University of Pavia

Department of Molecular Medicine

PhD course in Translational Medicine

XXXIV cycle

PhD thesis on:

Ageing-related impairments at the Neuromuscular Junction: nutritional and exercise interventions to attenuate neuromuscular dysfunctions

Tutor:

Prof. Maria Antonietta PELLEGRINO

Candidate:

Dr. Maira Rossi

Academic year: 2020/2021

TABLE OF CONTENTS

ABSTRACT

With an extended life expectancy in recent years, society is experiencing an increase in all the issues related to ageing. Older people face problems related to their own mobility, frailty and risk of injuries that can compromise their independence. In particular, an impoverished neuromuscular control and sarcopenia are mainly accountable for a reduced quality of life. Sarcopenia, defined as the evidence of a reduction in muscle mass (atrophy) and muscle strength, is nowadays recognized as a clinically diagnosed pathology in which incidence increases in the elderly population (> 70 years old). The origins of these manifestations are multifactorial and can affect human physiology in different districts and in different phases of life. Among all the processes that occur in the locomotor system during ageing, a great role is played by neurodegenerative changes. This is the reason why the study of molecular and morphological implications in the progression of ageing at the neuromuscular level is nowadays very important to give a face to the arising of these impairments, especially at the level of the neuromuscular junction (NMJ).

The NMJ is a chemical synapse that is formed between motor neurons and skeletal muscle fibers and its stability is crucial for the communication among these two compartments. Their functional interaction promotes a cascade of events that result in muscle contraction (excitation-contraction coupling, microscopically) and so movement (macroscopically). An intricate network of factors and molecules interacts with each other to maintain the high plasticity of this structure, meaning the ability to adapt and reorganize following stimuli. In elderly age, denervation, a defective molecular scaffold, mitochondrial dysfunctions and PGC1α impaired transcriptional control probably play an important role in NMJ degeneration and the decline of neuromuscular function.

Up to now, being a multifactorial pathology, neither pharmacological approaches nor therapeutical interventions are found to be successful for the treatment of age-related neuromuscular decline, but interventions useful to modulate and promote beneficial outcomes are usually applied to relief and delay NMJ-associated impairments. Exercise training and dietary supplementation are mainly used to treat sarcopenia and recently a greater interest is arising in the study of the beneficial combination of physical exercise and nitrate supplementation at the neuromuscular stability. Nitrates have been proven to ameliorate the physical performance in trained and untrained people, and their potential is mainly targeted to benefit at the level of mitochondrial biogenesis and functionality, a very relevant aspect in a highly active mitochondrial tissue such as skeletal muscle.

22-months old mice were subjected to 2 months' endurance exercise training (Old EX) and 1.5 mM inorganic $NaNO_3$ supplementation (Old N), separately or in combination (Old EX+N) and sacrificed for molecular and morphological evaluations at the age of 24-mo, in parallel with controls matching for the same age (Old CTRL). We primarily characterized the elderly cohort through the analysis of all the sarcopenia-related markers within the muscle compared to a young cohort of animals (7-months old, Young CTRL). In old mice, ageing promoted a decline of muscle mass concomitantly to the accumulation of hyper fused mitochondria, not correctly cleared by an impaired autophagic flux. Moreover, parameters indicative of innervation status and the structural stability of the junction were assessed, showing that denervation-related parameters such as NCAM1, Runx1, Myogenin and Gadd45α among all, were significantly upregulated in elderly animals, and structural maintenance of the postsynaptic side of this complex (namely the acetylcholine receptor, AChR) was perturbed due to a higher expression of AChR γ-subunit (indicative of denervation/instability). These results were confirmed by morphological evaluations of the NMJ through the acquisition of images at the confocal microscopy, revealing a highly fragmented postsynaptic structure and a reduced overlap between the pre and postsynaptic side, in parallel with an atrophic axon terminal to confirm a slow motor neuron degeneration. Treatments based on dietary nitrate supplementation and endurance exercise training promoted a slight benefit on those parameters related to muscle function: *ex vivo* functional assessments by muscle contractility assay and High-Resolution Respirometry (HRR, Oroboros-O2k) protocols were shown to highly ameliorate the functionality of aged muscles. Moreover, NMJ molecular parameters mildly ameliorated following interventions, even if a large improvement was visible in restoring NCAM1 molecular levels. Morphological evaluations following treatments then revealed an ameliorated postsynaptic organization with a reduced fragmentation in all the old groups under investigation compared to the Old CTRL, together with an increased compactness of the AChR clusters confined in a restricted endplate. The presynaptic side underwent remodelling in both exercise and nitrate groups, acting on different parameters.

As last purpose, we wanted to explain mechanisms underlying NMJ alterations and muscle deterioration by the characterization of muscular parameters that could be indicative of this. The focal regulatory factor PGC1α did not show changes in expression. The relevance of this marker is due to its involvement in mitochondrial biogenesis and the regulation of transcription of synaptic genes expressed in subsynaptic nuclei at the level of the NMJ. Changes in the expression of molecular factors involved in the postsynaptic organization were not perturbed following interventions, indicating that this factor is not merely involved in an ameliorated NMJ morphology

following nitrates intake and exercise training. Interventions did not change autophagic flux, reported in the literature as a pathway that influences the stability and turnover of NMJ components. Nitrate supplementation is found to regulate and increase factors involved in the Akt/mTOR synthetic pathway (demonstrated to be involved in beneficial remodelling of NMJ). Accordingly, a nitrate-induced muscle mass augment was observed. Exercise alone was highly affecting the neurotrophins' activity promoting a positive crosstalk between muscle and nerves which appeared hypertrophic and predisposed to reinnervation. Unfortunately, the combination of the two interventions did not promote a remarkable amelioration of neuromuscular and muscle metabolism-associated markers in comparison with the individual treatments.

In conclusion, the findings indicated that both treatments were effective in mitigating age-related NMJ dysfunctions in terms of morphology and organization. Improvement of muscle size, mitochondrial respiration and innervation were moreover representatives of an ameliorated muscle tissue functionality. The results obtained encourage thus the evaluations of nitrate supplementation in elderly sarcopenic humans to test its ability in counteracting age-related neuromuscular impairment.

LIST OF ABBREVIATIONS

4E-BP1 4E-binding protein 1

α-BTx α-Bungarotoxin

ACC acetyl-CoA carboxylase

ACh Acetylcholine

AChR Acetylcholine Receptor

ADP Adenosine diphosphate

Akt Protein Kinase B

AMP Adenosine monophosphate

AMPK AMP-activated protein kinase

ANT Adenine nucleotide translocator

AO Aldehyde Oxidase

ATG7 Autophagy related 7

ATP Adenosine triphosphate

BDNF Brain Derived Neurotrophic Factor

BNIP3 BCL2 Interacting Protein 3

BR Beetroot Juice

Ca^{2+} Calcium ion

CAF C-terminal agrin fragment

cGMP cyclic Guanosine Monophosphate

CHF Chronic Heart Failure

CLC-1 Chloride Channel 1

CoA Coenzyme A

COX Cytochrome c oxidase

CREB1 CAMP Responsive Element Binding Protein 1

CRF Cardiorespiratory Fitness

CS Citrate Synthase

CSA Cross-sectional area

CVD Cardiovascular Disease

DGC Dystrophin glycoprotein complex

DHPR Dihydropyridine Receptor

DMD Duchenne Muscular Dystrophy

DRP1 Dynamin-related protein 1

ECC Excitation-contraction coupling

ECM Extracellular Matrix

EDL Extensor Digitorum Longus

eIF2B eukaryotic Initiation Factor 2B

eIF4E eukaryotic Initiation Factor 4E

eNOS endothelial Nitric Oxide Synthase

ETC Electron Transport Chain

ETS Electron Transfer System

FA Fatty acids

FAPs Fibro-adipogenic progenitors

FGFBP1 Fibroblast-Growth Factor (FGF) Binding Protein-1

FoxO Forkhead Box O

FUNDC1 FUN14 domain containing 1

GADD45α Growth Arrest And DNA Damage Inducible Alpha

GAPDH Glyceraldehyde-3-phosphate dehydrogenase

GDNF Glial-derived neurotrophic factor

GLUT-4 Glucose transporter 4

GPx Glutathione peroxidase

GSH Glutathione

H_2O_2 Hydrogen Peroxide

HDAC4 Histone Deacetylase 4

HIF-1α Hypoxia-inducible Factor 1α

HRR High-Resolution Respirometry

HSG Human Salivary Glands

IGF Insulin like Growth Factor

IkB Inhibitory of NF-kB

IMM Inner Mitochondrial Membrane

iNOS inducible Nitric Oxide Synthase

LC3B Light Chain 3B

L-NAME L-N^G-Nitro arginine methyl ester

MAFbx/Atrogin-1 Muscle atrophy F-box (MAFbx)/atrogin-1

MARC1/2 Mitochondrial amidoxime-reducing component 1/2

Mfn1/2 Mitofusin 1/2

MHC Myosin Heavy Chain

MLC Myosin Light Chain

MLCK Myosin Light Chain Kinase

MLCP Myosin Light Chain Phosphatase

MPB Muscle Protein Breakdown

MPS Muscle Protein Synthesis

MRF Myogenic Regulatory Factor

mtDNA mitochondrial DNA

mTOR Muscle Target of Rapamycin

MuRF-1 Muscle Ring Finger 1

MuSK Muscle-specific kinase

MyoD Myoblast Determination protein 1

MyoG Myogenin

NCAM1 Neural Cell Adhesion Molecule 1

NF-H Neurofilament Heavy

NF-κB Nuclear Factor Kappa B

NF-L Neurofilament Light

NGF Nerve Growth Factor

NMDAR N-methyl-D-aspartate receptor

NMJ Neuromuscular Junction

nNOS neuronal Nitric Oxide Synthase

NO Nitric Oxide

NO_2 Nitrogen Dioxide

NO_2^- Nitrite

NO_3^- Nitrate

NOS Nitric Oxide Synthase

NSS Nitrosative Stress

NT4 Neutrophin 4

NRF2 Nuclear factor erythroid 2-related factor 2

O_2 Oxygen

O_2^- Superoxide

OMM Outer Mitochondrial Membrane

$ONOO^-$ Peroxynitrite

Opa1 Optic atrophy-1

OXPHOS Mitochondrial Oxidative Phosphorylation System

p62/SQSTM1 p62/sequestosome 1

p70S6K Ribosomal protein S6 kinase beta-1

PCr Phosphocreatine

PDE5 Phosphodiesterase 5

PFK Phosphofructokinase

PI3K Phosphoinositide 3-kinase

PKA cAMP-dependent protein kinase

PKG cGMP-dependent protein kinase

PGC1α Proliferator-Activated Receptor Gamma Coactivator 1α

PINK1 PTEN-induced kinase 1

PPARα/β/γ Peroxisome proliferator- activated receptor α/β/γ

RNS Reactive Nitrogen Species

ROS Reactive Oxygen SpeciesRunx1

Runx1 Runt-related transcription factor 1

RyR Ryanodine Receptor

sGC soluble Guanylate Cyclase

SERCA Sarco/endoplasmic reticulum Ca^{2+}-ATPase

SIRT1 Sirtuin 1

SLC17A5 Sialin receptor

SNO S-nitrosothiol

SOD1 Superoxide dismutase 1

TA Tibialis Anterior

TFAM Mitochondrial transcription factor A

TNF-α Tumour-necrosis factor α

UCP1 Uncoupling Protien 1

UPS Ubiquitin-proteasome system

VGCC Voltage-gated calcium channels

VO_2 Maximal volume of oxygen consumed during contraction

WT Wild Type

XOR Xantine Oxidoreductase

PREFACE

Skeletal muscle tissue is one of the major tissues that compose the body, and it is involved in different but very important vital functions: it acts as a reservoir for different compounds, it is involved in respiration and it promotes maintenance of posture and movement through the locomotor system. Its principal function, muscle contraction, is promoted by the highly organized sarcomere structures, which occupy the majority of the muscle fiber volume, and their interaction with specific structural proteins enable the fibers to maintain continuous activity and propagate the contractions, conferring those elasticity. Contraction and all the surrounding mechanisms are highly energy-demanding, that are accomplished through high levels of mitochondria, the primary energy suppliers of the cells.

Being exposed to different insults and stimuli, it is recognized as a tissue of high plasticity, due to its ability to remodel itself to cope with environmental changes and functional requirements. A fine balance among various opposite but complementary pathways is maintained to converge the system into homeostasis and to maximise the functionality. Interaction with other tissues and an intricate crosstalk through signalling molecules occurs, so as to excellently respond to all the demands the system encounters. Blood vessels, connective tissue and nerve terminals are finely intertwined among muscle fibers to provide nutrition, exchange gaseous compounds, distribute endocrine signalling molecules, maintain the structural spatial organization and propagate electrical inputs to elicit contraction. The latter interaction takes physically place in a confined area called neuromuscular junction (NMJ), in which nerve terminals and muscle fibers create a restricted cleft through which an exchange of signals occurs, directed to either trigger intracellular cascade of events leading to muscle contraction, and release trophic factors acting on both sides of the junction to maintain its functional organization. NMJ is a dynamic structure that is physiologically subjected to remodelling driven by an intricate network of factors that orchestrate its plasticity.

Changes in homeostasis occurring independently in the nerve terminals, in the muscle fibers and at the level of the junction, or impairments arising from one of these structures that can negatively affect the stability of the interconnected ones, can lead to a compromised transmission of signals, an instability of the assembled structures and eventually a degeneration of the activity-dependent interaction. Exogenous interventions and physiological changes such as a reduced physical exercise, a sedentary lifestyle, changes in dietary uptake, traumatic events, comorbidities and ageing modulate the stability of the junction so as to deal with changes. When the remodelling that are

triggered cannot be sufficient to restore a functional homeostasis, deregulation processes occur leading to an impaired activity.

Ageing is the result of a natural life course, but pathological spectra can emerge from this when subjects are clinically diagnosed with a reduced muscle mass and decreased strength developed by contractions, in a condition defined sarcopenia (with parameters officially indexed by the European Working Group on Sarcopenia in Older People (EWGSOP), Cruz-Jentoft *et al*, 2019). The arising frailty coming from this condition impairs the quality of life of elderly people which are no more independent and thus require more and more assistance. Sarcopenia and associated frailty have a multifactorial basis and for this reason it is difficult to approach pharmacological treatments aimed at treating the pathology, but rather therapeutic interventions are applied in order to mitigate or slow-down the course (Pascual-Fernandez *et al*, 2020). In this context, non-invasive strategies are covering a relevant role to ameliorate this condition.

INTRODUCTION

1. SARCOPENIA

During ageing, muscles undergo an inevitable and progressive loss of muscle mass accompanied by loss of force, a condition that is clinically defined sarcopenia. With an extended life expectancy in recent years, quality of older people is a priority. Especially in Italy, where the percentage of elderly people is one of the highest in the world, placing it among one of the "older" nations (in 2019, 22.9% of the population was over 65 years, and among those 28.4% with serious difficulties in basic functional activities, Istat survey 2019). Major hallmarks are loss of mobility, frailty, risk of injuries and falls, which can compromise individuals' independence and have dramatic impacts on the society, which nowadays is experiencing an increase in all the issues related to ageing. Most of the times, sarcopenic diagnosis is concomitant with comorbidities and the clinical picture of these patients undergoes increased morbidity. Besides a huge health care cost and thus the general economic impact they represent, it is now becoming very important to characterize the molecular pathways at the basis of sarcopenia. In fact, it is reported that worldwide sarcopenia affects about 5% to 13% of older adults (aged 60–70 years) and as many as 11% to 50% of those aged 80 years or older, with a rapid decline per decade from the age of 70. For this reason and all the associated features, it has become important to suggest methods and cut-off parameters for the evaluation of sarcopenia risk in clinical practice: it is well recognized as a muscle disorder and diagnosed by measuring muscle strength (function), muscle mass (quantity) and physical condition assessment (quality) (promoted by the EWGSOP, Cruz-Jentoft *et al*, 2019).

The aetiology of these manifestations are multifactorial and involve hormonal, biological, nutritional and physical activity factors, and can affect human physiology differently in various districts, leading to an inexorably muscle degeneration. Old muscles show a reduced regenerative capacity upon injury due to reduced number and activity of aged satellite cells (Brack and Rando, 2007). Moreover, age-related changes in muscle are driven by complex intrinsic mechanisms, histologically characterized by muscle atrophy, myofiber degeneration replaced by nonmuscular cells (i.e. adipocytes and connective tissue cells), fiber type grouping (following reinnervation by non-affected motor neurons), infiltration of connective fibrotic tissue and increase in inflammatory cytokines, presence of centrally-localized nuclei. Biochemical outcomes include altered anabolic, catabolic and metabolic pathways, selective loss of fast-twitch fibers and an increased heterogeneity in fiber composition, mitochondrial dysfunctions and uncontrolled oxidative stress. Functional features

regard weaker strength, contractile apparatus impairment and neuromuscular junction (NMJ) alterations. The age-related decline of NMJ is observable with altered structure and function that results in an impaired signal transmission and altered innervation (denervation/reinnervation cycles), with denervation representing one of the hallmark features of sarcopenia.

1.1 Age-related denervation

Denervation is one of the primary outcomes visible in age-related sarcopenia and muscle atrophy. This concept arises from a wide range of studies based on the morphology of the NMJ in which alterations at the endplate are clearly visible during ageing, with a reduction in motor unit number and eventually its loss. A lot of evidence have demonstrated that repeating cycles of denervation and reinnervation occur during lifespan and even in aged muscles (Hepple and Rice, 2016). During these processes, the motor neuron terminal transiently disconnects from its muscle fiber, rapidly followed by reinnervation of vacant sites by the original motor axon (if still intact) or through collateral sprouting from adjacent axons, guided by adhesion molecules ubiquitously expressed at the level of the NMJ. The motor neuron plasticity then maintains a mosaic distribution of fiber types in muscle cross-sections. Over the years, remodelling of motor units occur and fiber type grouping is more evident, with fibers of the same type being innervated by the same terminal beside one another, until axonal degeneration occurs, leading to grouped denervated fibers (Figure 1). Most of the long-term denervated fibers eventually undergo atrophy and will be entirely lost.

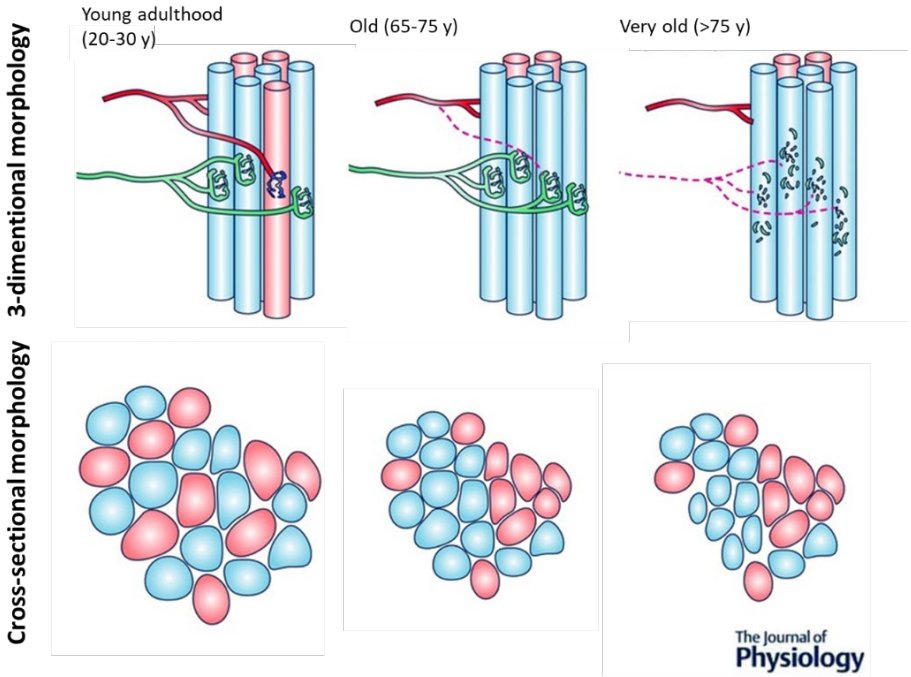

Figure 1. Morphological impact of motor unit alterations in aged muscle. *Young adulthood is characterized by an intermingling of fibers belonging to different motor units. This yields a mosaic distribution of fiber types in a cross-section view. Adulthood to old age is characterized by repeated cycles of denervation-reinnervation that result in fibers of the same type being beside one another (fiber type grouping) when viewed in cross-section. Very old age is characterized by increasing frequency of axonal degeneration and/or motor neuron death leading to grouped atrophic fibes when viewed in cross-section (modified from Hepple and Rice, 2016).*

Debate is ongoing regarding the relation between atrophy and denervation: in early aged rats (21 months), a significative denervation occurs in Plantaris muscles compared to young littermates, but no changes in muscle fibers size and fiber type composition occurs. Concomitantly, Soleus muscles from the same animals, involved in postural activity and therefore highly recruited throughout the day, show neither denervation nor muscle atrophy assessing that ageing and denervation act in a muscle-specific manner, and are not muscle atrophy-dependent (Deschenes *et al*, 2010). The reason why age-related denervation has little chances to undergo reinnervation can vary and be accounted for the instability of neuromuscular junction components, like the AChR organization, postsynaptic membrane proteins, decreased overlap between pre and postsynaptic elements, altered distribution of laminins and extracellular matrix (ECM) proteins, meaning all those components involved in the maintenance of the NMJ structure which are nomore able to cope with rearrangement requests. Another likely cause for the accumulation of persistently age-related denervated fibers can be caused by an impaired axonal regrowth. Aged animals (mice >20 months) subjected to acute nerve injury demonstrate little axon regeneration and branching due to obstruction of degenerated axonal debris, which incorrect clearance slows down the reoccupation of NMJ sites (Kang and Lichtman, 2013). Anyway, in very old female mice (29 months) no significant difference in the size or number of motor neuron cell bodies at the spinal cord are assessed, even if denervation is prominent in fast-twitch muscles (EDL) but not in slow-twitch Soleus. Despite the differences in denervation, fiber grouping is still visible in old animals, shifting Soleus in favour of a slower phenotype and Tibialis Anterior to a faster one, with no changes on mass (Chai *et al*, 2011). Axon guidance to reinnervation is a duty accomplished by the expression and active interaction with neurotrophins: overexpression of BDNF, GDNF and NGF in rat muscle facilitates axonal sprouting and thus reinnervation following 20 weeks' post-surgical denervation (Hoyng *et al*, 2014), but notably these factors show no significant trends in old rats (35/36 months old) compared to young, as an indication of a non-stimulated pathway during ageing (Aare *et al*, 2016). In this paper, factors known as denervation-related factors were also studied, and were found to be highly expressed and induced following denervation, in order to launch signals to sprouting axons so as to promote the

reinnervation. These factors are now recognized as hallmarks indicative of a denervated muscle fiber and thus highly studied in their expression. mRNA levels of these factors significantly increase in old rats (shown in the previously mentioned study) and in old female mice (Barns *et al*, 2014). Interestingly, 24 months old mice show a strong denervation profile compared to older animals: this is a proof that denervation-related factors are highly expressed to promote reinnervation (which turn-down their expression) and decrease after long-term denervation.

Among these factors, Runx1 covers an important role in denervation. Runx1/AML1 is a Runt-related transcription factor-1 (homolog of Runt transcription factor in Drosophila) found at very low expression levels in fully innervated muscle fibers and upregulated following denervation. It has been shown to have a protective role from severe muscle atrophy: in mice selectively deficient in muscle Runx1, its induction is required to prevent myofibrillar disorganization and so an extended muscle atrophy and wasting. Interestingly, major pathways involved in autophagy in muscle cells (FoxO/Atrogin-1 axis and NFκB/MuRF1 axis) are not excessively activated in Runx1-mutant mice, suggesting other pathways responsible for the decrease in muscle mass. Being a transcription factor, its activity regulates the expression of genes involved in cell growth, structural stability and function of muscle components, while its downregulation promotes a failure in the transcription of these genes, leading to atrophy and promoting autophagy. Among those, myosin heavy chain (MHC) IIA and AChR γ-subunit are found regulated by Runx1 activity, while none of the other denervation-related factors undergoes transcriptional regulation by Runx1 (Wang *et al*, 2005).

AChR γ-subunit is now widely used as a marker of denervation. Found expressed during embryonic and early postnatal development and selectively substituted by the adult ε-subunit in adulthood, during denervation its expression is again promoted and enhanced, together with all the other subunits highly expressed (studied in Vastus Lateralis of elderly women, Soendenbroe *et al*, 2020, and finely reviewed in different species and muscles by Bao *et al*, 2020). By the way, the denervation-induced increase in AChR subunits' gene expression does not persist in long-term denervated rat muscles. However, the adult isoform maintains high levels of expression in long-term denervated fibers, indicative of a preference in the adult isoform conformation of the receptors (Adams *et al*, 1995). The transcription of AChR subunits are regulated by the family of myogenic regulatory factors (MRFs), in particular MyoD (myoblast determination factor) and MyoG (Myogenin): both are highly increased in their expression after denervation, making them denervation-related factor themselves, but only MyoD maintains high levels of expression in long-

term denervation, while Myogenin decreases in parallel with AChR subunits in their embryonic conformation. Even in this case, contrasting assessments are made: following permanent tibial nerve injury in rats, Gastrocnemius mRNA levels of receptor's subunits and the MRF genes significantly increase in the seventh day after injury, but then stabilize their expression levels back to control ones, until reaching significant lower levels of expression one year after injury in comparison to control littermates (Ma *et al*, 2007). Different outcomes are seen in rat Gastrocnemius protein levels, in which α- and γ-subunits show no changes due to ageing, like Myogenin protein expression (Apel *et al*, 2009).

Another important modulator of denervation is represented by Gadd45α, the growth arrest and DNA damage-inducible 45α, a small myonuclear protein which promotes denervation-induced myofiber atrophy. Denervation *per se* strongly increases Gadd45α mRNA expression, which causes myonuclei reprogram and altered skeletal muscle gene expression, repressing genes involved in anabolic signalling, reducing mitochondrial efficiency and anti-atrophic pathways and stimulating thus pro-atrophic mechanisms. Its inhibition decreases denervation-induced muscle atrophy, while its overexpression is sufficient to induce muscle fiber atrophy even in the absence of denervation (Ebert *et al*, 2012). Induction of Gadd45α is mediated by HDAC4, a histone deacetylase which covers a relevant role in muscle denervation-reinnervation cycles. In this context, Gadd45α mediates several downstream effects of HDAC4, including the induction of both AChR γ-subunit and Myogenin and, most importantly, skeletal muscle mass loss and fiber atrophy (Bongers *et al*, 2013).

HDAC4 is a key enzyme which regulates gene expression by its histone deacetylation activity and mainly involved in satellite cell proliferation and differentiation. In last years, an important role was discovered in denervation-induced atrophy. Being highly expressed following denervation, it is promoter of atrogenes (muscle-specific E3 ubiquitin ligases) expression and autophagy-related proteins (Atg7, p62, LC3B, PINK1 and BNIP3). It was moreover found to cause the downregulation of the key regulatory factors SIRT1 and PGC1α and among all, induces Myogenin expression (through Gadd45α) and its downstream molecular factors. HDAC4 inhibition alleviates thus denervation-induced muscle atrophy by restrain all the previous pathways (Ma *et al*, 2021), but long-term inhibition leads to an impaired clearance apparatus for damaged components within the fibers that undergo denervation (Pigna *et al*, 2018). Its activity depends on the degree of phosphorylation, which confers its localization and activity: it is predominantly localized into the nuclei of fast-twitch fibers where it represses the oxidative metabolic gene program, while the

inactive cytoplasmic localization is associated with a hyper-phosphorylation in slow-twitch fibers (Cohen *et al*, 2015). It is important to note that denervation occurs primarily in fast-twitch fibers and the nuclear localization of HDAC4 can so accelerate all the downstream denervation-related mechanisms. The arising curiosity around HDAC4 led to the discovery of miR-206 as a regulatory element for its expression. It is able to inhibit HDAC4 activity, reversing muscle atrophy and promoting satellite cell differentiation (Huang *et al*, 2016). Another beneficial aspect it promotes is linked to the regeneration of neuromuscular synapses by induction of reinnervation. After denervation, there is a local increase in MyoD which promotes miR-206 expression. By inhibiting HDAC4 activity, this miRNA indirectly increases levels of the fibroblast growth factor binding protein-1 (FGFBP1), a secreted growth factor that interacts with FGF and promotes thus reinnervation (Bruneteau *et al*, 2013). miR-206 is also involved in the negative regulation of BDNF activity, due to a recurrent presence of binding sites along its transcript: by inhibiting its expression is thus able to modulate the retrograde signalling for promoting BDNF-dependent survival of motor neurons and NMJ remodelling (Miura *et al*, 2011).

Last, but not least, NCAM1 is highly studied in denervation and sarcopenia. It is a neural cell adhesion molecule that facilitates innervation processes and promotes synaptic stability by managing the distribution of presynaptic structures at developing and regenerating synapses. It was demonstrated that NCAM1-null mice undergo weaker and unstable reinnervation that ultimately degenerate after nerve injury. Moreover, incorrect redistribution of synaptic vesicles occurs in the active zone, promoting the scenario of NMJ instability and nerve terminal lower functionality (Chipman *et al*, 2014). It is found expressed in the cytoplasm of denervated fibers together with the neonatal isoform of MHC, a marker of regeneration, and both persist in highly atrophied muscle fibers of human biopsies, suggesting that loss of neural signal reverts certain muscle fiber proteins to an embryonic configuration (together with increased AChR γ-subunit; Soendenbroe *et al*, 2020). NCAM1, involved in myoblast fusion during development, is identified with lots of isoforms and localizations within a cell, and undergoes post-translational modifications. This is the reason why the main approach to study its expression levels is by the evaluation of its spatial localization (junctional or extra junctional, at the level of the NMJ, or cytoplasmic). The cytoplasmic localization is mainly found in highly atrophic muscles fibers, while the extra junctional expression is maintained following 2 weeks' denervation, even if in general elderly mouse skeletal muscle fibers have been demonstrated to have diminished capacity to upregulate NCAM1 production in response to denervation (Gillon and Sheard, 2015). On the contrary, NCAM1 was significantly upregulated in

both cytoplasmic and junctional localization at either 2 and 4 weeks after denervation in old rats (Hendrickse *et al*, 2018).

Taken together, the evaluation and expression profile of all these denervation-related factors contribute to the recognition of a denervated muscle which manifests functional impairment and eventually undergoes atrophy. However, it is still unknown whether the initial myofiber denervation is related to deleterious changes in muscle cells themselves or neurons or both components. It seems that the maintenance of NMJs depends on the healthy state of motor neurons and myofibers, and the profitable exchange of trophic signals by these two compartments.

1.2 Age-related instability of NMJ

Although the adult NMJ is a stable synapse under physiological conditions, it is also capable of remodelling to cope with various stimuli, exhibiting a dynamic expression of factors involved in its structural and functional organization (Figure 2).

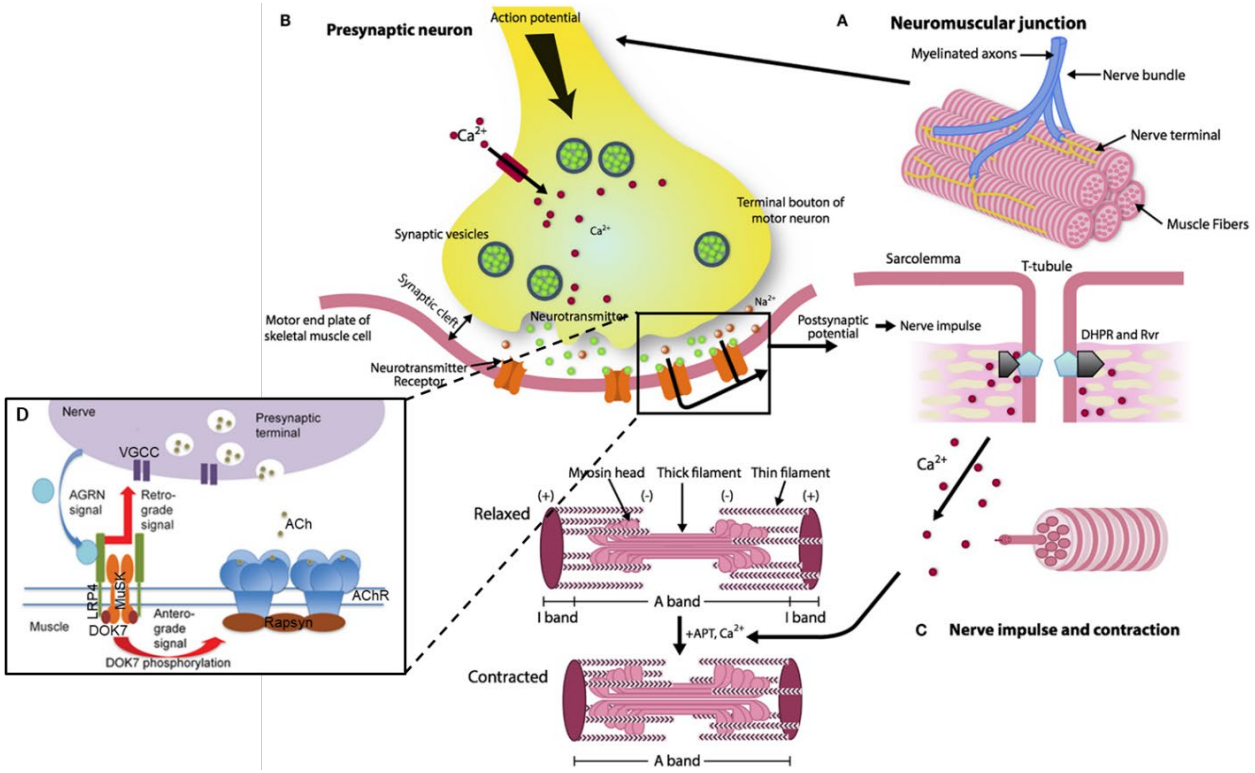

Figure 2. The architecture of a neuromuscular junction (NMJ). *(A, B) The NMJ is composed by three elements: presynaptic (motor nerve terminal), intrasynaptic (synaptic cleft), and postsynaptic component (muscle fiber). When the action potential reaches the motor nerve terminal, the voltage-gated calcium (Ca^{2+}) channels (VGCC) open and calcium ions enter in the terminal part of the neuron and delivers acetylcholine (Ach) in the synaptic cleft. (C) Activated AChRs promote a cascade of events within the muscle fiber and among those, the activation of the dihydropyridine receptors (DHPRs) located in the sarcolemma occurs, causing the induction of the ryanodine receptors (RyRs). Calcium released from the sarcoplasmic reticulum through the RyRs binds to troponin C and allows cross-bridge*

cycling and thus force production. (D) The intricate molecular scaffold composing the postsynaptic component. Modified from Gonzalez-Freire et al, 2014 and Koneczny et al, 2014.

However, with ageing the complexity and morphology of the NMJ become altered, appearing in rodents with a loss of the typical pretzel-like configuration (in a paper from 2013, Cheng and colleagues elegantly follow the timing evolution and changes of NMJ morphology of 2, 14, 19, 22, 25 and 28-months old mice). Nevertheless, different outcomes are seen in human NMJ morphologies, in which a slightly different postsynaptic structure (less complex and significantly smaller than rodents) is demonstrated to be less compelling across the entire adult lifespan, showing minor age-related instability and degeneration (Jones *et al*, 2017). However, a pivotal study in cadavers of elderly people showed an altered morphology and postsynaptic fragmentation, supporting a NMJ instability outcome (Oda K, 1984). These morphological alterations are thus reflective of a functional impairment (Willadt *et al*, 2018). In general, aged NMJs of most muscles show marked structural alterations, including nerve-terminal sprouting, disassembled active terminal zones, the previously described denervation accompanied by muscle fibers impairments, and fragmentation of the motor plaque.

Fragmentation of the postsynaptic side occurs when AChR clusters lose their spatial organization and thus disperse along the sarcolemma. This can be due to defects in all the cytoskeletal apparatus within the muscle fiber which can deteriorate during ageing and/or the loss of trophic activity which normally acts as a positive feedback for the maintenance of the structure. Activity at the level of the junction is maintained by the functional interaction of axon terminals with postsynaptic elements, but when nerve terminals detach to their fibers causing denervation, no active signal occurs within the cell and thus the trophism is nomore maintained. One of the key players for the maintenance of active NMJs is found in agrin. The synaptic signalling protein actively interacts with AChRs upon release maintaining their clustering. However, selective cleavage of agrin by neurotrypsin releases a soluble 22 kDa C-terminal agrin fragment (CAF), an inactive form of the protein that subsequently destabilizes AChR clusters. CAF is then dispersed in the extrasynaptic portions and has been found at high levels in the blood of sarcopenic diagnosed patients, rendering this factor a biomarker for sarcopenia (Hettwer *et al*, 2013).

During senescence, the percentage of denervated fibers augments and the compensatory sprouting of axon terminals seems to lose its efficiency, leaving muscle fibers without connection or connected with altered terminals and thus leading to a disruption of the postsynaptic neuromuscular organization and muscle fibers defects, with most of the times nuclei centrally located (Li *et al*,

2011). Because the maintenance of muscle mass requires normal innervation and regular activation, malfunction of any of these elements can lead to muscle deterioration and thus atrophy and loss of function.

Although degeneration of the NMJ in aged muscles is well known, the exact causes underlying its instability remain unclear. Many evidence indicate that mitochondria, a critical cellular organelle involved in energy production and cellular signalling, may be either a primary trigger or at least an important player in this process, in both junctional elements (Rygiel *et al*, 2016).

1.3 Age-related mitochondria adaptation

Mitochondria are the master producers of energy within the cell, so they play an important role in accomplishing metabolic demands and regulating many critical processes. They are particularly dynamic organelles in their structure and function, so as to be able to cope with any environmental change to preserve cellular homeostasis. Particularly enriched with these organelles, the muscle fibers require a large and constant energy supply to carry out their main activity, namely muscle contraction. But numerous other processes are occurring in the mitochondria as this organelle is critical for the regulation of signalling pathways relevant for muscle metabolism: not only ATP producer for the energetic sustainment of the cell, but also regulator of a balanced ROS (reactive oxygen species) equilibrium and inducer of the programmed cell death machinery under specific stimuli that collectively participate to the intrinsic apoptotic process. They are interspersed within the sarcoplasm and mainly localized in regions with high metabolic activity (especially in NMJs and among contractile myofilaments), found thus interconnected to boost their outcomes.

Given the relevant importance of mitochondria within muscle fibers, they need to be tightly controlled by a complex mitochondrial quality control system (Quiles and Gustafsson, 2020), essential to limit mitochondrial damage and for the maintenance of healthy organelles. It involves pathways related to protein folding and degradation as well as systems involved in organelle shape (mitochondrial dynamics) and turnover by the elimination of damaged organelles (mitophagy) and biogenesis of new ones (mitochondriogenesis) (Figure 3).

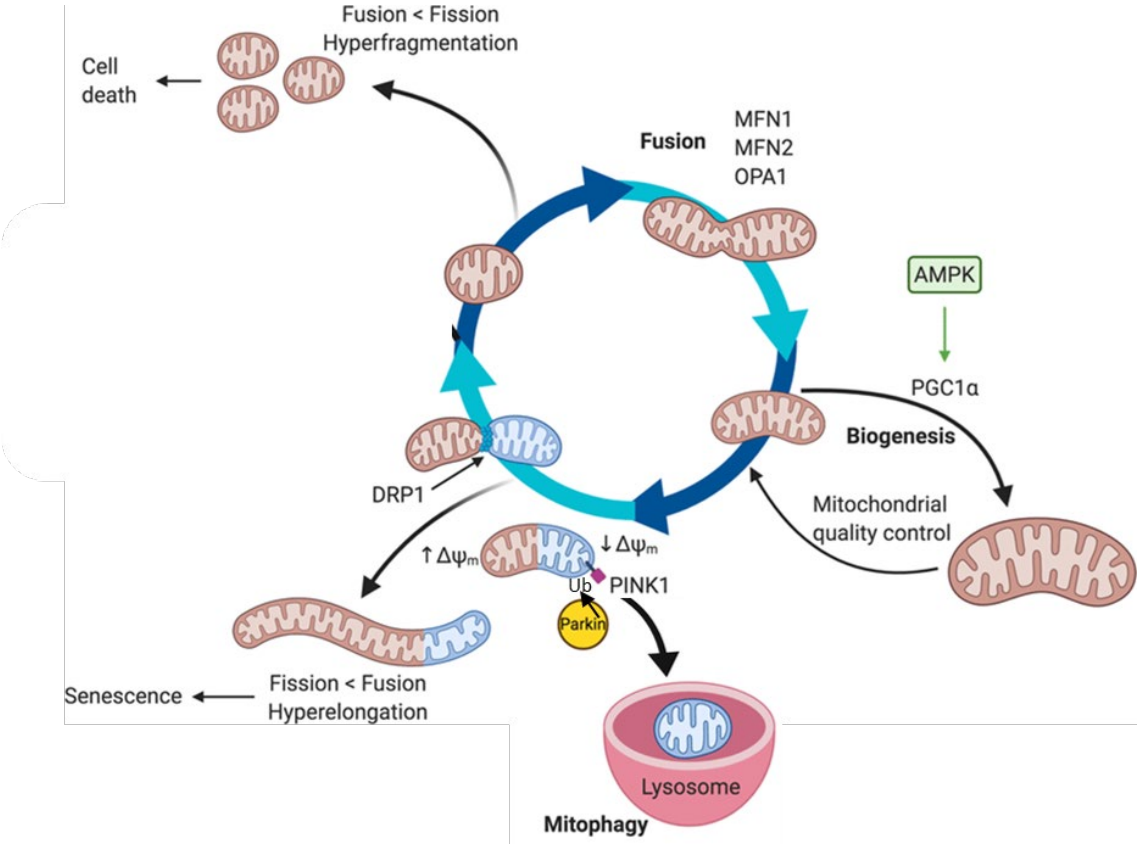

Figure 3. Mitochondrial dynamics and quality control. *Mitochondria undergo dynamic processes of biogenesis, fusion, fission, and mitophagy. A fine balance between fission and fusion processes are needed to maintain normal mitochondrial function. An imbalance of fission/fusion dynamics leads to mitochondrial dysfunction: excessive fission can lead to cell death and excessive fusion is often seen in senescence. Adapted from Garbern and Lee, 2021.*

Mitochondrial dynamics allow these organelles to undergo coordinated cycles of fission and fusion, in order to rapidly modulate their morphology and change in size, shape and distribution within the sarcoplasm (Tilokani *et al*, 2018). Mitochondrial fission (or fragmentation) is characterized by the segregation of one mitochondrion to two smaller organelles. They are mostly dysfunctional or damaged components of the mitochondrial network which are prepared for their removal via mitophagy. This process is mediated by a large cytoplasmic GTPase, the dynamin-related/-like protein 1 (Drp1), which is recruited to the outer mitochondrial membrane (OMM) where it oligomerizes and form a ring-like structure to drive membrane constriction. This recruitment is mediated by a family of membrane-anchored proteins, as Fis1. The final step of fission is the scission of the membranes and thus release of two separated organelles. A reduced fission and/or increased fusion lead to elongated mitochondria, while excessive fission and/or inhibited fusion generate isolated mitochondria, which are less efficient in ATP production and are thus dysfunctional because they focus ATP consumption for the maintenance of their membrane potential. Recent evidence also reveal that increased mitochondrial fission is causative of muscle wasting by promoting

apoptosis and atrophy of muscle fibers, while its inhibition leads to a diminished mitophagy followed by accumulation of dysfunctional organelles that over time promotes cell death. Further, fragmentation occurring in damaged mitochondria results in energy stress and AMPK-induced activation of FoxO3 that could induce expression of atrophy-related genes, protein breakdown and muscle loss, and eventually promote the release of pro-apoptotic factors (Romanello *et al*, 2010).

Conversely, mitochondrial fusion is the union of two mitochondria resulting in just one elongated organelle. This mechanism can occur between healthy and damaged organelles in order to dilute the damaged material into the healthy network, avoiding the local accumulation of defective or abnormal mitochondria and maintaining their overall fitness (function). It is promoted by specific melting of the OMMs and even in this case, two large GTPases guide this phenomenon: Mfn1 and Mfn2 (mitofusins), accumulated at the level of the contact areas of two adjacent mitochondria. The docking of the two organelles occurs when even the inner mitochondrial membranes (IMMs) fuse, and this is mediated by the Mfn1-dependent activation of OPA1 (Optic Atrophy 1, part of the dynamin-like GTPase family). This pathway increases the bioenergetic capacity of the cell and is essential for the excitation-contraction coupling (ECC) in skeletal muscles. In addition, under high-energy demand conditions, mitochondrial fusion covers a survival function, by protecting mitochondria against mitophagy, decreasing the probability of activation of the apoptotic regulatory elements, reducing ROS production and optimizing ATP synthesis (Romanello and Sandri, 2015). However, fusion events can repair membranes only when an intact membrane potential is maintained (which can dissipate when there is damage). Instead, fission processes can occur following loss of membrane potential and allows damaged portions of the mitochondrion to be degraded by mitophagy (Johnson *et al*, 2013). Fusion processes are moreover found to maintain mtDNA stability, contrary to fission events in which mtDNA can undergo more frequent mutations and eventually get lost (Chen *et al*, 2010). Notably, damage in mtDNA would trigger a vicious cycle in which the synthesis of defective electron transport chain (ETC) subunits results in decreased ATP production and higher ROS generation.

The importance in maintaining an equilibrium among these two phenomena is fundamental: they do not act separately but instead pro-fission and pro-fusion proteins cooperate to maintain a balance in mitochondrial dynamics and control mitochondrial mass (Yu *et al*, 2020). This equilibrium can be perturbed in pathological conditions or when the cellular homeostasis is impaired. During ageing, a remodulation in the mitochondrial dynamics occurs, leading to changes in mitochondrial

morphology and so elongated organelles, even if discrepancies in these observations are recurrent. Mitochondrial content was evaluated in young (8 months) versus old (24 months) mice in which ageing showed atrophic profile, and no changes in quantitative mass parameters were visible between the two cohorts. On the other hand, evaluations of the mitochondrial morphology through the electron microscopy (EM) technique revealed larger mitochondria with complex shapes in old animals, indicative of major fusion processes, but not sustained by changes in pro-fusion and pro-fission proteins (Leduc-Gaudet *et al*, 2015). Augmented mitochondrial volume was confirmed in old mice compared to young, accompanied by a changed orientation of mitochondria from a longitudinal towards a transverse orientation (which looked alike smaller fragmented mitochondria), with a decrease in pro-fusion proteins but no changes in Drp1 levels (del Campo *et al*, 2018). The constancy in Drp1 expression during ageing is explained by knockdown and overexpression experiments on old mice, demonstrating in both cases atrophic muscles and a decreased mitochondrial quality (Dulac *et al*, 2021). Physiologically, a reduced mitochondrial fusion machinery is linked to age-related sarcopenia and atrophy, demonstrated in Mfn2 deficient mice, in which age-induced mitochondrial dysfunction was enhanced and number of mitochondria reduced but with a wider volume, accompanied by a reduction in the autophagic pathway (Sebastian *et al*, 2016). In rats it was demonstrated that giant mitochondria accumulate during ageing, with low inner membrane potential and low levels of OPA1, but no changes in Mfn2, in an impoverished autophagic scenario (Navratil *et al*, 2008). However, it was even reported upregulation of both pro-fusion and pro-fission proteins in old rats together with a diminished mitochondrial content (Koltai *et al*, 2012).

Among the mitochondrial quality control systems, mitochondrial turnover covers a relevant role in parallel with mitochondrial dynamics pathways: degradation of dysfunctional or unnecessary mitochondria through a mitochondrial-specific autophagic flux, called mitophagy; generation of new organelles promoted by biogenesis. These two processes are well coordinated to maintain a constant amount of functional mitochondria that correctly supply energetic demands within the cell. Mitophagy is found strictly connected with fission phenomena as previously mentioned: a fragmented (small) mitochondrion becomes easily encapsulated in a double membrane system to form an autophagosome delivered to a proximal lysosome. The primary pathways involved in this process are the PTEN-induced putative kinase 1 (PINK1)/Parkin pathway and mitophagy receptors exposed in the OMM, as a result of loss in mitochondrial membrane potential. Accumulation of PINK1 in the outer membrane promotes the recruitment of the E3 ubiquitin ligase Parkin, which in turn ubiquitinates numerous proteins found on the surface of the OMM. This leads to recruitment

of the autophagosome machinery and sequestration of the mitochondria. Other receptors exposed in the OMM (BNIP3 and FUNDC1) directly tether the mitochondrion to the autophagosome membrane via their interaction with the active lipidated LC3B factor and p62 to facilitate its clearance.

Autophagy is essential for the maintenance of muscle mass, as demonstrated in Atg7 (a crucial factor in autophagy) null muscles. Accumulation of abnormal mitochondria and disorganization of sarcomeres lead to a loss of mass and force production, exacerbated with denervation (Masiero *et al*, 2009). Without provoking the denervation, inhibition of autophagy (Atg7 null mice) shows major impact on neuromuscular synaptic function and structure (Carnio *et al*, 2014), which seems to be restored by reactivating autophagic flux through Beclin-1 induction (Baraldo *et al*, 2020). On the contrary, excessive fission events lead to augmented autophagy which precede muscle atrophy in denervated animals (Romanello *et al*, 2010), as demonstrated in old (35 months) denervated rats which show greater levels of autophagy-related machinery factors Atg7, p62 and Parkin (O'Leary *et al*, 2013). However, in non pathological aged muscles, autophagy proteins are downregulated, causing alteration in mitochondrial turnover. AMPK, a key player in autophagy, is mostly found diminished in its activation in elderly skeletal muscles. Specific muscle deletion of AMPK causes an increase in mitochondrial size along with a significant decline in mtDNA copy numbers. Together with these observations, accumulations of p62 and Parkin proteins were seen, thus indicating a link between AMPK and mitophagy in ageing muscle. In addition, the ratio of LC3B-II to LC3B-I was increased in old mutated mice (Bujak *et al*, 2015).

AMPK (5' AMP-activated protein kinase) is a focal factor in sensing energetic levels within the cell. It is a cellular kinase able to sense low ATP availability and mediate metabolic adaptations in response to energy stress. ATP depletion shifts the AMP/ATP ratio in favour of AMP that can now be able to bind effectively the γ-subunit of AMPK. This leads to an increase in phosphorylation at Thr-172 residue and subsequent augment in activity. Once activated, AMPK inhibits the anabolic pathways by blunting energy-consuming processes such as protein and lipid synthesis and, in parallel, it stimulates catabolism by switching on the energy-producing pathways such as glucose transport and lipid oxidation for the conservation/restoration of ATP. A growing body of evidence indicates that the activation of AMPK results in signalling events that promote an increase in protein degradation, associated with an increase in the expression of Atrogin-1 and MuRF1 via a FoxO-dependent mechanism. The increase in AMPK activity is triggered by the expression of pro-fission

proteins (Romanello *et al*, 2010), promoting mitochondrial fragmentation (prior to autophagy) through phosphorylation of a specific Drp1 receptor, which recruits high amounts of Drp1 on the mitochondrial surface (Herzig and Shaw, 2017). AMPK is moreover involved in mitochondrial homeostasis through direct stimulation of mitochondrial biogenesis, the opposite process to mitophagy, useful to re-establish a rich organelle network in response to increased energy expenditure. Highly induced by exercise, this process can be molecularly promoted by AMPK hyper activation, which in turn increases PGC1α expression (Garcia-Roves *et al*, 2008).

The peroxisome proliferator-activated receptor-γ coactivator 1α (PGC1α) is a regulatory transcription factor involved in the promotion of oxidative metabolism and master regulator of mitochondrial biogenesis and fitness. It is regulated by several post-translational modifications (among which AMPK-mediated phosphorylation and SIRT1 deacetylation, a NAD^+-dependent protein deacetylase enzyme whose activation can attenuate age-related metabolic disorders), and it modulates itself the activity of several nuclear transcription factors. Regarding external stimuli, exercise greatly stimulates PGC1α activation through its translocation from the cytosol to the nucleus and within mitochondria where it can modulate the expression of important genes necessary for the metabolic adaptations of skeletal muscle. This subcellular relocalization, furthermore, helps nuclear and mitochondrial crosstalk to promote mitochondrial biogenesis and regulation of the expression of mitochondrial proteins required for ATP synthesis. PGC1α is also involved in the regulation of skeletal muscle mass: its overexpression prevents transcription of FoxO3 and downstream degradative pathways via AMPK (Cannavino *et al*, 2015, Gill *et al*, 2019). With ageing a downregulation of PGC1α is visible and may also contribute to skeletal muscle atrophy and the destabilization of the NMJ (Gouspillou *et al*, 2013). On the contrary, its overexpression preserves NMJ structure in aged muscles (Wenz *et al*, 2009), therefore recognizing a prominent role in the maintenance of NMJ.

Regarding the beneficial effects on NMJ, it is well known that PGC1α is a transcription regulator of synaptic genes in an activity-dependent manner. Neuregulin-stimulated phosphorylation of PGC1α allows its recruitment and transcription of a broad neuromuscular junction gene program (Handschin *et al*, 2007). In a fascinating study about sarcopenia, a negative age-related correlation among mitochondrial energy metabolism proteins and neuromuscular junction proteins was visible through proteomic analyses of rats aged 6, 12, 18, 21, 24, and 27 months, where the sarcopenic profile was visible at the 21st month, with loss of muscle mass, depletion of mitochondrial functional

proteins, deterioration of NMJ-related pathways (as denervation phenomena and postsynaptic remodelling, Ibebunjo *et al*, 2013). Mitochondrial impairments show their detrimental effects at the NMJ starting from the axon, in which mitochondrial mass is significantly reduced and even lost in 35% of terminal axons in elderly post-mortem subjects, with a reduced mtDNA copy number and smaller cell bodies suggesting mitochondrial deficiency-driven atrophy (Rygiel *et al*, 2014). This could be causative of a lack of efficient reinnervation. In aged rats, it was demonstrated a morphological change in the majority of mitochondria at the axon terminal (but not detected in cell bodies), with swollen and larger conformations and ruined membranes (Garcia *et al*, 2013). A "dying back" phenomenon is thus visible in aged axons in which dysfunctional mitochondria, accumulated by an impaired fusion and thus forming fragmented dysfunctional organelles, promote apoptotic signals guided until the cell body, promoting thus nerve cell death.

Because of its involvement in the energetic metabolism of muscle fibers, mitochondria are responsible for the 85-90% of the oxygen consumption in humans, required for an efficient mitochondrial respiration and utilized thus in the final steps of the electron transport chain (ETC), relevant to be the main source of ATP in mammalian cells (Taylor, 2008). In all stages of the ETC, a small amount of the electrons that flow through the respiratory chain leaks prematurely and causes one-electron reduction of oxygen, producing a relatively stable free radical, the superoxide anion (O_2^-). This molecule is part of the so-called reactive oxygen species (ROS), physiologically produced by functional mitochondrial metabolism. Chemically, these oxygen-free radicals are molecules containing one or more unpaired electrons in atomic or molecular orbitals, which render them particularly reactive. In healthy conditions, mitochondria are able to keep the concentration of free radicals under control, through the balance between their rate of production and their neutralization mediated by a network of antioxidant mechanisms, in order to reduce any risk of oxidative damage. During exercise, for example, the production of ROS significantly increases due to higher energy demand and thus augmented ETC activity, but the preservation of cell homeostasis is promoted through neutralization of these and maintenance of a functional activity of the cell. During ageing, oxidative stress increases (Dobrowolny *et al*, 2021) and the uncontrolled levels of ROS can be attributable to lower expression/activity of antioxidant enzymes caused by reduced NRF2 redox sensor levels. In fact, inhibition of NRF2 leads to premature senescence (Matsumaru and Motohashi, 2021) and NRF2 deficiency in aged mice causes an exacerbated sarcopenic profile (decreased mitochondrial biogenesis and fusion dynamics, with less mitochondrial content, Huang *et al*, 2019; increased AMPK levels and ROS signals, causative of an excessive autophagy, Huang *et*

al, 2020). For these reasons, nowadays one of the main transgenic mouse models used for the study of sarcopenia are mice lacking the antioxidant enzyme Cu/Zn SOD ($Sod1^{-/-}$ mice). This transgenic line is characterized by a relatively shorten lifespan compared to wild-type littermates and lots of features resembling sarcopenia: decline in muscle mass and function, a reduced nerve conduction, decline in the number of motor units, partial denervation, degeneration of NMJs and increased muscle mitochondrial ROS generation accompanied by mitochondrial dysfunction (Deepa *et al*, 2017).

Another critical pattern through which ROS can be produced is caused by the uncoupling proteins (UCP) activity: it is known that under cachectic conditions (pathological muscle mass loss), UCP complexes augment in the mitochondrial membranes leading to the entry of uncoupled (not linked to the ETC) protons within the mitochondrial matrix, increasing thus H^+ concentration and the risk of reacting with oxygen to produce high levels of ROS (Riuzzi *et al*, 2018).

At the level of NMJ stability, age-related mitochondrial instability promotes high levels of ROS, which inevitably damage the presynaptic components and cross through the axon until the cell body, according to the "dying back" theory (Pollari *et al*, 2014). NMJ impairments were shown in UCP-1 overexpressing mice, in which an age-dependent deterioration of the junction was correlated with progressive denervation. Moreover, NMJ recovery was profoundly delayed following sciatic nerve injury, and mitochondrial uncoupling was highly exacerbated (Dupuis *et al*, 2009).

Notwithstanding, ROS are well recognized for playing a dual role since they can be either harmful (oxidative stress, Schicchitano *et al*, 2018) or beneficial (defence against infectious agents or promotors of signalling paths, Zhang *et al*, 2016) to living systems.

Altogether, these findings suggest a prominent role of mitochondria in NMJ detrimental outcomes during ageing, correlating those with sarcopenia, even if the pathways involved are very intricate and complex to extrapolate and clarify.

1.4 Age-related muscle mass maintenance pathways adaptation

Being defined as a resultant of loss of muscle mass and force, sarcopenia is characterized by impairments in molecular signals that are physiologically tightly regulated in order to maintain a functional cell homeostasis. Primary signals of ageing in muscle fibers are represented by muscle atrophy and concomitant shift of fibers towards a more oxidative phenotype. Then, an unbalanced

metabolism is often assessed, due to loss of equilibrium among anabolic and catabolic pathways which regulate the turnover of organelles or proteins/enzymes within the cell (Figure 4).

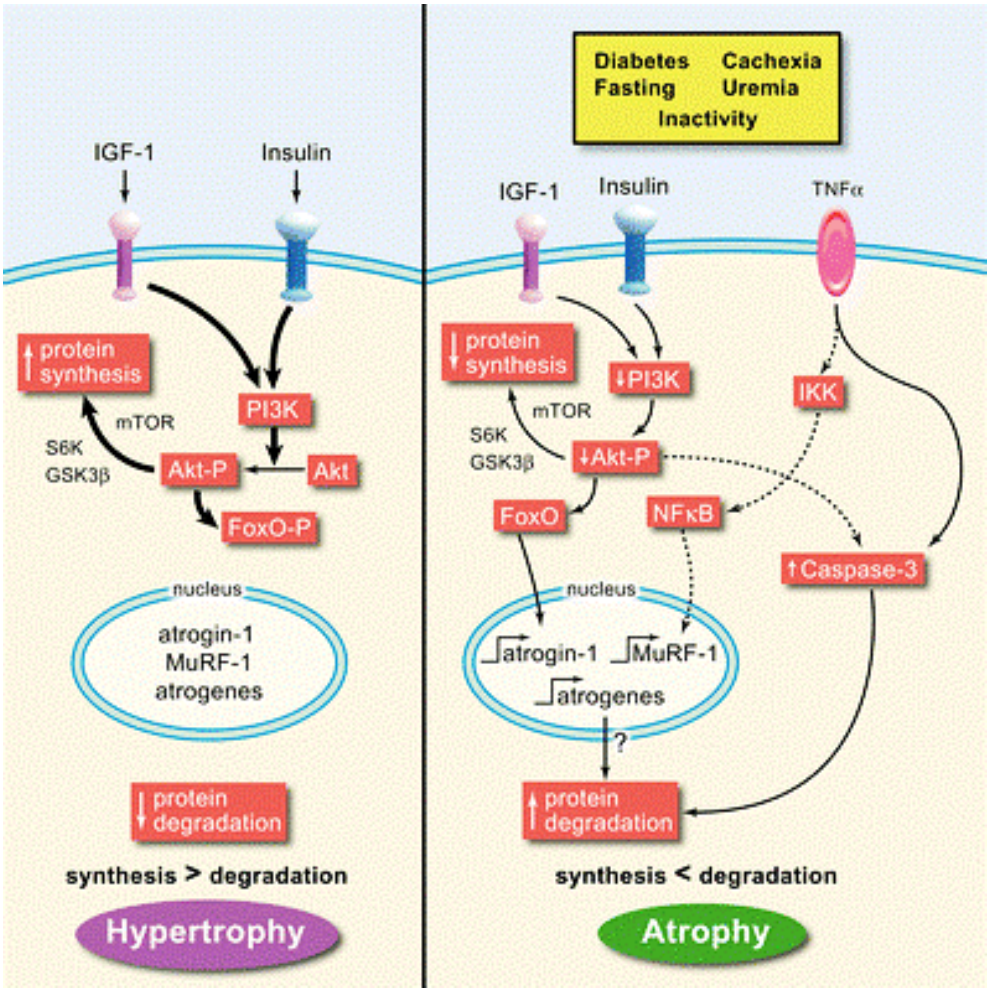

Figure 4. Schematic representation of molecular determinants of muscle protein synthesis (MPS) and breakdown (MPB). *The balance between muscle hypertrophy and atrophy depends on whether anabolism prevails on catabolism or vice versa. When anabolic pathways are elicited, insulin-like growth factor (IGF)-1 leads to increased phosphatidylinositol 3-kinase (PI3K), which promotes Akt phosphorylation and the activation of the downstream Akt/mTOR/S6 axis, leading to an increased protein synthesis. Akt also phosphorylates the forkhead (FoxO) transcription factor, preventing it from entering the nucleus to promote expression of atrogenes, thereby blocking protein degradation. When catabolism is promoted, the opposite pathway happens, but additionally, decreased Akt leads to increased caspase-3 activity, further promoting degradation. During inflammation, it is thought that tumour necrosis factor (TNF)-α and other inflammatory cytokines phosphorylate the inhibitor of nuclear factor (NF)-κB (IκB), to leave NF-κB free to enter the nucleus and promote MuRF-1 expression and, ultimately, muscle protein degradation. From Rajan and Mitch, 2008.*

Muscle protein synthesis (MPS) is formed by an intricate network of factors that either interact among each other to promote anabolic pathways and inhibit factors and molecules involved in muscle protein breakdown (MPB), and vice versa. The main actor that orchestrates these two opposite events is the protein kinase B (Akt). Upon activation through phosphorylation, it is involved

in a complex axis that leads to two different endpoints: through the insulin/IGF1/PI3K pathway, it is able to increase protein synthesis via activating the downstream mechanistic target of rapamycin complex 1 (mTORC1) signalling. Simultaneously, Akt blocks FoxO transcription factors via phosphorylation and subsequent reduction of protein degradation, in a general activation of a hypertrophic signalling within the muscle. mTORC1 is found in its inactive form on the cytoplasm, while once activated it is critically localized on the surface of lysosomes. Different downstream targets are under mTORC1 control: one of the effectors is the 70-kDa ribosomal protein S6 kinase (p70S6K), a kinase involved in the phosphorylation of the ribosomal protein S6 to promote transcription of a subset of genes involved in protein synthesis. The other mTORC1 effector is the eukaryotic initiation factor 4E binding protein (4E-BP1). This protein binds and inactivates the eukaryotic translation initiation factor eIF4E; once 4E-BP1 is phosphorylated by mTORC1, it dissociates from eIF4E which is now able to start the translation process.

mTOR is becoming a focal factor for the NMJ maintenance (Castets *et al*, 2020). Even if it is not locally found in proximity of the NMJ, some direct targets are, like 4E-BP1 and S6 kinases. mTORC1 activity is also strongly regulated by innervation status, with experimental denervation potently stimulating mTORC1 activity in fast-type mouse skeletal muscle fibers, and highly expressed following prolonged denervation (Tintignac *et al*, 2015). Muscle-specific mTOR deficient (mTORmKO) mice show a prominent denervation profile, while Raptor depletion (a regulator of mTOR stability) increases again the proportion of denervated fibers and the fragmentation of the motor endplate (Baraldo *et al*, 2020).

During ageing, the anabolic pathway is generally downregulated (Kim and Hwang, 2020) compared to young mice, and a parallel increase in proteolytic pathways decree muscle atrophy and loss of force. However, in a captivating longitudinal study in which rat muscles were evaluated in their mass and protein synthesis patterns, from 1 to 24 months, a significant decrease in muscle mass was not accompanied by a decrease in protein synthesis factor, but on the contrary eIF2B activity, relative eIF2 expression, and S6K1 phosphorylation all increased, speculating a model wherein protein synthesis is enhanced during ageing in a futile attempt to maintain muscle mass (Kimball *et al*, 2004, Joseph *et al*, 2019). Similarly, Sandri and colleagues demonstrated in old humans and mice that the IGF1/Akt pathway is not downregulated during ageing, and neither FoxO and proteolytic systems were upregulated (Sandri *et al*, 2013). Only the increased phosphorylation of the ribosomal protein S6, indicative of increased activation of mTORC1, was found in aged mice. But either overexpression

of Akt and inactivation of Atrogin-1 (proteolytic factor) separately are causative of muscle pathology and a reduced lifespan. Studies and observations in elderly humans moreover focus on the decrease in habitual physical activity and protein ingestion as causes for a decreased protein synthesis, which can induce anabolic resistance phenomena due to lower substrate presence. Recovery from immobilization (bed-rest) followed by essential amino acid ingestion results in muscle mass loss due to a highly blunted anabolic machinery in elderly subjects compared to young (Tanner *et al*, 2015), even assessed after exercise training (Francaux *et al*, 2016). Other authors by the way speculate about no variations in the protein synthesis rate in elderly versus young subjects (Volpi *et al*, 2001).

Another factor which decreases during ageing is the circulating IGF1, due to an increased insulin resistance occurring over the years (Huffman *et al*, 2016). IGF1 triggers the activation of the IGF1/Akt/mTOR pathway so any decrease in its concentration can interfere with the correct activation of this anabolic axis. So in conclusion, the study and framing of specific trends in the anabolic pathway during ageing seems complicated and does not return a plain pattern of events which can be indicative of muscle mass loss. Surely, an impairment at different levels of these signalling molecules occurs, in parallel with changes in proteolytic pathways (Anisimova *et al*, 2018).

A correct protein synthesis is always matched with functional protein folding, promoted by a family of enzymes (chaperones) recruited in normal conditions but highly enhanced under stress conditions (oxidative stress and cellular damage). Misfolded and/or non-functional proteins physiologically undergo rapid degradation to prevent the accumulation of damaged molecules within cells that could then hinder the proper functioning of the fibers, and replace those with newly synthesized proteins. But when the cell undergoes stress, it can happen that these scavenging pathways are nomore efficient to counteract the accumulation of damaged residues within the cell, leading to reduced health of the cell and activation of stress-driven mechanisms that can lead to massive atrophy and eventually apoptosis. Among the proteolytic pathways activated within the cell, a major role is covered by the ubiquitin-proteasome system (UPS).

UPS accomplishes selective protein degradation via labeling of a specific substrate with a polyubiquitin chain, which can then be quickly ferried to the 26S proteasome. The proteasome is an ATP-dependent protease complex formed by a macromolecular scaffold of different protein subunits: a catalytic core known as 20S proteasome is organized in a way to create a pore in which proteolytic enzymes are exposed within. Two regulatory caps, the so-called 19S regulatory particles, are associated in both extremities of the main structure and serve as recognition and attachment

site for polyubiquitinated proteins. Once degraded, reusable ubiquitin monomers are released. Three enzymes cooperate in the primary polyubiquitination step in a series of catalytic reactions mediated by the E1 (ubiquitin activating), E2 (ubiquitin conjugating), and E3 (ubiquitin ligase) enzymes. E2-E3 complex is the catalytically active ubiquitin ligase that shows specific substrate recognition function. Once the first ubiquitin is transferred into residue Lys-48 of the target protein, a covalent tandem linkage of additional ubiquitin molecules occurs in order to deliver the selected protein to the proteasome.

Many catabolic conditions correspond to an increase in the expression of a number of E3 ligases, some of which broadly exist in different cell types and others exclusively expressed into the skeletal muscle. Two muscle-specific E3 ubiquitin ligases that are part of the atrogenes family controlled by FoxO transcription factor, namely Muscle RING Finger 1 (MuRF1) and Muscle Atrophy F-box (MAFbx)/Atrogin-1, are studied in their expression levels during various states of muscle catabolism and atrophy (Bodine and Baehr, 2014). In its Akt-dependent phosphorylated state, FoxO remains confined to the cytosol but in the absence of the active Akt, FoxO translocates to the nucleus where it can exert transcription of atrogenes necessary for the production of ubiquitin ligases, and its activation is sufficient to increase protein degradation and promote net protein loss. It is good to know that muscle Akt phosphorylation could be reduced during short-term energy deficit, fasting and ageing, with a concomitant reduction in muscle protein synthesis, which likely activates FoxO and thus upregulates Atrogin-1 and MuRF1. In atrophying muscles, the ubiquitin-proteasome system is found widely increased and controls the half-life of sarcomeric proteins: the selective inhibition of proteasomal-dependent degradation has been described to reduce muscle atrophy (Sandri M, 2010). Moreover, knockout mice lacking Atrogin-1 and MuRF1 are largely resistant to muscle atrophy induced by denervation (Sandri *et al*, 2013). Conversely, a study evaluating Atrogin-1 and MuRF1 expression in old mice identified no age-related differences in mRNA expression of the two atrogenes (Gaugler *et al*, 2011). The same situation was found in elderly human subjects, where levels of E3 ubiquitin ligases did not show any change (Gumucio *et al*, 2013). In conclusion, even in this case as for the anabolic pathway, it is difficult to outline a trend in the expression of Atrogin-1 and MuRF1 in older subjects, even if the UPS is found strictly correlated with atrophic outcomes.

Another catabolic mechanism within the cell, that promotes clearance and functional maintenance of the cells, is represented by the autophagic flux, previously explained as regards of the

mitochondria (going through mitophagy). This process of organelles' clearance is highly conserved through the species and allows the removal of all damaged/dysfunctional organelles or protein complexes interspersed in the cytoplasm. An impaired autophagic system causes the accumulation of abnormal organelles and toxic proteins that lead to myofiber degeneration, with the outcome of atrophy. Of course, at the level of the NMJ, an altered age-related autophagic flux leads to accumulation of damaged elements which hamper the normal function of the synapse (Carnio *et al*, 2014, Khan *et al*, 2014).

Taken together, all these pathways physiologically involved in the maintenance of the cellular homeostasis show a dynamic equilibrium among opposite pathways which crosstalk among each other, in an intricate and complex network, sometimes difficult to clarify. Ageing and age-related sarcopenia are generally promoters of an impairment in these patterns, and the degree of involvement of one or more signalling pathways is certainly influenced by multiple factors. Up to now, being such multifactorial and variegate in severity and symptoms, there is no specific pharmacological treatment available for sarcopenia. The most successful therapeutic intervention to mitigate or slow down age-related sarcopenia is based on lifestyle adaptations. They basically include beneficial changes in caloric intake and dietary regimen combined with physical exercise based on aerobic training (recently reviewed in Pascual-Fernandez *et al*, 2020).

2. NITRATES

In the last few decades, the literature has shown a consistent growing interest regarding the metabolism of NO (nitric oxide) and its effects, especially within the skeletal muscle tissue. Being a widespread signalling molecule, it has been widely studied for its role as a novel messenger of biological processes, ranging from vascular control to tissue inflammation and mitochondrial metabolism.

NO and its derivatives could be endogenously synthesized by following two different pathways: the enzymatic and non-enzymatic pathway. The latter path involves production of NO from nitrite via multiple pathways, particularly under acidic conditions and mainly occurs in tissues (Zweier *et al*, 1995). The former pathway occurs within cells of our organism through specialized enzymes called nitric oxide synthases (NOSs, Figure 5).

2.1 Endogenous synthesis of NO

Substrates of these enzymes are body proteins stored in our organism or amino acids supplemented by the diet. Their catalytic activity is based on the oxidation of the guanidinium nitrogen residue of the amino acid L-arginine which is converted to L-citrulline. This reaction releases reactive NO as a free radical (Wu and Morris, 1998) which thus can give birth to a variety of NO-related molecules including S-nitrosothiol (SNOs), metal NO complexes and higher oxides of nitrogen (NO_x), including peroxynitrite ($ONOO^-$) and nitrogen dioxide (NO_2).

Three NOS isoforms are known, resulting from the encoding of three different genes and named after the cells or systems from which they were originally discovered and are thus designated neuronal (n)NOS (NOS1), Ca^{2+}/calmodulin-independent or “inducible” (i)NOS (NOS2), and endothelial (e)NOS (NOS3). They share a similar structure with about 60% of sequence identity and are only active as dimers. A very complete and exhaustive review from 2001 describes the expression of NOSs relative to different species and diverse muscles that compose the body (Stamler and Meissner, 2001). A fourth isoform, namely mitochondrial NOS (mtNOS) has been recently demonstrated to be expressed at the inner membrane of mitochondria, but debate on this is still open (Carreras *et al*, 2007).

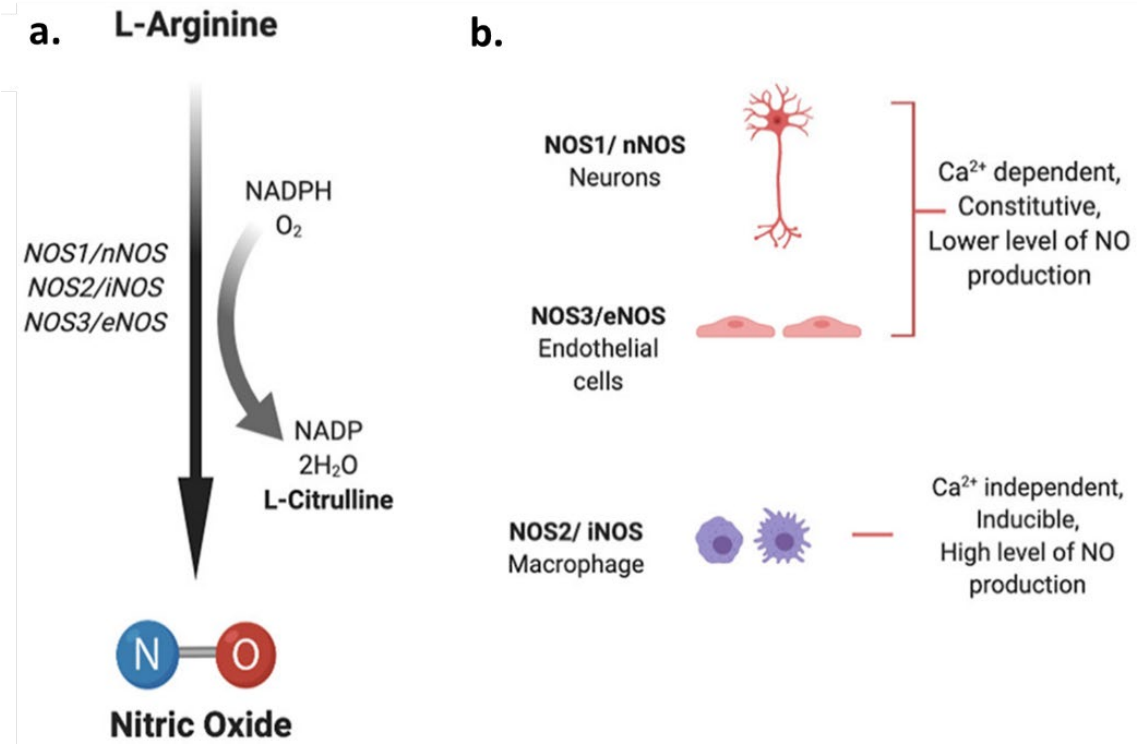

Figure 5. Nitric oxide synthesis and endogenous enzymes involved. *a) Synthesis of nitric oxide. b) Nitric oxide synthase (NOS) isoforms: neuronal (NOS1/nNOS), inducible (NOS2/iNOS), and endothelial (NOS3/eNOS) isoforms catalyse the process of NO generation in the presence of cofactors via oxidation of L-arginine to L-citrulline. From Mishra et al, 2020.*

nNOS and eNOS are constitutively expressed within the muscle fiber and are regulated by intracellular Ca^{2+}/calmodulin interaction, while the inducible isoform is not sensitive to these factors but seems to be transcriptionally controlled following inflammatory responses. Their activity is maintained at low rates under resting conditions while functional stimuli and the activity of the muscle promote an increase in NO production, as demonstrated by different research groups when performing *in vivo* electrical stimulation of Tibialis Anterior and EDL muscles of rabbits (Reiser *et al*, 1997) or *in vitro* cyclic stretching of myotubes (Tidball *et al*, 1998), assessing nNOS activity. In addition to previous regulations, all of the isoforms are regulated by post-translational modifications which determine their activity. They are even regulated by cytokines and sensitive to hypoxia. NO covers a fundamental role in cellular oxygen sensing at the cellular and systematic level, participating in O_2 homeostasis and modulating the hypoxia-inducible factor (HIF-1α), notoriously involved in the promotion of cellular survival under conditions of impaired oxygen supply. One of the pathways through which NO regulates its stability is its S-nitrosylation. On the other hand, O_2 homeostasis maintained by NO activity is itself a key player in NO synthesis, modulating the enzymatic activity of NOSs (Jeffrey Man *et al*, 2014).

nNOS is ubiquitously expressed, with its main expression in central and peripheral neurons. In 1996, Silvagno and colleagues showed that alternative splicing returns a functional enzyme containing a 34-amino acid insertion in mature skeletal muscle and heart, namely nNOS-mu. The structural arrangement in its N-term domain allows the formation of the functional PDZ domain, act to the interaction with the dystrophin complex through spectrin-like repeats 16 and 17 (R16/17) and the α1-syntrophin PDZ domain (Patel *et al*, 2018) and with postsynaptic density proteins (PSD93 and PSD95, Murciano-Calles *et al*, 2020) at the level of synaptic membranes. Syntrophins are even directly involved in the colocalization of utrophin and nNOS-mu at the level of the neuromuscular junction (NMJ), being a key component of the dystrophin protein complex scaffold that functions to stabilize AChR clusters (Adams *et al*, 2010). Absence of α1-syntrophin at the postsynaptic scaffold results in structurally aberrant NMJs with reduced levels of AChR clustered at the motor end plate, in favour of a spatial misallocation in small spikes, and a missing nNOS-mu expression on the sarcolemma and NMJ, although still present in the cytosol. Under pathological conditions (i.e. dystrophies such as the Duchenne Muscular Dystrophy, DMD), the absence of dystrophin causes loss of nNOS at the level of NMJ and in general in the sarcolemma, resulting in decreased activity. The subsequent decrease in endogenous NO production results detrimental to diseased muscles due to NO involvement in muscle metabolism, function and mass (enucleated later), blood flow and glycolytic rate. The latter one occurs through the interaction of nNOS with phosphofructokinase (PFK), a regulatory enzyme of glycolysis, which is down-activated in dystrophic mice, explaining muscle fatigability and glycolytic impairments (Timpani *et al*, 2017).

In rodents, nNOS immunostaining experiments supported by biochemical approaches demonstrate a higher NOS activity in muscles enriched in type II (EDL, Gastrocnemius and Plantaris) than type I (Soleus) fibers (Kobzik *et al*, 1994), while in humans this distinction is not so evident, meaning that nNOS expression is about equal in the two types of fibers. However, nNOS location at the NMJs was not related to skeletal muscle fiber type, as experiments demonstrate nNOS activity highly present in either rat EDL and Soleus end plates (Kusner and Kaminski, 1996). It covers a wide range of functions, including synaptic plasticity in the central nervous system (CNS), central regulation of blood pressure, smooth muscle relaxation, and vasodilatation. Its expression is increased by injuries, muscle activity and chronic exercise whereas it decreases during ageing due to denervation. Denervation of rat sciatic nerve decreases nNOS and iNOS reactivity after 15 days, with a complete loss after 30 days from denervation (Tews *et al*, 1997). Modulatory effects of nNOS are then

promoted by post-translational modifications such as phosphorylation at Ser-847 (with an inhibitory effect) and 1412 (which promotes its activity, Rameau *et al*, 2007).

iNOS transcripts are found at very low levels in rodents' skeletal muscles and its activity varies depending on disease state and the species investigated. As nNOS, it was reported that iNOS coimmunoprecipitates with the sarcolemmal caveolae membrane protein caveolin-3 (Gath *et al*, 1999), a muscle-specific member of the caveolin family, thus giving a further proof of their sarcolemmal localization. Caveolin-3 is also expressed at the neuromuscular junction (Carlson *et al*, 2003) and it was reported to be involved in the clustering and thus the activity of the AChRs (Hezel *et al*, 2010). It has been found highly increased in skeletal muscle cells of patients with chronic heart failure but it is more generally expressed in response to autoimmune inflammation and high inflammatory cytokines persistence, contributing to the pathophysiology of inflammatory diseases (Zamora *et al*, 2000).

eNOS expression is widely found in endothelial cells of vessels and microvessels, but it was demonstrated a muscular localization due to its interaction with the caveolae structural protein Caveolin-1. Found at very low expression levels in muscles, immunolocalization studies showed its colocalization with mitochondrial markers in a subset of fibers within muscles of different phenotypes (Kobzik *et al*, 1995). It exerts its activity following dimerization, as a resultant of a kinase activity that phosphorylates Ser-1177. It is involved in the maintenance of blood vessels dilatation, control of blood pressure and other vasoprotective effects. It is upregulated by chronic exercise due to continuous stimulation of the contractile apparatus.

Skeletal muscle is highly enriched with NOSs enzymes and given the fact that muscle is recognized as an amino acid reservoir in the body, the high availability of arginine is a thriving substrate for NOS activity and therefore production of NO. Their activity depends on age and developmental stage, innervation, muscle contractility and fiber composition, cytokines interaction and exposure to growth factors. Moreover, the fact that their localization is mostly confined and anchored to the NMJ architectural scaffold, depicts their functionality as strictly activity-dependent, producing so NO as a signalling molecule under functional stimuli at basal low concentrations.

2.2 Exogenous uptake of NO

NO and its derivatives may also be supplemented exogenously through a targeted nitrate dietary, a growing field of interest as a sports nutrition supplement. Inorganic nitrate is abundant in green

leafy vegetables and roots such as lettuce, spinach, rocket, celery, cress, and beetroot, which typically contain over 250 mg (>4 mmol) of nitrate per 100 g fresh weight (Lundberg *et al*, 2009). Nitrate from the diet is rapidly assimilated into the plasma following the bloodstream and rapidly expelled. Only a small percentage (about 25%) of nitrate in circulation is actively taken up by the salivary glands, leading to a significant increase in its concentration in the saliva. Subsequently, commensal facultative anaerobic bacteria located at the dorsal surface of the tongue catalyse nitrate to nitrite by the activity of nitrate reductase enzymes (Govoni *et al*, 2008). These bacteria use nitrate and nitrite as final electron acceptors in their respiration and meanwhile help the host to convert nitrate to NO as the first step (NO_3^--NO_2^--NO pathway). Because of the arising interest on this pathway, a lot of studies are now focusing on the effects of mouthwash formulations and their outcomes in the processing of nitrate/nitrite in the oral cavity (Woessner *et al*, 2016). Part of the processed nitrite is reduced to NO in the acidic environment of the stomach, but a substantial portion of it enters the systemic circulation, elevating the plasma nitrite concentration. Following bolus nitrate ingestion, plasma nitrate concentration peaks after 1-2 hours and plasma nitrite concentration peaks after 2-3 hours, after which both gradually fall, arriving back at baseline values after about 24 hours (Webb *et al*, 2008). A variety of enzymes and proteins can subsequently catalyse the one-electron reduction of nitrite to NO in blood and other tissues. This process is facilitated under low oxygen availability conditions (ischemia and hypoxia) and low pH, enabling NO to be produced where it is most required, due to the fact that NOS activity is oxygen dependent and thus may decrease in its functionality. Interestingly, these conditions (low partial pressure oxygen and pH) may exist in skeletal muscle during exercise (Lemieux and Birot, 2021).

In rodents and in humans, skeletal muscle serves as a nitrate reservoir with nitrate levels greatly exceeding those in blood or other internal organs, augmented more by dietary nitrate ingestion. Following the same baseline nitrate diet, some muscle groups store nitrates at concentrations higher than the blood (as for example Gluteus, Soleus and Gastrocnemius) and some do not (as EDL and TA), as widely demonstrated in rat skeletal muscles (Park *et al*, 2021). This difference in nitrate concentration could depend either by different request and local consumption and by different expression of proteins involved in its transport. During high-intensity exercise, nitrate levels decrease due to its functional demand, only when there is a high concentration stored (Wylie *et al*, 2019). This could be explained by the demonstration that muscle cells do not only have elevated activity rates of NOSs, but they also own a molecular apparatus for the transport, storage and

metabolism of nitrate. It has been recently demonstrated by Srihirun and colleagues that skeletal muscle fibres themselves possess an intracellular NO_3^--NO_2^--NO pathway (Figure 6).

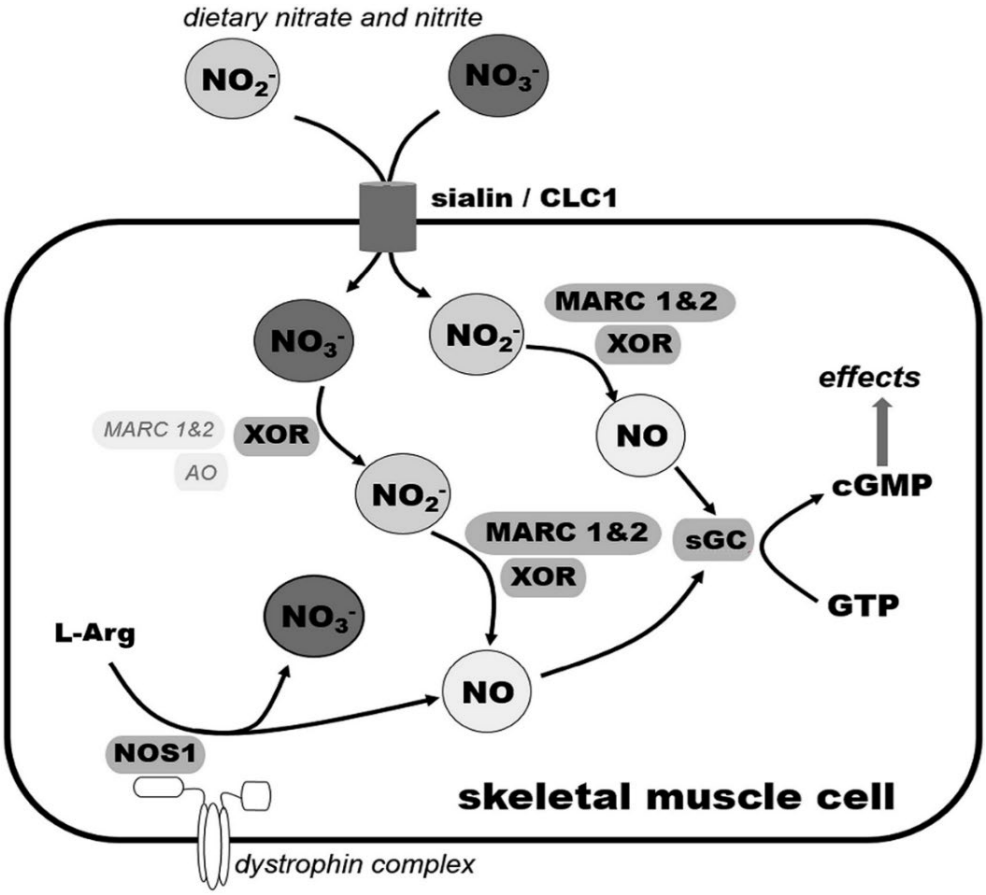

Figure 6. Schematic representation of NO_3^--NO_2^--NO pathway in human skeletal muscle cells. *Different enzymes are recruited for the transport and metabolism of dietary nitrate/nitrite in the muscle fiber. From Srihirun et al, 2020.*

Experimental setups on cultured cells show increased uptake of exogenous nitrates following supplementation in both myoblasts and myotubes but increased nitrite levels only in myotubes. This was explained by the increased expression of factors (the molybdenum-containing proteins and nitrate and nitrite reductases) following the differentiation of myoblasts into myotubes. These factors include the mitochondrial amidoxime-reducing component (MARC1 and 2), aldehyde oxidase (AO) and among all the xanthine oxidoreductase (XOR). All these reductases have been demonstrated to work at high rates when environmental pH is lower than the physiological pH 7.4, markedly demonstrated following an exhaustive severe intensity exercise protocol, where muscle pH falls to 6.6 – 6.8 (Gilliard *et al*, 2018). Transporters responsible for NO_3^- uptake into the skeletal muscle were identified in Sialin (SLC17A5) and chloride channel 1 (CLC-1): an intriguing experiment demonstrates how Sialin knockdown decreases nitrate uptake and hence nitrate concentration within the myoblasts. Sialin, together with XOR, have been demonstrated to be major players on

NO homeostasis due to an increase in their protein levels as a compensatory mechanism in mice lacking other proteins involved in nitrates' muscle metabolism (in eNOS-deficient mice, Peleli *et al*, 2016; in myoglobin-deficient mice, Park *et al*, 2019).

Sialin receptor is a well-known sialic acid (SA)/H^+ cotransporter which is more generally identified as an anion transporter, primarily identified in tissues as liver and salivary glands. Due to its structural nature, several anions that could interact with the receptor were investigated: chloride (Cl^-) was the less interactive, while glutamate (Glu) and aspartate (Asp) displayed a higher membrane current in human salivary gland (HSG) tested cells at pH 4. Nevertheless, NO_3^- among all has shown a particular affinity with this receptor in a pH-dependent manner (lower pH displays higher membrane current), even if transporting anions represents itself an intracellular acidification of the environment (Qin *et al*, 2012).

2.3 Bioactivity of NO and metabolic pathways

Nitric oxide, as the smallest gaseous signalling molecule known, functions as a messenger molecule affecting numerous cellular processes through different molecular targets in different body districts. It has a short half-life (0.1-2.0 seconds) but its highly diffusible property allows to reach other cells and tissues in a short period of time (Thomas DD, 2015). Being a very reactive molecule, NO is present in low nanomolar concentrations and it is likely to be "made on demand" rather than stored, and rapidly converted into less reactive species (i.e. nitrate) upon storage. The activity of nitric oxide is mainly occurring through the activation of the soluble NO-sensitive guanylate cyclase (sGC) and increased formation of cyclic guanosine monophosphate (cGMP), which activates cGMP-dependent protein kinases. This NO–sGC–cGMP signalling pathway mediates many of the favourable effects that NO bioactivity systemically promotes, on cardiovascular, kidney and metabolic functions (schematized in Figure 7).

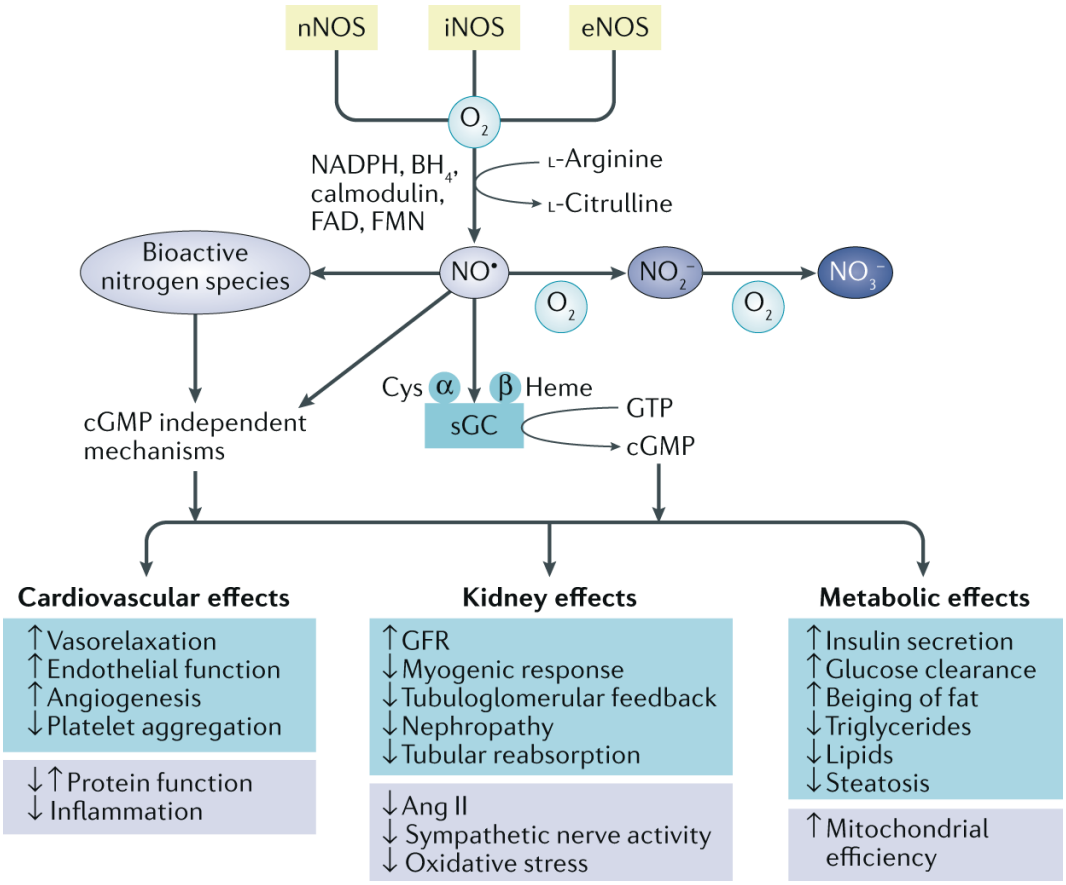

Figure 7. Nitric oxide biosynthesis, metabolism and bioactivity in the body system. *Representative flow-chart resuming the systemic effects that are occurring in different compartments, in a cGMP-dependent pathway, although cGMP-independent mechanisms have also been reported (Carlström M, 2021).*

One of the major roles NO covers in the body function is the control of vascular tone and blood flow through the NO-dependent sGC-cGMP axis. The cGMP activates protein kinase G which leads to a cascade of signalling events leading to the activation of the myosin light-chain phosphatase (MLCP). This inhibitory modification eventually dephosphorylates myosin light chain and, along with a reduced intracellular Ca^{2+} levels, results in the relaxation of the smooth muscles and thus vasodilation (MacDonald and Walsh, 2018). This phenomenon is reversed by calcium release in the cytoplasm from the sarcoplasmic reticulum with concomitant activation of Ca^{2+}/Calmodulin, a positive regulator of myosin light-chain kinase (MLCK), involved in phosphorylation of MLC and thus its activation and muscle contraction. The activity of cGMP is then rapidly terminated by phosphodiesterase 5 (PDE5), which hydrolyses active cGMP to inactive 5'-GMP.

It covers an important task at the level of the brain by regulating the local blood flow and can be released postsinaptically as a retrograde neurotransmitter. It diffuses across the synaptic cleft up to the presynaptic nerve terminal, where it improves the release of the neurotransmitter glutamate

through the sGC-cGMP axis. This event is mainly associated to N-methyl-D-aspartate receptor (NMDAR) activation, involved in the physiological mechanism of learning and memory (Picon-Pages *et al*, 2019).

NO regulates gene transcription and mRNA translation (by binding to iron-responsive elements) and produces post-translational modifications of proteins which can modulate their activity (for example histone post-translational modifications, S-nitrosylation of cysteine residues, ADP ribosylation of proteins, Mengel *et al*, 2013). The control of NO on protein translation is exerted through direct regulation of factors involved in protein synthesis. The mTOR (mammalian target of rapamycin) signalling pathway controls the anabolic metabolism by phosphorylating two downstream proteins: the eukaryotic initial factor 4E-binding protein 1 (4E-BP1) and the ribosomal p70S6 kinase 1 (p70S6K). *In vitro* experiments demonstrate that dietary supplementation of L-Arg was protective against muscle wasting by increasing protein synthesis in an mTOR-dependent manner: both mTOR phosphorylation at Thr-2446 and p70S6K at Thr-389 increase in their levels following NO-donor supplementation in cell culture, and this effect was counteracted by L-NAME inhibitory effect on NOS activity (Wang *et al*, 2018).

In addition to the improved synthetic pathway, nitric oxide acts as a signalling molecule to preserve mass and protect the muscles from excessive proteolysis. In stressing conditions, cytosolic calcium levels are increasing (i.e. during ageing), leading to the activation of Ca^{2+}-dependent enzymes, including calpains. This family of proteases are involved in the cleavage of substrates at specific sites, so as to target the resultant small fragments to the ubiquitin/proteasome system. Their activity is controlled by different factors as calpastatin, which decreases during ageing promoting proteolysis of myofibrillar components and thus muscle weakness (Schroder *et al*, 2021). Moreover, ageing displays a decrease in NO content and its synthesis by lower NOS enzyme levels and thus loss of S-nitrosylation, which decrees an increase in calpain-mediated myofibril degradation (Samengo *et al*, 2012). NO, which covalently binds and modifies calpain through S-nitrosylation, is able to prevent its excessive activity.

Another relevant role nitric oxide promotes within the cells is through a beneficial modulation of the mitochondrial metabolism, operating on various patterns. A NO-dependent cGMP activity directly stimulates mitochondrial biogenesis by the activation of PGC1α (Nisoli *et al*, 2003), a key transcription factor in mitochondrial biogenesis and general muscle metabolism. It has been demonstrated in L6 myotubes that cultured cells treated with NO-donors were able to induce

biogenesis of functional mitochondria through elevated AMPKα phosphorylation that cooperates with NO to upregulate PGC1α mRNA and protein levels (Lira *et al*, 2010). AMPKα moreover exerts its kinase activity on both endothelial and neuronal NOS, promoting their activation (Chen *et al*, 2000) and thus regulating NO production. Another pathway through which NO stimulates mitochondrial biogenesis is represented by the sGC/cGMP-dependent activation of PKA (cyclic AMP-dependent protein kinase) that promotes the phosphorylation of CREB1 (cAMP response element-binding protein 1). This one, together with its coactivator TORC1 (transducer of regulated CREB binding protein 1, a well-known potent activator of PGC1α transcription) fosters increased mRNA levels of PGC1α and mitochondrial mass markers in primary mouse skeletal muscle cultures (Tengan *et al*, 2012, Piantadosi and Suliman, 2012).

It is well established that SIRT1, a deacetylase member of the sirtuins family, is involved in mitochondrial biogenesis by means of its deacetylation-activating modification on factors previously mentioned (PGC1α, AMPK and CREB1). Nisoli and colleagues demonstrated that SIRT1 expression is regulated by NO. Treatments with NO donors augment SIRT1 and cGMP expression in cultured cells, while suppression of eNOS contrasts its increment, speculating that SIRT1 undergoes NOS-derived NO expression (Nisoli *et al*, 2005). On the other hand, a feedback mechanism exists in this reaction chain, by the regulatory activity of SIRT1 on eNOS due to deacetylation of Lys-496 and 506, involved in the calmodulin-binding domain of eNOS and thus its functional activation (Mattagajasingh *et al*, 2007).

cGMP was even found responsible to promote AMPKα activation, which inhibits acetyl-coenzyme A (CoA) carboxylase (ACC), a notorious regulator of the metabolism of fatty acids (FA). When in its active form, ACC catalyses the irreversible carboxylation of acetyl-CoA to produce malonyl-CoA, a building block for new fatty acid synthesis but on the other hand an inhibitor of the catabolic β-oxidation of FA in the mitochondria (Glund *et al*, 2012). The positive regulation of AMPK driven by nitric oxide promotes thus the FA oxidation within the mitochondria, by mediating the expression of PPARβ/δ and PPARα transcript regulation on the induction of FA oxidation enzymes (Ashmore *et al*, 2015). Moreover, following NO-donor supplementation in L6 myotubes, mRNA levels of GLUT-4 significantly increase through the cGMP-dependent AMPK activation, an effect completely ablated by cotreatment with AMPK inhibitor. Selective inhibition of nNOS hence confirms a reduction in GLUT-4 expression demonstrating the major importance of NO and its role in the activation of cGMP

and AMPK to enhance GLUT-4 expression (Lira *et al*, 2007). An increase in GLUT-4 translocation (the major glucose transporter in muscles) contributes to a better glucose uptake.

Nitric oxide not merely acts on various metabolic parameters linked to the mitochondrial biogenesis and metabolism: functional improvements at the level of the mitochondrial respiratory chain were demonstrated. Low concentrations of NO reversibly inhibit the Cytochrome c oxidase (COX) (Sarti *et al*, 2012), thus decreasing its "slippage" phenomenon. Slippage is an uncoupling process that depends mainly on flux and contributes to a reduction in the biochemical coupling efficiency of ATP production, so by the reduction of this phenomenon, ATP synthesis capacity is maximised from the proton pumps activities and a beneficial reduction in energy waste occurs (Clerc *et al*, 2007). A study based on nitrate supplementation on healthy humans showed the decrease in expression of adenine nucleotide translocase (ANT), a protein involved in mitochondrial proton conductance. This event reduces leak respiration and improves the efficiency of oxidative phosphorylation. The amount of oxygen consumed per ATP produced (mitochondrial P/O ratio) was ameliorated following nitrate supplementation, demonstrating a reduction in proton leakage across the inner mitochondrial membrane (Larsen *et al*, 2011). Another study on healthy males demonstrates that nitrate supplementation reduces the ATP cost of muscle force production, an index of the coupling between ATP hydrolysis and muscle force production. A decreased ATP hydrolysis is indicative of a reduced muscle ATP turnover requirement, demonstrated by a reduced phosphocreatine (PCr) catalysis in treated subjects. This was explained by a NO-mediated inhibitory effect on Ca^{2+} cycling proteins (Ca^{2+} handling pumps in the sarcoplasmic reticulum, Ca^{2+}-ATPase, SERCA) which then consume less ATP, ending up with an improved tolerance to high-intensity exercise (Bailey *et al*, 2010).

However, some experimental observations demonstrated mild or even plain effects on the efficiency of mitochondrial respiration following inorganic nitrate supplementation either in mice and humans, in which no altered mitochondrial coupling efficiency (the relationship between mitochondrial respiration and ATP generation) was seen, together with unchanged expression of mitochondrial proteins involved in proton leak and uncoupling (Ntessalen *et al*, 2020).

An improved functional efficiency promoted by NO is not only confined to the mitochondrial respiration, but even at the level of muscle contraction and functionality. *In vitro* studies on isolated diaphragms of 24-months old mice supplemented with 1mM $NaNO_3$ for 14 days demonstrated a significant increase in contractile properties (i.e. the peak power and the maximal rate of isometric force development) that were independent by the phosphorylation rate of key myofibrillar proteins

and the amount of calcium handling proteins (Kumar *et al*, 2020). The diaphragm is mainly composed of fast-twitch fibers, even if with ageing a shift of type IIx/IIb fibers occurs in favour of type IIa (intermediate oxidative) fibers (Greising *et al*, 2013). Nitrate effects on skeletal muscle are more pronounced in fast-twitch fibers, due to a lower oxygen pressure that promotes nitrate and nitrite reduction and thus the promotion of its metabolism, so this is the main reason a functional effect of supplementation is seen in this muscle (Hernandez *et al*, 2012). But it is still uncertain the mechanism through which nitrates enhance diaphragm contraction. Moreover, 8-weeks supplementation of 0.6 mM $NaNO_3$ in old mice (20-24-months old) has been shown to attenuate the decline in motor function (through grip strength and rota-rod endurance tests) compared to untreated old animals, and this ameliorated physical profile was accompanied by a reduction of inflammatory cytokines, markedly increased in elderly animals, which return to young reference levels after treatment, establishing a positive correlation between motor function and inflammation rate (Justice *et al*, 2015).

Macroscopically, muscle function and so exercise tolerance has been demonstrated to ameliorate following nitrate supplementation in chronic heart failure (CHF) patients. NO supplementation lowers the systemic vascular resistance (as molecularly mentioned previously) and thus elevates the O_2 delivery in the skeletal muscles. The resultant microvascular coupling between oxygen delivery and utilization in this highly demanded tissue is thus essential to support faster rates of oxidative phosphorylation at the level of mitochondria (Hirai *et al*, 2015). The beneficial effects of NO on exercise tolerance will be further discussed in *Chapter 2.5*.

Motor function was even evaluated regarding NMJ stability and the activity nitric oxide has on it. As mentioned before, nNOS is widely enriched at the level of the postsynaptic side through α1-syntrophin and the dystrophin-glycoprotein complex (DGC), contributing in its stability. Loss of expression of any of these DGC members leads to a reduction of NOS from the sarcolemma and defects in NMJ structure. Studies based on *mdx* mice (dystrophic mouse model, in which NOS localization and activity is lost) subjected to NOS implementation show important reduction in NMJ structure defects, with a major increase in the concentration of AChRα subunit and AChR density compared to normal *mdx* mice. However, NOS implementation in α and β1-syntrophin knockout mice causes accumulation of NOS in the cytoplasm, bringing no benefits for the AChR structural organization, demonstrating the importance of the anchored functional NOS to the DGC at the level of the NMJ (Shiao *et al*, 2004).

NO is also involved in the agrin signalling. NOS activity correlates with agrin-induced aggregation of AChRs through the sGC-cGMP-PKG (cGMP-dependent protein kinase) axis. During development, inhibition of those factors reduces receptors' aggregation in cultured embryonic muscle cells, while their overexpression highly improves the organized areas of these aggregates (Godfrey *et al*, 2007). Moreover, NO elicits pathways for the maintenance of AChR aggregates by means of PKG (protein kinase G), found involved in the binding between actin and dystrophin, anchoring and stabilizing the AChR structural organization during maturation (Jones and Werle, 2004). The structural stability is also maintained by the family of src kinases, which activity is NO-mediated. Src are also responsible for the tyrosine phosphorylation of the β-subunit of AChR, the one supposed to interact directly with rapsyn and cytoskeletal elements, controlling the primarily stabilization of AChR clusters (Godfrey and Schwarte, 2003). Stability of the NMJ is even promoted by NO signalling at the level of the presynaptic side, in which it covers an important positive role in neuronal growth and synaptic remodelling after nerve injury (Cooke *et al*, 2013).

2.4 Dose-dependent efficiency and toxic effects: nitrosative stress

All the beneficial effects nitric oxide shows at the level of different districts are mostly occurring under physiological NO concentrations, through a controlled activity of both endogenous and exogenous NO metabolisms. NO needs to be tightly regulated in its intracellular concentrations to avoid pathophysiological outcomes namely oxidative stress (in the specificity of this case would be nitrosative stress, NSS) which, if not properly counteracted, can cause irreversible damage to cell components, altering their activity, leading to a pro-inflammatory scenario and eventually causing cell death. Dysfunctional endogenous production or an excessive nitrate intake for prolonged periods can thus create an oxidative stressed environment which promotes the formation and accumulation of the reactive nitrogen species (RNS). These detrimental effects were unfortunately evaluated following NO implementation on DMD patient-derived myotubes and *mdx* mice, in which muscle damage and nitrosative stress were exacerbated, returning to the aforementioned damaged scenario (Timpani *et al*, 2020). The authors accounted for this in the prolonged chronic treatment or mistaken dosage, which is nowadays still debated. The NO dosage to be administered has always been a point of discussion as in the past a carcinogenic effect has always been feared due to studies on cancer progression and the role NO covered in the chronic inflammatory processes and reactive species-induced cell damage and dysfunction (Tamir and Tannenbaum, 1996).

RNS are the resultant of an overproduction of secondary metabolites by the oxidation of nitric oxide caused by an elevated iNOS stimulation or by the uncoupled activity of eNOS, exacerbated in their toxicity when found in an oxidative stress environment, i.e. high concentrations of superoxide anions (O_2^-) (Lancaster Jr, 2006). Reactive nitrogen species (RNS) include peroxynitrite ($ONOO^-$), nitrogen dioxide ($\bullet NO_2$), peroxynitrous acid (HNO_3), dinitrogen trioxide (N_2O_3), nitroxyl (HNO), peroxynitrous acid (ONOOH), peroxynitrate (O_2NOO^-), peroxynitric acid (O_2NOOH), nitrosonium cation (NO^+), nitrate (NO_3^-), nitrite (NO_2^-) and nitroxyl anion (NO^-) and can lead to nitrosative stress (NSS). Out of all RNS, $ONOO^-$ is the most abundant and the widely cytotoxic.

Being highly reactive species, they rapidly interact and crosslink with different cell components, mainly causing lipid peroxidation, changing lipid membrane composition, causative of an increased membrane permeability and reduced fluidity, which together lead to disorders in intracellular signal transduction and receptor dysfunction (Morris *et al*, 2016). They are even involved in DNA damage by the formation of hydroxydeoxyguanosine and 8-nitroguanidine, causative of breaks and single-strand formation in DNA (Tripathi *et al*, 2014). RNS can even damage intracellular proteins at different levels, rendering them enzymatically non-functional or structurally misfolded, by nitration of tyrosine residues resulting in the formation of 3-nitrotyrosine, formally recognized as an index of RNS formation (Radi, 2004). Misfolded and functionally impaired proteins could so accumulate in the cell and could not be easily degraded due to irreversible modifications of proteins involved in the degradation pathway, as finely reviewed by Ju and colleagues (Ju *et al*, 2021). 3-nitrotyrosine has been even directly correlated to the induction of cell death signalling pathways (Franco and Estevez, 2014). Another way through which RNS cause damage within the cell is at the level of organelles, especially mitochondria. Nitrosative stress could alter the activity of the electron transport chain and enzymes involved in fatty acid metabolism (Poderoso *et al*, 2019), as well as damage the integrity of mitochondrial DNA, more susceptible than the nuclear counterpart due to its non-protected exposure without histones. Since mtDNA encodes for 13 polypeptides, all of which are subunits of complexes I, III, IV and V (ATP synthase) of the mitochondrial electron transport chain, its instability due to nitrogen species covers a relevant role (Moon *et al*, 2006). Under high inflammatory conditions, iNOS activity is highly stimulated and causes an excessive production of NO which alters the anabolic pathway, dramatically decreasing protein synthesis through the downregulation of mTOR and its substrates (Frost *et al*, 2009, Hall *et al*, 2011).

Oxidative stress is generally defined as an imbalance between exposure to toxic reactive oxygen species and antioxidant systems. It plays relevant roles at different levels of the body districts, by mainly causing and participating in endothelial dysfunction, arterial stiffness, activation of inflammatory events, neurodegenerative and cardiovascular diseases, and metabolic impairments (Mozos and Tudor Luca, 2017; Perez-Torres *et al*, 2020).

Physiological methods are adopted by cells to counteract this phenomenon and so maintain redox homeostasis (Figure 8): antioxidant mechanisms, namely enzymatic and non-enzymatic systems, are involved in the neutralization of radical reactivity which act in a synergetic coupling within the cell, coping with free radical damage. One of the primarily enzymatic lines of defence implemented are the superoxide dismutases (SOD), a family of enzymes firstly recruited by the cells against the oxidative injury caused by O_2^-, partitioning it into ordinary O_2 and H_2O_2. Regarding NSS, SOD neutralizes the reactive $ONOO^-$ decreasing the formation of 3-nitrotyrosine in tissues. By the way, in high oxidative stress conditions, $ONOO^-$ itself can be causative of the loss of SOD activity through 3-nitrotyrosine modification in its catalytic site (Yamakura and Kawasaki, 2010). Catalase, an oxidoreductase enzyme containing a heme group, is subsequently recruited and intervenes when SOD processes large quantities of its substrate, to neutralize the by-products. It is found predominantly confined to the peroxisome and following an accumulation of hydrogen peroxide (H_2O_2) in the cell, it promotes catalysis into molecular O_2 and H_2O. Reactive $ONOO^-$ damages the enzyme and inhibits its activity since it reacts with the catalase heme group with a ferric-nitrosyl irreversible interaction, thus hampering any interaction among H_2O_2 and the metal ion. Moreover, NO molecules can react with a catalase tetramer, creating a complex sequestered by its native activity (Brunelli *et al*, 2001). Finally, glutathione peroxidase (GPx) isoforms are antioxidant enzymes which catalyse the oxidation of glutathione (GSH), present at high concentrations in cells, so as to reduce their substrates. They prevent the accumulation of intracellular damage by H_2O_2 and they also act as a peroxynitrite reductase to modulate $ONOO^-$ reactivity, converting these species to water or alcohol while simultaneously oxidizing GSH. Excess of NO inhibits glutathione reductase activity and reduces the concentration of GSH. $ONOO^-$ could irreversibly react with GSH by forming S-nitrosoglutathione, a promotor of apoptosis and progression of NSS and OS (Presnell *et al*, 2013).

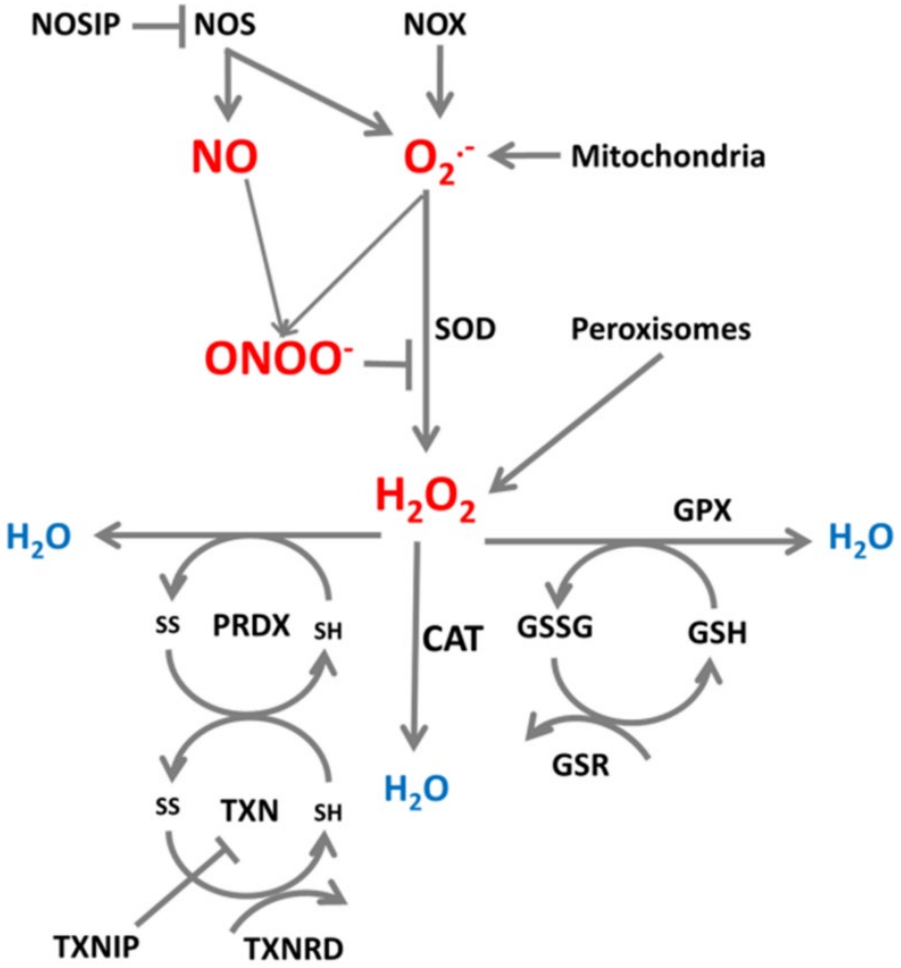

Figure 8. ROS/RNS production and neutralization. *Cellular superoxide (O_2^{-}•) and nitric oxide (NO) are produced and further converted to peroxynitrite ($ONOO^-$) by reaction of NO with O_2^{-}•, or to H_2O_2 by superoxide dismutase (SOD). H_2O_2 can be further neutralized and transformed to H_2O by catalase (CAT), glutathione peroxidase (GP_X) and peroxiredoxins (PRDX) which are reduced by thioredoxins (TXN). TXN is reduced by thioredoxin reductase (TXNRD), and glutathione (GSH) is reduced by glutathione-disulfide reductase (GSR). From Ciesielska et al, 2021.*

Other ways to counteract oxidative/nitrosative stress are represented by all those non-enzymatic factors such as Vitamin E, Vitamin C (ascorbic acid) and thiol antioxidants such as glutathione, thioredoxin, α-Lipoic acid, N-acetylcysteine, melatonin, carotenoids and flavonoids, mainly absorbed as a part of diets. They act or by directly neutralize free radicals or by solely enhance endogenous enzymatic activity, finely reviewed by Kurutas (Kurutas EB, 2015).

2.5 Nitrate supplementation as exogenous beneficial intervention on physical performance

Consistently with all the functions NO fulfills within the muscle and all the modulatory effects it exerts at different levels of muscle metabolism, muscle contraction and respiratory efficiency under controlled concentrations, this small gaseous molecule is growing in popularity in the field of sport

sciences and performance implementation, with a wide range of the literature now focusing on the effects of exogenous nitric oxide (i.e. nitrate supplementation) on the physical performance.

In 2007 Larsen and colleagues firstly demonstrate that nitrate supplementation improves exercise efficiency by means of lower oxygen demand during submaximal work. The oxygen cost of exercise was significantly reduced after nitrate supplementation compared with placebo, demonstrated by a reduction in average VO_2 during the submaximal test, while no changes were seen in VO_{2max} between treatments. VO_{2max} is a fundamental biological parameter for testing the physical aerobic performance of an individual, developed by the oxidative metabolism. It represents the maximal oxygen volume consumed per unit of time, during exercises of increasing intensity (incremental exercise). This parameter is widely used as an indicator of cardiorespiratory fitness (CRF), considering that lower fitness levels are associated with high risk of cardiovascular disease (CVD) or all-cause mortality (Kodama *et al*, 2009).

In 2009, Bailey and colleagues introduce into this randomized designed protocol a natural nitrate-rich dietary source (500ml/day of beetroot juice (BR), which contains 5.6 mmol NO_3^-) as the nitrate supplement, opening to an ongoing field of study based on this way of supplementation. In this protocol, the subjects were pushed until task failure as a measure of exercise tolerance and VO_{2peak} was measured. VO_{2peak}, directly reflective of VO_{2max}, is the highest value of VO_2 attained upon an incremental or other high-intensity exercise tests, designed to bring the subject to the limit of tolerance. Even if VO_{2peak} did not show any difference at the end point of the two treatments, the BR significantly delayed time of exhaustion and reduced the VO_2 "slow component". The VO_2 slow component, finely reviewed by Jones and Grassi (Jones *et al*, 2011), represents an index of muscle fatigability. It is well established that during constant aerobic exercise (endurance training), type I muscle fibers are recruited. These fibers enjoy a highly oxidative metabolism which allows them to maintain their work load for a long time. The slow component of VO_2 represents a progressive loss of skeletal muscle contractile efficiency, mainly associated with the progressive recruitment of additional (type II) muscle fibers that are presumed to have lower efficiency, due to a higher ATP demand for contractile activity and thus higher oxygen consumption. A year after, the same group identifies less ATP hydrolysis as the leading cause of an improved tolerance of high-intensity exercise, guided by the NO-mediated modification of calcium handling proteins (Bailey *et al*, 2010).

Consistent with these promising outcomes on physical performance on healthy subjects tested after BR intake, interest arises in the evaluation of parameters related to exercise training performances.

Acute dietary nitrate has been shown to improve cycle performance of club-level competitive male cyclists (Lansley *et al*, 2011); it reduced the metabolic costs of twelve well-trained apnea divers promoting an increased apneic duration (Engan *et al*, 2012); it lowered steady-state VO_2 of trained cyclists exposed to moderate simulated altitude (approx. 2500 mt, Muggeridge *et al*, 2014). Regarding chronic BR supplementation (6-day), physically active men reached an important reduction in O_2 cost of medium- and high-intensity running, concomitant with an increased time of exhaustion during severe-intensity running (up to 15%, Lansley *et al*, 2011); trained male cyclists significantly improved submaximal VO_2 and increased tolerance of high-intensity work rates (Cermak *et al*, 2012); moderately trained male swimmers showed a reduction in aerobic energy cost (Pinna *et al*, 2014).

For these and other studies related to the beneficial effects of BR on exercise tolerance and oxygen consumption, there are just as many which demonstrate no BR effects on exercise performance in highly trained endurance athletes. Acute dietary nitrate did not improve 1-hour time-trial cycle performance (Cermak *et al*, 2012) and no improvement in 50-mile time trial performance in well-trained cyclists (Wilkerson *et al*, 2012). No particular beneficial effects have been found on the evaluation of time to exhaustion at high altitudes (4000 mt) and 10-km treadmill time-trial at 2500 mt simulated altitude of well-trained runners (Arnold *et al*, 2015). Combined studies made up on acute and chronic BR supplementations at the same level did not show any improvement on physical performance and oxygen consumption assessed by VO_2 measurement in well-trained athletes performing 40-min endurance tests (Bescos *et al*, 2012), in elite distance runners (Boorsma *et al*, 2014) and in highly trained cyclists (Nyakayiru *et al*, 2017).

These observations open up about the heterogeneous responsiveness of subjects to BR supplementation, depending on individual-specific nitrate assimilation, the long duration of tests and the training status (Porcelli *et al*, 2015). High-trained athletes flatten the benefits of nitrates that are seen in moderately athletic subjects. This could be explained by higher nNOS expression and activity following endurance exercise training (McConell *et al*, 2007), which render the NO_3^--NO_2^--NO pathway relatively less important for NO production. Moreover, nitrite is reduced to NO in hypoxia and under acidic environment, conditions in which NOS function is compromised. Highly trained subjects which develop a great intricate net of skeletal muscle capillarization are thus able to maintain a sustained hyper fusion of metabolites and molecules required during exercise,

reducing the NO demand and avoiding the onset of conditions that can promote nitrate reduction phenomena.

2.6 The role of nitric oxide in ageing

Ageing process is associated with a number of structural changes that most of the times lead to compromised cardiovascular and muscular functions, such as decreased capillarity density and blood flow in the microcirculation, inflammatory outcomes, vascular stiffness as well as mitochondrial impairments (changes in density and oxidative function; Conley *et al*, 2000, Gouspillou *et al*, 2010). All together, these alterations may perturb efficient O_2 delivery and utilization (and so a slower VO_2 kinetics) within different body districts and exercise, naturally involved in increasing skeletal muscle blood flow due to higher energy requests, has shown attenuated outcomes with increasing age (Wahren *et al*, 1974). Moreover, the overproduction of reactive oxygen and nitrogen species is one of the main problems encountered in senility and pathological conditions and they are believed to play a relevant role in the functional losses of molecular components which lead to the accumulation of oxidative/nitrosative-induced damages. It occurs due to mitochondrial dysfunction caused by age-related mitochondrial damages, besides NOSs altered activities.

The concentration of nitric oxide in plasma has found to be negatively correlated with physiological advancing age (Di Massimo *et al*, 2006). At the level of skeletal muscle tissue, measurements of NO levels on human muscle biopsies of various age-related cohorts demonstrate that basal nitrate concentration in healthy young controls (~80 µmol/l) was 1.5-fold greater than in older healthy subjects (~54 µmol/l), speculating that aged muscle tissue may be altered in nitrate transport, metabolic pathways and proper storage. This result therefore opens up the possibility of considering the nitrate dietary supplementation as a promising intervention to improve the availability and storage of nitrates in old muscles (Nyakayiru *et al*, 2017). Following NO_3^- metabolism and circuitry within the body starting from salivary glands, variation in the oral microbiota could influence nitrate reduction and furthermore, the expression of the putative NO_3^- transporter Sialin decreases at the level of submandibular glands of mice and human parotid gland, limiting the physiological function of salivary glands of older individuals (Li *et al*, 2018).

Furthermore, an altered NOS enzymes expression and/or activity occurs in ageing. Despite changes in expression are still a source of debate due to contradictory studies, it is well accepted that the activity of eNOS and nNOS are reduced in ageing. The loss in activity could be due to a decreased

availability of substrates (L-arginine is considered a non-essential amino acid and could not be implemented in old individuals' diet) or cofactors, changes in post-translational modifications which modulate their activity and subcellular localization. eNOS and nNOS are functionally found anchored in the plasma membrane of the cells but during ageing the amount of these enzymes localized in the membrane decreases (Cau *et al*, 2012). In particular, eNOS seems to play a harmful role in ageing. Under conditions of substrate depletion, NOS becomes a radical generating enzyme, a phenomenon referred as NO uncoupling. As a result of a lack of Ser-1177 phosphorylation, monomeric eNOS was found increased in mesenteric arteries of old rats, and has been demonstrated to be involved in the generation of O_2^- (Yang *et al*, 2009). Being NO a superoxide anion scavenger, it decreases its bioavailability because of its reaction with the reactive oxygen, promoting peroxynitrite ($ONOO^-$) accumulation and subsequent intracellular damage. This reaction is then facilitated in the pro-oxidant environment of old tissues. On the other hand, iNOS is found widely expressed during ageing, due to its involvement in pro-inflammatory events extensively occurring in different districts in elderly subjects. Ageing-associated iNOS up-regulation is therefore accompanied by $ONOO^-$ production, due to the same aforementioned reaction.

Given all the positive observations that nitrate supplementation has in terms of blood flow, oxidative metabolism and generally in physical performance, a lot of curiosity has emerged about whether NO_3^- supplementation can somehow improve contractility and therefore ameliorate physical performance and enhance exercise tolerance in the elderly, consistent with all the NO-metabolic impairments due to ageing.

Regarding studies of aged human profiles, lots of observations were made in the time window of senescence. Despite no significant improvements in exercise tolerance and oxygen consumption under medium-high intensity exercise were assessed in middle to older-aged well-trained adults (41 to 64 years old subjects who consume 9.9 mmol of NO_3^-/day for 7 days; Berry *et al*, 2020), the literature that focused on ageing showed off positive effects of supplementation in physical performances.

Acute nitrate supplementation (~13.4 mmol) improved muscle functional contractility, assessed through the maximal knee extension test at angular velocities, in a group of elderly subjects (about 70 yo), (Coggan *et al*, 2020). Muscle oxygenation and time to recovery were ameliorated in acute nitrate intake (~12 mmol) of randomized aged individuals (de Oliveira *et al*, 2017). Moreover, 9.4 mmol nitrate treatment reduced aortic blood pressure promoting thus beneficial cardiovascular

effects (Hughes *et al*, 2016), confirmed by 4-weeks supplementation in which aged subjects showed a reversed vascular dysfunction and thus a better cardiovascular prognosis (Rammos *et al*, 2014). 3-days supplementation (~9.6 mmol/day NO_3^-) improved then VO_2 kinetics during treadmill walk, reduced blood pressure with no changes in O_2 cost of exercise in 60-70 years old subjects (Kelly *et al*, 2013). However, even in this case, the literature showed contrasting results regarding the effects of dietary nitrates on old subjects. In particular, Siervo and colleagues did not find any change in physical exercise-related functional parameters after 1-week BR supplementation (~12 mmol/day) (Siervo *et al*, 2016). This could be in part explained by interindividual variability of nitrate absorption and metabolism, worsened during ageing (Coggan et al, 2018).

Taken together, all these evaluations and studies on the impact of nitrate supplementation on physical performance could open a window of study regarding the combined effects they could have in the elderly, who are known to be prone to high fatigue and exercise intolerance.

RATIONALE AND AIM

The rationale of the study is based on several observations (see also Introduction for details):

- Neuromuscular junction (NMJ) deterioration, mitochondrial dysfunction, increased ROS production, and decreased PGC1α expression have been reported in skeletal muscle with ageing. Muscle mitochondria are believed to be crucially important for the maintenance of NMJ. Recent findings point to changes in myofiber PGC1α expression as a key process involved in NMJ impairments with ageing.
- Loss of nNOS in skeletal muscle with ageing has been shown to be associated with structural defects at the NMJs, impaired mitochondrial biogenesis and muscle wasting.
- Exercise intolerance is experienced during ageing, with higher fatigability and associated muscle wasting which devoid the subjects to perform it as therapeutical intervention.
- Nitric oxide (NO) has been shown to induce mitochondrial biogenesis in skeletal muscle cells via modulation of PGC1α.Inorganic nitrate supplementation has been shown to increase NO bioavailability and exercise performance in both untrained and trained conditions.

Based on the above evidence, the specific goals of the present study were to a) determine the efficacy/ability of nitrates in counteracting NMJ alterations and muscle wasting in ageing through exogenous supplementation of inorganic $NaNO_3$ alone and in combination with exercise, b) evaluate whether the combination of the two treatments promotes additive or synergistic effects on elderly muscles and c) characterize the molecular mechanisms underlying the effects induced by the interventions.

MATERIALS & METHODS

Animals: C57BL/6

Wild-type C57BL/6 male mice were used to perform all the experiments, in a natural physiological ageing course of life (22-months old) and in 7-months old mice. Mice were housed in a conventional laboratory animal facility, in pathogen-free and controlled conditions, at constant temperature and controlled humidity, with 12 hours of light/dark cycles to ensure natural circadian rhythm. Animal handling and experimentation were performed in line with approved Institutional Animal Care and Use Committee protocols at the University of Pavia and conformed to Italian law concerning animal testing (D. Lgs n° 2014/26, implementation of the 2010/63/UE).

Following behavioural tests performed by collaborators of the University of Pavia, old mice were randomly assigned to the experimental groups under investigation, in order to minimize intrinsic heterogeneity among groups. Five groups were assessed: young control mice (Young CTRL, 7-mo), old control mice (Old CTRL, 24-mo), old mice supplemented with $NaNO_3$ through water intake (Old N, 24-mo), mice subjected to incremental endurance exercise (Old EX, 24-mo) and mice underwent combined $NaNO_3$ supplementation and exercise protocols (Old EX+N, 24-mo). All interventions lasted for two months starting from the 22nd month of age. During the experimental procedure, mice had full access to food and water *ad libitum*, except for $NaNO_3$ supplemented animals which underwent surveilled beverage daily. Seven to eight animals per group were used.

Dietary nitrate supplementation

Dietary nitrate supplementation consisted of 1.5 mM $NaNO_3$ (Sigma-Aldrich) dissolved in the drinking water of old mice allocated in the N and EX+N group, whereas the other cohorts received regular water. 1mM inorganic nitrate has been widely used in other rodent studies (Hernandez *et al*, 2012; Ivarsson *et al*, 2017), representing a concentration that is readily obtainable in the diet (Hord *et al*, 2009). So, for preliminary data sets, we augmented inorganic nitrate concentration to emphasize their action. Nitrate solutions were prepared daily by dissolving a concentrated stock solution of $NaNO_3$ in drinking water. Aliquots of the concentrated stock were stored at -20° C to prevent nitrate degradation (Corleto *et al*, 2018) and thawed daily to prepare the drinking solution. Both groups received $NaNO_3$ and water in similar containers (bottles) available *ad libitum* for all the experimental period (nine weeks). Regular water and $NaNO_3$ solution volumes were measured to assess the correct concentration of nitrates intake and replaced daily.

Exercise training protocol

To familiarize themselves with the treadmill device, mice were acclimatized for four days prior to the beginning of the nine weeks' protocol by walking 20 min/day at 5 to 7 m/min at 0° inclination on a motorized treadmill (Exer 3/6 Treadmill, Columbus Instruments, Columbus OU, USA) (Figure 9).

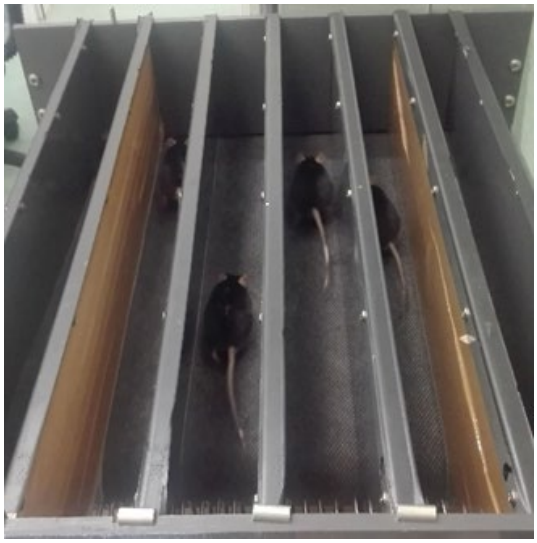

Figure 9. Old mice subjected to exercise training protocol in six-lane animal exerciser treadmill. *Lanes were obscured to not influence the animals' run.*

After a short period of acclimation, the exercise protocol was performed as follows: 5 min of warmup at 5 m/min after which time the speed was increased to 0.5 m/min for 10 min until the speed of 7 m/min. Then the mice ran until the 30th min in the first weeks and progressively incrementally increased in end time and speed until the last two weeks in which they were able to perform 60 min of exercise training eventually reaching 10 m/min velocity. Exercise protocols were performed five out of seven consecutive days a week for nine weeks. This medium-intensity exercise protocol was designed for old animals to promote aerobic endurance training, with an incremental time and speed approach due to the sedentary lifespan of mice which renders them highly prone to fatiguing and to interrupting the exercise before the scheduled time.

Behavioural tests and locomotor evaluations

In vivo experiments were performed for investigating the locomotor abilities of old mice. Protocols were performed by collaborators from the University of Pavia and details are described in Roda *et al*, 2021. Briefly, all mice, at different experimental times, performed two spontaneous behavioural tests: open-field arena and emergence tasks. In the open arena test, mice were left free to explore an empty arena of 63 × 42 cm. During the emergence test, mice were placed in a familiar cage with

a hole through which they can emerge in a larger arena without walls. Both tests lasted 8 min. Mean speed (cm/s), resting time (s), and max speed (cm/s) were evaluated. Mice performances were measured by SMART video tracking system (2 Biological Instruments, Besozzo, Varese, Italy) and Sony CCD colour video camera (PAL).

Nitrate concentration

In order to quantify NOx concentration in the muscles, Soleus was used as a reference muscle because it is indicated by the literature as a NOx reservoir (Park *et al*, 2021). Samples were homogenized in PBS (phosphate buffer aqueous solution containing 136 mM NaCl, 2 mM KCl, 6 mM Na_2HPO_4 and 1 mM KH_2PO_4) pH 7.4 on ice and rapidly centrifuged at 10000 x g for 30 min and supernatant used for quantification through the RC-DC™ (reducing agent and detergent compatible) protein assay (supplied by Bio-Rad). RC-DC™ is a colorimetric assay for protein determination in the presence of reducing agents and detergents, based on the Lowry protocol (Lowry *et al*, 1951), one of the most used methods to evaluate protein amount. The absorbance value of each sample was read by a spectrophotometer settled at a wavelength of 750 nm. According to Lambert-Beer law, absorbance of a protein is directly proportional to its concentration. Thus, protein sample concentration was calculated by interpolating the values on a calibration reference curve whose points are scalar concentrations of a solution of a known concentration of BSA.

Concentration of NOx was measured using a commercial colorimetric assay kit (Griess Reagent Kit, Cayman Chemical, USA), which provides an accurate and convenient method for measurement of nitrate and nitrite concentration. The Griess Reagent System is based on the chemical reaction which uses sulfanilamide and N-(1-Naphthyl) ethylenediamine dihydrochloride (NED) under acidic (phosphoric acid) conditions. For nitrate measurements, a reducing reaction needed to occur through the addition of an Enzyme Cofactor that sustain the Nitrate Reductase Mixture activity (both provided by the kit). 40 µg of each sample were used, in duplicate. After three hours' incubation with the enzymes at room temperature, samples were read by the addition of Griess reagents at 545 nm in a microplate reader spectrophotometer (CLARIOstar® Plus, BMG Labtech, Germany). A linear calibration curve was computed from pure nitrate standard (ranging from 0 to 35 µM). Both nitrate and nitrite were quantified, following manufacturer's datasheet.

Sample collection

Animals of all experimental groups were fasted 2 hours prior to the sacrifice. Groups subjected to exercise protocols were sacrificed 24 hours after the last training session. Mice were weighted and subsequently sacrificed by cervical dislocation, and muscles from the hindlimb were finely dissected within 15 min post-mortem, weighed and immediately snap frozen in liquid nitrogen and stored at -80° C for further evaluations. For the *ex vivo* experiments, muscles were excised and preserved in physiological environments to maintain their functionality. The respiratory muscle diaphragm was dissected and stored following different methods due to different outcomes. The central part was destined to the intact muscle contractility assay plunged on Krebs oxygenated solution, part of the dorsal section snap frozen in liquid nitrogen and a ventral well oriented portion embedded in OCT medium (Killik, O.C.T. for cryostat, Bio-Optica) at room temperature prior to snap frozing in liquid nitrogen to be further cryosectioned for morphological analyses. One of the foot dorsiflexor Tibialis Anteriores (TA) was then used for the high resolution respirometry (HRR) assay through rapid dissection in cold BIOPS buffer.

Ex vivo Analysis: Oxygraph-2k for High-Resolution Respirometry

For the measurements of mitochondrial respiration, the Oxygraph-2k (O2k, OROBOROS Instruments, Innsbruck, Austria) was used. Experiments using permeabilized skeletal muscle fibers were performed in miR05 (mitochondrial respiration medium: 110 mM sucrose, 60 mM K-lactobionate, 0.5 mM EGTA, 3 mM $MgCl_2$, 20 mM taurine, 10 mM KH_2PO_4, 20 mM HEPES, pH 7.1 at 30° C, and 0.1% BSA essentially fatty acid free; Gnaiger *et al*, 2000). All experiments were performed at 37° C in hyperoxic conditions (concentration of oxygen up to 400 µM) to avoid O_2 limitations in respiration, and the medium was reoxygenated with pure gaseous O_2 when oxygen concentration diminishes under the threshold of 280 µM. Standardized instrumental and chemical calibrations were performed to correct for back-diffusion of O_2 from the various components into the chamber (e.g. leak from the exterior, O_2 consumption by the chemical medium and by the sensor O_2) (Pesta & Gnaiger, 2012). Because the Oroboros-O2k machinery has two chambers for the experimental session, two samples can be evaluated in parallel. The excised TA was washed in ice-cold BIOPS (biopsy preservation solution: 2.77 mM CaK_2EGTA, 7.23 mM K_2EGTA, 5.77 mM Na_2ATP, 6.56 mM $MgCl_2 \bullet 6\ H_2O$, 20 mM Taurine, 15 mM Na_2Phosphocreatine, 20 mM Imidazole, 0.5 mM Dithiothreitol (DTT), 50 mM MES, pH 7.1 at 0° C) and properly dissected so as to obtain a compacted piece of well-oriented fibers of about 6 µg. Two of those were prepared to perform the analysis in double during

the day. Contiguous pieces of the ones subjected to HRR were then cleaned and weighed. The continuity of the fibers with the one destined to HRR allows to analyse it with composition and properties as much close as the assessed one. The muscle fibers needed to be enlarged so as the medium could penetrate easily in every part of it, with the help of small fine-tipped tweezers under the microscope. Then it underwent 30 min of permeabilization with 20 µg/ml Saponin (Sigma-Aldrich) in BIOPS in agitation at 4° C so all the fibers of the tissue sample could be reached by the substrates/inhibitors inserted into the chambers during the experimental procedure. At last they were washed with miR05, the medium in which all the experimental protocol was performed, for 10 min and then transferred into Oroboros-O2k chambers. Experiments were performed in the presence of the myosin II-ATPase inhibitor (Blebbistatin, 25 µM, dissolved in 5 mM DMSO) (Perry *et al*, 2011) in order to prevent spontaneous contraction in the respiration medium.

Respiration of permeabilized muscle fibers was determined using substrate-uncoupler-inhibitor titration (SUIT) protocols previously described (Makrecka-Kuka *et al*, 2015; Zuccarelli *et al*, 2021) with modifications. All the chemicals used were purchased from Sigma-Aldrich, otherwise differently mentioned.

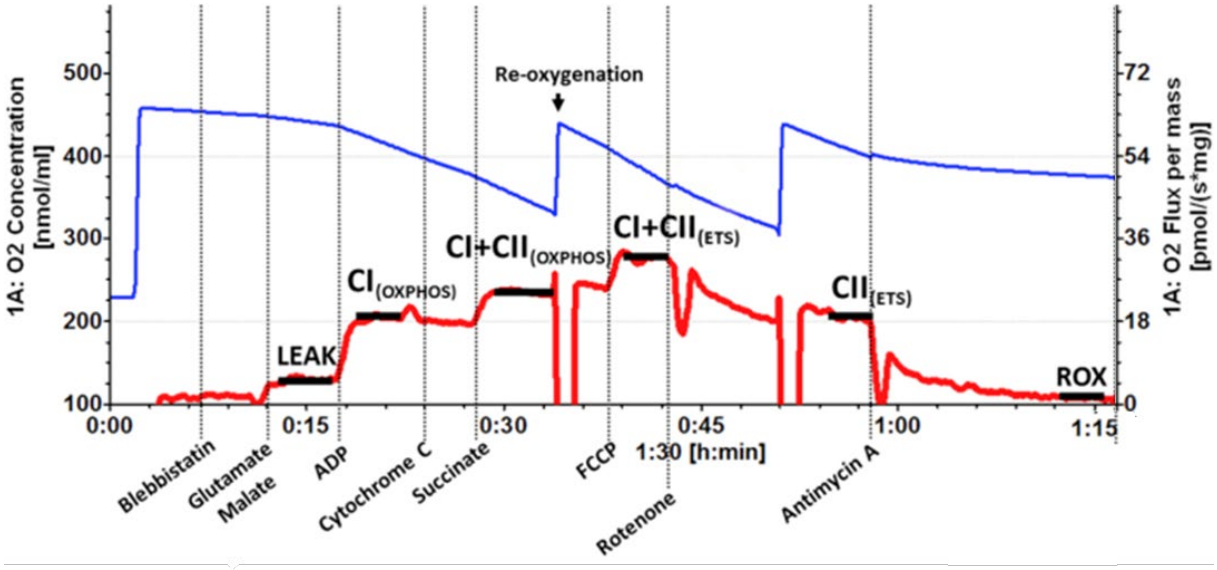

Figure 10. Representative scheme of a HRR experiment performed with Oroboros-O2k machinery. *Red line is the oxygen flux produced by the sample under investigation, while the blue line represents the oxygen concentration within the chambers. Our protocol added Succinate prior to ADP and Cytochrome C prior to Rotenone. Adapted from Cheng et al, 2019.*

Glutamate (G) and malate (M) (10 mM and 4 mM, respectively) were added to measure non-phosphorylating resting mitochondrial respiration in absence of adenylates, so that O_2 consumption was mainly driven by the back leakage of protons through the inner mitochondrial membrane

('LEAK' respiration). Succinate (Succ, 10 mM) was then used to support convergent electron flow into the Q-junction through Complexes I and II (determining the LEAK of both Complexes I (CI) and II (CII). ADP was added at increasing submaximal concentrations to build up a titration curve until reaching a 4 M final concentration, which was saturating for oxygen flux to obtain maximal ADP-stimulated mitochondrial respiration (OXPHOS capacity). Additional substrates were added sequentially to reconstitute convergent CI&II-linked respiration. Titrations with the uncoupler protonophore carbonylcyanide-p trifluoromethoxyphenylhydrazone FCCP (a few steps of 1 µM) were performed to determine the electron transfer system (ETS) capacity. Rotenone (Rot, 0.5 µM added to inhibit Complex I) and Antimycin A (AmA, 2.5 µM to inhibit Complex III and thus mitochondrial respiratory chain) were added for the determination of maximal respiratory uncoupled efficiency and residual oxygen consumption (ROX) independent by mitochondria, respectively. Prior to AmA, Cytochrome C (CytC, 10 µM) was added to the chambers to evaluate the integrity of the outer mitochondrial membrane: an increase in oxygen flux of more than 15% would indicate damaged organelles. At the conclusion of each experiment, muscle samples were removed from the chambers, washed in PBS and centrifuged for 10 min at 14000 g at 4° C, and immediately frozen in liquid nitrogen to be stored at -80°C until further determinations.

Volume-specific O_2 fluxes were calculated real-time by the DatLab software (OROBOROS INSTRUMENTS, Innsbruck, Austria) over time. Only the stable portions of the apparent fluxes were selected and artefacts induced by additions of chemicals or re-oxygenations were excluded. All the mitochondrial respiration indices were corrected for O_2 flux resulting from residual O_2 consumption (ROX). The obtained mitochondrial respiration values needed to be normalized by citrate synthase activity (see below), taken as an estimate index of mitochondrial mass (Larsen *et al*, 2012). Contiguous pieces of the ones subjected to HRR were analysed due to their conserved properties and the similar composition of the ones subjected to the SUIT protocol.

Citrate synthase activity

Citrate synthase (CS) activity was determined as described in Zuccarelli *et al*, 2021. Briefly, muscle samples were thawed and homogenized in a glass potter (Wheaton, USA), resuspended 1:50 w/v in a homogenization buffer containing 250 mM Sucrose, 20 mM Tris, 40 mM KCl and 2 mM EGTA, with 1:50 v/v protease (Sigma-Aldrich) inhibitors. Prior to the last of the 20 strokes (at 500 rpm), Triton X-100 (0.1% v/v) was added to the solution. Then, after 30 min incubation in ice, the homogenate was centrifuged at 14.000 g for 10 min. The supernatant was used to evaluate protein concentration

and the quantified extracts (5–10–15 µg) were added to each well of a 96-well-microplate along with 100 µl of 200 mM Tris, 20 µl of 1 mM 5, 5'-dithiobis-2-nitrobenzoate (DTNB), freshly prepared, 6 µl of 10 mM acetyl-coenzyme A (Acetyl-CoA) and MilliQ water to a final volume of 190 µl. A background ΔAbs, to detect any endogenous activity by acetylase enzymes, was recorded for 90 s with 10 s intervals at 412 nm at 25°C by an EnSpire 2300 Multilabel Reader (PerkinElmer). The ΔAbs was subtracted from the one given after the addition of 10 µl of 10 mM oxalacetic acid that started the reaction. All assays were performed at 25°C in triplicate on homogenates. Activity was expressed as nmol min^{-1} (mU) per mg of protein.

Ex vivo Analysis: Intact Muscle Contractility

Diaphragm muscle from mice was dissected and portioned for different purposes. An isolated and well-oriented diaphragm strip between two opposite portions of rib cages was transferred in Krebs solution at room temperature (22° C) and constantly oxygenated. Non-absorbable 4-0 silk sutures were then applied to the two ends of the sample (one extremity of the ribs and the central tendon) in order to firmly anchor it vertically to the hooks that make up the force transducer (FT-03; AstroNova) (Figure 11).

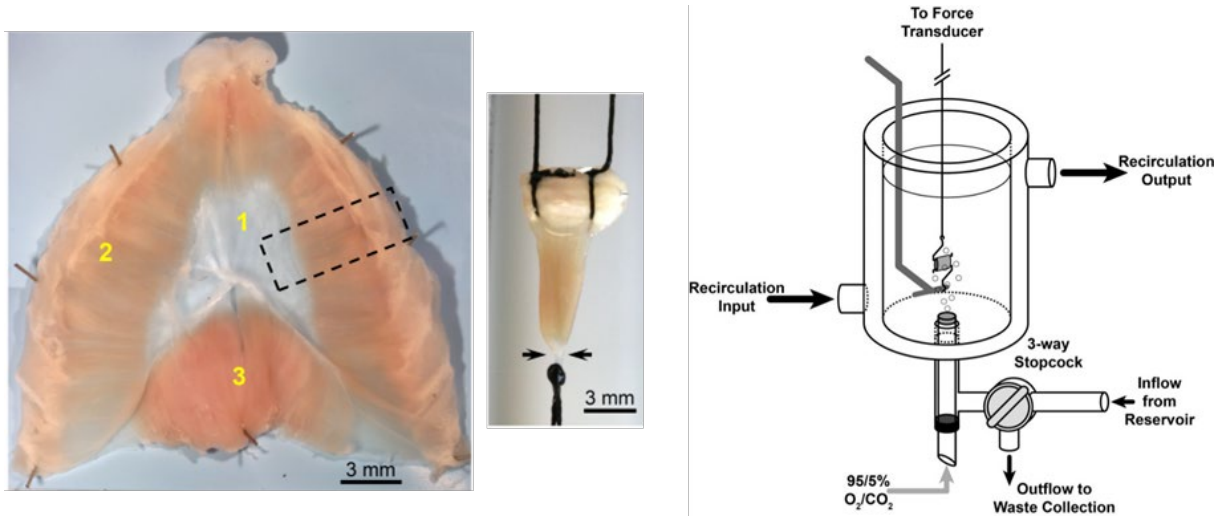

Figure 11. Schematized representation of the intact muscle contractility assay performed on diaphragm. *Silk sutures are applied on the extremities of the hemi-diaphragm (the non-contractile portions, adapted from Hakim et al, 2019). On the right, an exemplified bath in which muscle is anchored and plunged in oxygenated Krebs solution to perform the assay (adapted from Jespersen et al, 2015).*

Preparations were placed in an organ bath containing Krebs solution (120 mM NaCl, 2.4 mM KCl, 2.5 mM $CaCl_2$, 1.2 mM $MgSO_4$, 5.6 mM glucose, 1.2 mM KH_2PO_4, and 24.8 mM $NaHCO_3$, pH 7.4) bubbled with a blend of 95% O_2 and 5% CO_2 and kept at constant temperature (22° C). Force

transducer is formed by a fixed hook and a movable lever arm used to adjust the muscle length, stretched to L_o (muscle optimal length for maximal twitch force). On both sides of the perfusion bath at a distance of about 2 mm from the preparation, plate platinum electrodes connected with a stimulator (S48 Grass-stimulator; AstroNova) allow electrical field stimulation. Tetanic isometric contractions were evoked (110 Hz, 120 ms, supramaximal amplitude) at L_o. A fatigue test was performed by measuring the drop-in force of the maximal tetanic force following 20 repeated contractions in a ramp protocol at 0.03, 0.09, and 0.3 Hz. Data were normalized to muscle cross-sectional areas (CSA) and expressed as force/CSA ($Po/\mu m^2$) unless otherwise specified. A 1401 A/D converter (Cambridge Electronic Design) and CEA Spike2 software (Cambridge Electronic Design) were used for the analysis (Tirone *et al*, 2018).

Cross-Sectional Area (CSA) Analysis

Muscle fibers' CSA was performed to assess the size of muscle fibers. CSA was obtained by cutting in the mid-belly region of fusiform muscles under investigation (Gastrocnemius and Soleus) and in transversally oriented diaphragm OCT-embedded muscles. Briefly, serial transverse sections with a thickness of 10 µm each were obtained from muscles by using a cryostat with a working temperature of -20° C. Sections were collected on the surface of polarized glass slides which guarantees the permanent adhesion. Images of the sections were then captured from a light microscope (Leica DM/LS, Wetzlar, Germany) equipped with a camera (Leica DFC450 C, Wetzlar, Germany). Fibers' CSA was measured with Image J analysis software (NIH, Bethesda, MD, USA) and expressed in μm^2. Glass slides were then conserved at -20° C for further immunohistochemical and fluorescence investigations.

Immunohistochemistry Analysis

MHC isoforms staining

In order to evaluate the composition of fiber types present in each muscle of all the groups, the cross-cryosections were immunostained with two mouse monoclonal antibodies separately: the antibody specific for slow MHC isoforms (Abcam) and the one specific for the fast MHC isoforms (Abcam). Primary antibodies were diluted 1:2000 and 1:1000 respectively in a solution of PBS and BSA (bovine serum albumin, Merck) 1% (w/v) and distributed on the surface of the slides so as to completely cover each section. After 1 hour of incubation at 37° C, slides were washed three times, 5 min each in PBS at room temperature. Then, the slides were incubated for 30 min at 37° C with a secondary rabbit anti-mouse immunoglobulin G (IgG) antibody conjugated with peroxidase (DAKO,

Glostrup, Denmark), diluted 1:500 in PBS + BSA 1% solution. At the end, three consecutive washes in PBS were performed to remove the exceed of antibody solution. In order to visualize the positive immunostained transverse cells where the reaction antigen-antibody occurred, hydrogen peroxide needed to react with peroxidase in an environment containing DAB (diaminobenzidine), which produces at last a brownish coloration where the secondary antibody is found linked. The colorimetric reaction was carried out at room temperature in about 5 min, and in order to devoid overreaction and aspecific oxidation of negative cells, it was blocked by dipping the slides in PBS. A dehydration step in alcoholic solutions of increasing concentration was performed, for a few seconds each (40% ethanol, 60% ethanol, 80% ethanol, 95% ethanol, 50% ethanol and 50% xylene and a long wash in xylene). Finally, the slides were closed by using cover slips fixed with the Eukitt® Mountant (Bio-Optica). The sections of muscles so coloured were examined using a computerized image analyser, consisting of a camera (Digital Vision) placed on a light microscope (Leica DM/LS, Wetzlar, Germany) and connected through a digital interface to a computer equipped with specific software (Leica DFC450 C, Wetzlar, Germany). With this system, it was possible to view images of preparations on the screen and to evaluate the distribution of the two different MHC isoforms within a muscle, further counted based on acquisition of images at 10X magnification and reconstruction with imaging software (Image J, NIH). The results were displayed as a percentage of the positive fibers on the total amount that composes the section under investigation.

Picro Sirius Red staining for fibrotic tissue

Sirius Red staining in formerly used for the staining of collagen present in tissues, and in our case is particularly indicative of the fibrotic infiltration within muscle tissue sections. Sections stored at −20°C were dried at room temperature for 10 min before rehydration in alcoholic solutions of decreasing concentrations (xylene 100%, xylene/ethanol 50%, ethanol 95%, 80%, 70% and 50%) and subsequent fixation in a neutral buffered formaldehyde solution 3.7% for 1 hour at room temperature. Following incubation in Sirius Red (Direct Red 80, Sigma-Aldrich) 0.1% (w/v) in a saturated aqueous solution of picric acid (1.3% saturated in water, Sigma-Aldrich) for 1 hour at room temperature, two washes in acidified water (0.5% acetic acid in water) were performed to remove exceeding stain. Dehydration in two changes of 100% ethanol is then required, with a subsequent wash in ethanol/xylene in a 1:1 ratio and final clear in xylene. Finally, the slides were closed by using cover slips fixed with the Eukitt® Mountant (Bio-Optica). The sections of muscles so coloured were examined as previously described, with a 10X magnification acquisition and analysed with Image J software as the percentage of the fibrotic area on the total area of the section.

Immunofluorescence Analysis

NCAM1+ fibers

In order to evaluate the expression of NCAM1 as a marker of denervation, immunofluorescence on transverse muscle sections was performed to assess the presence of any positive fibers and whether the localization of the adhesion molecule was on the sarcolemma or within the sarcoplasm, indicative of different degrees of denervation/reinnervation occurring on that site. Sections stored at −20°C were dried at room temperature for 10 min and fixed in cold methanol (-20° C) for other 10 min and further permeabilized with a solution based on PBS and Triton X-100 2% (v/v) for 30 min. Then, the sections were incubated for 1 hour in BSA 2% and Normal Goat Serum 2% in PBS, in order to saturate non-specific sites, in a humidified chamber. After two washes in PBS, sections underwent incubation with primary antibodies against NCAM1 (anti-mouse, 1:500, Abcam) and Dystrophin (anti-rabbit, 1:500, Abcam) in saturation solution, overnight at 4° C in humid chamber. Then, three washes in PBS, 5 min each were performed, and secondary antibodies added on the sections to allow specific reaction with their targets. Conjugated anti-mouse Alexa Fluor™ 594 and anti-rabbit Alexa Fluor™ 488 (Invitrogen) were diluted 1:500 in saturation solution and incubated for 1 hour at room temperature, in humid chamber and under dark conditions to devoid any damage of the photo-sensitive fluorophores, a condition maintained in all the further passages. Repeated washes in PBS were performed and nuclei were counterstained for 5 min with DAPI 1:5000 in PBS. Negative controls (without the primary antibody incubation) were performed in parallel with the standard protocol to demonstrate the specificity of the fluorescence signals. Slides were mounted with a glycerol-based anti-fade mounting medium and images were acquired at 10X magnification with a fluorescence microscope (Olympia microscopes), and elaborated and analysed with the support of Image J software. Total number of cells, centralized nuclei and cells positive for NCAM1 signal were counted and analysed for comparison between control and treatment groups.

Confocal microscopy for NMJ morphology

The chosen muscle for the study and morphological evaluation of the neuromuscular junction structure was the Extensor Digitorum Longus (EDL) in order to allow the whole-mounted evaluation of the entire muscle and thus preserve the complete architecture of the tissue. EDL is moreover a small fusiform muscle that allows a high efficiency of in-depth analysis, with strong tendons that serve as anchors for immunostaining fixed passages. Snap-frozen muscles were divided in half along the length to reduce the thickness of the tissue and so allow a profound investigation. Prior to

defrost, the half-muscles were pinned in silicon-based dishes and plunged within cold 4% paraformaldehyde (PFA) for 1 hour at room temperature to allow fixation of all the structures. After long washes in PBS, tissue was permeabilized with 4% Triton X-100 for 90 min and subsequently incubated in a blocking solution of 4% BSA and 2% Triton X-100 in PBS, at room temperature for 1 hour. Then, primary antibodies for visualizing presynaptic structures were added and left to react for 48 hours at 4° C. Rabbit anti-Neurofilament-L (the most represented of the axonal neurofilaments; NF-L, Cell Signalling) and mouse anti-synaptophysin (part of the synaptic vesicles apparatus; Syn, Cell Signalling) were made up in blocking solution with dilutions of 1:400 and 1:200 respectively. After a long wash in PBS, samples were incubated with 4% BSA and 2% Triton X-100 in PBS for 30 min and then with the secondary antibodies targeting the primary ones together with the conjugated primary antibody labelling the postsynaptic AChRs: the α-bungarotoxin (α-BTX, Invitrogen). Conjugated anti-mouse and anti-rabbit Alexa Fluor™ 488 (Invitrogen) were diluted 1:500 in blocking solution and incubated for 120 min at room temperature under dark conditions together with TRITC-conjugated α-BTX. At the end, repeated washes in PBS were made and in between, samples were plunged in DAPI 1:5000 in PBS for 5 min to mark the nuclei, and then repeatedly washed in PBS. Finally, muscles preparations were stored for short terms in PBS at 4° C protected from excessive light exposure prior to imaging.

Samples were then mounted on glass slides in VECTASHIELD Vibrance® Antifade Mounting Medium (Vector Laboratories, US) and acquired on a TCS SP8 confocal laser scanning microscope (Leica Microsystems, Heidelberg, Germany). Confocal settings were optimized to achieve the best compromise between image quality and acquisition rate: 8-bit depth, 512 × 512 frame size, ×20 magnification, ×2 zoom and 1 µm z-stack interval, with sequential image acquisition to minimize bleed through (red channel—543 nm excitation, 565–615 nm collection; green channel—488 nm excitation, 500–550 nm collection). Confocal micrographs of immunolabelled mouse NMJs were acquired from whole-mounted muscle preparations using standard image capture approaches. For accurate analysis, each image captured a single en-face NMJ with a short length of its terminal axon in the centre of the field of view. NMJs that were partially oblique to the field of view were only included if the oblique portion constituted less than approx. 10% of the total area. All image analyses were performed on maximum intensity projections of the z-stacks, using Image J software and related plugins (BinaryConnectivity). Specific analyses of NMJ morphology and characteristics were assessed as previously finely described by Gillingwater lab, in which the group was able to develop the “NMJ-morph” workflow, specifically designed to facilitate quantitative analysis of both pre and

postsynaptic structures at the NMJ, based on a standardized and repeatable workflow suitable for use on confocal z-stack projections of individual NMJs. In total, 21 individual morphological variables were evaluated into the NMJ-morph platform, divided into 'core variables', 'derived variables' and 'associated nerve and muscle variables', following the flowchart by using standard ImageJ functions as depicted in the panel below. At the end, about 40 NMJ structures were analysed per experimental group.

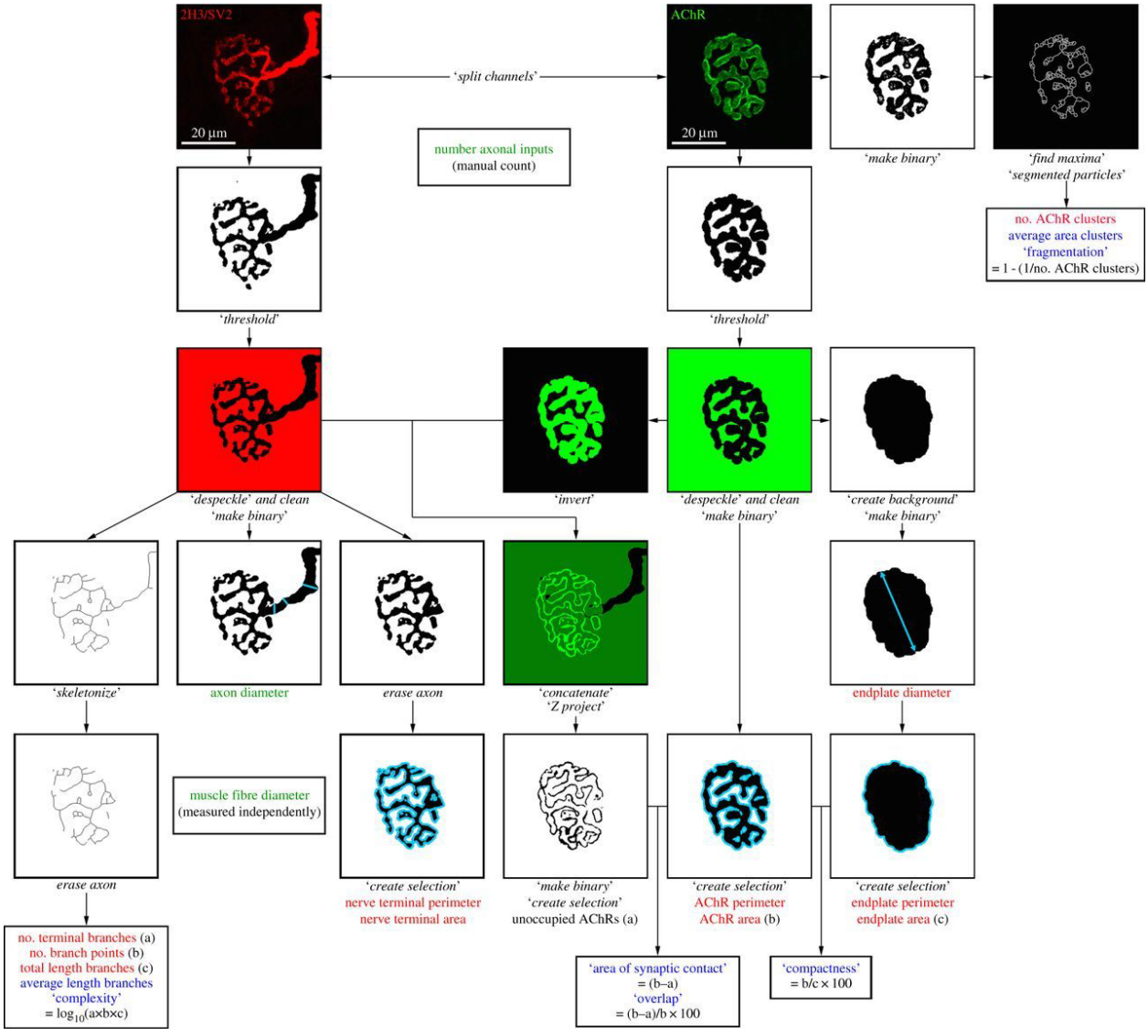

Figure 12. Representative scheme depicting all the passages/commands to perform manual NMJ morphological analyses. *21 morphological variables can be analysed following this flowchart. Taken from Jones et al, 2016.*

Western Blot Analysis

For decades, the Western Blot technique represents a major technique that allows the separation and identification of proteins. This task is accomplished by a first separation of proteins based on

molecular weight through electrophoresis on a polyacrylamide gel. Then, separated lysates are transferred up to a high-affinity protein membrane, whether it is a nitrocellulose or Polyvinylidene Fluoride (PVDF) membrane. Finally, target proteins are marked thanks to the natural specificity of primary antibodies to recognize specific epitopes discriminative from all the protein content. Secondary antibodies species-specific bind then to the primary ones, and the conjugation with fluorophores or peroxidases allows an easy detection of the signal through coloured products or chemiluminescence methods.

For the preparation of proteins, still frozen muscles were pulverized in a steel mortar using a ceramic pestle, with the constant addition of liquid nitrogen in order to maintain muscle components' properties. The powder thus obtained was homogenized with a lysis buffer containing 20mM Tris-HCl, 1% Triton X-100, 10% glycerol, 150 mM NaCl, 5 mM EDTA, 100 mM NaF and 2mM NaPPi supplemented with protease inhibitor 5X, phosphatase inhibitors 1X (Protease Inhibitor Cocktail, Sigma-Aldrich) and 1 mM PMSF. The lysis of tissue was performed on ice for 40 min. The homogenate obtained was centrifuged at 13500 rpm for 20 min at 4° C and the supernatant was transferred to clean Eppendorf® tubes and stored at -80° C until use. Quantification of proteins was performed as previously described, using the RC-DC™ (reducing agent and detergent compatible) protein assay (Bio-Rad) and measuring concentration of proteins at 750 nm wavelength, taking advantage of a reference standard curve made up by known concentrations of BSA.

The previously prepared and quantified samples were mixed in a buffer called Laemmli Buffer 4X (8% SDS, 20% β-mercaptoethanol, 40% glycerol, 0.25 M Tris-HCl pH 6.8 and bromophenol blue traces; Laemmli, 1970). SDS is an anionic detergent that strongly binds to and intercalates to proteins in a ratio of one anion every two amino acids of the polypeptide chain, firstly favouring the denaturation of proteins in combination with other reducing agents (β-mercaptoethanol), which promote the loss of the secondary and tertiary structures associated and then cancel differences in electric charge, rendering the proteins negatively charged. Proteins can thus be well resolved in accordance with their molecular weight during the electrophoretic run. To enable visualization of the migration of proteins it is common to include in the loading buffer a small anionic dye molecule (i.e. bromophenol blue). Since the dye is anionic and small, it will migrate faster than any other component in the mixture to be separated and will provide a migration front to monitor the separation progress. We arbitrarily set the end volume of the wells to 16 µl so Laemmli Buffer 4X was added referred to this value. The total amount of protein loaded into gels depends on the

expression level of the target protein evaluated by a linear standard curve prior to saturation signals that we assessed and at the end PBS 1X was added in order to reach the end volume. 40 µg of lysates are standardly used for phosphoprotein evaluations. To allow complete denaturation, samples were left at 95° C for 5 min. After 5 min at room temperature to acclimate, samples were ready to be loaded on SDS-PAGE.

For all the experiments performed in this study, a gradient Precast gel purchased from Bio-Rad (AnykD or 4-20% gradient) was used. In these gels, the percentage of the acrylamide/bisacrylamide polymers varies uniformly from a lower percentage in the upper part to a higher concentration at the bottom of the gel, designed to provide a complete and well-resolved molecular weight protein separation pattern (300 kDa-5 kDa), being these percentages the reflection of the pore sizes created by the polymerizing net of acrylamide/bisacrylamide. Equal amounts of protein sample were loaded on the gel and subjected to electrophoresis. Due to the elevated number of samples under investigation, a reference sample is prepared and loaded in every gel during the same experimental session to then make the comparison possible among the samples. Electrophoretic run was carried out at constant current (100V) for about 2 hours in a running buffer at pH 8.8 (25mM Tris, 192Mm Glycine, 1% SDS, Bio-Rad). To monitor protein separation, a protein molecular weight marker constituted by a mixture of proteins with known molecular weight (Preistained Protein Ladder Marker, Bio-Rad) was loaded on the gel. At the end of the gel run, the electrophoretic apparatus was disassembled and the gel recovered for the next step.

In order to make the proteins accessible to antibody detection, they were moved from within the gel onto a membrane made of nitrocellulose or PVDF. Their disposition and organization are maintained by applying an electric field in which the proteins still negatively charged migrate from the negative (gel) to the positive (membrane) pole (the assembly of the so-called "sandwich" is shown in Figure 13). As a result of "blotting" process, the proteins are exposed on a thin surface layer for detection (see below). Protein binding is based upon hydrophobic interactions, as well as charged interactions between the membrane and protein. In this study, the proteins resolved by electrophoresis were transferred (blotted) to a PVDF membrane that needed to be activated for few seconds in methanol. The transfer was carried out at constant voltage at 100V for 2 hours at 4° C or at constant 35mA overnight (O/N) in a cold transfer buffer containing 25 mM Tris, 192 mM Glycine and 20% methanol. The effective protein transfer to the membrane was verified by staining with Ponceau S (Merck) red staining in acetic acid (0.2% Ponceau S in 3% acetic acid) for 15 min under

gentle shacking at room temperature, followed by washes to remove the excess and clear the membrane.

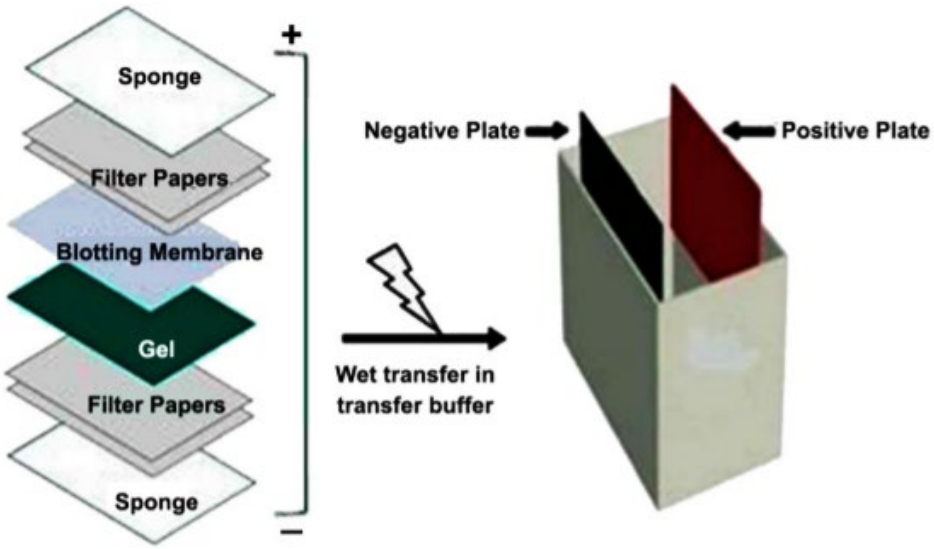

Figure 13. A schematic example of the Western Blot assembly for protein transfer. *The so-called "sandwich" is thus prepared, to allow the transfer of the negatively charged proteins onto the membrane, following the electric flow through the positive pole. Adapted from www.thermofisher.com*

To minimize the background, nonspecific binding sites present on the PVDF membrane were saturated with a blocking solution consisting of 5% fat-free milk in TTBS 1X (0.02 M Tris, 0.05 M NaCl and 0.1% Tween-20) for 2 hours at room temperature with constant shaking. At the end of incubation, the membrane was washed with TTBS 1X for three times 10 min each and incubated O/N at 4° C with the specific primary antibody appropriately diluted in a solution of TTBS 1X containing 5% BSA or 5% fat-free milk (depending on specificities of antibodies by datasheet) (Table 1). Subsequently, the membrane was washed three times in TTBS 1X and then incubated 1 hour at room temperature at constant agitation, with a secondary antibody diluted suitably as previously referred to as primary antibodies. The nature of secondary antibodies depends on the species from which the primary ones in use were produced, but with the peculiarity of being conjugated with the enzyme HRP (Horseradish Peroxidase). After removing the excess of antibodies used with three washes of 10 min each in TTBS 1X, the last one was made in TBS 1X (0.02 M Tris and 0.05 M NaCl). Proteins detection was made using the Amersham ECL Select™ detection system (Cytiva Life Sciences, ex GE Healthcare) which highlights the HPR substrate by a chemiluminescent reaction. The membrane was gained through the analysis software ImageQuant™ LAS 4000 (GE Healthcare Life

Sciences) and the exposure time adjusted in an automatic manner or editable depending on the intensity of the emitted signal.

Protein target	*Antibody dilution*	*Host species*	*Company*	*Indicative pathway*
p-Akt (Ser473)	1:1000 in BSA 5%	In rabbit	Cell Signalling	Protein synthesis
Akt	1:1000 in BSA 5%	In rabbit	Cell Signalling	Protein synthesis
p-mTOR (Ser2448)	1:1000 in BSA 5%	In rabbit	Cell Signalling	Protein synthesis
mTOR	1:1000 in BSA 5%	In rabbit	Cell Signalling	Protein synthesis
p-p70S6K (Thr389)	1:1000 in BSA 5%	In rabbit	Cell Signalling	Protein synthesis
p70S6K	1:1000 in BSA 5%	In rabbit	Cell Signalling	Protein synthesis
p-S6 (Ser235/236)	1:1000 in BSA 5%	In rabbit	Cell Signalling	Protein synthesis
S6	1:1000 in BSA 5%	In rabbit	Cell Signalling	Protein synthesis
p-AMPK (Thr172)	1:1000 in BSA 5%	In rabbit	Cell Signalling	Protein synthesis
AMPK	1:1000 in BSA 5%	In rabbit	Cell Signalling	Protein synthesis
TOM20	1:1000 in Milk 5%	In rabbit	Santa Cruz	Mitochondrial mass
Citrate Synthase	1:2000 in Milk 5%	In rabbit	Abcam	Mitochondrial mass
SIRT1	1:1000 in BSA 5%	In mouse	Cell Signalling	Metabolism
PGC1α	1:1000 in Milk 5%	In rabbit	Abcam	Metabolism
p62	1:1000 in Milk 5%	In rabbit	Cell Signalling	Autophagy
LC3B II / I	1:1000 in Milk 5%	In rabbit	Abcam	Autophagy
PINK1	1:500 in Milk 5%	In rabbit	Invitrogen	Mitophagy
Parkin	1:1000 in Milk 5%	In rabbit	Invitrogen	Mitophagy
Mfn1	1:1000 in Milk 5%	In mouse	Abcam	Mitochondrial dynamics
Mfn2	1:1000 in Milk 5%	In rabbit	Abcam	Mitochondrial dynamics
OPA1	1:3000 in Milk 5%	In mouse	Abcam	Mitochondrial dynamics

p-DRP1 (Ser616)	1:1000 in BSA 5%	In rabbit	Cell Signalling	Mitochondrial dynamics
p-DRP1 (Ser637)	1:1000 in BSA 5%	In rabbit	Cell Signalling	Mitochondrial dynamics
DRP1	1:1000 in BSA 5%	In rabbit	Cell Signalling	Mitochondrial dynamics
Fis1	1:1000 in Milk 5%	In rabbit	Abcam	Mitochondrial dynamics
p-MuSK (Tyr755)	1:1000 in Milk 5%	In rabbit	Abcam	Postsynaptic scaffold
MuSK	1:1000 in Milk 5%	In rabbit	Abcam	Postsynaptic scaffold
Neurofilament H	1:1000 in Milk 5%	In mouse	Cell Signalling	Presynaptic organization
Neurofilament L	1:1000 in BSA 5%	In rabbit	Cell Signalling	Presynaptic organization
Xanthine Oxidoreductase	1:1000 in Milk 5%	In rabbit	Abcam	Nitrate metabolism
Sialin	1:1000 in Milk 5%	In rabbit	Abcam	Nitrate metabolism
GAPDH	1:3000 in Milk 5%	In rabbit	Abcam	Housekeeping
HRP-conjugated α-mouse	1:5000 in Milk 5%	In donkey	Dako	Secondary antibody
HRP-conjugated α-rabbit	1:10000 in Milk 5%	In donkey	Cell Signalling	Secondary antibody

Table 1. List of antibodies used for Western Blot evaluations. *GAPDH is the housekeeping used for normalization. Secondary antibodies are the last two of the list.*

The inverted bands presented on the scanned images were quantified with Adobe Photoshop program and a BAP value (Brightness Area Product), given by the product of the brightness and the area of the band itself, is defined. The target protein levels were then normalized with respect to the amount of a housekeeping protein (ubiquitously and stably expressed and well conserved in any of the conditions under investigation), or evaluated between two different isoforms (as for example a phosphorylated and unphosphorylated total forms) of the same protein. The housekeeping protein is a protein ubiquitously and stably expressed in the cells and well conserved in any of the conditions under investigation at high rates and so GAPDH (glyceraldehyde 3-phosphate dehydrogenase, a key cytoplasmic enzyme involved in glycolysis) was chosen for this duty. Data were expressed as the ratio between the BAP of target protein and of housekeeping/total protein form (arbitrary units, AU).

Western Blot for poli-Ubiquitinated proteins

Following the previously well described procedure for general Western Blot protocol, the detection of poli-Ubiquitinated proteins was performed in a similar way. 15 µg of quantified proteins were prepared with adjusted amounts of Laemmli Buffer 4X and PBS 1X and denatured at 95° C for 5 min. Following 5 min of acclimation at room temperature, a protein molecular weight marker and samples were loaded on gradient Precast acrylamide/bisacrylamide gels (Bio-Rad) and electrophoresis was carried out at constant current (100V) for about 2 hours in running buffer. At the end of the gel run, gels underwent transfer of proteins to a nitrocellulose membrane which, unlike PVDF membrane, do not need to be activated in methanol. The transfer was carried out at constant voltage at 100V for 2 hours at 4° C or at constant 35mA overnight (O/N) in cold transfer buffer. The effective protein transfer onto the membrane was verified by staining with Ponceau S red staining in acetic acid for 15 min under gentle shacking at room temperature, followed by washes to remove the excess and clear the membrane.

Then, nonspecific binding sites present on the nitrocellulose membrane were saturated with a blocking solution consisting of 2% BSA in TTBS 1X for 2 hours at room temperature with constant shaking. At the end of incubation, the membrane was washed with TTBS 1X for three times 10 min each and incubated O/N at 4° C with the specific primary antibody against mono- and poly-ubiquitinated proteins (1:2000, EnzoLife) in 2% BSA in TTBS 1X. Subsequently, membranes were washed three times in TTBS 1X and then incubated 1 hour at room temperature with constant agitation, with the HRP-conjugated donkey anti-mouse secondary antibody (1:5000, Dako) in 5% fat-free milk in TTBS 1X. After final three washes of 10 min each in TTBS 1X, the last one was made in TBS 1X. Proteins detection was made by using Amersham ECL Select™ detection system (Cytiva Life Sciences, ex GE Healthcare) and the membrane was gained through the ImageQuant™ LAS 4000 software (GE Healthcare Life Sciences), with the exposure time adjusted in an automatic manner or editable depending on the intensity of the emitted signal. Analysis of these protein signals occurred as previously mentioned, with the exception of the normalization passage, performed with respect to the amount of total protein content evaluated in the nitrocellulose membrane through a digitalized image of the membrane stained with Ponceau S. Data were expressed as the ratio between the BAP of target protein and of total protein amount stained with Ponceau S (arbitrary units, AU).

Western Blot for OXPHOS

Following the previously well described procedure for general Western Blot protocol, the detection of the five mitochondrial complexes that make up the respiratory chain can be performed in the same PVDF membrane by using a cocktail of the five antibodies targeting the five proteins. 5 µg of quantified proteins were prepared with adjusted amounts of Laemmli Buffer 4X and PBS 1X and denatured at 37° C for 5 min. Following 5 min of acclimation at room temperature, a protein molecular weight marker and samples were loaded on gradient Precast acrylamide/bisacrylamide gels (Bio-Rad) and electrophoresis was carried out at constant current (100V) for about 2 hours in running buffer. At the end of the gel run, gels underwent transfer of proteins to a PVDF membrane prior to methanol activation. The transfer was carried out at constant voltage at 100V for 2 hours at 4° C or at constant 35mA overnight (O/N) in cold transfer buffer.

Then, nonspecific binding sites present on the PVDF membrane were saturated with a blocking solution consisting of 5% fat-free milk in TTBS 1X for 2 hours at room temperature with constant shaking. After that, membranes were washed three times, 10 min each, with TTBS 1X and incubated O/N at 4° C with the specific primary antibody against the mitochondrial complexes of the respiratory chain (OXPHOS 1:1000, Abcam) in 5% fat-free milk in TTBS 1X. Subsequently, membranes were washed three times in TTBS 1X and then incubated 1 hour at room temperature in constant agitation, with the HRP-conjugated donkey anti-mouse secondary antibody (1:10000, Dako) in 5% fat-free milk. After final three washes of 10 min each in TTBS 1X, the last one was made in TBS 1X. Proteins detection was made by using Amersham ECL Select™ detection system (Cytiva Life Sciences, ex GE Healthcare) and membranes gained through the ImageQuant™ LAS 4000 software (GE Healthcare Life Sciences), with the exposure time adjusted in an automatic manner or editable depending on the intensity of the emitted signal. After, to visualize the total protein amount present on the membrane, these were subjected to a Coomassie PVDF-specific staining (0.1 % Coomassie Blue R-250, 50 % Methanol, 10 % Acetic Acid) for 20 min and destained with a destain solution composed by 40% Methanol and 10% Acetic Acid. Air dried membranes were then digitalized with a scanner and analysed. Data were expressed as the ratio between the BAP of samples from each of the five complexes and of total protein amount stained with Coomassie (arbitrary units, AU).

Gene Expression Analysis

- *RNA extraction from muscle tissue*

Frozen muscle tissues were pulverized using a sterile pestle and mortar previously treated with RNase Zap (Sigma-Aldrich) to remove any trace of RNase presence. Approximately 20 mg of powder

of each sample was used to RNA extraction with SV Total RNA Isolation System (Promega, Italia). The successful isolation of intact RNA requires four essential steps: (i) effective disruption of cells or tissue, (ii) denaturation of nucleoprotein complexes, (iii) inactivation of endogenous ribonuclease (RNase) activity and (iv) removal of contaminating DNA and proteins. The most important step is the immediate inactivation of endogenous RNases that are released from membrane-bound organelles upon cell disruption. The SV Total RNA Isolation System combines the disruptive and protective properties of guanidine thiocyanate (GTC) and β-mercaptoethanol to inactivate the ribonucleases present in cell extracts. GTC, in association with SDS, acts to disrupt nucleoprotein complexes, allowing the RNA to be released into solution and isolated free from proteins. Dilution of cell extracts in the presence of high concentrations of GTC causes selective precipitation of cellular proteins, while the RNA remains in solution. After centrifugation to clear the lysate of precipitated proteins and cellular debris, the RNA is selectively precipitated with ethanol and bound to the silica surface of the glass fibres found in the Spin Basket. By effectively clearing the lysate of precipitated proteins and cellular debris, these cleared lysates may be bound to the Spin Baskets by a centrifugation filtration method. The binding reaction occurs rapidly due to the disruption of water molecules by the chaotropic salts, thus favouring the absorption of nucleic acids to the silica. RNase-Free DNase I is applied directly to the silica membrane to digest contaminating genomic DNA. The total bound RNA is further purified from contaminating salts, proteins and cellular impurities by simple washing steps. Finally, the total RNA is eluted from the membrane by the addition of Nuclease-Free Water. This procedure yields an essentially pure fraction of total RNA after only a single round of purification without organic extractions or precipitations. Quantification of extracted RNA was then performed by using the Nano Drop. Basically, a drop of an mRNA sample (equal to 2 µl) is exposed to ultraviolet light at 260 nm and, through a photodetector, the light that passes through the sample is measured. The more the light is absorbed by the sample, the higher the concentration of nucleic acid content is. We also evaluated any contamination by proteins and aromatic components by evaluating the ratio of the absorbance at 260 and 280 nm (A260/280), which for pure RNA is ~1.98-2.

In order to measure messenger RNA (mRNA), it is necessary to convert mRNA into complementary DNA (cDNA) by the activity of a reverse transcriptase enzyme. The nucleic acid product will be then amplified by Real Time PCR. In this study, 300 ng of RNA for each sample were reverse transcribed using the Superscript III enzyme (Invitrogen). The protocol was as follows: in 300 ng of RNA of each sample were added 1 µl of random primers, 1 µl of deoxyribonucleosides (dATP, dGTP, dCTP and

dTTP 10mM each at neutral pH) and RNase-free water to reach the end volume of 13.5 µl. The mix obtained was denatured at 65° C for 5 min to eliminate secondary complex structures and incubated on ice for at least 1 min. Then, 4 µl of First-Strand Buffer 5X, 1 µl of DTT 0.1M, 1 µl of RNaseOUT™ Recombinant RNase Inhibitor (40 units/µl) and 0.5 µl of SuperScript™ III RT (200 units/µl) were added. The mixture thus composed was incubated at 25° C for 5 min and at 50° C for 60 min (annealing and extension steps). After that, the temperature was increased to 70° C for 15 min to inactivate the reaction and the samples stored at 4° C, or eventually stored at -20° C for further analyses.

- *Primer evaluation*

Primers were previously designed using Primer3Plus (Bioinformatics) software, and tested in order not to pair to each other. Moreover, they were purchased lyophilized from Sigma-Aldrich Company and resuspended in sterile water at the final concentration of 100 µM. The concentration suitable for the Real Time PCR protocol is 50 µM each. They are currently available stored at -20° C. The primers used for this project are listed below (Table 2).

Gene target	*Forward 5' – 3'*	*Reverse 5' – 3'*	*Indicative pathway*
MuRF1	ACCTGCTGGTGGAAAACATC	CTTCGTGTTCCTTGCACATC	Catabolism
Atrogin-1	GCAAACACTGCCACATTCTCTC	CTTGAGGGGAAAGTGAGACG	Catabolism
HDAC4	CAGACAGCAAGCCCTCCTAC	AGACCTGTGGTGAACCTTGG	Denervation
Gadd45α	GAAAGTCGCTACATGGATCAGT	AAACTTCAGTGCAATTTGGTTC	Denervation
MyoG	GTGCCCAGTGAATGCAACTC	CGAGCAAATGATCTCCTGGGT	Denervation
Runx1	CGGTAGAGGCAAGAGCTTCAC	CGGGCTTGGTCTGATCATCT	Denervation
NCAM1	TGTTCAAGCAGACACACCGT	GGTTTCCACTCAGAGGCGAG	Denervation
AChRα	GTAGAACACCCAGTGCTTCCA	GCCCGACCTGAGTAACTTCAT	Postsynaptic scaffold
AChRγ	CCTGTGGATATTGAGGGTGCC	CCAGTAGATACAACCGTCGGG	Postsynaptic scaffold
SIRT1	Purchased from TaqMan® (Promega)		Metabolism
PGC1α	ACCCCAGAGTCACCAAATGA	CGAAGCCTTGAAAGGGTTATC	Metabolism
TFAM	Purchased from TaqMan® (Promega)		Metabolism
p62	CCCAGTGTCTTGGCATTCTT	AGGGAAAGCAGAGGAAGCTC	Autophagy
BNIP3	TTCCACTAGCACCTTCTGATGA	GAACACCGCATTTACAGAACAA	Autophagy

IGF1	CTCAGAAGTCCCCGTCCCTA	ATTTTCTGCTCCGTGGGAGG	Metabolism
BDNF	TGGCCCTGCGGAGGCTAAGT	AGGGTGCTTCCGAGCCTTCCT	Presynaptic organization
NT4	AGCGTTGCCTAGGAATACAGC	GGTCATGTTGGATGGGAGGTATC	Presynaptic organization
GAPDH	CACCATCTTCCAGGAGCGAG	CCTTCTCCATGGTGGTGAAGAC	Housekeeping

Table 2. List of primers used for rt-PCR evaluations. *GAPDH is the housekeeping used for normalization. Both primers (forward and reverse) are written in 5' -> 3'.*

- *Real Time PCR*

Real Time Polymerase Chain Reaction (rt-PCR) is the ability to monitor the progress of the PCR as it occurs (i.e. in real time) and represents a quantitative method for the amplification of DNA. The reaction is characterized by the point in time during cycling when amplification of a target achieves a fixed level of fluorescence rather than the amount of traditional PCR product accumulated after a fixed number of cycles (PCR end-point). Data is therefore collected throughout the PCR process, rather than at the end of the PCR. To make this possible, the use of fluorescent molecules or probes is required, which allow following in real time and quantifying the amplification reaction. In our case, the SYBR Green I dye probe is used, a highly specific, double-stranded DNA binding fluorescent molecule that is able to detect all double-stranded DNA, including non-specific reaction products through binding to the minor groove of the DNA double helix. This is the reason why a primer evaluation is required in order to eliminate any chance to have artefacts in fluorescence levels given by primer pairs or amplification of unwanted genes.

cDNA samples were prepared using the SYBR™ Green PCR Master Mix (Applied Biosystems, Warrington, UK) consisting of a HotStart Taq DNA Polymerase, a SYBR Green I probe, $MgCl_2$ at a concentration of 5 mM, dNTPs and the fluorescent ROX passive reference dye. The latter serves as an internal reference to normalize the signal emitted by the SYBR Green I probe, thereby enabling to correct possible variations between the wells due to experimental errors and/or due to fluctuations of the fluorescence. For each gene to be studied, the reaction was carried out in duplicate. The mixture is thus composed: 15 µl of SYBR Green PCR Master Mix 2X, 0.6 µl of oligo primers (50 µM) specific to each gene, 3 µl of cDNA mold of each sample and 12 µl of sterile H_2O to bring to an end volume of 30 µl. The reaction was performed using the AB PRISM 7500 instrument (Applied Biosystems, Warrington, UK). The protocol used for the reaction of gene amplification consists of four steps: a pre-incubation cycle of 10 min at 95° C to activate the HotStart Taq polymerase and denature the cDNA. 45 cycles of amplification, each of them divided into a phase in

which the sample is brought to 95° C for 15 sec for denaturation, a step of 60 sec at 60° C in which there is the annealing of primer and a step of 30 sec at 72° C in which the elongation of the cDNA strand occurs. In this last phase, the probe intercalates cDNA and acquires the basic fluorescence to be quantified.

- *Analysis of Melting curve*

Through the analysis of a graph, in which the abscissa is the number of cycles and the ordinate the logarithm of the fluorescence (Rn), a sigmoid is obtained for each sample, in which three phases can be discrimined: a flat trend, a region of exponential increase and a plateau phase (Figure 14). An amplification plot graphically displays the fluorescence detected over the number of cycles that were performed.

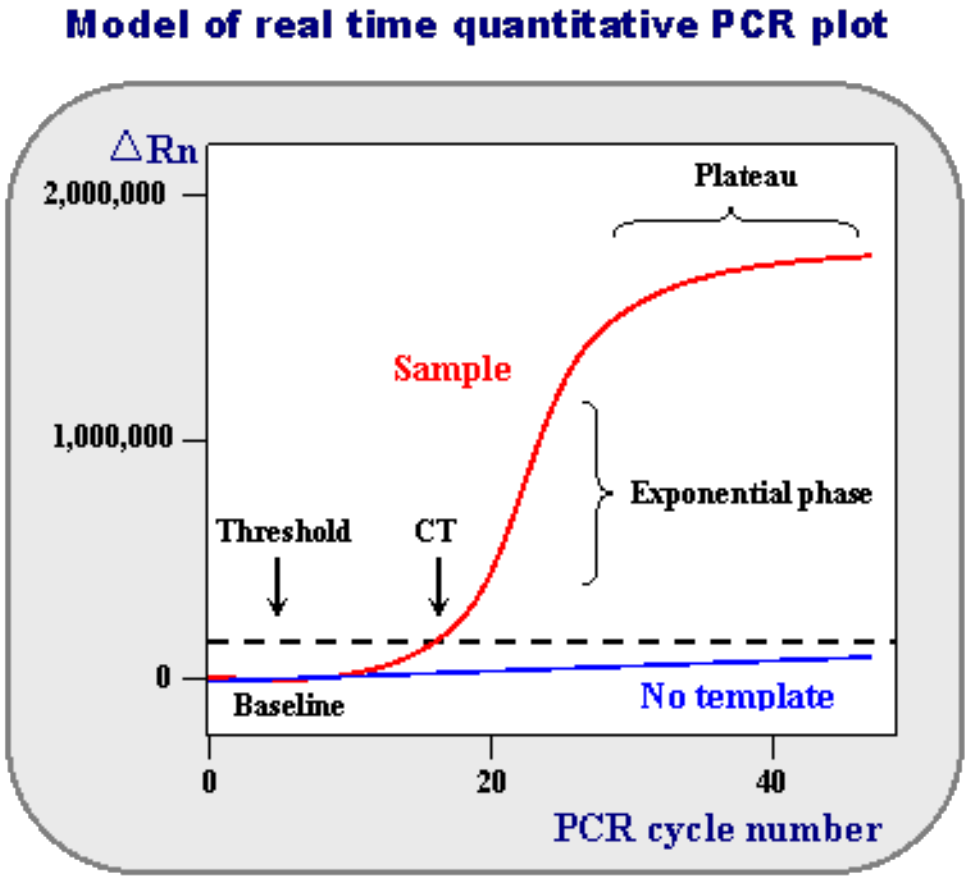

Figure 14. Model of a single sample amplification plot. *In the baseline, no significant change in fluorescence signal (Rn) occurs; in the exponential phase, fluorescence signal increases in proportion to the increasing formation of amplification products. The threshold line is the level of fluorescence signal automatically determined by the software and it is set to be above the baseline and sufficiently low to be within the exponential growth region of the amplification curve. The Ct cycle is the number of*

amplification cycles when the fluorescence signal cross the threshold (from https://www.ncbi.nlm.nih.gov/genome/probe/doc/TechQPCR.shtml).

As schematized in Figure 14, during the initial cycle of PCR there is no significant change in fluorescence signal. This predefined range of PCR cycles is called baseline. The software generates a baseline subtracted amplification plot by calculating a mathematical trend using Rn values (the fluorescence emission intensity of the reporter dye) corresponding to the baseline cycles. Then, on the amplification plot, an algorithm searches for the point at which the ΔRn (Rn - baseline) crosses the threshold. The fractional cycle at which this occurs is defined as the Ct. Data is automatically analysed by the software once you have chosen the central point of the exponential part of the curve for the sample with the highest concentration (the one that reaches the loop-line after a smaller number of cycles). In the relative quantification, the concentration of the gene of interest (target) is expressed as a function of the concentration of a reference gene (housekeeping gene), which is assumed to be constant between the different tissues of an organism, in all stages of development (constitutively expressed) and should not suffer modifications due to the experimental treatment. In our case, to normalize the samples it was chosen the housekeeping gene GAPDH (Glyceraldehyde 3-phosphate dehydrogenase). The ΔCt was calculated by subtracting the Ct of control mice (Young CTRL) to the Ct of Old groups for both target genes and housekeeping gene. Values thus obtained by the target genes were normalized on the values obtained by the housekeeping gene.

Statistical Analysis

Data are represented as mean values ± SD. Data were tested for normal distribution by the Shapiro-Wilk test. The statistical significance of differences between two groups (Young CTRL vs Old CTRL) was evaluated by Student's t-test (unpaired, 2-tailed) with Welch's correction. The statistical significance of differences between more than two groups (Old groups) was evaluated by ordinary one-way ANOVA followed by the Tukey multiple comparisons using statistical hypothesis testing. The level of significance was set at $p < 0.05$. The statistical analyses were performed by GraphPad Prism software (GraphPad Software, San Diego, CA, USA).

RESULTS AND DISCUSSION

1. Age-related changes in male wild-type mice

1.1 Body composition, muscle phenotype and muscle mass

Body weight of Young CTRL (7-months old) and Old CTRL (24-months old) male mice was measured prior to sacrifice. Following hindlimb muscle dissection, the four major muscles that compose the posterior legs of the mouse (Gastrocnemius, Soleus, Tibialis Anterior and Extensor Digitorum Longus) were weighted and compared between the two cohorts (Table 3). The choice to dissect and analyse these muscles finds its basis in the variegated phenotypic characteristics that each muscle has, in parallel with the different roles they cover in the activity of the hindlimb (postural or movement).

	Young CTRL	**Old CTRL**
Age (mo)	7	24
n	8	7
Body weight (gr)	31 ± 1.92	35.14 ± 4.67
Individual weights of hindlimb muscle (normalized on body weight)		
Gastrocnemius (mg)	5.48 ± 0.43	3.94 ± 0.25 ****
Soleus (mg)	0.33 ± 0.01	0.25 ± 0.01 ****
Tibialis Anterior (mg)	1.79 ± 0.20	1.37 ± 0.16 ***
Extensor Digitorum Longus (mg)	0.36 ± 0.03	0.28 ± 0.02 ***

Table 3. Body weight of mice and individual weights of hindlimb skeletal muscles. *Body weights are expressed in grams (gr) and are presented as the means ± SD. Weights of hindlimb muscles are the resultant of the weight of isolated muscles normalized by the body weight of the mouse, depicted as means of left and right muscles and expressed in milligrams (mg). The * denotes a significant difference among the groups. Difference is considered significant when P < 0.05.*

Body weight, the first line of evaluation of body mass, increased in old littermates even if no significance is valuable ($p = 0.06$). On the other hand, individual hindlimb muscles normalized per body weight showed a strong significant decrease in their weight, assessing a loss of muscle mass at the level of the hindlimb. The effects of ageing in these parameters suggested us a decrease of muscle mass, the main parameter used to decree a sarcopenic profile, in a physiological system that replaced this mass with other tissues (i.e. adipose tissue and fibrotic infiltrations, see Figure 17, panel a/c).

In order to characterize the phenotype of aged mice in comparison with a young cohort, different muscles were taken under investigation to have a plenary scenario of the time window we were evaluating and discriminate the key features representative of ageing. Gastrocnemius, a massive muscle involved in movement and posture, Soleus mainly recruited in postural maintenance, and Diaphragm, the major respiratory muscle, were evaluated in their phenotypic profile by assessing the percentage of myosin heavy chain (MHC) fast and slow isoforms on transversal sections (Figure 15).

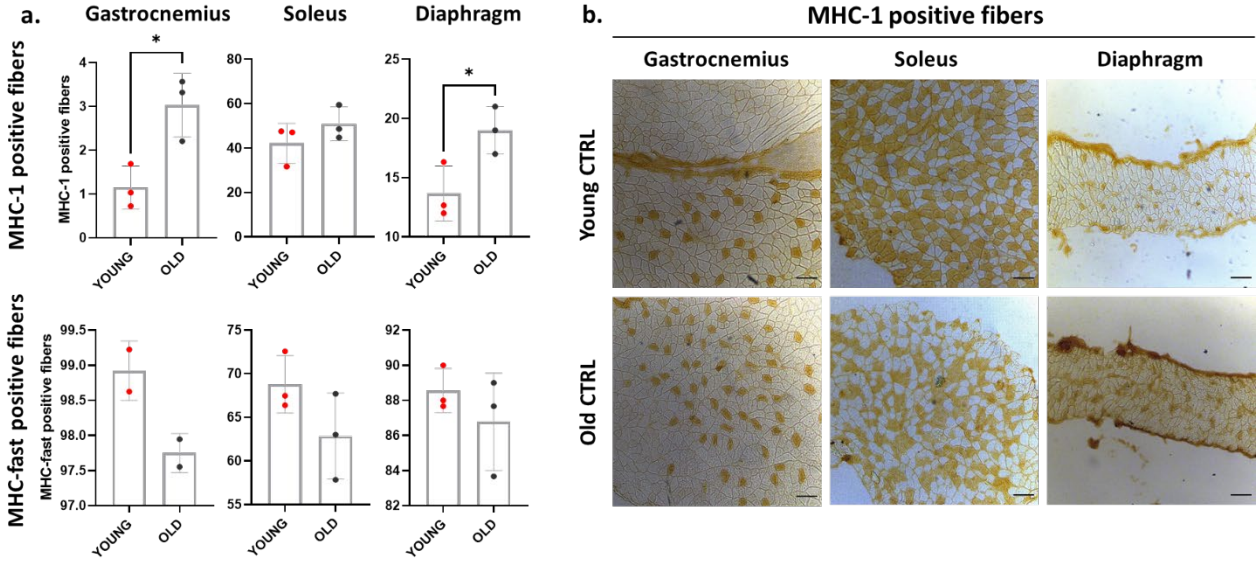

Figure 15. Immunohistochemical analyses for the evaluation of MHC isoforms that constitute the muscles under investigation*. a) graphic representation of Gastrocnemius, Soleus and Diaphragm evaluated in their MHC content. First row expresses the percentage of fibers positive for MHC-1 isoform over the entire fiber population; second row expresses the percentage of fibers positive to MHC-fast isoforms over the entire fiber population. Exception is made by diaphragm, where the percentage is calculated over a fixed amount of cells (300), due to a partial dissection of this muscle, even involved in other evaluations. The * denotes a significant difference among the groups. Difference is considered significant when P < 0.05. b) Representative images of IHC in muscles subjected to MHC-1 specific staining, scale bar 100 µm.*

Elderly muscles showed a significant increase in slow MHC-1 positive fibers, except for Soleus, and no significative changes in the presence of MHC-fast positive fibers, with a visible tendency to decrease in all the three old muscles under investigation. The reduced experimental number studied could be explicative of a missing significant difference in some cases. An increase in oxidative fibers within a muscle is notoriously associated with ageing (Brocca *et al*, 2017): an augment in slow MHC expression can be the resultant of a gradual shift of isoforms from the glycolytic to the oxidative ones. This event favours the protection of the muscle from atrophy and loss of fibers due to degeneration. Glycolytic fast fibers are the ones more susceptible to detrimental stimuli and ageing

can cause a numerical reduction of those fibers with consequent loss of mass (Nilwik *et al*, 2013), while oxidative ones are more resistant to this outcome, in an effort to reduce muscle mass loss and preserve it. In our experimental groups, old mice fitted perfectly into an oxidative phenotypic scenario, independently from muscle type. Soleus, which is representative of a highly oxidative muscle, did not show any significant variance in MHC composition, speculating that the oxidative component was not particularly affected and so this muscle was preserved from an age-dependent MHC isoform shift.

Regarding loss of muscle mass, a relatable parameter useful to assess atrophy is the analysis of the cross sectional area (CSA), by means the average area of transversal fibers (Figure 16). We measured the CSA of Gastrocnemius, Soleus and Diaphragm of young and elderly mice and we assessed a significant reduction of the fibers' areas in Gastrocnemius, which is strongly linked to the isolated dissected muscle weight shown in Table 3. Despite the overt atrophy of Gastrocnemius fibers, Soleus and Diaphragm did not show significant loss of mass, in accordance with the literature, in which selective atrophy of fast glycolytic fibers is assessed (Greising *et al*, 2013; Mobley *et al*, 2017). Considering that Soleus is mainly composed by oxidative fibers and Diaphragm of 24-mo mice displays a shift in favour of slow fibers, it is not surprising that atrophy is not strongly visible: the function of these two muscles, mainly involved in postural maintenance and respiration, needs to be maintained and their activity so stimulated because of their requirement throughout the lifespan of an individual.

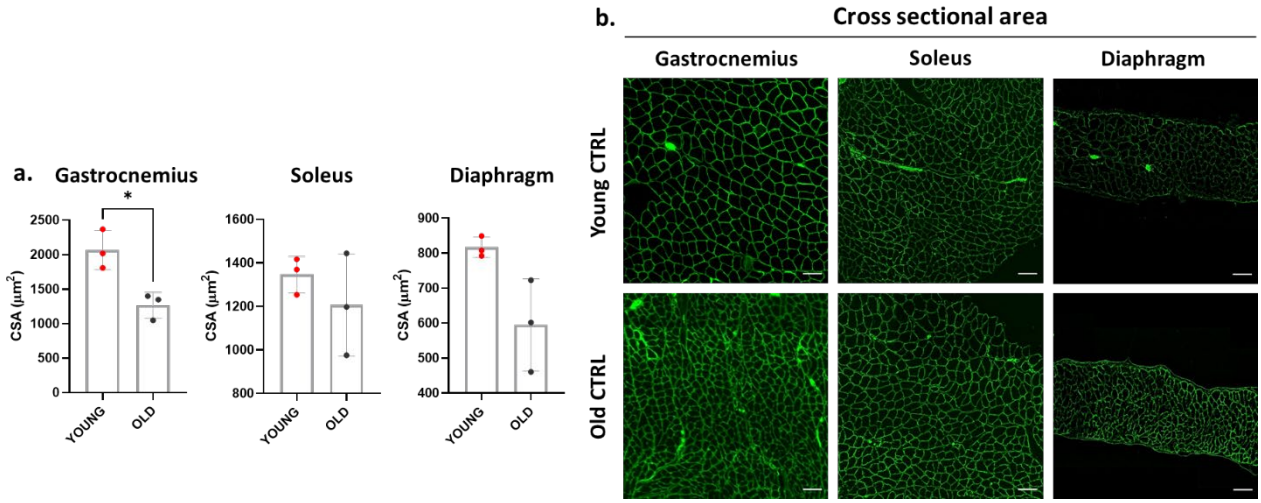

Figure 16. Cross sectional area (CSA) analyses of transversal fibers from Gastrocnemius, Soleus and Diaphragm. *a) graphical representation of CSA of the muscles under investigation, in their total amount of fibers, expressed in µm². The * denotes a significant difference among the groups. Difference is considered significant when P < 0.05. b) Representative images of transversal sections of muscles*

subjected to immunofluorescence. Green channel represents the dystrophin, a marker of the plasma membrane. Scale bar 100 µm.

Loss of muscle mass or, at least, a decrease in fibers' average area can be related to degenerative phenomena and associated regeneration, in an attempt to recover from a damaged condition. Moreover, atrophy and degeneration of muscle fibers can leave space to interstitial infiltrates and growing adipose tissue presence, which together can be causative of a dysfunctional activity of the skeletal muscle (Shang *et al*, 2020).

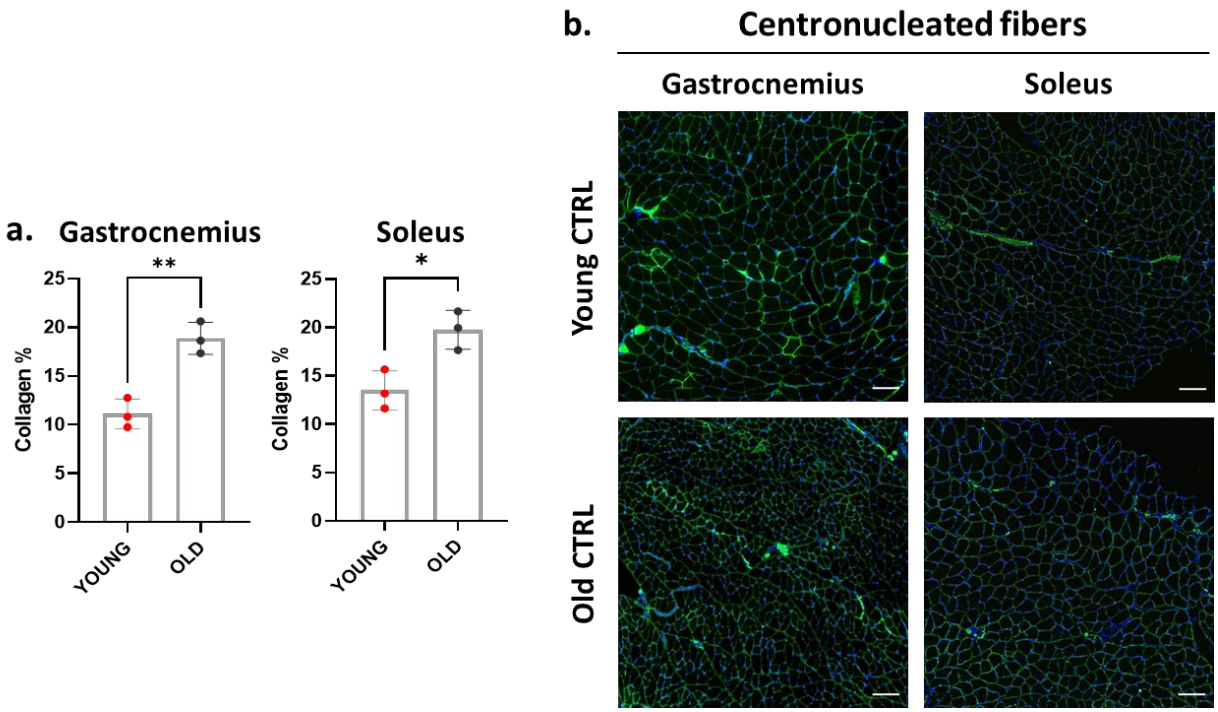

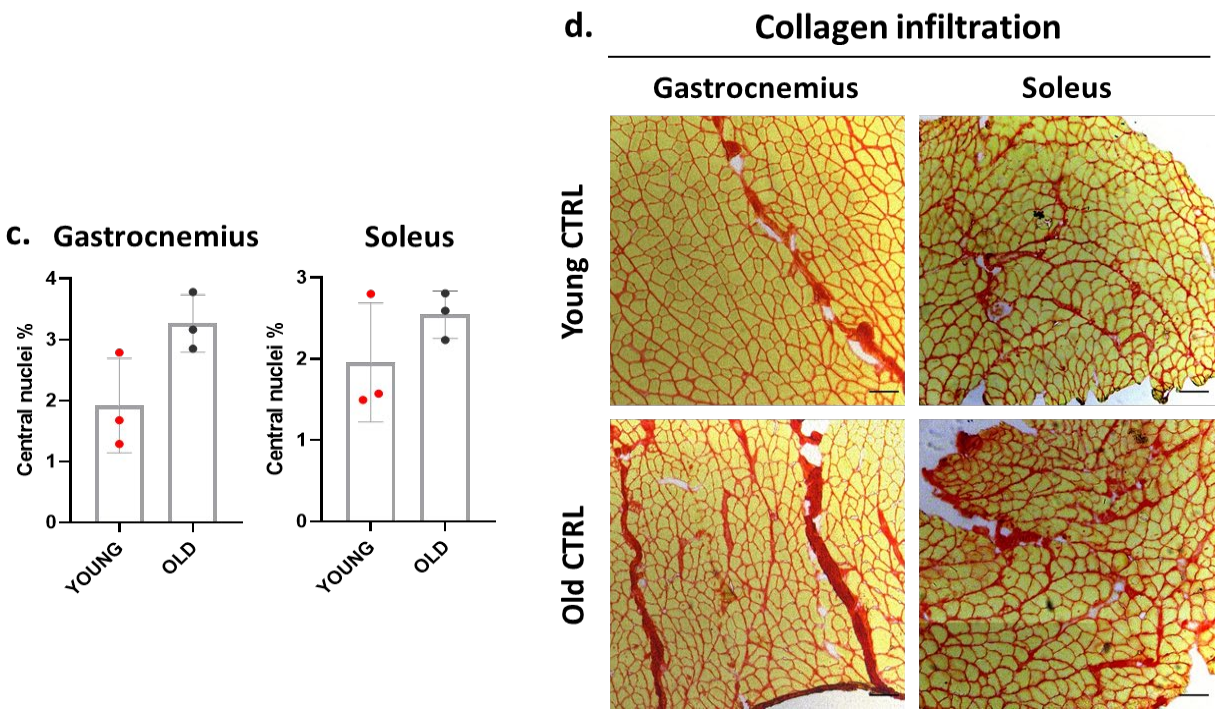

Figure 17. Histochemical evaluations on Gastrocnemius and Soleus. *a) and b) display the percentage of fibers with central nuclei up to the total amount of fibers composing the muscle section. c) and d) display the percentage of collagen infiltrated among the fibers and stained with Picro Sirius Red. Percentage is calculated as the ratio between the fibrotic area stained in red over the total area of the muscle section. The * denotes a significant difference among the groups. Difference is considered significant when P < 0.05. b) Representative images of transversal sections of muscles acquired with a fluorescence microscopy. Green channel represents the dystrophin, a marker of the plasma membrane; blue channel represents the muscle nuclei marked with DAPI. Scale bar 100 µm. d) Representative images of transversal section of muscles acquired with an optical microscope. Red staining identifies collagen and yellow areas denote the transversal skeletal muscle fibers. Scale bar 100 µm.*

By the histochemical analyses of Gastrocnemius and Soleus depicted in Figure 17, an increase in centronucleation was visible in both muscles, with a prominent trigger of the central localization in the Gastrocnemius ($p = 0.07$). One of the peculiarity of the post-mitotic skeletal muscle tissue is the peripheral localization of the nuclei following maturation and establishment of the contractile apparatus within the sarcoplasm, which pushes the nuclei in the periphery of the fiber. A damage of fibers can be causative of a rearrangement in the localization of the myonuclei, which are indicative of a regenerative process triggered by the stimulus of maintaining a homeostatic equilibrium and restore the damage. During ageing, damages of fibers arose from different causes and the loss of muscle mass, clearly occurring in Gastrocnemius, stimulated the regeneration processes to recover in part from an advancement of atrophy (Srikuea *et al*, 2020). Regarding the evaluation of the fibrotic infiltration within the muscle, old mice showed a significant increase in collagen deposition among the fibers in both muscles evaluated. The deposition of a non-contractile tissue can compromise the function of the muscle, in line with the typical outcomes of sarcopenia

(Mann *et al*, 2011). Diaphragm data are not shown in these panels due to a non-significant presence of centronucleated fibers and fibrotic tissue infiltration.

A decrease in CSA and a damaged outline of muscle fibers found in the old mice cohort framed our elderly animal model in an atrophic profile. Different mechanisms are found to be involved in the progression of atrophy, by means of alterations of molecular pathways involved in maintenance of muscle mass and turnover of proteins/components in order to sustain a functional homeostasis within the muscle. Two parallel phenomena are notoriously involved in this pattern: muscle protein synthesis (MPS, Figure 18a) and muscle protein breakdown (MPB, Figure 18b/c). From now on we decided to focus our studies and observations on Gastrocnemius due to the preliminary important age-related changes and to the relevance this muscle covers in the hindlimb movement.

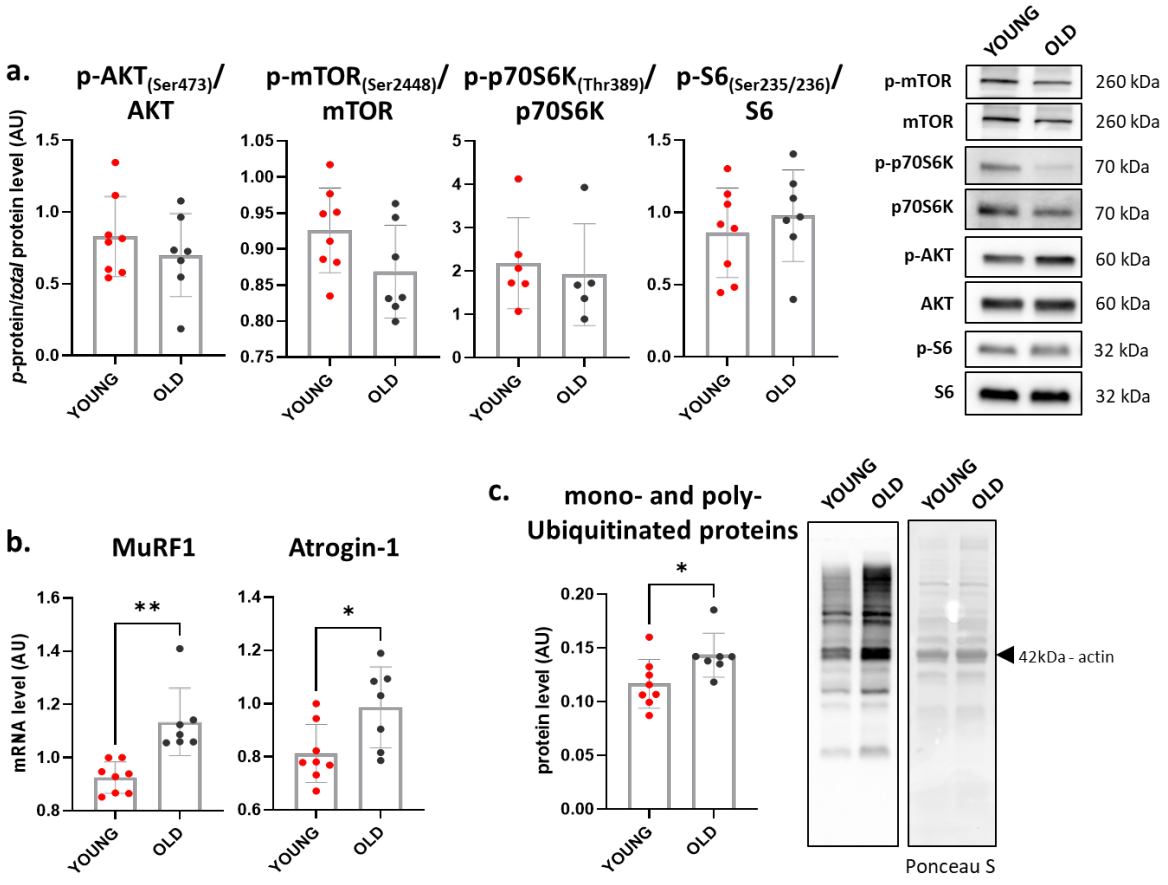

Figure 18. Muscle protein synthesis and muscle protein breakdown in Gastrocnemius. *In panel a) the major factors involved in the mTOR synthetic pathway, juxtaposed with representative Western Blot images. Analysis is the result of the ratio between the phosphorylated isoform of the protein and the amount of the total protein. In panel b) the transcript levels of the two main muscle atrogenes involved in protein degradation, accompanied by the levels of mono- and poly-ubiquitinated proteins (c) in Young and Old cohorts (with representative Western Blot image and corresponding Ponceau S staining). The * denotes a significant difference among the groups. Difference is considered significant when P < 0.05.*

MPS and MPB are normally found in equilibrium in a physiological system and a cross-talk is necessary for the maintenance of muscle mass. Once an unbalance occurs, the predominance of one over the other or a downregulation of one not compensated by the other can lead to a loss of mass. We analysed the protein levels of the phosphorylated active factors involved in the protein synthesis promotion guided by mTOR, a key protein for this pathway (Yoon, 2017). No change was visible in this pathway in any of the different levels of the cascade activity studied. Levels of phosphorylation did not change, meaning that there was no stimulus in pushing the synthesis of newly functional proteins all over Gastrocnemius. Conversely, degradation of proteins promoted by ubiquitin-ligase atrogenes MuRF1 and Atrogin-1 had a significant upregulation in elderly animals, confirmed by the levels of mono- and poly-ubiquitinated proteins significantly increased in old mice. Induction of atrogenes is modulated by FoxO transcriptional activity, mainly controlled by Akt. A decrease in Akt levels diminishes the probability to phosphorylate its substrates and thus inactivate FoxO, which can then translocate into the nucleus and promote transcription of atrogenes. Upregulation of atrogenes is found strictly related to atrophy (Sandri *et al*, 2004). In our case, a basal level of Akt phosphorylation was maintained in both ages under investigation, as it occurred for all the downstream factors involved in the Akt-mTOR pathway (as previously demonstrated by Perry Jr *et al*, 2016). By the way, basal levels of Akt in both ages did not match to increased expression of atrogenes only in ageing, meaning that other pathways interfered to activate FoxO transcriptional activity and thus to enhance the degradative pathway during ageing. No variances in the protein synthesis pathway in the Gastrocnemius was even observed by Kim and colleagues, in which ageing did not particularly affect mass maintenance-related pathways in muscles under investigation, apart from the diaphragm in which synthesis was enhanced in an effort to preserve the vital function of respiration. The idea that maintenance and any variances in muscle mass occur in a muscle type-dependent manner, as demonstrated in Kim's work, strengthens us to deeply focus on Gastrocnemius (Kim *et al*, 2020).

Overall, 24-months old mice showed a general atrophic profile strictly linked to an age-related sarcopenia in which muscle mass was lost due to an enhanced degradation pathway not counterbalanced by protein synthesis and thus correct protein turnover. Loss of muscle mass was even associated with fibrotic infiltration and regenerative phenomena in order to restore from the advancement of atrophy, in part counteracted by a shift to slow MHC, notoriously resistant to atrophy and final degeneration.

1.2 Effects of ageing on the autophagic flux

Autophagy is the process though which cells remove damaged components, promoting clearance of dysfunctional organelles (or part of those) and avoiding accumulation of abnormal organelles and toxic elements that eventually lead to an impairment in basal cell function and its degeneration. This process is modulated in order to find a balance with the synthesis of newly functional components in a turnover model which should reward the health of the cell. The autophagic flux is modulated by various stimuli and signalling processes triggered by different physiological contexts. Uncontrolled activation or an unexpected delay in autophagic interventions can be detrimental for the stability of the cell and, regarding muscle fibers, can compromise the maintenance of muscle mass and the ability of the contractile apparatus to properly function (Masiero *et al*, 2009). We firstly evaluated key proteins involved in the progression of the autophagic machinery in order to evaluate the state of the art in Gastrocnemius of 24-mo mice (Figure 19).

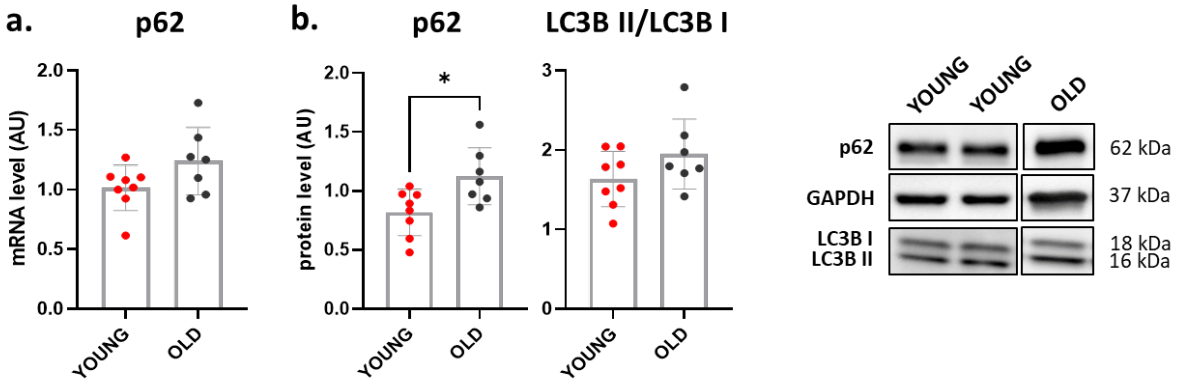

Figure 19. Factors involved in the progression of autophagy. *a) Transcript levels of p62 in Young CTRL vs Old CTRL mice. b) Protein levels of p62 normalized on GAPDH and LC3B II normalized on LC3B I in Young CTRL vs Old CTRL mice. Graphs are accompanied by representative Western Blot images. The * denotes a significant difference among the groups. Difference is considered significant when P < 0.05.*

p62, a scaffold protein that specifically binds to ubiquitinated protein aggregates to target them for degradation, did not show any perturbation in its transcript levels in Old CTRL compared to Young littermates. It was interesting, however, to see significantly high protein levels of p62 in elderly mice. An accumulation in p62 is mostly associated with a slower or inhibited autophagic flux, while lower protein levels are linked to an active process that leads to degradation of marked ubiquitinated elements, with the attached targeting proteins (as for example p62; Bjørkøy *et al*, 2009). Protein levels that significantly increase did not reflect the transcript levels, meaning that the accumulation of p62 was not positively provoked by transcription of its mRNA.

p62, being recognized as an ubiquitin-linked flag of components that need to be degraded, is recognized by factors exposed on the surface of the phagosome to initiate the process. Among those, LC3B is the main studied for the evaluation of autophagy. Two isoforms are physiologically found: the lipidated LC3B II isoform, that is actively found exposed in nascent phagosomes and the pre-assembled LC3B I isoform. To monitor the autophagic flux, LC3B II levels are usually taken into account. In Old CTRL group, no changes in LC3B II levels compared to young littermates were visible, meaning that the autophagic flux had no fully efficient outcomes at the level of autophagosome formation. p62, accumulated within the cell and on the surface of damaged components, was thus not sufficiently bound to LC3B II and those components were not efficiently degraded. This theory is in line with the sarcopenia features, in which an impaired autophagy is causative of muscle mass loss and impaired functionality (Sakuma *et al*, 2016).

To complete the evaluation of this pattern, factors specifically involved in mitochondrial degradation were then studied. Upon activation and recruitment on the outer mitochondrial membrane, these factors trigger modifications of specific residues so as to promote the recognition of the damaged organelle by the autophagic machinery (in a process called mitophagy). PINK1 accumulates on the surface of the mitochondria when a depolarization of mitochondrial membrane potential occurs, decreeing its dysfunction. It is a kinase that causes the phosphorylation of different molecules to activate a signal cascade. Among those, cytosolic Parkin, an ubiquitin-ligase, once phosphorylated by PINK1, is recruited itself by the damaged organelle and promotes ubiquitination of mitochondrial components that are eventually recognized by p62. BNIP3, on the other hand, when exposed on the outer mitochondrial membrane, directly binds to and so recruits autophagosomes. In Figure 20, age-related changes in mitophagy were studied.

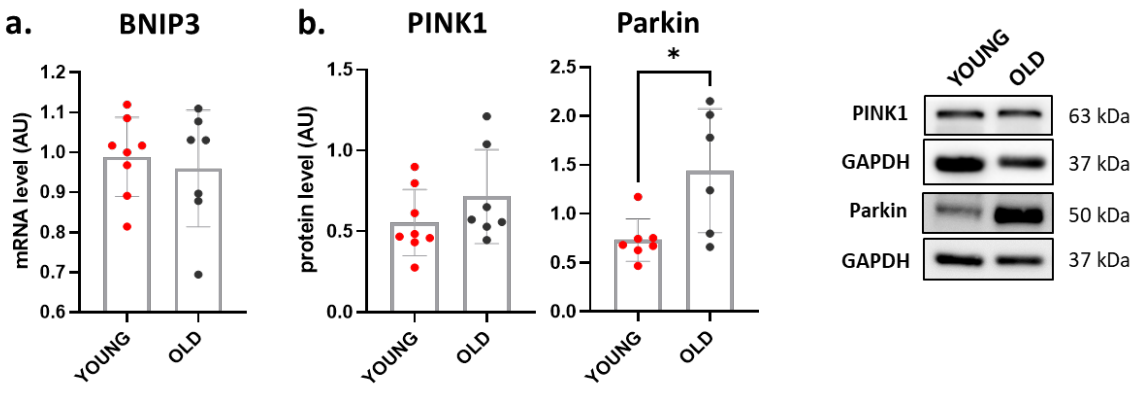

Figure 20. Factors involved in the progression of mitophagy. *a) Transcript levels of BNIP3 in Young CTRL vs Old CTRL mice. b) Protein levels of PINK1 and Parkin, with GAPDH as housekeeping, evaluated*

*in Young CTRL vs Old CTRL mice. Graphs are accompanied by representative Western Blot images. The * denotes a significant difference among the groups. Difference is considered significant when P < 0.05.*

BNIP3 transcript levels did not change during ageing, so there was no enhancement of autophagosome recruitment at the level of mitochondria in elderly mice. PINK1 protein levels, in the same way, did not change in 24-mo mice compared to the young cohort, but interestingly, Parkin levels were highly increased during ageing. The fact that Parkin promoted its "ubiquitinating" activity was demonstrated in part by increased p62 levels previously assessed. The impairment in this flux was still ascribable to LC3B II levels, which did not cope with increasing Parkin/p62 protein levels.

Overall, by evaluating the autophagic/mitophagic flux in 24-mo mice compared to young CTRL, an impaired autophagic flux was assessed, due to p62 accumulation that was not correctly degraded by LC3B II-mediated phagosomes. Moreover, mitophagy process was maintained at baseline levels, apart from Parkin overexpression. In the literature, the accumulation of p62/Parkin, together with other autophagic factors, was demonstrated to be detrimental for mitochondrial quality (Goljanek-Whysall *et al*, 2020).

1.3 Effects of ageing on mitochondrial parameters

It is well known from the literature that mitochondrial function and its health is highly relevant for a general beneficial homeostasis of cells. Since skeletal muscle is a tissue of a high energy demand, maintaining an efficient mitochondrial network in this district is of particular importance for carrying out all the functions of this tissue.

We firstly investigated parameters relative to mitochondrial mass in order to evaluate how ageing affects the density of these organelles. Protein levels of TOM20, a component of the translocase of the outer mitochondrial membrane, and Citrate Synthase (CS), an enzyme of the mitochondrial matrix, were studied (Figure 21).

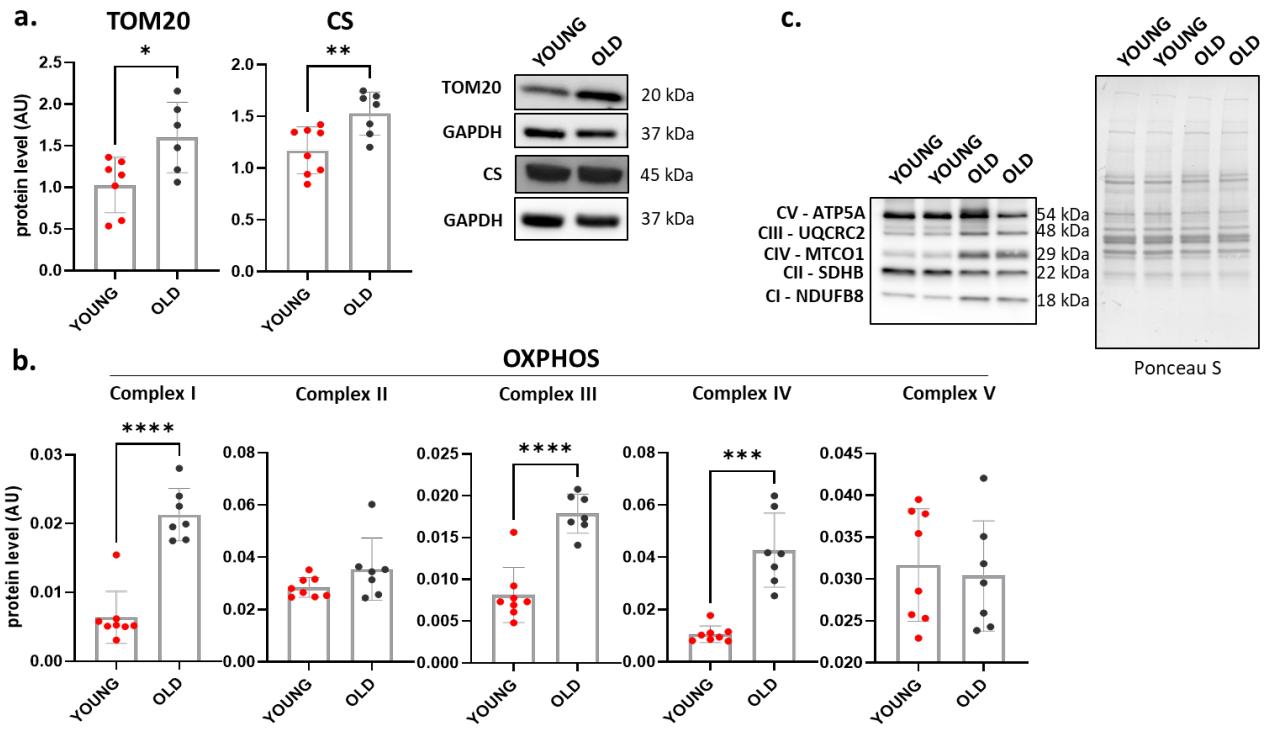

Figure 21. Protein levels of mitochondrial mass markers TOM20 and CS and relative amount of complexes that form the mitochondrial respiratory chain in Gastrocnemius. *a) A significant increase in protein level is assessed in old mice compared to young littermates. Beside, representative Western Blot images of the two proteins with corresponding GAPDH levels for normalization. b) Protein level of the five complexes the respiratory chain is formed by, juxtaposed with representative Western Blot images (c). Significative trends are not visible in all the complexes, suggesting different involvements and implications in mitochondrial function. The * denotes a significant difference among the groups. Difference is considered significant when P < 0.05.*

Levels of both mitochondrial mass markers significantly increased during ageing. This result goes in contrast with the notion that ageing promotes a decrease in mitochondrial density and therefore the respective altered functionality. By the way, a change in mitochondrial morphology and the surveys of larger organelles with a higher density has been demonstrated in elderly mice through the electron microscopy technique (Leduc-Gaudet *et al*, 2015), accompanied by a changed orientation of mitochondria from longitudinal towards transverse orientation, in which assume a bigger elongated and branched shape (del Campo *et al*, 2018). Moreover, we investigated the amount of the complexes composing the mitochondrial respiratory chain, indicative of mitochondrial density and function: a significant increase in protein content was not equal among all the five complexes during ageing. Complexes I, III and IV were found to be highly expressed in elderly mice compared to young littermates. These three complexes are strongly assembled and dependent to each other to form the so-called supercomplexes (respirasome). Different experiments demonstrate how a selective downregulation of one of those reduces the probability

to form the functional respirasome (Li *et al*, 2007 on complex IV; Bhardwaj *et al*, 2021, on complex I positively regulated by IGF1 and negatively by FoxO-mediated downregulation). A direct relation is even occurring between the supercomplexes assembly and the shape of the cristae (Cogliati *et al*, 2013), highly important for mitochondrial functionality and undergoing remodelling during ageing, altering thus the mitochondrial membrane potential which causes ATP synthase loss of functional dimerization (Daum *et al*, 2013). However, even complex II is involved in the assembly of the functional respirasome, establishing thus a functional interaction beyond the respiratory chain (Jang and Javadov, 2018). It was demonstrated that an increase in the expression of the supercomplexes lead to lowered levels of Complex II, resulting in accumulation of succinate and downstream metabolic effects (Jiang *et al*, 2020). At the same level, an impairment in ATP synthase activity can occur, due to baseline levels our elderly mice cohort maintains. We can thus speculate a dysfunction in 24-mo mice mitochondria due to heterogeneous levels of mitochondrial complexes.

Different explanations can be given and different pathways up- and/or downstream these factors can be called into question. We evaluated factors involved in mitochondrial biogenesis as a possible pattern causative of an increased mitochondrial mass. PGC1α (peroxisome proliferator-activated receptor-gamma coactivator-1α) is the major regulatory factor involved in the mitochondrial biogenesis and general energetic metabolism. During ageing, a decrease in mitochondrial mass is mostly associated to a decrease in PGC1α levels, but in our case the opposite trend of TOM20 and CS was not linked to PGC1α levels, which did not change in both ages under investigation (Figure 22). Basal levels of this factor together with an inefficient autophagy could not correctly degrade mitochondria, leading to an accumulation.

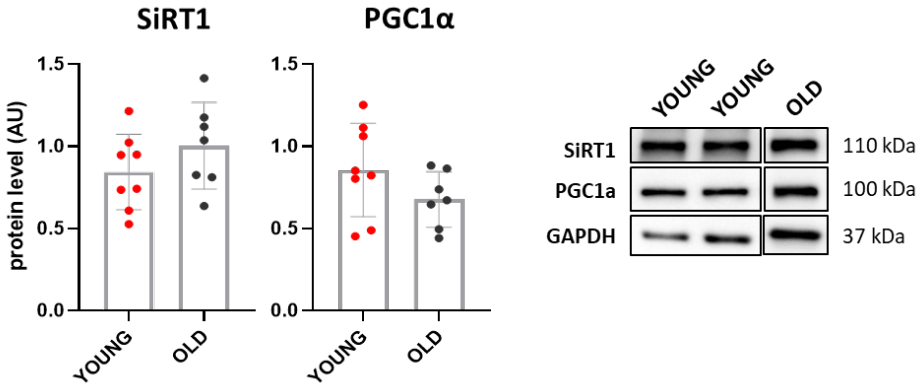

Figure 22. Protein levels of SIRT1 and PGC1α in Gastrocnemius, two of the major markers of mitochondrial biogenesis and energy sensors for the modulation of the metabolism. *SIRT1, a deacetylase, and PGC1α, targeted by SIRT1 post-translational modification, do not change during*

ageing. Beside, representative Western Blot images of the two proteins with corresponding GAPDH levels for normalization. Difference is considered significant when P < 0.05.

However, PGC1α is strictly controlled and modulated in its biological activity by different factors, modification and interactions, due to its key role within the skeletal muscle and all the pathways, mechanisms and transcriptional factors it promotes to cope with environmental stimuli. A major aspect to take into account for this factor is its very short half-life (about 30 min, Adamovich *et al*, 2013) which can hamper a real quantification of protein content within a muscle. Another aspect important for the regulation of its function and activity is related to all the post-translational modifications it undergoes. SIRT1, a NAD-dependent deacetylase sirtuin-1, is one of the upstream factors involved in the deacetylation of PGC1α and subsequent translocation into the nucleus, so as to favour its transcriptional activity. Ageing did not affect SIRT1 protein levels, meaning that its activity was maintained constant over its targets, especially on PGC1α.

Another relevant factor involved in the modulation of PGC1α activity is AMPK. AMP-activated protein kinase, as the name suggests, is a kinase which activity is dependent by AMP concentration within the cell. It is well established as an energy sensor because of its activation following ATP depletion and subsequent increase of AMP concentration, meaning that cell is starving from the highly energetic molecule indispensable for various muscular functions. The activation of AMPK sets up a cascade of events in order to augment mitochondrial activity and blunt irrelevant energy-consuming processes, preferring the stimulation of catabolism. These assumptions found a confirmation in the activity levels of MPS and MPB in 24-mo mice we studied (Figure 18).

Anyway, together with SIRT1, AMPK promotes a post-translational modification on PGC1α (Cantò and Auwert, 2009), which can then translocate into the nucleus and induce transcription of genes involved in mitochondrial biogenesis, genes involved in oxidative metabolism and genes involved in the maintenance of a functional muscular apparatus in all its districts. Protein levels of AMPK and its activating phosphorylated modification were analysed in our experimental groups (Figure 23).

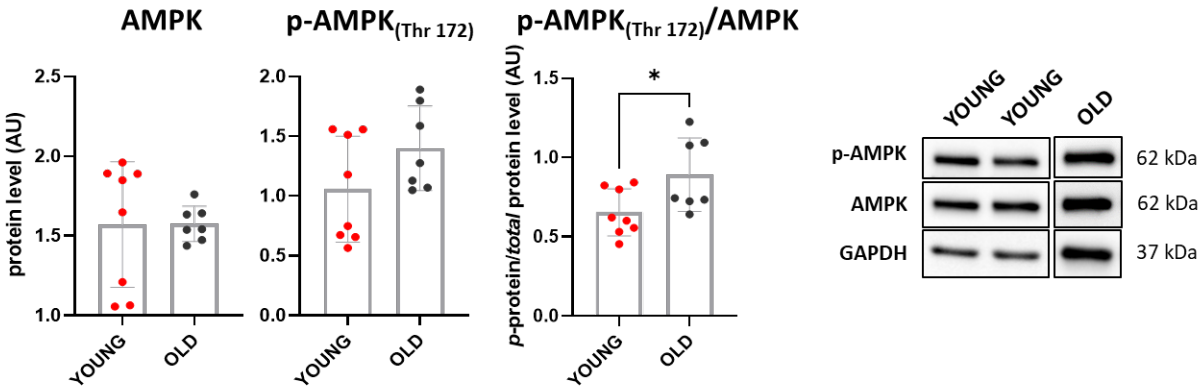

Figure 23. Protein levels of energy sensor AMPK, a sensor for the energetic status within the muscle fiber. *The total protein amount and the phosphorylated (actively functional) are normalized by GAPDH housekeeping, while the amount of the active isoform over the total protein amount is depicted on the right, together with Western Blot images analysed. The * denotes a significant difference among the groups. Difference is considered significant when P < 0.05.*

Protein levels of the AMP-energy sensor in elderly mice did not show any age-dependent perturbation in its absolute protein content, but a significant increase of phosphorylation over the total protein content was visible in old littermates. This result suggested a compromised energetic status in Gastrocnemius fibers and a stimulated pathway due to an impaired AMP/ATP ratio. Even if the other parameters of the SIRT1/AMPK/PGC1α axis were not significantly changed in their protein level, the high phosphorylation of AMPK could be speculative of an increased kinase activity on those factors. This could be in part indirectly explicative of an increased mitochondrial mass, reinforced by an impaired autophagic flux (Figures 19/20). Moreover, an indirect but not remote interaction exists between ATP synthase and AMPK, which is activated following inhibition of ATP synthase in order to support a rapid glycolytic switch and elicit catabolic events (Hall *et al*, 2018; Contreras-Lopez *et al*, 2021). The increase in AMPK activation level found in old mice could be thus reflective of a heterogeneous expression level of ETC complexes that could be inefficient in the final ATP synthesis passage.

Mitochondrial mass and health of this important organelle is regulated by dynamic processes it undergoes following different stimuli/signals. Mitochondrial dynamics enclose all those factors exposed on mitochondrial membrane which trigger and drive two different opposite processes, depending on the final aim and the issues it has to cope with. Fusion induces the formation of an extended interconnected mitochondrial network enabling the mitochondria to mix and redistribute their contents of metabolites, proteins, and mitochondrial DNA (mtDNA). An interconnected mitochondrial network prevents the local accumulation of defective/abnormal mitochondria.

Conversely, mitochondrial fission or fragmentation is a mechanism that segregates components of the mitochondrial network, which are dysfunctional or damaged, facilitating their removal via autophagy. Hence, dynamic regulation of the fusion-fission events adapts mitochondrial morphology to the bioenergetics requirements of the cell, in a system maintained under a balanced and controlled equilibrium. By the analysis of mitochondrial dynamics factors in order to evaluate any linkage among these processes and an increased mitochondrial mass, pro-fusion protein levels have been demonstrated to significantly increase in ageing (Figure 24).

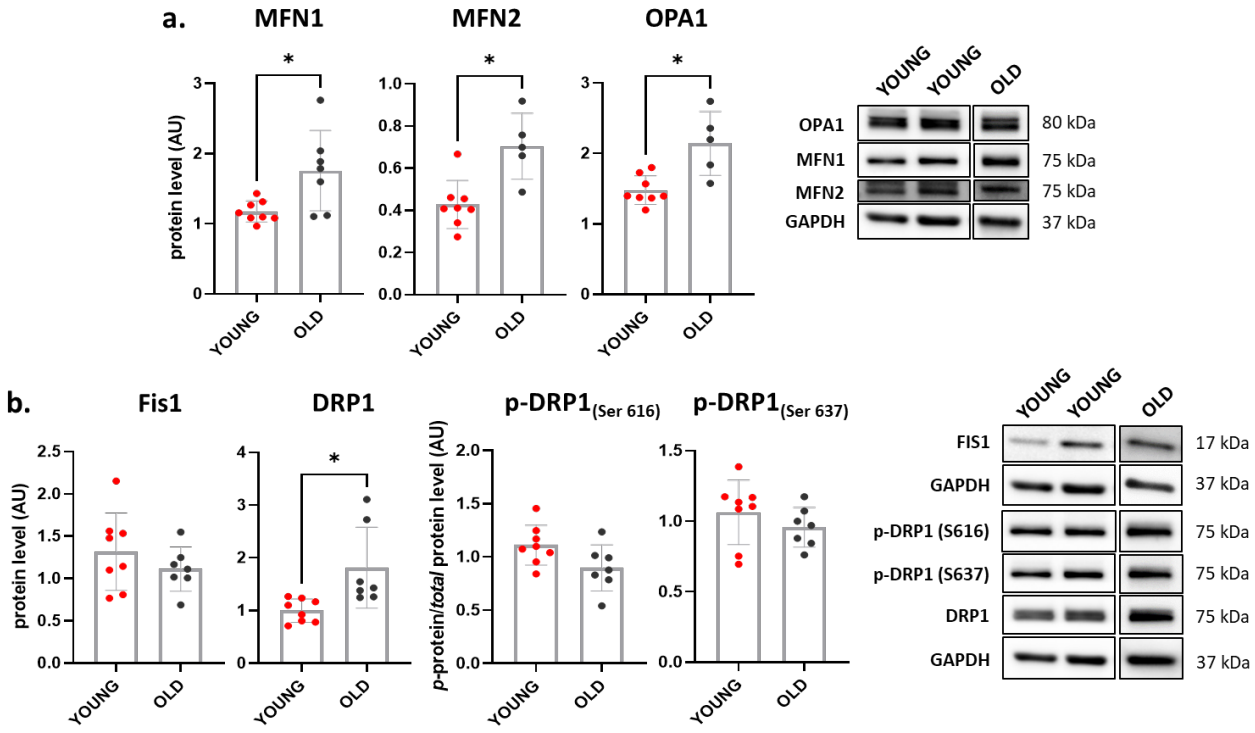

Figure 24. Mitochondrial dynamics on Gastrocnemius. *In the upper panel a) pro-fusion proteins involved in the promotion of fusion processes among close mitochondria. All evaluated by protein amount over the housekeeping. In the lower panel b) pro-fission proteins involved in the advancement of fission of damaged portions of mitochondria to be easily cleared and removed. FIS1 and DRP1 are analysed over the housekeeping, while the phosphorylated isoforms of DRP1 are depicted here as the ratio among the phosphorylation and the total protein amount. Phosphorylation on Serine 616 promotes fission pattern, while phosphorylation on Serine 637 hampers the activation of this mechanism. Graphs are accompanied by representative Western Blot images. The * denotes a significant difference among the groups. Difference is considered significant when P < 0.05.*

Fission parameters did not significantly change, despite DRP1 (dynamin-1-like protein) total protein content was increasing. An interesting work demonstrates how overexpression of DRP1 in elderly female mice promotes a mild atrophy and altered mitochondrial quality with dysfunctional respiration parameters and an increased expression of Complexes III and V only, together with an increased CS expression (Dulac *et al*, 2021). The overexpression of these mitochondrial parameters

did not correlate with an ameliorated mitochondrial respiration (ETC unequal components), meaning that this increase acted as a compensatory mechanism in order to try to recover. High levels of DRP1 *per se* can be either linked to other mechanisms beside fission, as mitochondrial localization within the muscle (due to its interaction with kinesin-1 complex that promotes a microtubule-dependent trafficking so as to place them within the nucleus, Giovarelli *et al*, 2020) and its shape remodelling and involvement in calcium homeostasis (Favaro *et al*, 2019). By the way, DRP1 undergoes itself post-translational modification in different residues, and this causes different effects on its activity. Phosphorylation at Ser-616 promotes a higher binding affinity to FIS1, in a pro-fission model; while the attachment of a phosphate group at Ser-637 hampers the interaction site with FIS1, thus leaving the soluble DRP1 in the cytosol and inhibiting its functional translocation on the surface of mitochondria. In our conditions, there were no fluctuations in any of the phosphorylation levels of DRP1. These data suggested an unbalanced equilibrium of mitochondrial dynamics in favour of fusion, which promoted the formation of hyper fused tubular mitochondria not counteracted by an increased fission.

In some conditions as exercise and starvation, elongated and interconnected mitochondria are evaluated as a defence mechanism to protect them from autophagosomal degradation, which could permit mitochondria to maximize energy production (Rambold *et al*, 2011). Nevertheless, in our elderly animals, autophagy/mitophagy was demonstrated to be impaired in its functional flux, indicating a non-correct clearance of damaged organelles: autophagic apparatus removes rather small fragmented mitochondria than huge ones, with the risk that damages accumulate in hyper fused ones. Elongated and fused mitochondria have been demonstrated to spare from autophagic degradation, possess more cristae (evaluated through electron microscopy approaches) and increase levels of dimerization and activity of ATP synthase in order to maintain ATP production under starvation (Gomes *et al*, 2011). In our case, an increase in mitochondrial pro-fusion proteins and an augment in mitochondrial mass markers independently by biogenesis suggested us an increase in the size of those organelles which, on the other hand, missed an increase in ATP synthase (Complex V of OXPHOS panel, Figure 21, panel b) so an impairment in the final step of the respiratory chain, speculating a malfunction of mitochondria in our 24-mo mice.

To sum up, mitochondria, highly relevant due to their energy supply for all the functional requirements within the fibers, have been demonstrated to increase in their mass, mainly caused by a significant augment of fusion processes together with a reduced autophagic flux. The formation

of a hyper fused and interconnected network of mitochondria devoided these organelles from autophagy and most of the times is causative of accumulation of mtDNA mutations (Chen *et al*, 2010) and dilution of mitochondrial components in a wider environment. Moreover, respiratory chain complexes were found increased in their levels in old mice, as predicted by data of mitochondrial mass, even if this augment was not homogeneously preserved in all the complexes. ATP synthase in this case covered a relevant role because it is the last component of the respiratory chain but, contrary to the increase in the expression of complexes I, III and IV, its levels remained unchanged, suggesting an impairment in the electron flux within the transport chain that ended up with ATP synthase protein amounts that did not compensate for age-related mitochondrial mass increase and diminished efficient ATP production yield. This was inevitably linked to an energy stress condition in which AMPK was strongly induced (Figure 23), as a sensor for a decreased ATP concentration within these elderly fibers.

1.4 Effects of ageing on denervation and neuromuscular junction stability

During ageing, other important aspects enclosing the functionality of the muscle undergo detrimental impairment, determining the loss of function typical of sarcopenia. One of the major interactions the muscle tissue has with its surrounding environment is with the nervous system, and the interaction among these two is responsible for the formation of the neuromuscular junction (NMJ). NMJ is a synapse involved in the propagation of an action potential that is converted to a chemical input so as to terminally release calcium within the cytoplasm and allow the initiation of muscle contraction. During ageing, this cascade of events can be perturbed at different levels of activity. Impairments can arise from the nervous presynaptic side or from the muscular postsynaptic side, and a lot of molecular mechanisms and pathways cross-talk and intertwine among each other in both the isolated confined apparati and even among the two compartments in a paracrine fashion. Different factors/molecules are expressed by the muscle as neurotrophic factors that act on axon terminals to maintain their trophism and attachment on the active zone of the NMJ.

Denervation occurs in conditions in which axon terminals detach from the muscle they innervate, caused by neuronal degeneration, muscular instability on the site of the NMJ and missing trophic signals required for the maintenance of a functional interaction. In this situation, muscle increases the expression of some specific factors indicated as markers of denervation. We evaluated through rt-PCR the quantification of histone deacetylase-4 (HDAC4), growth arrest and DNA damage-inducible 45α (Gadd45α), Myogenin (MyoG) and Runt-related transcription factor-1 (Runx1) in

Gastrocnemius, because expression of these genes increases in denervated muscles (Barns *et al*, 2014, just to cite one) (Figure 25).

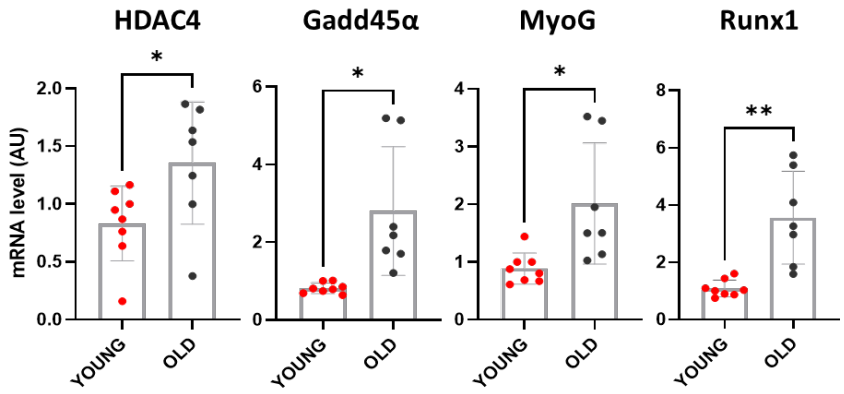

Figure 25. Transcriptional expression of denervation-related factors in Gastrocnemius. *The expression of these factors is directly linked to loss of axonal innervation and subsequent attempt of the muscle to recall back innervation. Ageing strongly induces the expression of all the factors evaluated. The * denotes a significant difference among the groups. Difference is considered significant when P < 0.05.*

The gene expression of all the denervation-related factors we investigated significantly increase in elderly animals. As they are known to be closely related in their expression/activity, it is no wonder that they all follow the same pattern. HDAC4 is primarily involved in promoting the transcription of Gadd45α, a factor induced by denervation and with a negative outcome into the muscle, associated to muscle atrophy progression (Bongers *et al*, 2013). HDAC4 is even found to be the modulator of the expression of MyoG, inducing its expression during denervation, as we have evaluated in our old mice in comparison with the young cohort. Even in this case, MyoG is considered a negative modulator of muscle mass leading to atrophy through its interaction and activation of the atrogenes (MuRF1 and Atrogin-1; Moresi *et al*, 2010). In our study, overexpression of MyoG correlated finely with the overexpression of atrogenes (Figure 18b) in Gastrocnemius, reinforcing our assumptions to face with animals undergoing muscle mass loss and so atrophy (sarcopenic phenotype). Furthermore, Runx1 levels were highly increased following ageing. In the literature, up-regulation of Runx1 during denervation has been known to have a protective role from severe muscle atrophy (Wang *et al*, 2005).

Taken all together, the over expression of these denervation-related factors projected us into a scenario of an impaired stability of muscle innervation and a general instability at the level of the neuromuscular junction. Another very powerful factor studied that can be linked to a denervation outcome is the Neural Cell Adhesion Molecule-1 (NCAM1), notoriously strongly expressed during

development and in stressing conditions where innervation is lost. It has been confirmed as a marker of denervation in a study on elderly humans and, beside the classical factors, NCAM1 expression and validation through immunofluorescence localization assays decrete its involvement in denervation (Soendenbroe *et al*, 2019).

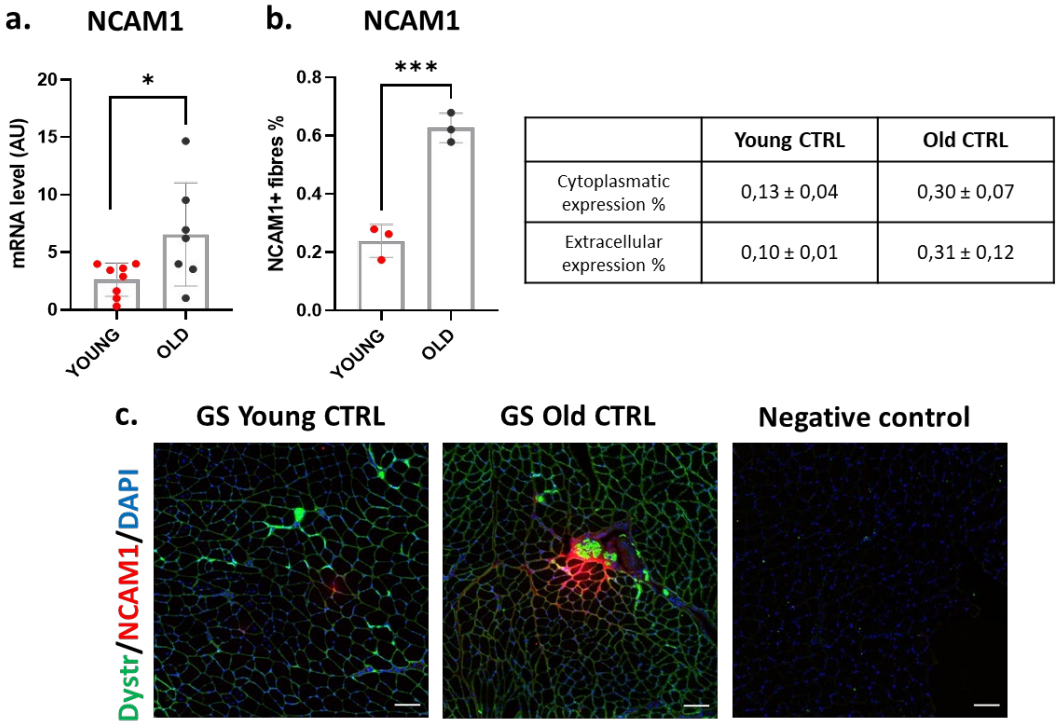

	Young CTRL	Old CTRL
Cytoplasmatic expression %	0,13 ± 0,04	0,30 ± 0,07
Extracellular expression %	0,10 ± 0,01	0,31 ± 0,12

Figure 26. Analysis of Neural Cell Adhesion Molecule 1 (NCAM1) expression and localization in Gastrocnemius. *a) Transcript level of NCAM1 is significant in older animals. b) Percentage of NCAM1 positive fibers over the total amount of fibers counted in a transversal section of Gastrocnemius. Positive fibers are the sum of fluorescence positive signal located within the cytoplasm and confined on the membrane (extracellular signal). Values are expressed in means ± SD in the nearby table. c) Fluorescent representative images of NCAM1 induction in young and old cohorts. Green channel represents the dystrophin; red channel represents NCAM1; blue channel represents the muscle nuclei marked with DAPI. Negative control to assess the specificity of secondary antibodies. Scale bar 100 µm. The * denotes a significant difference among the groups. Difference is considered significant when P < 0.05.*

In Figure 26, mRNA levels of NCAM were highly up-regulated in our old experimental group compared to young. Further analyses of this factor were then performed in order to evaluate the percentage of expression within the muscle and its localization. An increase in transcript levels found its correspondence in NCAM1 positive fibers through immunofluorescence (Figure 26, panel c). Despite the low numerosity of the samples, it was visible at first glance the augmented expression of NCAM1 (red signal) in elderly Gastrocnemius sections over the young cohort group. Following denervation and so loss of neural interaction at the level of the NMJ, NCAM1, in order to restore nerve contact and attract again any axon terminal, begins to be expressed at the level of the

sarcolemma, firstly in the junctional area, then in the extrajunctional spreaded region and at the end ubiquitously in the cytoplasm of denervated fibers. The impossibility for the muscle fiber to restore a functional innervation lead to a down-regulation of this nomore fruitable factor and an inevitably degeneration of the fiber (Gillon and Sheard, 2015). The importance and the relevance of this factor is even demonstrated at the level of the nervous terminal side, in which NCAM1 selective expression in partially denervated muscles promote and enhance functional expansion of synaptic territory in order to accomplish a regenerative reorganization of motoneurons in favor of a reinnervation of skeletal muscles, guided by postsynaptic NCAM1 overexpression (Chipman *et al*, 2014).

Regarding the postsynaptic stability, apart from the denervation-related factors previously analyzed, other factors (proteins/receptors) are primarily involved in NMJ stability and in the maintenance of the functional structure exposed in the sarcoplasm. The postsynaptic structure is formed by acetylcholine receptors (AChR) closely grouped in a confined active zone where contact with the nerve terminal occurs. Other factors interact with the AChR in order to maintain its spatial organization and promote the signal cascade required for muscle initiation of contraction. AChR is an heteropentamer formed by five subunits and, among those, subunit-α and subunit-γ cover a very important role in the primary evaluation of NMJ stability and/or perturbations. Subunit-γ is nowadays considered a denervation-related factor, because its expression is related to fetal/embryonic expression to establish the correct assembly of the receptor, but rapidly substituted by the subunit-ε in healthy mature muscles. A re-expression of the fetal/embryonic expression occurs under stress conditions in which a destabilization of the AChR structure and denervation happen. Subunit-α, on the other hand, is an important marker for junctional stability because the pentameric AChR structure is formed by two isoforms of this over the other heterogeneous three. By the evaluation of both subunits, in all cases ageing promoted a significant increase in these subunits (Figure 27, panel a).

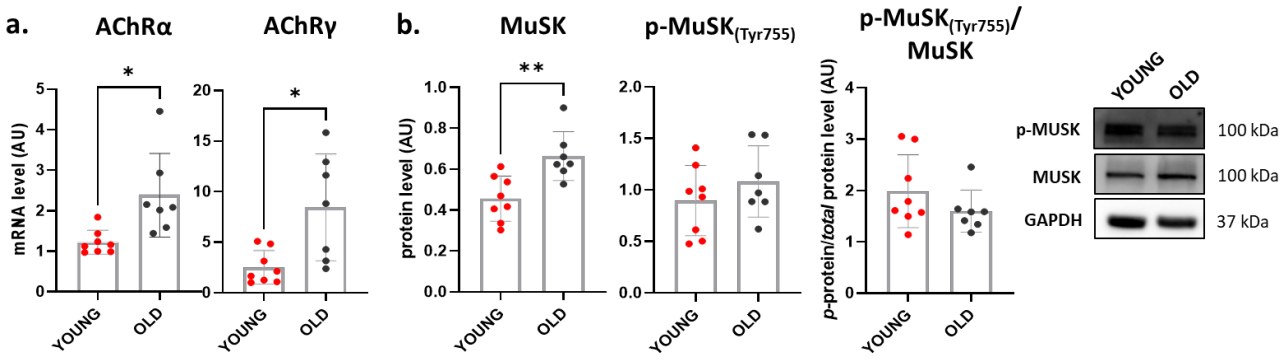

Figure 27. Factors involved in postsynaptic neuromuscular stability. *a) Transcription level of two of the main acetylcholine receptor (AChR) subunits: the alpha subunit is of relevance due to its stoichiometric presence in the pentameric receptor assembly (2 out of 5 are alpha subunits). The gamma subunit is the foetal/embryonal subunit highly induced following denervation, damage and traumatic events. It is notoriously recognized as one of the main denervation-related factors. b) Protein level of Muscle Specific Kinase (MuSK) in its total protein content and its phosphorylated content over the housekeeping GAPDH. The last graph depicts the phosphorylated isoform levels over the total protein amount. Representative Western Blot analyses are presented close by. The * denotes a significant difference among the groups. Difference is considered significant when P < 0.05.*

It is well established from the literature that subunit-α increases in ageing as a reflection of the fragmented and disorganized spatial disposition of the receptors: a wider area covered by the receptors suggests an increase in the expression of the main subunits, in order to increase the probabilities of a reorganization. Regarding subunit-γ, elderly animals showed a significant increase in its expression which is in accordance with the expression of the other denervation-related factors previously commented (Figures 25 and 26).

Moreover, MuSK protein levels and its active phosphorylation were evaluated as responsible for the beginning of the postsynaptic signalling cascade. MuSK is a transmembrane receptor that interacts with the AChR and is activated following agrin interaction through the agrin/LRP4/MuSK pathway. Levels of phosphorylated (active) protein did not increase in elderly animals, but MuSK total protein content was highly expressed in old compared to young littermates. An increase in protein levels of MuSK could be comparable to an increase in AChR subunits (especially the subunit-α, Brown *et al*, 2019), on an attempt to try to recover from a damaged and fragmented postsynaptic situation. An increase in total protein level was not accompanied by the phosphorylation of residue Tyr-755, depicting a situation in which in elderly mice there was an increase in protein levels related to the postsynaptic part, but a non-functional amelioration.

Overall, data collected on neuromuscular junction stability and levels of the markers involved in denervation/reinnervation gave us a general framework of a compromised system in 24-mo mice.

Especially denervation-related factors were highly induced in elderly Gastrocnemius muscles, suggesting an impaired trophic interaction of the muscle with the nervous system. Most of the up-regulated factors had a negative effect on muscle mass, because of their involvement in pro-atrophic pathways (as confirmed by the CSA evaluations), even if they were found in a balanced overexpression with Runx1, a denervation factor involved in the reinnervation and reestablishment of a nerve contact. Ageing, in this scenario, was subjected to NMJ instability and the overexpression of all these factors respect to young littermates suggested us an elderly system not capable to remodel and face with detrimental outcomes of age.

2. Interventions-related changes in aged mice

2.1 Mice characterization and in vivo effects of treatments

Following two months of intervention on 24-months old male mice, animals were characterized in their body weight and hindlimb muscles weight (Table 4). Moreover, histological investigations were performed on Gastrocnemius (the same muscle we focused in the first part of Results and Discussion) by assessing MHC isoform composition of treated mice and damage/regeneration parameters for the evaluations of the sarcopenic status (centronucleated fibers and fibrotic infiltration, Figure 28).

	Old CTRL	Old N	Old EX	Old EX+N
Age (mo)	24	24	24	24
n	7	7	7	7
Body weight (g)	35.14 ± 4.67	39.71 ± 5.08	35.71 ± 5.55	36.85 ± 3.23
Individual weights of hindlimb muscle (normalized on body weight)				
Gastrocnemius (mg)	3.94 ± 0.25	3.62 ± 0.41	4.08 ± 0.59	4.06 ± 0.22
Soleus (mg)	0.25 ± 0.01	0.24 ± 0.02	0.27 ± 0.02	0.27 ± 0.03
Tibialis Anterior (mg)	1.37 ± 0.16	1.24 ± 0.15	1.46 ± 0.21	1.45 ± 0.13
Extensor Digitorum Longus (mg)	0.28 ± 0.02	0.27 ± 0.03	0.28 ± 0.04	0.27 ± 0.02

Table 4. Body weight of mice and individual weights of hindlimb skeletal muscles. *Body weights are expressed in grams (gr) and represent the means ± SD. Weights of hindlimb muscles are the resultant of the weight of isolated muscles normalized by the body weight of the mouse, depicted as means of left and right muscles and expressed in milligrams (mg).*

The animals undergoing interventions did not differ in body weight values and hindlimb muscles weight respect to the Old CTRL. Histological evaluations on MHC isoforms that compose

Gastrocnemius did not reveal any change or shift in isoform following interventions (data not shown). However, the count of centronucleated fibers (Figure 28, panel a/b) displayed a decreasing trend on the percentage of regenerative fibers over the total amount of fibers. Even if significances were not reached (Old CTRL vs Old Ex+N, *p = 0.06*), treatments seemed to ameliorate the health of fibers. In the end, collagen infiltration within Gastrocnemius of treated mice (Figure 28, panel c/d) significantly decreased in all conditions compared to Old CTRL. This result was very important regarding exercise training protocol, because it demonstrated a non-traumatic impact on muscles of aged mice. It was demonstrated a cross-talk among regeneration, fibrotic infiltration and exercise: senescence of fibro-adipogenic progenitors (FAPs) in response to exercise-induced muscle damage is needed to establish a state of regenerative inflammation that induces muscle regeneration (Saito *et al*, 2020). In our case, after two-months exercise training, Gastrocnemius of 24-mo mice seemed to have reached a steady state, with both of the preocesses downregulated after being stimulated and induced by exercise. All these data suggested an improvement in histological features of old animals supplemented with nitrates and subjected to exercise, even if no macroscopic changes were visible (body weight).

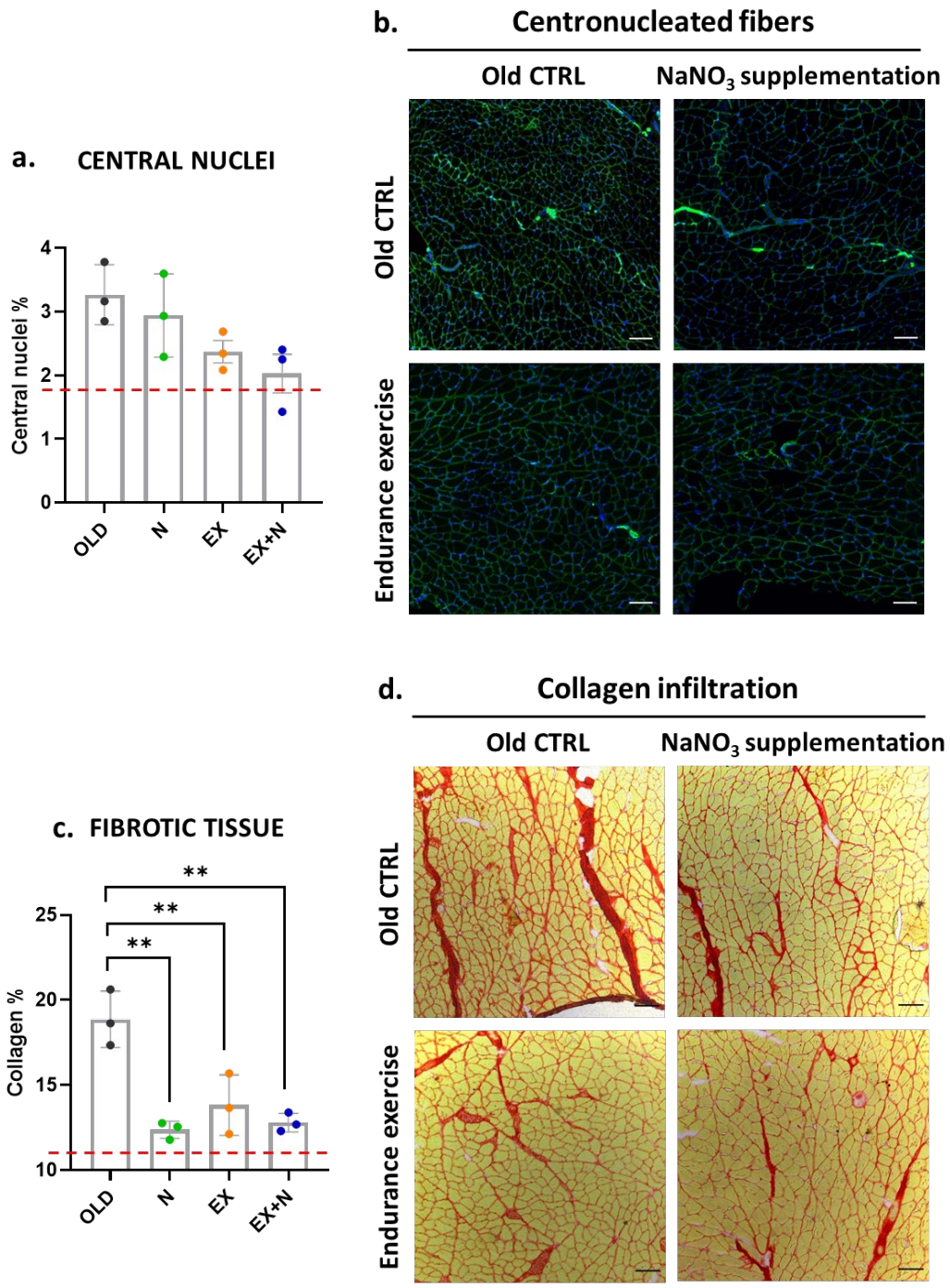

Figure 28. Histochemical evaluations of Gastrocnemius. *a) Percentage of fibers with central nuclei up to the total amount of fibers composing the muscle section. b) Representative images of transversal sections of muscles acquired with a fluorescence microscopy. Green channel represents the dystrophin, a marker of the plasma membrane; blue channel represents the muscle nuclei marked with DAPI. Scale bar 100 µm. c) Percentage of collagen infiltration stained with Picro Sirius Red. Percentage is calculated as the ratio between the fibrotic area stained in red over the total area of the muscle section. The * denotes a significant difference among the groups. Difference is considered significant when P < 0.05. d) Representative images of transversal section of muscles acquired with an optical microscopy. Red staining identifies collagen and yellow areas denote the transversal skeletal muscle fibers. Scale bar 100 µm.*

In order to confirm the effectiveness of the interventions, we evaluated the effects of 1.5 mM nitrate supplementation and endurance exercise training protocol by analysing nitrate concentrations within the muscle (Figure 29) and the effects of exercise on physical responsiveness of mice from all experimental groups (Figure 30).

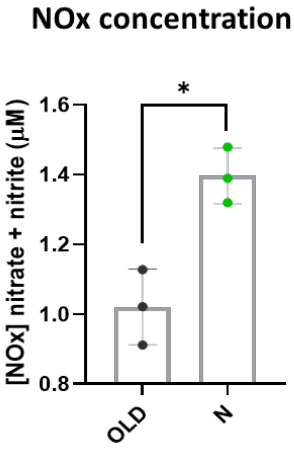

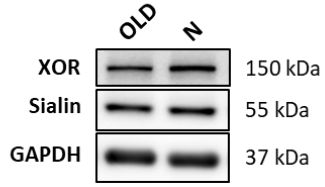

	Sialin	XOR
Old CTRL	0.67 ± 0.12	0.43 ± 0.06
Old N	0.79 ± 0.03	0.57 ± 0.18

Figure 29. Nitrate and nitrite concentration in Soleus muscle (µM). *Accompanied by a scheme reporting protein levels of Sialin, a specific nitrate transporter, and Xanthine Oxidoreductase (XOR) in Gastrocnemius (means ± SD). Representative Western Blot images are shown. Difference is considered significant when P < 0.05.*

Nitrate and nitrite concentration within the Soleus were evaluated. Due to the difficulties in the measurements of these compounds (especially nitrites, which are known to be highly unstable and so difficult to detects, and moreover their concentration is very low compared to nitrates), we measured the concentration of both molecules, taking advantage of the Griess Reagent protocol.

In order to evaluate the effective concentration of [NOx] following a targeted treatment, we only compared Old CTRL and Old N groups, revealing a significant increase of NO compounds in supplemented mice compared to the controls. Moreover, we evaluated protein levels of two components involved in NOx transport and metabolism within the muscle cell: Sialin and Xanthine Oxidoreductase (XOR), respectively. In this case, no statistical relevance was assessed in Old N cohort compared to the Old CTRL, but an interesting trend was visible for the Sialin transport expression (*+ 19%*) and XOR protein levels (*+ 32%*), indicative of their elicited activity (referred to the scheme of Figure 29). Hence, we can consider 1.5 mM $NaNO_3$ supplementation treatment as effective in order to increase bioavailability and distribution of NOx compounds within the muscle.

We then evaluated if the endurance exercise protocol which mice performed for two-months, 5-days/week had beneficial effects on their physical health (Figure 30).

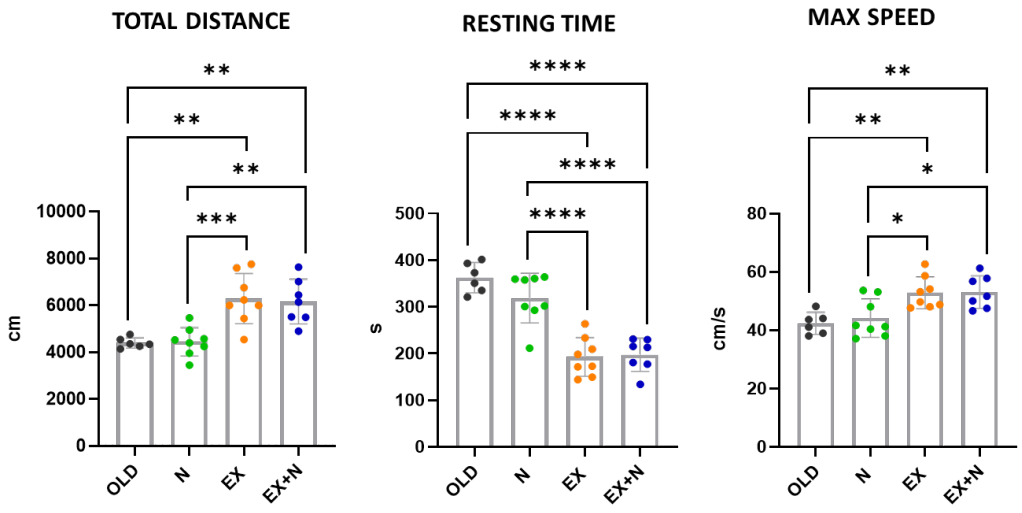

Figure 30. In vivo physical responsiveness of treatments compared to Old CTRL mice. *The * denotes a significant difference among the groups. Difference is considered significant when P < 0.05.*

Collaborators with a higher experience in behavioural tests and observations of spontaneous physical activity on controlled environments, measured, after two months of interventions, spontaneous total distance (cm) walked by animals in a restricted environment for 8 min, resting time (sec) during this test and the maximal speed (cm/sec) calculated from the total distance walked over the time of the experimental observation (ref. to Material and Methods). As depicted in Figure 30, significant ameliorations were visible in the cohort of animals undergoing endurance exercise protocol (both Old EX and Old EX+N littermates), while no changes among Old CTRL and Old N were visible. We can conclude that mice undergoing two-months exercise showed beneficial effects on their spontaneous walking inputs and reduced resting time during their daily activity, indicating an ameliorated physical fitness and higher stimuli to undergo spontaneous activity. Furthermore, maximal speed was increased in exercised mice compared to Old CTRL and Old N, as a reflection of an augmented muscular responsiveness stimulated by the exercise training protocol.

2.2 Ex vivo effects of treatments

We performed an *ex vivo* evaluation of the respiratory muscle diaphragm in order to evaluate force-frequency production and the resistance to fatigue in old mice in order to characterize functional changes, if any. Maximal tetanic force production did not change through our experimental groups (Table 5), so neither values of peak twitch force (P_o/CSA expressed in mN/mm^2) and related time to peak and time to relaxation (bot expressed in sec), meaning that interventions did not modulate the responsiveness of the diaphragm to electrical stimuli.

	Old CTRL	Old N	Old EX	Old EX+N
Maximal tetanic force (mN/mm²)	57.83 ± 17.14	70.31 ± 34.37	45.30 ± 14.00	54.18 ± 13.87
Peak twitch force (mN/mm²)	11.95 ± 2.51	12.10 ± 8.47	7.15 ± 2.67	10.55 ± 3.89
Time to peak (s)	0.05 ± 0.01	0.06 ± 0.01	0.06 ± 0.01	0.06 ± 0.01
Time to relaxation (s)	0.09 ± 0.01	0.10 ± 0.02	0.10 ± 0.02	0.11 ± 0.02

Table 5. Intact muscle contractility evaluations on Diaphragm of old mice. *No significant variances are assessed in the parameters under investigation, in neither of the treated groups compared to the Old CTRL. Values are represented as means ± SD.*

These results were not properly surprising, because diaphragm is one of the most protected muscles in the musculoskeletal system, due to its involvement in the vital function of the respiration, so its function and activity tends to be maintained at basal levels. Exercise did not show any beneficial effect on force production-related parameters because old muscles may be resistant to change following stimuli, depicting a minor plasticity-driven adaptation.

Regarding the intermittent fatigue protocol, results are depicted in Figure 31. Muscle fatigue is defined by a decline in muscle force linked to repeated muscular activation, in this case electrical stimulation at increasing frequencies (Hz). Tetanic force, expressed in percentage over the pre-fatigue force at time 0, showed a rapid drop in Old CTRL group, while treatments displayed a better trend and in most cases, evident divergences in favour of a positive resistance to fatigue.

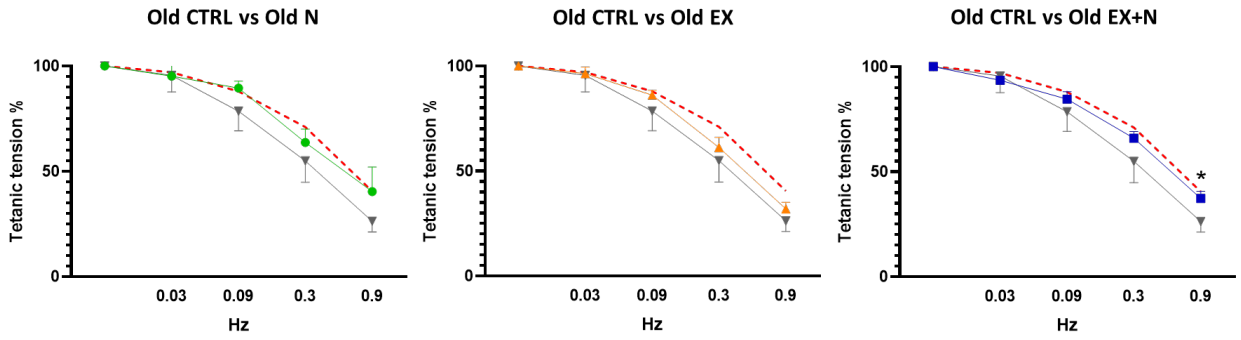

Figure 31. Resistance to fatigue assay in diaphragm of elderly mice with interventions (N, EX, EX+N) compared to Old CTRL, at increasing frequencies (0.03, 0.09, 0.3 and 0.9 Hz). *The dashed red line in the graphs represent the trend of the Young CTRL, to compare the decay of resistance. The * denotes a significant difference among the groups. Difference is considered significant when P < 0.05.*

An ameliorated resistance to fatiguing stimuli was mainly occurring on nitrate treated mice, as confirmed by the literature (Bailey *et al*, 2019 on mice; Porcelli *et al*, 2015 on humans). Even if a statistical significance was missing, the overall trend of the treatments over the Old tetanic tension

trace showed a delayed decay to fatigue. Apart from exercise, some points in nitrate supplemented mice (at 0.09 Hz, *p = 0.09* and at 0.9 Hz, *p = 0.08*) curve and in the combined supplementation with exercise (at 0.3 Hz, *p = 0.1* and at 0.9 Hz, *p = 0.01**) curve had a relevant difference that could be augmented by increasing the number of subjects evaluated. The dashed red line on each graph depicted the trend of the Young CTRL mice diaphragms. The almost precise overlap between the Old N and the Young CTRL fatigue-dependent decay of tension demonstrated an overall ameliorated resistance to the increasing frequencies stimuli, totally superimposed at 0.09 Hz, in which Young CTRL were significantly more resistant to fatigue compared to Old littermates (p = 0.009). An appreciable trend could be even assessed for EX+N mice if compared to the young cohort, thus speculating that dietary nitrate supplementation mildly acted as an ergogenic factor on diaphragm, ameliorating resistance to intermittent fatigue stimuli compared to Old CTRL groups.

We next moved on through the investigation of the modulatory effects the two-months interventions have on mitochondrial function of 24-mo mice. We evaluated the efficiency of the mitochondrial ETC through the Oroboros-O2k technique (ref. Materials and Methods). Briefly, the substrate-uncoupler-inhibitor titration (SUIT) protocol we performed focuses on Complexes I and II activity and major results are depicted in Figure 32, below. The muscle used for this study was the Tibialis Anterior, a muscle of mixed fibers composition.

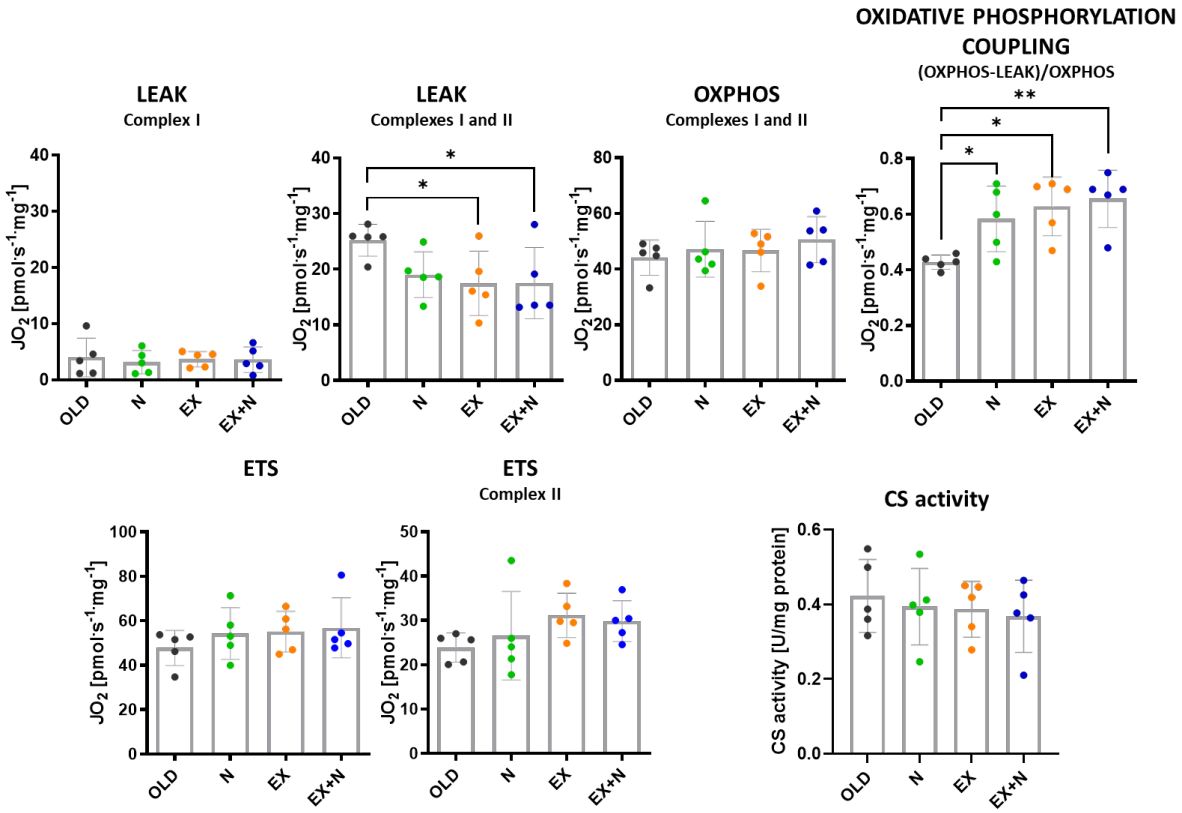

Figure 32. High resolution respirometry on Tibialis Anterior mitochondria through SUIT protocol performed with Oroboros-O2k. *LEAK (Complex I) represents the proton dissipation following G+M (glutamate+malate). LEAK (Complexes I and II) represents the proton dissipation following S (succinate). OXPHOS (complexes I and II) represents the mitochondrial respiration following the addition of submaximal ADP concentrations. ETS (electron transport system) is the maximal uncoupled respiration following the addition of FCCP (an uncoupler). ETS (of Complex II) is the maximal uncoupled respiration following Rotenone, which inhibits Complex I activity. Oxidative Phosphorylation Coupling is the maximal capacity of the oxidative phosphorylation solely finalized to mitochondrial respiratory chain and thus, indirectly, ATP production. Data are shown in JO_2 [pmol*s^{-1}*mg^{-1}], depicting the oxygen flux measured by the machinery. CS activity, in the last panel, is evaluated in TA samples in proximity of the one used for the SUIT protocols. The * denotes a significant difference among the groups. Difference is considered significant when P < 0.05.*

LEAK phase, which is indicative of proton dissipation not associated with the oxidative phosphorylation, was assessed in Complex I alone (stimulated by the addition of substrates Glutamate+Malate) and together with Complex II with further addition of Succinate. While no changes were visible in proton leak in Complex I of interventions compared to the Old CTRL, the proton leakage from Complexes I+II following Succinate injection showed a significant decreasing trend in both exercised groups (Old EX and Old EX+N) compared to the Old CTRL. The fact that protons did not dissipate during the mitochondrial respiration means that the system devoided to spare protons that were thus highly involved in the ETC mechanism, maximising their transport. Nitrate supplementation *per se* did not show any significant trend, even if raw data positioned them closer to the exercise interventions than the control mice (Old CTRL: *25.22 ± 2.86*; Old N: *19.03 ± 4.11*; Old EX: *17.48 ± 5.78*; Old EX+N: *17.50 ± 6.39*). By the analysis of OXPHOS, then, we evaluated the oxidative phosphorylation capacity following ADP submaximal saturating titrations. In this case, the system did not show any intrinsic change in all the conditions investigated in 24-mo mice. But when we evaluated the maximal capacity of the oxidative phosphorylation (without leak proton dissipation) of these mice, all treatments showed a significant positive trend. Both exercise and nitrate (on their own or in combination) displayed a higher intrinsic oxidative phosphorylation efficiency, attributable to the beneficial effects these treatments had on the leak phase (rather than the OXPHOS; Clerc *et al*, 2007).

Regarding the maximal electron transport system (ETS) efficiency (with both Complexes I and II stimulated and with the inhibition of Complex I following Rotenone injection), no changes were visible among interventions in comparison with the Old CTRL. A tendency to increase was valuable in the exercised groups when Complex I is inhibited. The evaluation of ET system is referred to the degree of uncoupling of mitochondria and it is strictly linked to ATP production. A significant increase in uncoupling of mitochondria was considered a side-effect of the swelling and structural

abnormalities seen in individuals with malignant-hypertermia susceptible phenotype (Lavorato *et al*, 2016). ETS, thus, evaluates the capacity of the electron transport chain not associated to ATP production, meaning all the electron fluxes promoted by the ETC and the uncoupled proteins and not finalized to the oxidative phosphorylation. The importance of this value is revealed when compared to the OXPHOS capacity. When the ET capacity reaches major values than the OXPHOS (as in our case, for all the groups), the phosphorylation system limits OXPHOS capacity, and there is an apparent E-P (ETS-OXPHOS) excess capacity, but this is considered a physiological parameter, postulated in healthy human skeletal muscle mitochondria (Pesta *et al*, 2011).

The parameters evaluated for the mitochondrial respiratory efficiency needed to be normalized to the activity of CS (Eigentler *et al*, 2020). In these panels, normalization was not performed but the levels of CS activity *per se* did not change all over the Old groups, as seen in the last panel of Figure 32. Normalizing all the respirometry values for the CS activity will not change the outcomes discussed previously. This means that the interventions on Old mice promote a beneficial effect on the quality of mitochondrial respiration, independently by the quantity.

Overall, data relative on mitochondrial respiration suggested an ameliorated functionality of mitochondria from mice subjected to two-months exercise training, with and without nitrate supplementation. The effects of nitrate were milder but we can speculate a beneficial effect of this treatment based on the positive maximal oxidative phosphorylation evaluated in this group, compared to Old CTRL. In particular, by specifically studying Complexes I and II, we can conclude that Complex II is shown to have an ameliorated functionality while Complex I did not show any change in mice subjected to interventions and Old CTRL. A decrease in proton leakage was strongly visible in the exercised groups only when Complex II was stimulated, and ETS following inhibition of Complex I showed a mild increase in the Old EX group, representing an insult of the ET chain not visible with Complexes I and II togheter. The ameliorated functionality of Complex II not accompanied by complex I could be attributable to the heterogeneity of responses that the mitochondrial respiratory chain had, following different stimuli, and to a degree of resistivity in changes typical of ageing.

Overall, treatments submitted to 22-mo animals for two months have been demonstrated to be effective on indicative parameters: NOx concentration increased following supplementation so to augment bioavailability within the muscle tissue, confirmed by a mild improvement of force decay following intermittent fatigue protocol; aerobic exercise training ameliorated the spontaneous

mobility and thus the locomotor behaviour of elderly mice. Moreover, mitochondrial quality was ameliorated following functional evaluation, in all the conditions studied and compared to the Old CTRL.

2.3 Effects of interventions on neuromuscular junction in aged mice

We next evaluated the impact of the two interventions (N and EX) and the combination of two (EX+N) in 24-mo mice on different aspects of the NMJ, starting from its stability, morphology and then the denervation-related factors, all parameters found highly impaired in ageing. It is well known that exercise generally acts on muscle so as to ameliorate some trophic aspects of it and induce a remodelling that concerns many aspects of this tissue. On the other hand, interest on nitrate supplementation start arose few decades ago (ref. Introduction) because of their beneficial outcomes in ameliorating time to exhaustion and VO_{2max} in sport science evaluations. In the following paragraphs we elucidate all the effects these interventions promote at the level of the NMJ, the synapse involved in the primary triggering of muscle contraction.

2.3.1 Factors involved in NMJ postsynaptic stability

We firstly analysed the expression of factors involved in the stability of the NMJ. As demonstrated before, during ageing the expression of proteins involved in the postsynaptic assembly of the synapse are strongly induced in their expression. This increase is justified in a compromised elderly system as the latest insult to compensate for structural deficiencies and try to reconstitute a spatially well-organized and functional postsynaptic framework. Transcript levels of the subunit-α and -γ were evaluated in Gastrocnemius of all the Old groups (Figure 33). While the subunit-α did not change following interventions, the subunit-γ significantly increased in the combined EX+N intervention against both Old CTRL and Old N. Overall, an increase in subunit-γ could be ascribed as an exercise-related effect (because nitrate supplementation alone did not promote any change in expression), and a mild trend to increase of subunit-α could confirm this point of view (proven by Mor Huertas *et al*, 2020). In conditions of skeletal muscle atrophy, exercise has been shown to maintain muscle function through adaptations to the NMJ, which can induce its hypertrophy through an increase in the number of acetylcholine (ACh)-containing vesicles, acetylcholinesterase and the number of AChRs within the motor endplate in an attempt to stabilize the structure and cluster the receptors in a confined area (Gonzalez-Freire *et al*, 2014, Nishimune *et al*, 2014).

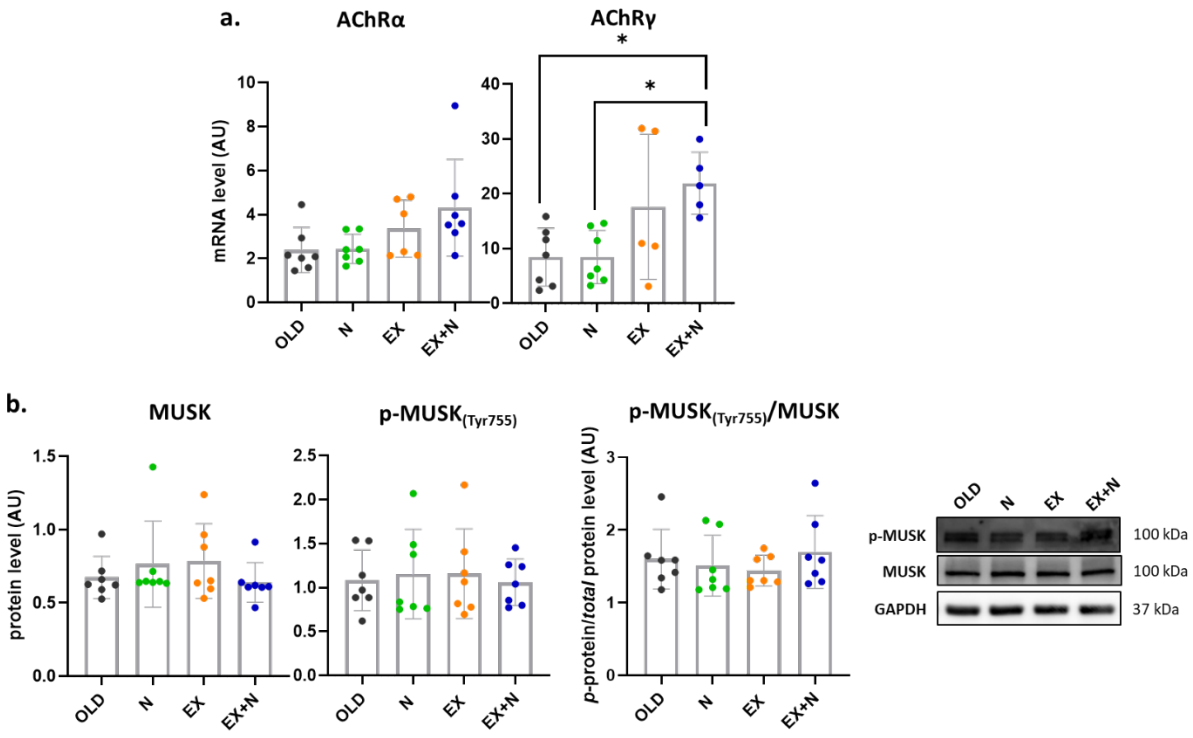

Figure 33. Factors involved in postsynaptic neuromuscular stability. *a) Transcription level of two of the main acetylcholine receptor (AChR) subunits: the alpha subunit is of relevance due to its stoichiometric presence in the pentameric receptor assembly (2 out of 5 are alpha subunits). The gamma subunit is the foetal/embryonal subunit highly induced following denervation, damage and traumatic events. It is notoriously recognized as one of the main denervation-related factors. b) Protein level of Muscle Specific Kinase (MuSK) in its total protein content and its phosphorylated content over the housekeeping GAPDH. The last graph depicts the phosphorylated isoform levels over the total protein amount. Representative Western Blot analyses are presented close by. The * denotes a significant difference among the groups. Difference is considered significant when P < 0.05.*

We thus evaluated the protein levels of MuSK in all the experimental groups under investigation, in both its total protein content and its activating phosphorylation at Tyr-755. No trends or changes were visible in any of the interventions, and especially (and surprisingly) on the exercised groups, in which, as previously explained for the AChR subunits, a remodelling of the postsynaptic side of the junction could be stimulated by exercise in order to ameliorate muscle function, starting from the NMJ structure. By the way, MuSK levels in ageing were previously demonstrated to be augmented in an effort to preserve the postsynaptic structure.

On the whole, exercise intervention increased the expression of AChR subunits, not accompanied by an increase in MuSK protein levels and phosphorylation, which remained expressed at basal levels of Old CTRL. Conversely, nitrate supplementation did not show any particular beneficial trend on the indirect molecular markers of the postsynaptic NMJ structure stability.

2.3.2 Morphological evaluations of NMJ

We continued our investigation regarding how NMJ responded to these interventions and so which aspects of the junction were modulated by external inputs in a physiological elderly system (Figure 34). Morphological analyses were performed on Extensor Digitorum Longus (EDL) muscles, due to the feasibility of the immunofluorescence protocol on this muscle (explained in Materials & Methods). Young CTRL data are represented in all the morphological parameters in order to have a reference value that can be compared with the data relating to the treatments, while a direct statistic was made between Young CTRL and Old CTRL so as to monitor how much the neuromuscular structure has been affected by ageing. This prompted us to visualize the effects of treatments from a critical point of view and could therefore suggest us the significance of trends and/or remodelling of the junction. Any change that is promoted by a treatment compared to the Old CTRL, if it moves towards levels of the Young CTRL, can be considered as a beneficial change.

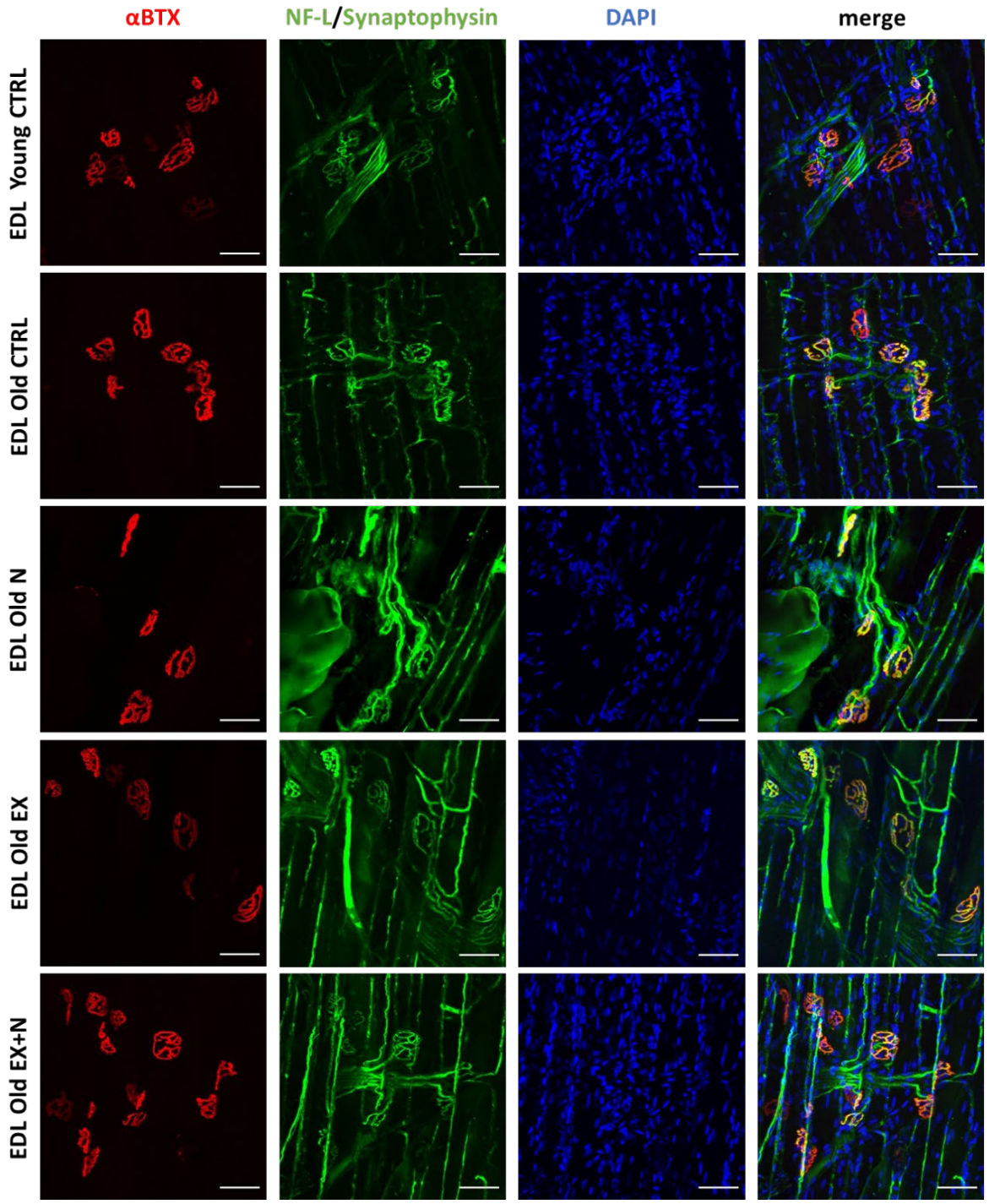

Figure 34. Panel depicting representative images of NMJ morphologies from EDL of all the experimental groups. *Red channel represents the αBTX; the green channel is the combination of Nf-L and Synaptophysin, which together stain the presynaptic side. Nuclei are marked with DAPI (in blue). Merge is the combination of the three channels. Scale bar 50 µm.*

Parameters under investigations can be divided in three macro-areas: presynaptic and post-synaptic parameters, and values related to the interaction among the two sides a NMJ is formed. We used this approach according to Jones *et al*, 2015. We firstly measured indicative parameters related to the presynaptic nervous part remodelling in ageing and following interventions (Figure 35).

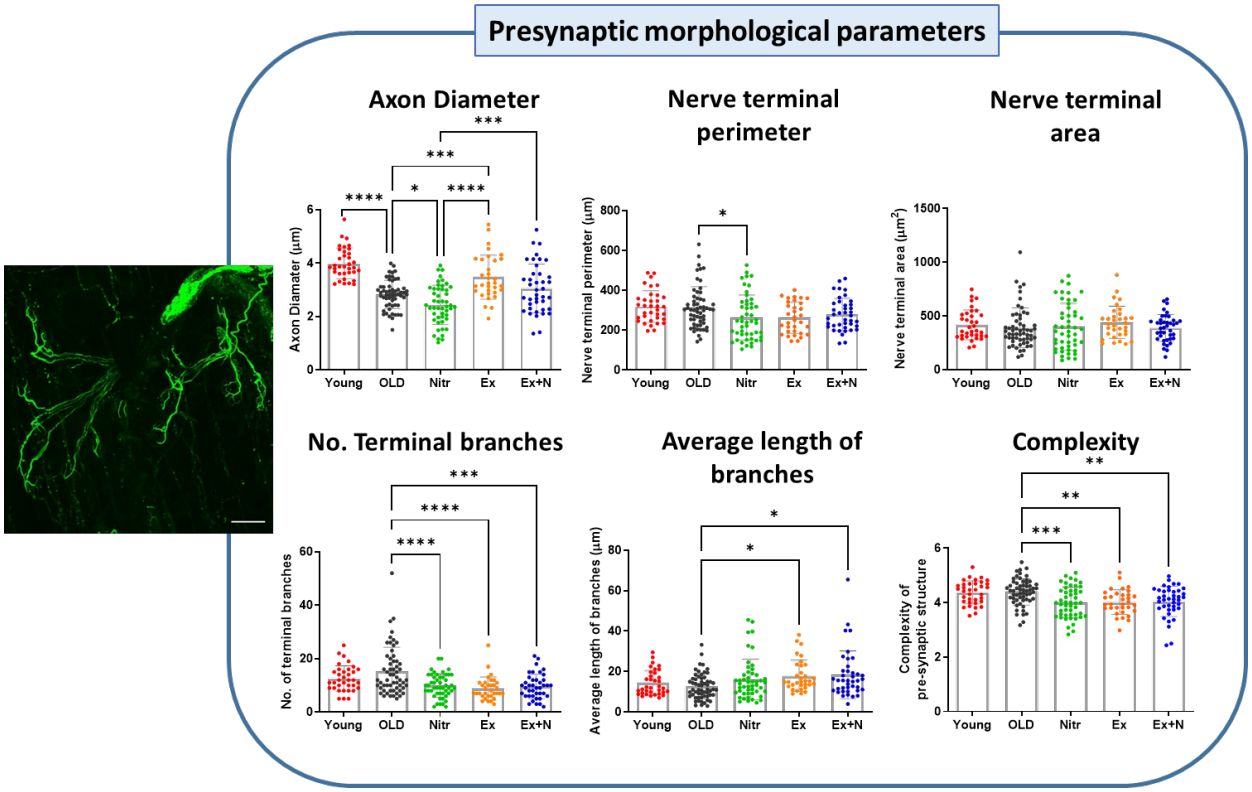

Figure 35. Morphological evaluations of the presynaptic side of the NMJ. *Panel depicting the analysis of parameters indicative of the presynaptic stability and adaptations. Parameters and measures are written in the Y axis of each graph. Young CTRL is depicted together with Old groups only as a reference for Old groups trending assessments. For statistical references, one-way ANOVA was performed only among cohorts of the same age (Old CTRL, N, EX, EX+N), while statistics between Young CTRL and Old CTRL is based on the student t-test. On the left, a representative image of the presynaptic side, from an EDL Young subject. Scale bar 100 µm. The * denotes a significant difference among the groups. Difference is considered significant when P < 0.05.*

Axon diameter value was significantly decreased during ageing (Krishnan *et al*, 2017), but exercise seemed to hardly re-establish a strong axon remodelling. Nitrate supplementation seemed not to improve terminal axon trophism, in fact axons from Old N groups seemed to undergo further atrophy, and in mice cohort undergoing combined interventions, nitrates seemed do diminish axonal "hypertrophy". The fact that axon diameter assumed so many variegate values is based on the high plasticity this structure is subjected from the development to late stages of lifespan. Repeating cycles of denervation and reinnervation occur during lifespan, when motor neuron terminal transiently disconnects from its muscle fiber, rapidly followed by reinnervation of vacant sites by the original motor axon (if still intact) or through collateral sprouting from adjacent smaller axons (Hepple and Rice, 2016). When a strong interaction among adhesion molecules ubiquitously expressed in both faces of the NMJ structures is established, axon can develop a hypertrophic phenotype to strengthen the interaction with the muscles. So, with these assumptions, smaller axons are indicative of a denervation/reinnervation process frequently occurring, trying to remodel

the junctional interaction and strongly maintain it (in Krishnan and colleagues' paper, axon diameter values in ageing resemble the values of very young mice, when maturation and bond balances need to be defined).

Nerve terminal perimeter and area did not particularly change, due to a wide distribution of the values calculated from the terminal branched axonal portion. The variety of these parameters is not surprising due to a very heterogeneous variability of NMJ morphology and their frame that may be referred to different time of remodelling following different physiological and external (our interventions) stimuli.

Terminal branches were calculated as the number of branches composing a presynaptic junction and the average length each branch has in that structure. All the treatments showed a significant diminished number of branches compared to Old CTRL. Old CTRL, then again, had an increased number of branches likened to Young CTRL ($p = 0.05$): this result suggested us that a decrease in branching numerosity pushed the nervous organization of old treated groups very close to a younger condition. This datum was reinforced by the average length of these branches, highly increased in Old animals in an exercise-dependent manner. As a whole, these analyses described presynaptic nerve undergoing continuous remodelling, especially promoted and much prominent in Old group of mice subjected to exercise training (with and without N), in which a simpler branching was established, but of a wider extent. In fact, Old EX showed a *13%* increase in nerve terminal area spatially covered, in comparison with Old CTRL. Complexity of presynaptic side, calculated as a logarithmic function of branchings and areas occupied, was significantly decreased in all the Old cohorts undergoing interventions (Old N, EX, EX+N) compared to Old CTRL. These results suggested the establishment of a simplistic presynaptic structural organization arosen from a stimulated remodelling of the NMJ.

We next moved on with the analyses of postsynaptic parameters indicative of AChR clustering, compactness and dispersal on the surface of the sarcolemma (Figure 36).

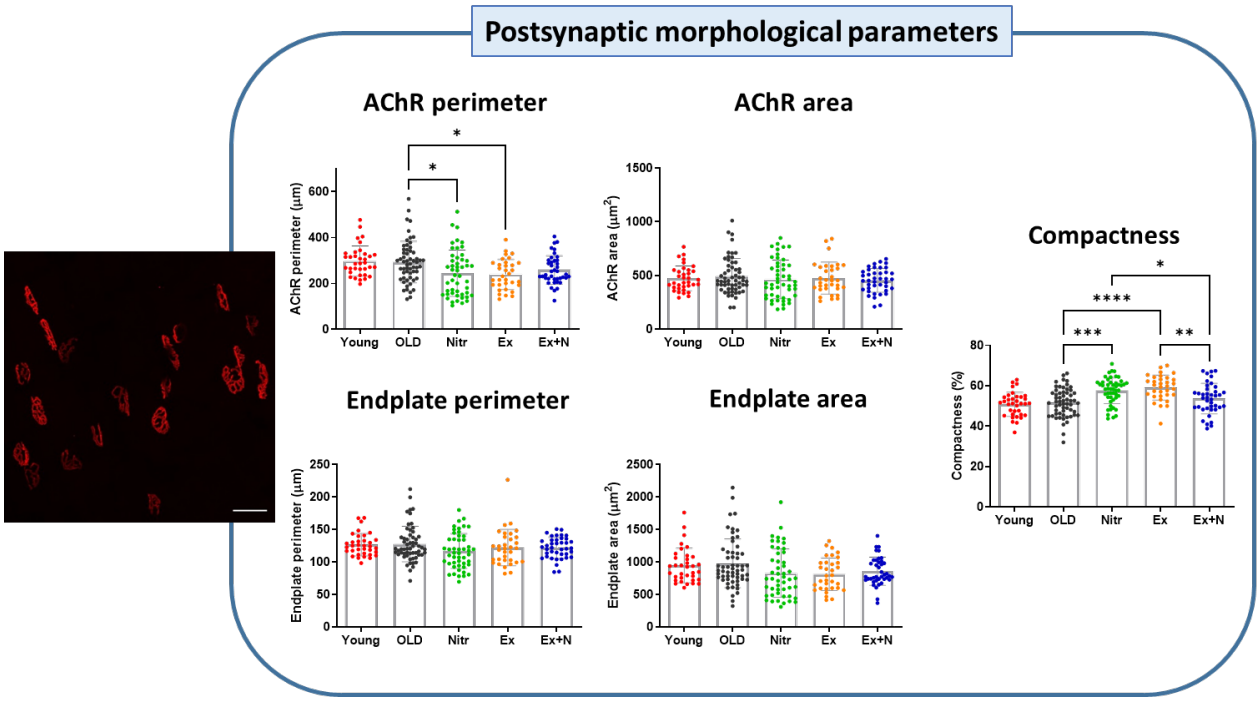

Figure 36. Morphological evaluations of the postsynaptic side of the NMJ. *Panel depicting the analysis of parameters indicative of the postsynaptic stability and adaptations. Parameters and measures are written in the Y axis of each graph. Young CTRL is depicted together with Old groups only as a reference for Old groups trending assessments. For statistical references, one-way ANOVA was performed only among cohorts of the same age (Old CTRL, N, EX, EX+N), while statistics between Young CTRL and Old CTRL is based on the student t-test. On the left, a representative image of the postsynaptic side, from an EDL Young subject. Scale bar 100 µm. The * denotes a significant difference among the groups. Difference is considered significant when P < 0.05.*

Postsynaptic parameters can be divided into the strict perimeter delimiting the area of AChR spatial organization, and the perimeter of the overall average area in which AChR clusters are distributed (endplate). In this case, no significant differences were found in perimeter and area of both AChR pretzel-like structure and endplate. Nitrate supplementation and exercise, separately, showed a significant decrease in the perimeter of the AChR clusters respect to Old CTRL, but the average level did not rank in line with the perimeter of Young CTRL animals. This could suggest, as for the presynaptic side, a simplistic spatial organization of the receptors, which could be a synonym of primary steps of reorganization. Regarding the other parameters indicative of a postsynaptic spatial distribution, no significant trends and changes were assessed among the old mice and even compared to the young cohort. A valid explanation can be ascribable to the heterogeneous distribution of values each group has within, speculative of the variety of structures every cohort has. Any strong changes in morphological AChR parameters were even evaluated in Young, Old, and Old Exercised EDL from rats by Brown *et al*, 2019, while, as the majority of the literature reports, exercise tend to increase pre and postsynaptic areas (in TA of 25-mo mice, Cheng *et al*, 2013).

Different outcomes can arise by the evaluation of different muscles, as described by Arnold *et al*, 2014, in which they study NMJ molecular and morphological parameters in transgenic mice overexpressing and downregulating PGC1α, mimicking thus an exercised molecular phenotype. Morphological analyses on EDL muscle follow our same trend regarding exercise and control elderly mice (an increased average length of the branches and a reduced AChR area), while evaluations on Soleus muscle do not show any perturbation in NMJ morphology. Overall, morphological changes could be muscle-dependent and exercise could act differently on those parameters. Regarding nitrate supplementations, the literature is poorly enriched of studies on NMJ morphology adaptations following supplementation so it is quite difficult for us to give an interpretation to the solely data related to Old N cohort. A fashioned study on Drosophila and NOS (the enzyme involved in the endogenous production of NO) demonstrated how overexpression and inhibition of NOS, with the subsequent increase and decrease of NO production, changes morphological features during development of this animal model (Robinson *et al*, 2017). But the majority of the papers on NO and NMJ is mainly focused on characterizing the activity and regulation of the synaptic transmitter release: this branch of observations is still controversial, with some studies demonstrating enhancement (Nickels *et al*, 2007) and others suggesting suppression (Etherington and Everett, 2004) of transmitter release by NOS activity and thus NO concentration.

Compactness, at the end, represents the percentage of the distribution of AChR clusters within the endplate area. Nitrate supplementation and exercise, independently, showed a significant trend in Old mice compared to the Old CTRL, while combination of the two, again, did resemble the same percentage levels of the CTRL. A highly compact postsynaptic structure means that AChR clusters do not disperse throughout the area delimited by the endplate perimeter, but they are found closely organized.

Finally, we studied the interaction among the pre and the postsynaptic structures by calculating the percentage of overlap among the two structures and so the unoccupied AChR area, the one not covered by nerve terminal and so that did not receive direct nervous signals. At last, we evaluated the fragmentation of the postsynaptic area based on the clusters the AChR forms and their average area based on AChR area (Figure 37).

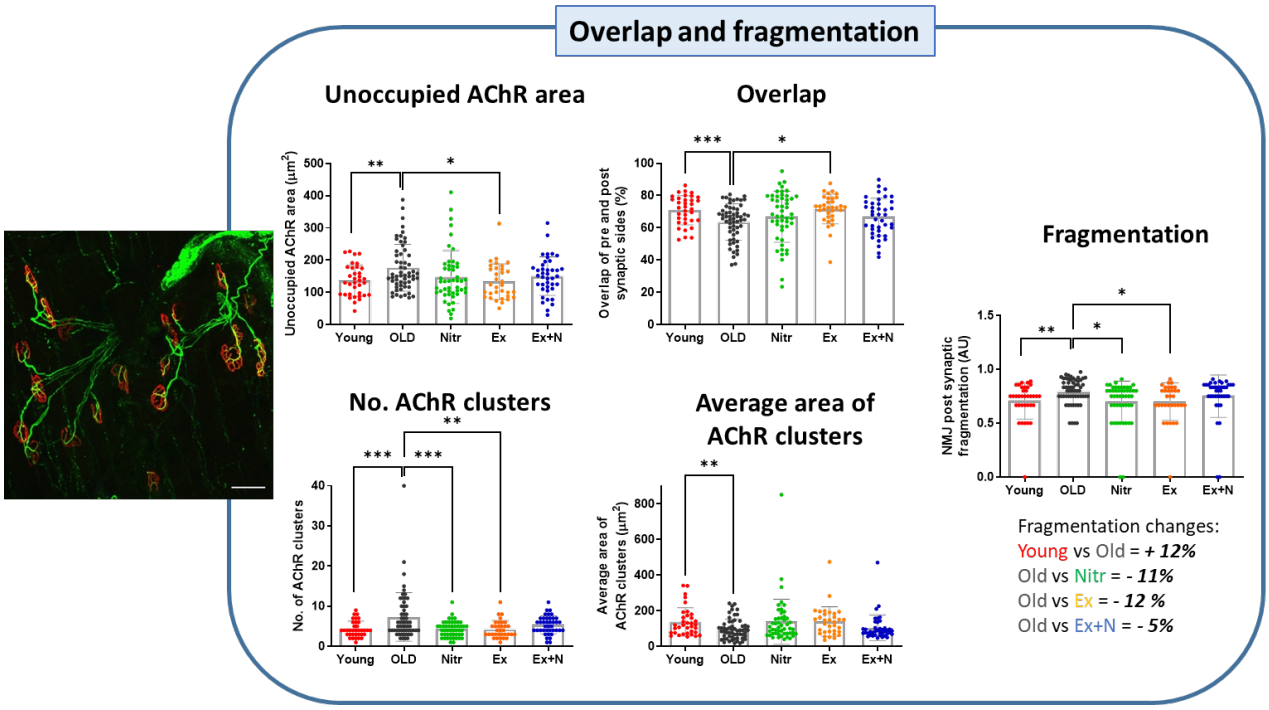

Figure 37. Morphological evaluations of the interaction between pre and postsynaptic sides of the NMJ, and fragmentation index. *Parameters and measures are written in the Y axis of each graph. Young CTRL is depicted together with Old groups only as a reference for Old groups trending assessments. For statistical references, one-way ANOVA was performed only among cohorts of the same age (Old CTRL, N, EX, EX+N), while statistics between Young CTRL and Old CTRL is based on the student t-test. On the left, a representative image of the merge, from an EDL Young subject. Scale bar 100 µm. The * denotes a significant difference among the groups. Difference is considered significant when P < 0.05.*

The unoccupied AChR area of all Old groups was measured as a subtraction of the presynaptic area from the postsynaptic one. By this value, the overlap of the two structures was calculated as percentage. Old CTRL junctions showed a significant decrease in overlapping areas compared to Young CTRL littermates: despite no significant changes in pre and postsynaptic areas were assessed in the previous panels (Figures 35/36; nerve terminal area in µm^2 of Young CTRL: *417.89 ± 138.11* vs Old CTRL: *389.35 ± 183.94*; AChR area in µm^2 of Young CTRL: *473.94 ± 116.38* vs Old CTRL: *494.00 ± 165.86*), a higher unoccupied AChR area was assessed in the Old cohort, due to the fluctuations of the values' distribution. Intrinsic variances inside each group could thus assume combinations among the pre and postsynaptic areas so as to establish an inverse correlation among the two (meaning a low presynaptic value correlating with a higher postsynaptic one). Physiologically, an increased AChR area that is not superimposed by the nerve terminal is indicative of a junction that does not fully receive the nervous stimulus and thus can be defined not fully active. Missing the nervous contact and so the trophic activity in some areas can lead to a dispersal of those AChR

clusters away from the junctional area, disrupting the positive feedback mechanism that arise from their interaction and the exchange of trophic factors, to preserve and maintain the NMJ.

Among the interventions proposed on Old animals, the percentage of overlap between the pre and postsynaptic areas displayed a significant amelioration in the exercised group, resembling the values of the Young cohort. Nitrate supplementation did not significantly change this parameter in both isolated and combined intervention (Old CTRL vs Old N, $p = 0.06$ and Old CTRL vs Old EX+N, $p = 0.05$). A higher distribution was visible in both cohorts and this could be indicative of a higher intrinsic variance that diminished the probability of significance. However, the average value of both groups were graphically shifted in favour of the Young cohort rather than the Old CTRL, so we could speculate a mild effect of this intervention on the maintenance of trophic interaction between the two synaptic sides.

To conclude, fragmentation of the junctions was calculated in all groups under investigation starting from the number of AChR clusters counted for each junction. Old CTRL mice had a higher fragmentation compared to Young littermates (*+ 12%*), and this goes in accordance with the literature. NMJ fragmentation is often referred as a hallmark feature of ageing and pathological conditions (Rudolf *et al*, 2014), and our 24-mo mice are totally found enclosed within this characteristic. Fragmentation is the reflection of the physiological consequence of a missing overlap with the nerve terminal: as aforementioned, unoccupied AChR areas are missing those nervous-based maintenance stimuli and thus undergo slow dispersal in the nearby area, leading to a fragmented postsynaptic appearance.

Regarding all the interventions promoted in Old mice, nitrate supplementation and exercise training, separately, significantly decreased the fragmentation index (- *11%* and - *12%*, respectively) of the postsynaptic side of the junction. This is occurring due to lower number of AChR clusters found in the structures of these mice. The positive effects of these interventions alone (because the combined one shows a faint *5%* decrease in fragmentation compared to Old CTRL) showed a beneficial outcome for the postsynaptic side of the junction, that has been demonstrated to be highly compacted in Figure 36 (Compactness %). Moreover, the overlap values of Old EX group were significantly increased compared to the Old CTRL, establishing thus a positive feedback among pre and postsynaptic sides. Regarding Old N group, overlap percentage was not significant but very close by ($p = 0.06$), so we can speculate this beneficial feedback even in this treatment. The final parameter studied was the average area of AChR clusters. A decrease in the average area was

assessed in elderly CTRL mice, that had a higher number of clusters compared to young littermates: elevated numbers of small clusters supported the fragmentation spread significantly present in our 24-mo animals. Aged mice with interventions did not have significant trends in clusters' areas but mean values of Old N (*138.88 ± 126.59* μm^2) and Old EX (*139.47 ± 83.16* μm^2), independently, closely resembled the one of young cohort (*137.66 ± 79.18* μm^2), meaning that postsynaptic organization undergoes beneficial remodelling.

To sum up this huge part related to morphological evaluations of NMJ and the structure it is composed, an impairment in the Old CTRL group compared to young littermates is established (a decreased axon diameter, mild impoverishment of presynaptic morphology and an augmented fragmentation caused by a missing complete overlap among pre and postsynaptic parts). Among all the interventions our 24-mo mice underwent (nitrate supplementation, exercise training and the combination of the two), exercise strongly promotes a positive remodelling of both pre and postsynaptic sides in most of the aspects under investigation, that ends up with a beneficial amelioration of the physical interaction among the two sides and so less fragmented junctions. Nitrate supplementation, likewise, follows almost the same positive trend the exercise promotes, but in a milder way (some parameters are missing in statistical relevance), speculating a beneficial remodelling even in this case. Surprisingly, the combination of the two interventions do not show the expected trend, maintaining most of the times values relatable to the Old CTRL condition. There may be some mechanism in this combined treatment that hampers the beneficial effects these treatments promote on their own, separately.

A very important aspect needs to be taken into account regarding the study of the morphological features of the NMJ. As visible in Figure 38, and as widely said during the discussion of different parameters, NMJs are depicted as highly heterogeneous structures regardless of the developmental conditions, the passing of time and so ageing, the arising and progression of pathologies. This means that in adult muscles it is possible to see fragmented structures, nonlinear postsynaptic tubuli, as well as detachment of the axon terminals and decreased definition of the presynaptic branches. The analyses of these impaired structures can lead to a non-homogeneous distribution of values that can interfere with the arising of significant differences. This is explained by the high plasticity that characterizes the NMJ: denervation/reinnervation phenomena naturally occur during the lifespan, and spatial remodelling of the junction is continuously promoted and stimulated by endogenous and/or exogenous signals in order to cope with any environmental change and load. On the other

hand, the processing of images from elderly muscles may return continuous postsynaptic tubuli that can be underestimated in terms of number of clusters. By visualising these structures, however, it can happen that a disorganized structure with irregular jagged edges is clearly visible, demonstrating an impaired not-healthy structure. The huge variability of the morphological features visible in the following figure shown is thus an important variable to keep in mind every time these analyses are performed.

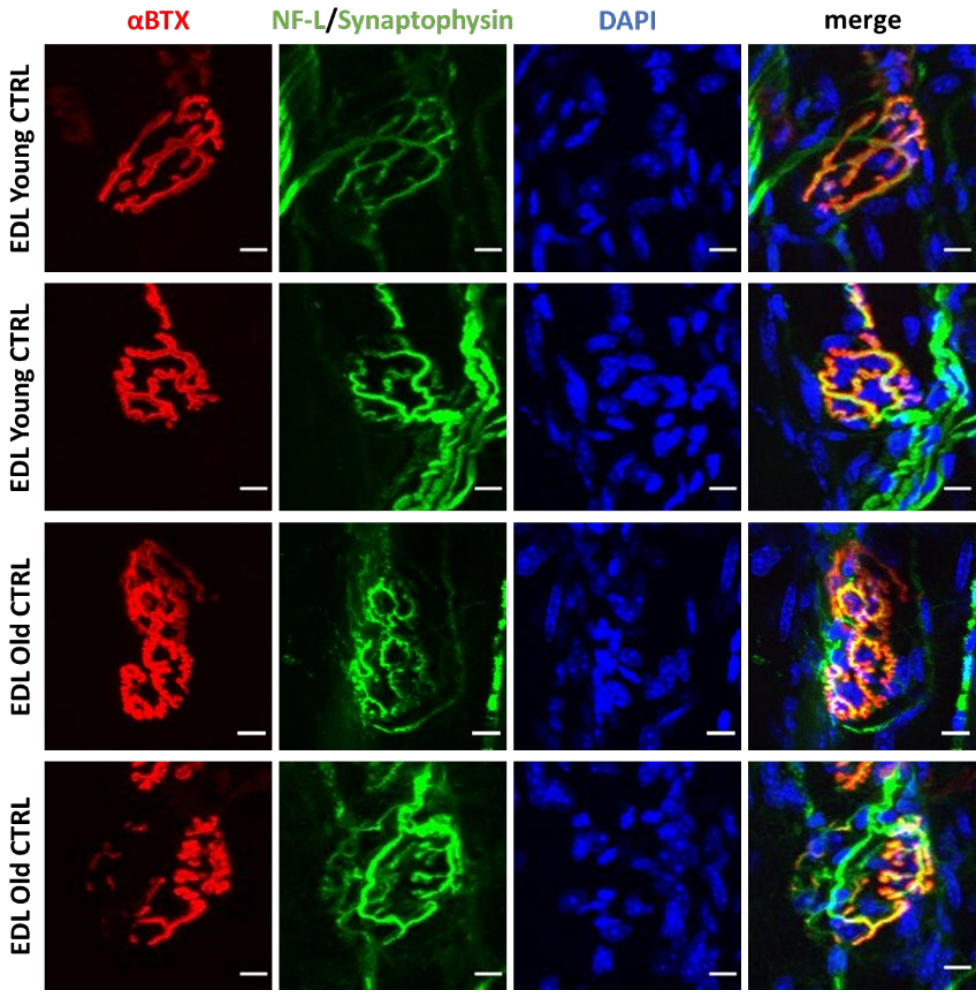

Figure 38. Maximal Z-stack projection images of NMJ morphology from EDL muscles acquired through the confocal microscopy technique. *Only Young CTRL and Old CTRL are represented here in order to give an example of the heterogeneity these structures undergo, in an age-independent manner. αBTX marks the postsynaptic side due to its specific binding to AChRs (in red); light neurofilament (NF-L) and synaptophysin (Syn) label the presynaptic structure (in green); nuclei are stained with DAPI (in blue). Merge is the superimposition of the three channels. Magnification 20x, digitally zoomed post-acquisition. Scale bar 10 µm.*

2.3.3 Denervation-related factors

To better evaluate the interaction among the pre and postsynaptic structures and the cross-talk that occurs among them, we studied the expression of the denervation-related factors so as to assess

the effects of interventions on denervation/reinnervation cycles in ageing. We previously demonstrated how these factors were highly induced in elderly mice, indicative of an impaired junctional interaction. Transcription levels of the main factors were evaluated (Figure 39).

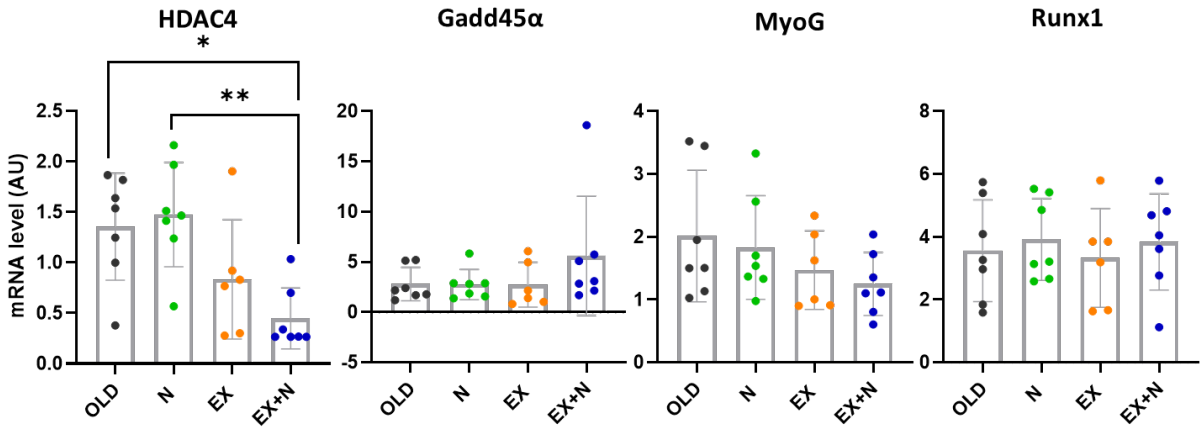

Figure 39. Transcriptional expression of denervation-related factors in Gastrocnemius. *The expression of these factors is directly linked to loss of axonal innervation and subsequent attempt of the muscle to recall back innervation. Ageing strongly induces their expression but treatments show to have an effect only on HDAC4 expression. The * denotes a significant difference among the groups. Difference is considered significant when P < 0.05.*

Histone deacetylase-4 (HDAC4) significantly decreased in its expression in the combined Old EX+N cohort compared to the Old CTRL and the Old N. The clear trend to decrease of the exercised group, but not of the nitrate alone, suggested a downregulation of HDAC4 modulated by exercise. This pathway is mediated by AMPK, which is found induced by exercise and associated with increased glucose intake (McGee *et al*, 2003). In this paper, even if AMPK transcript and protein levels do not augment following exercise (as it happens in our 24-mo mice subjected to exercise training compared to Old CTRL, data not shown), its functional activity was associated to its nuclear translocation, where it can modulate gene and protein expression and, among all, negatively regulate HDAC4 activity (Niu *et al*, 2017). Because HDAC4 is associated with a denervation-related atrophy and thus assume negative shades on muscle mass and maintenance, exercise seemed to ameliorate this negative outcome by decreasing HDAC4 transcript levels.

Surprisingly, being HDAC4 a positive regulator of the other factors Gadd45α and MyoG, these transcripts did not follow the same trend the histone deacetylase underwent, as conversely viewed by Yoshihara and colleagues, in which atrophy of elderly rats is attenuated by exercise-modulating HDAC4/Gadd45α downregulation (Yoshihara *et al*, 2019). Gadd45α is known to be regulated by other transcription factors, as for example the activating transcription factor 4 (ATF4), that is

strongly induced in stressing conditions as denervation, ageing, fasting, in which it promotes atrophic pathways (Ebert *et al*, 2012) and may not be influenced by our interventions. MyoG did not change in expression levels but a mild trend resembling HDAC4 was visible. In the end, Runx1 did not change its transcript levels following intervention, assuming the same transcription levels of the Old CTRL.

Taken together, denervation-related factors were strongly modulated by none of the interventions the old animals underwent. Exercise had only mild effects on the modulation of HDAC4, strengthened by the combination with nitrates, but still not sufficient to strongly decrease MyoG transcript levels. The last denervation-related factor taken under investigation was NCAM1, evaluated in its transcript levels and cellular expression and localization (Figure 40).

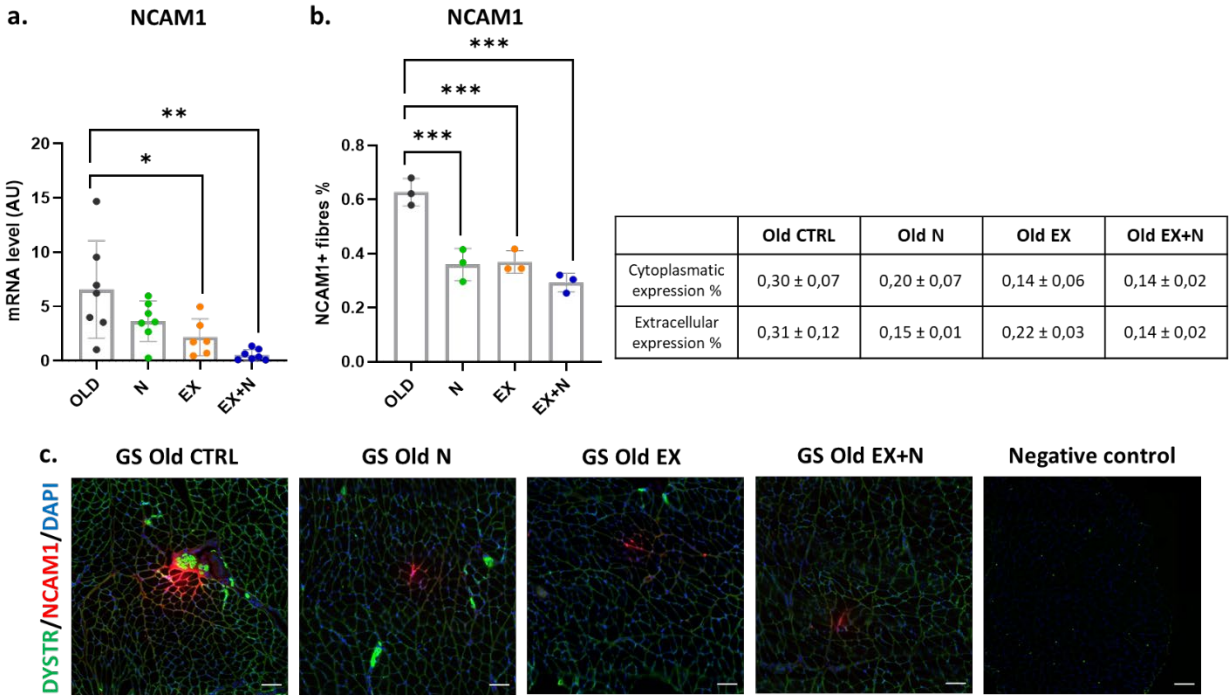

	Old CTRL	Old N	Old EX	Old EX+N
Cytoplasmatic expression %	0,30 ± 0,07	0,20 ± 0,07	0,14 ± 0,06	0,14 ± 0,02
Extracellular expression %	0,31 ± 0,12	0,15 ± 0,01	0,22 ± 0,03	0,14 ± 0,02

Figure 40. Analysis of Neural Cell Adhesion Molecule 1 (NCAM1) expression and localization in Gastrocnemius. *a) Transcript level of NCAM1 significantly decrease in mice subjected to exercise protocol (Old EX and EX+N). b) Percentage of NCAM1 positive fibers over the total amount of fibers counted in a transversal section of Gastrocnemius. Positive fibers are the sum of fluorescence positive signal located within the cytoplasm and confined on the membrane (extracellular signal). Next, a table resuming the percentages of cytoplasmic and extracellular/membranous expression of NCAM1, expressed in means ± SD. c) Fluorescent representative images of NCAM1 induction in old cohorts, with (Old N, EX, EX+N) and without (Old CTRL) interventions. Negative control to assess the specificity of secondary antibodies. Scale bar 100 µm. The * denotes a significant difference among the groups. Difference is considered significant when P < 0.05.*

All the interventions promoted appreciable changes in 24-mo mice. Transcription of NCAM1 was strongly downregulated in Old EX and Old EX+N compared to the Old CTRL, indicating the exercise

as the intervention that mainly modulated its expression. By the analyses of immunofluorescence on transversal sections, the percentage of fibers that positively express NCAM1 significantly decreased in all the treated old groups in comparison with the Old CTRL. Together with HDAC4 and MyoG, we can conclude that exercise promoted a beneficial effect on the expression of these denervation-related factors by means of decreasing their transcription. The combination with nitrates strongly induced this downregulation, even if nitrates alone only had effects on NCAM1 cellular expression. Improvements in the denervation/reinnervation molecular patterns driven by exercise training was thus found to be closely related to all the beneficial effects studied and evaluated through morphological evaluations.

3. Events involved in interventions-related changes in NMJ of aged mice

According to the literature, different pathways are found to be implicated in NMJ stability and plasticity, through the activation of a cascade of molecular events that contribute to remodel and adapt the junction following diverse stimuli. We focused our evaluations on four aspects that can potentially modulate NMJ features, in order to assess which of those pathways were modulated by the interventions we promoted on 24-mo mice. Based on the literature assumptions, metabolic aspects driven by master regulator PGC1α can be involved in NMJ remodelling (Arnold *et al*, 2014). PGC1α covers a relevant role in the regulation of NMJ stability through the transcriptional activity it elicits on synaptic genes expressed in the myonuclei positioned below the synaptic bouton (Handschin *et al*, 2007). The contribution it has on the expression of subsynaptic genes is mainly increased following an activity-dependent feedback signalling from the neurons, mostly elicited by exercise (Nishimune *et al*, 2014). It is moreover found implicated in mitochondrial biogenesis and the control of metabolism within the fibers, positioning it to a relevant role in the context of the muscle homeostasis. Because a wide part of the literature indicates mitochondria as one of the key features of muscular and neuromuscular impairments during ageing and pathological conditions (ref. Introduction), PGC1α can represent an important factor for the elucidation of NMJ integrity even related to this pattern.

Moreover, a dysregulation in the autophagic flux can be causative of a severe impairment of the NMJ (Carnio *et al*, 2014) with a precocious ageing spectrum, presenting this pathway as one of the mostly important in the stability and functionality of the junction. On the other hand, factors notoriously recognized as part of the synthetic pathway within the cell are now covering an interesting role in the stability of the junction: recent literature started focusing on the interaction

between NMJ stability and the synthetic pathway orchestrated by mTOR pathway (Castets *et al*, 2020), which is found to be critical for proper innervation (Baraldo *et al*, 2020). To conclude, neurotrophins and growth factors are often recalled as important factors for the innervation and thus the maintenance of an established activity-dependent interaction, through a beneficial crosstalk among the two sides of the junction (Saini *et al*, 2021). In particular, insulin growth factor-1 (IGF1) has been presented as a key factor in muscle trophism and plasticity, modulating a wide range of molecular aspects. During ageing, overexpression of IGF1 promotes beneficial effects on mass through an ameliorated mass, mitochondrial biogenesis and autophagic flux and an improved NMJ appearance (Ascenzi *et al*, 2019).

Nevertheless, it is noteworthy to say that all these observations and assessments are evaluated in transgenic mouse models or cell systems in which a genetic manipulation of factors involved in the pathways under investigation was performed, pushing thus the system to an extreme in adaptations and modulations of the responses driven by the modification. In a physiological condition as ageing, in which the system undergoes changes and detrimental outcomes, a situation in which some of the pathways previously mentioned are completely dismissed is not always evident, but conversely, complementary mechanisms are established to cope with changes and to compensate in an attempt to restore back to a functional situation.

3.1 Evaluation of PGC1α modulatory effects following interventions

Due to its main relevance on NMJ assembly and maintenance, we firstly evaluated levels of PGC1α in all the old mice groups under investigation (Figure 41).

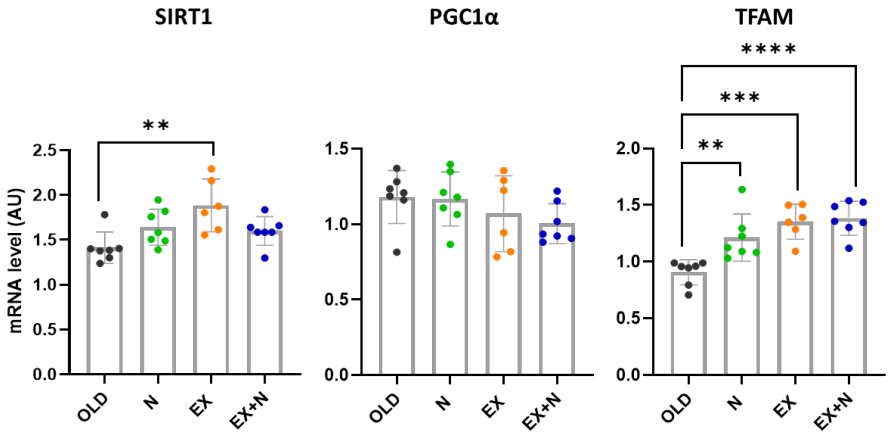

Figure 41. Transcript levels of SIRT1, PGC1α and TFAM in Gastrocnemius, three of the major markers of mitochondrial biogenesis and energy sensors for the modulation of the metabolism. *SIRT1 is an enzyme recruited for substrate deacetylation. PGC1α, one of SIRT1 targets, is a master regulator of*

*muscle and mitochondrial metabolism. TFAM (transcription factor A) is involved in mtDNA replication and transcription. The * denotes a significant difference among the groups. Difference is considered significant when P < 0.05.*

SIRT1 significantly increased in the Old EX group, while nitrates did not show any particular trend, neither alone nor in combination with EX. SIRT1 is proven to be highly expressed following exercise (Radak *et al*, 2020) as a response to stimulate and increase mitochondrial adaptations to exercise training, mainly through PGC1α deacetylation and subsequent nuclear translocation. In this case, PGC1α transcript levels and protein levels (not shown) in our elderly animals did not change in any of the treatments proposed. It is known by transversal studies on PGC1α protein levels that its overexpression is limited to few hours after exercise bouts (Tadaishi *et al*, 2011) and depends on the intensity of the exercise (Tanaka *et al*, 2017). Moreover, its transcriptional activity is dependent by its localization (active when translocated into the nucleus) and its post-translational modifications (as for example phosphorylation promoted by AMPK and deacetylation by SIRT1). Due to a higher SIRT1 induction following exercise, we can speculate that PGC1α transcriptional activity is promoted due to SIRT1-mediated deacetylation, even if SIRT1 has been demonstrated to have a nuclear activity independent by its protein content that positively correlates to mitochondrial biogenesis factors (Gurd *et al*, 2011). This assumption is confirmed by high levels of TFAM (transcription factor A) expressed at the level of the myonuclei, which translocates within the mitochondria to replicate the mtDNA and to promote transcription of the mitochondrial genes (mainly the ETC complexes). In our experimental groups, we found TFAM surprisingly overexpressed even in Old N. A strict correlation among inorganic nitrate and TFAM induction was studied at the level of the kidney (Zhang *et al*, 2021), while increasing NO concentrations in pluripotent stem cells is found to activate endoplasmic reticulum stress responses and so PGC1α activity in an attempt to recover from this situation (and thus upregulate all the mitochondrial genes it transcribes, Caballano-Infantes *et al*, 2017). What is clear is that TFAM overexpression, induced by all the intervention our 24-mo mice underwent, is considered beneficial for mitochondrial health. Moreover, transcriptional activity of TFAM on mtDNA promotes transcription of complexes forming the respiratory chain which can be more efficient in their activity, replacing the old ones (as evaluated through the High Resolution Respirometry).

On the other hand, PGC1α role for the transcription on subsynaptic genes does not seems to occur since the genes involved in the structural organization of the postsynaptic junction (AChR subunits and MuSK) were substantially not modulated by any of the intervention (Figure 33), as a reflection

of the unchanged PGC1α content. This is quite surprisingly especially for the exercised condition: genetic manipulation of mice for the overexpression of PGC1α is mainly justified as for the creation of a molecular scaffold resembling all the beneficial effects the exercise has on the metabolism through PGC1α.

To conclude, the master regulator PGC1α was not modulated by neither nitrate supplementation nor exercise, and this is reflected by the expression of the genes directly involved in the NMJ assembly and stability which were not changed in elderly animals following intervention. Moreover, no changes at the level of mitochondrial mass were evaluated (TOM20 did not change following interventions, data not shown), meaning that PGC1α did not promote biogenesis.

3.2 Evaluation of autophagic flux following interventions

We investigated key proteins involved in the progression of the autophagic machinery in order to evaluate the consequences of interventions on 24-mo mice and if this pathway could be directly related to NMJ changes (Figure 42).

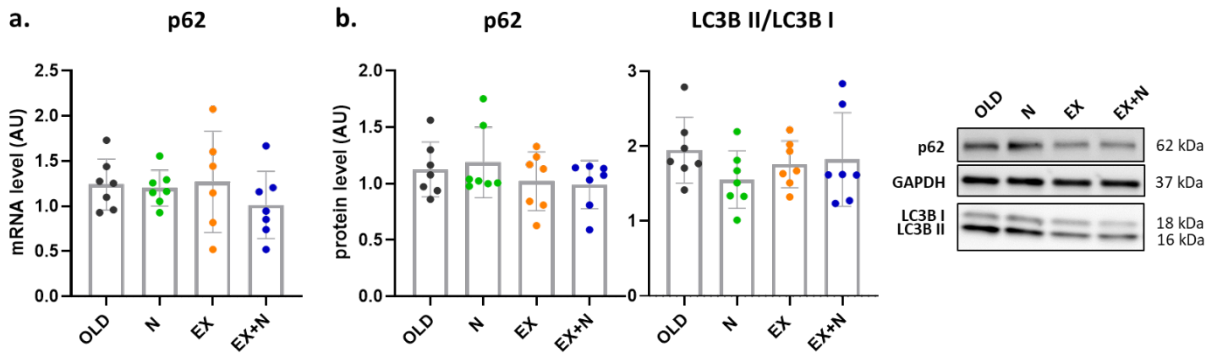

Figure 42. Factors involved in the autophagic flux. *a) Transcript levels of p62 in Old CTRL vs Old N, Old EX and Old EX+N. b) Protein levels of p62 normalized on GAPDH and LC3B II normalized on LC3B I in old mice groups. Graphs are accompanied by representative Western Blot images. Difference is considered significant when P < 0.05.*

Autophagic flux in 24-mo mice was demonstrated to be impaired in its progression, due to an accumulation of p62 in old mice compared to young littermates. Nitrate supplementation and endurance exercise did not promote any change in the expression of factors involved in autophagy. Because it is a process involved in the clearance and turnover of damaged components to allow correct functionality of active structures, among which the NMJ, the changes in NMJ stability were not thus attributable to changes in the autophagic flux due to a non-efficient modulation of the interventions on this pathway. However, this outcome was quite unexpected due to the notion that different exercise intensities, even during ageing, modulates the autophagic flux (Zeng *et al*, 2020).

3.3 Evaluation of the synthetic pathway following interventions

According to the literature, we evaluated the expression of key factors involved in protein synthesis in the Gastrocnemius of 24-mo mice subjected to nitrate supplementation and exercise training. The Akt/mTOR axis is thus elucidated in Figure 43.

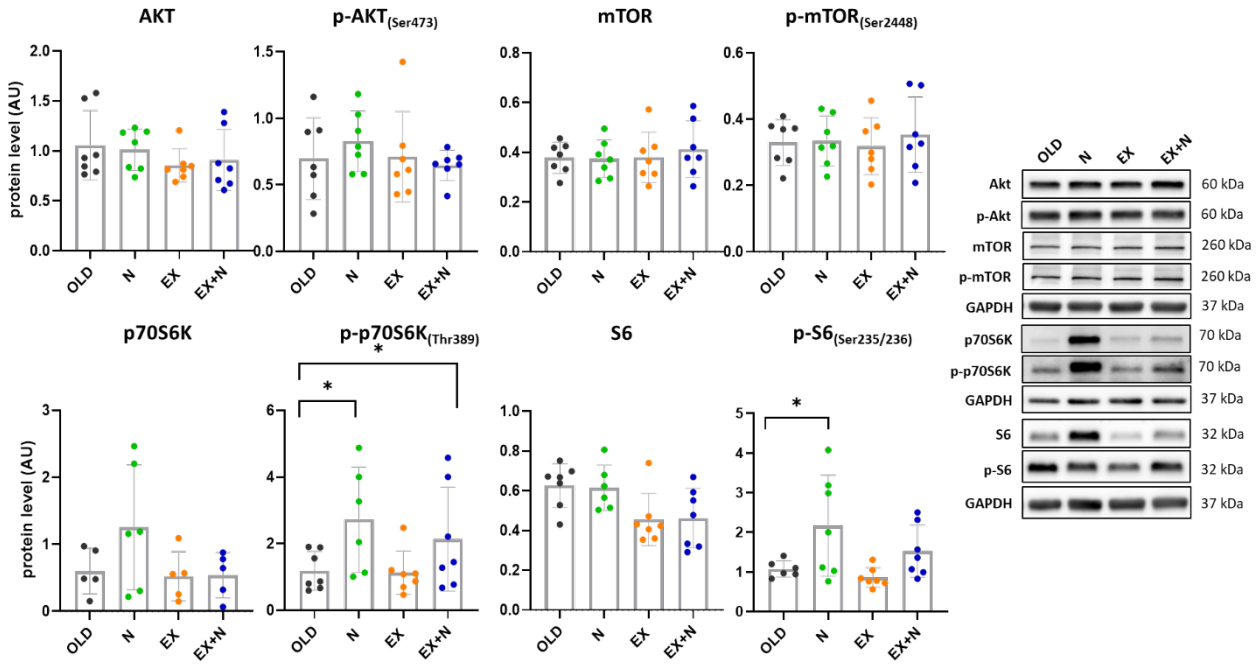

Figure 43. Muscle protein synthesis in Gastrocnemius of old mice. *Protein levels of the major factors involved in the mTOR synthetic pathway, all normalized for the housekeeping GAPDH. Juxtaposed, representative Western Blot images relative to the synthetic pathway. The * denotes a significant difference among the groups. Difference is considered significant when P < 0.05.*

Akt and mTOR protein level of both total and phosphorylated isoforms maintained the same levels among the different groups of mice: the two interventions were not able to modulate the activity of this axis in elderly mice. Conversely, phosphorylated p70S6K and its downstream factor S6 (directly involved in the translation initiation) showed a significant increase in Old N group compared to the CTRL animals. Moreover, p70S6K significantly increased in the combined EX+N group of mice, suggesting a nitrate-dependent augment of this factor. Total protein content of p70S6K was at the same level increased in nitrate supplemented animals compared to old, while the S6-kinase showed an increase in its protein content either in the total and in the active phosphorylated isoform. Moreover, its increased activity was even demonstrated by the higher levels of its downstream regulated factor S6, which showed an increased phosphorylation percentage compared to Old CTRL. The mechanism through which nitrate supplementation improves the latter stages of the synthetic pathway are not fully elucidated in the literature, but it was demonstrated that dietary

supplementation of NO-donor protects muscle from wasting by increasing protein synthesis in an mTOR-dependent manner, promoting increase in both mTOR phosphorylation at Thr-2446 and p70S6K at Thr-389 (Wang *et al*, 2018).

A major consequence of an increased protein synthesis was visible through muscle mass evaluations: in a system in which some treatments promoted MPS (with no changes at the level of the protein breakdown, data not shown), a modulated muscle plasticity in favour of a hypertrophic-like scenario could be promoted. Cross-sectional areas of transversal sections from Gastrocnemius were evaluated in all Old groups (Figure 44).

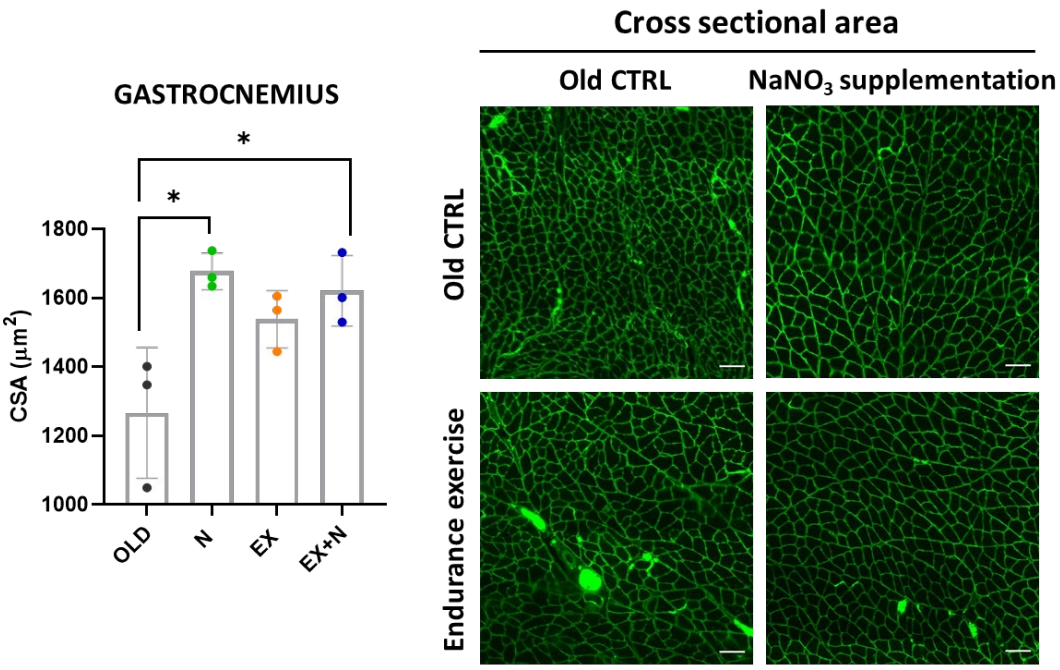

Figure 44. Cross sectional area (CSA) analysis of transversal fibers from Gastrocnemius and representative immunofluorescences. *Green channel represents the dystrophin. Scale bar 100 µm. The * denotes a significant difference among the groups. Difference is considered significant when P < 0.05.*

CSA of 24-mo mice strongly increased following nitrate supplementation. Significant results were even reached in the combined Old EX+N group, compared to the Old CTRL. Exercise alone did not promote hypertrophy of old mice. By the analysis of CSA, nitrate had beneficial outcomes on muscle mass, mainly explained by the increased p70S6K induction and higher levels of phosphorylated S6 factor. The combined treatment aswell underwent hypertrophy compared to the Old CTRL, attributable to high levels of phosphorylated p70S6K. Synthesis could thus promote an increase in

muscle mass related to nitrate-treated groups. Exercise alone did not cause a significant increase of CSA, that could therefore be labelled as a NO-dependent event.

Overall, muscle mass increased following NO supplementation, while exercise did not show hypertrophic patterns. This was sustained by a boost in phosphorylation of factors downstream the Akt/mTOR pathway. An increase in synthesis of proteins may concern beneficial turnover of muscle components in old mice, even if no counterbalanced protein degradation is stimulated. To conclude, by modulation of the synthetic pathway and the remodelled plasticity the muscle underwent, NO supplementation alone could be explicative of ameliorated NMJ morphology through the activity of this pathway.

3.4 Evaluation of trophic factors and neurotrophins following interventions

We evaluated transcript levels of IGF1 in 24-mo mice subjected to interventions to assess any modulatory effects nitrates and exercise promoted on it (Figure 45). Transcript levels were solely augmented in the combined EX+N group compared to Old CTRL mice. Exercise alone favoured its expression, even if no significant trends were visible. Nitrate supplementation alone did not change IGF1 levels. At the level of mitochondria, IGF1 overexpression could be linked to an ameliorated mitochondrial function (ref. to High Resolution Respirometry) in elderly mice (Poudel *et al*, 2020), even if factors involved in mitochondrial remodelling were not significantly changed following EX+N combination, apart from TFAM higher levels. IGF1-mediated neurotrophic and neuroprotective role in the central and peripheral nervous system is well known and solid (Bianchi *et al*, 2017), as the effects the exercise promote on neurotrophic factors like IGF1 and BDNF (Hachisu *et al*, 2020). In line with this, we can speculate that IGF1 is involved in the remodelling of the presynaptic side (no. of branches, average length of branches and overall complexity of presynaptic side, ref. "morphological evaluations of NMJ", *Paragraph 2.3.2*), acting on NMJ stability and morphological features.

In addition, neurotrophic factors BDNF and NT4 were evaluated in their transcript levels in all Old cohorts (Figure 45), to evaluate if interventions modulate their expression and thus if they can be considered promotor of presynaptic remodelling at the NMJ.

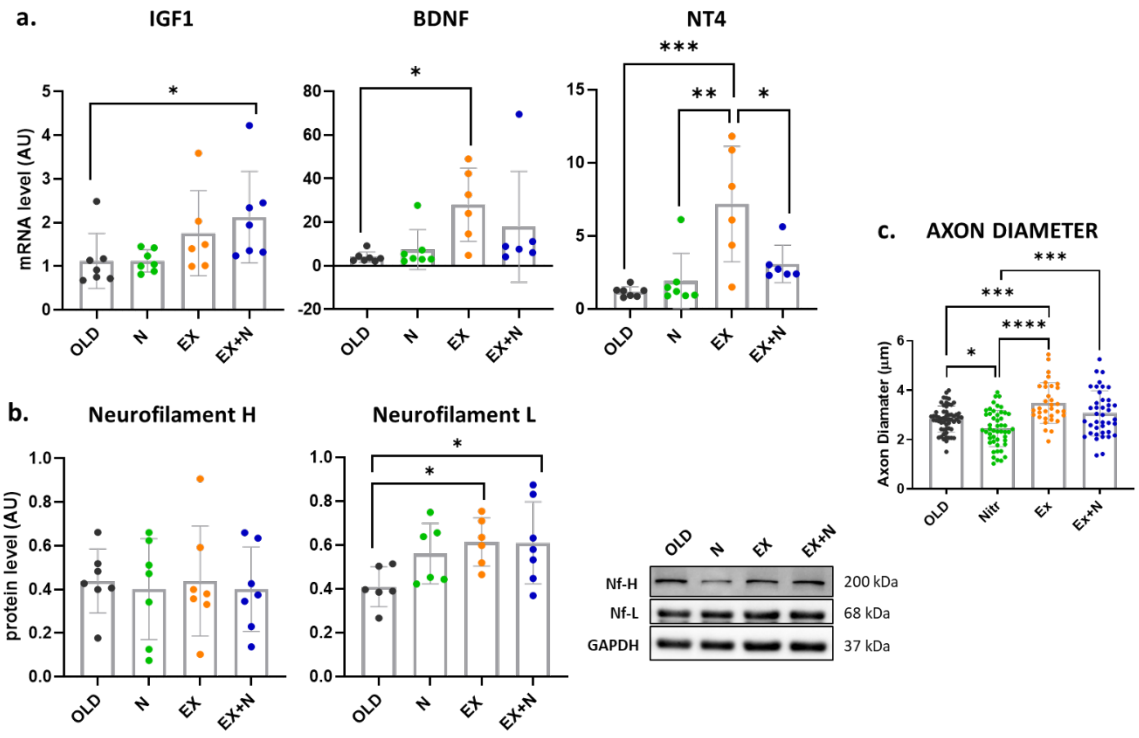

Figure 45. Growth factor IGF1 and neurotrophins' expression on Gastrocnemius. *a) Upper panel depicts transcript levels of IGF1 and relevant neurotrophins. b) Lower panel depicts protein levels of Neurofilament H (heavy) and Neurofilament L (light), juxtaposed with their representative Wester Blots. c) On the right, evaluation of axon diameter from all 24-mo mice with and without intervention (in µm). The * denotes a significant difference among the groups. Difference is considered significant when P < 0.05.*

Both brain-derived neurotrophic factor and neurotrophin-4 were highly induced following exercise training. Transcript levels neither changed following nitrate supplementation nor with the combined intervention. As a matter of fact, NT4 was significantly increased in Old EX group compared to both nitrate treated groups. BDNF acts on muscle as a powerful regulator of its plasticity (Sakuma and Yamaguchi, 2011), being stimulated by neuromuscular activity and acting as an autocrine factor on muscle to activate TrkB receptor, to initiate a cascade of events involving Akt and AMPK pathways. Together with NT4, they are moreover released from the muscle to promote a paracrine activity on the axon terminal at the NMJ, boosting neuronal survival and stimulating axon sprouting. The increase in transcript levels of both BDNF and NT4 are not IGF1-dependent, but as the literature suggests, we can consider them as a result of the exercise stimulation from the activity of the interacting nerves.

To better evaluate the effects of the neurotrophins on presynaptic parameters, we evaluated the amount of neurofilaments that compose the motor neuron axon. Motor neuron axons are finely formed by a maintained stoichiometric assembly of Neurofilament Heavy, Medium and Light chains

(Nf-H:Nf-M:Nf-L in a 7:3:2 proportion, as suggested by Zucchi *et al*, 2018). Changes in proportions can be subordinated to adaptive modulations of their expression following physiological and pathological outcomes. We analysed the protein levels of Nf-L and Nf-H, the most and the least represented filaments composing the motor neuron axon, respectively. We were not measuring the relative proportion of those, but only the protein level, due to the assumption that Nf-L is the one that undergoes high plasticity in its expression. As expected, no changes in Nf-H was visible following two months' intervention, while regarding Nf-L levels, exercise training and the combination with nitrate supplementation highly increased its expression, meaning that axon was stimulated to remodel itself through Nf-L higher levels. Nitrate alone did not show a significant trend but an increase in neurofilament-L content is clearly visible (*+ 37%*).

The significant increase in neurotrophins following exercise training were thus explicative of an increase in Nf-L polymerization in the formation of the axon, that was thus confirmed by the morphological analysis of the axon diameter, in which we demonstrated that axon terminal underwent hypertrophy, compared to the Old CTRL. The mild increase of neurotrophins in the EX+N group reflected the trend assessed for the axon diameter analysis, while the high levels of Nf-L for this treatment could be attributed to IGF1 activity.

Overall, we can conclude that neurotrophins and IGF1 together were associated with the remodelling of the presynaptic neuromuscular junction mainly induced by exercise training. Old EX and Old EX+N seemed to be subjected to complementary activity of these factors on the NMJ outcomes. The remodelling was confirmed by the axon diameter analysis in which the diameter of axon terminals of the motor neurons was measured and compared to the Old CTRL. To strengthen these results, we evaluated the protein levels of the neurofilaments, among which an increase in Neurofilament-L was assessed, the stoichiometrically mostly represented in the formation of the axon. Nitrate alone did not promote any change in these parameters, despite changes in morphological features were evaluated, regarding the presynaptic organization.

CONCLUSIVE REMARKS

In order to evaluate the beneficial effects of interventions such as exercise training and dietary supplementation on sarcopenic subjects, we investigated the key molecular pathways downstream of the structural organization and maintenance of the NMJ in an attempt to understand the molecular muscular mechanisms that drive the adaptations of the junction in elderly. We promoted our study in a wild-type animal model that physiologically undergoes ageing. We primarily started by the characterization of our elderly male animals (24-months old) in comparison with young adult littermates (7-months old), so as to evaluate all the age-related features this model shows. In doing so, we studied the molecular pathways involved in the stability and innervation status of the old mice, to have a primary framework of NMJ changes during ageing. We then promoted two-months intervention on 22-months old mice to evaluate NMJ molecular and morphological changes modulated by endurance training and nitrate supplementation, so as to compare animals of the same age (24-mo). The combination of the two was even evaluated as suggested by experimental evidence coming from the sports science literature (ref. "Nitrate supplementation as exogenous beneficial intervention on physical performance", *Chapter 2.5*). Evaluation of NMJ changes and remodelling patterns was then combined with the study of molecular pathways involved in muscle plasticity, to describe the relationship between NMJ and muscular adaptations triggered by the interventions.

- *Sarcopenia-related adaptations*

We compared different aspects of the skeletal muscle from elderly and young mice to characterize the mouse model within the sarcopenic profile. The choice of this age was suggested mainly by the literature (Xie *et al*, 2021), but also by comparative studies of age between mice and humans (Figure 46; Ratto *et al*, 2019), in which biological senescence arising at early sixties in humans is corresponding to 18 months in mice. Our 24-mo mice are thus reflecting 80 years old humans (an age in which statistically the decline of sarcopenia-related features is assessed in 11 to 50% of worldwide subjects).

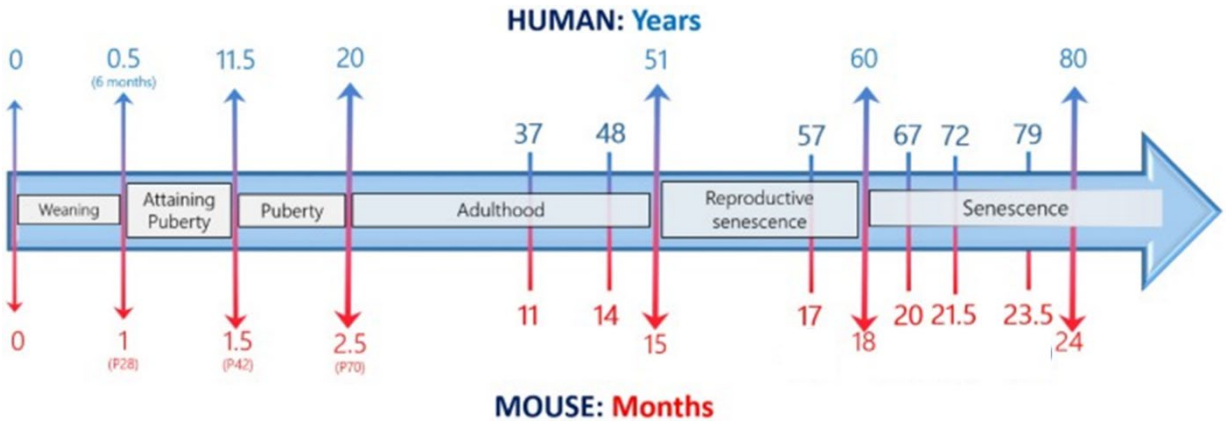

Figure 46. Comparative age between men and mice. *Observations were obtained following transversal behavioural studies during their life span (adapted from Ratto et al, 2019).*

Most of the analyses were focused on the fast Gastrocnemius muscle, based on the assumption that during lifespan, the remodelling of muscle fiber type composition is caused by continuous cycles of denervation/reinnervation, with a much prominent denervation occurring in type-II fast fibers with the passing of time, that eventually lead to atrophy and loss of muscle mass (Gouspillou *et al*, 2013). On the contrary, oxidative type-I fibers display resistance to denervation, with slow motor neuron strongly interacting with oxidative fibers, which thus increase in their percentage as a protective effort against age-related atrophy (assessed in rodents by Kung *et al*, 2014, in humans by Brocca *et al*, 2017).

Elderly mice showed a decrease in body weight and isolated muscle weight to body weight ratio, a widely used index of sarcopenia (Ezzat-Zadeh *et al*, 2017), confirmed by a significant decrease in the fibers cross-sectional area. Muscle phenotype of old animals showed a significant increase in the percentage of slow type-I fibers, with no changes in fast-type composition, in line with the typical increase of hybrid fibers during ageing (Moreillon *et al*, 2019), namely the co-expression of different MHC isoforms within the same fiber. Muscle exhibited typical histological features of aged muscle, i.e. central nuclei and fibrotic infiltration, the latter depicting a deposition of a non-contractile tissue that can hamper the function of the muscle, in a typical sarcopenic-like model (Mann *et al*, 2011).

Molecular pathways underlying age-related atrophy revealed that an increase in muscle protein breakdown is highly elicited and causative of a reduced muscle mass (Sandri *et al*, 2004). Conversely, protein synthesis did not change, limiting the turnover exchange that physiologically occurs under the plasticity remodelling of muscle tissue. Autophagy, another mechanism involved in the maintenance of muscle mass and clearance of damaged components (Masiero *et al*, 2009), was found impaired in old mice compared to young littermates. An accumulation in p62 is mostly

associated to a slower or inhibited autophagic flux whenever other pro-autophagic factors are not changing, as in our case, to finalize the degradative process (Sakuma *et al*, 2016). Mitophagy, the selective removal of damaged mitochondria, in the same way, is impaired due to the accumulation of Parkin, which recruits p62 on the surface of compromised organelles, in a heterogeneous system maintained at baseline levels (LC3B II does not change in elderly animals compared to the young cohort). In agreement with an impaired degrading process, the augmented levels of pro-fusion proteins not accompanied by increased mitochondrial biogenesis factors suggest the presence of hyper fused mitochondria in ageing condition. In rodents, it was demonstrated that giant mitochondria accumulate during ageing, with a declined inner membrane potential, in an impoverished mitophagic scenario (Navratil *et al*, 2008, Garcia *et al*, 2013, Leduc-Gaudet *et al*, 2015). The high AMPK phosphorylated levels found in old mice, indicative of an impaired AMP/ATP ratio, suggest an ineffectiveness in energy production.

The last characteristic to define mice as sarcopenic was the evaluation of denervation and the NMJ stability, by means of studying molecular patterns involved in these phenomena. As previously mentioned regarding fiber type shift, lots of evidence have demonstrated that repeating cycles of denervation and reinnervation occur during lifespan and even in aged muscles (Hepple and Rice, 2016). We evaluated transcript levels of the well-established denervation related factors HDAC4, Gadd45α, MyoG, Runx1, AChRγ and NCAM1 in Gastrocnemius of old mice (Barns *et al*, 2014, Soendenbroe *et al*, 2020), revealing a high expression level of all these parameters.

Overall, these data confirm that the frame window we evaluated on mice is falling within the sarcopenic pathology, showing all the hallmark features of ageing as relevant markers for muscle trophism and junctional innervation.

- *NMJ morphological evaluations: effects of interventions*

As regards with dietary supplementation, notions from sports science suggest an improvement in muscle contractile properties (Haider and Folland, 2015) and tolerance to exercise efforts (Husmann *et al*, 2019) in humans following nitrate-rich beetroot juice supplementation. In mice, 1mM $NaNO_3$ supplementation ameliorates exercise tolerance and voluntary exercise inputs (Ivarsson *et al*, 2017, Ferguson *et al*, 2020), but little is known regarding the molecular mechanisms at the basis of this beneficial outcome and, in the specific, at the level of the NMJ. We intervened on 22-mo mice through 2 months' endurance training exercise and 2 months' $NaNO_3$ supplementation to modulate muscular aspects impaired by ageing. We thus studied the effects of these interventions on the

morphology of the NMJ to evaluate any effect leading to a remodelling of the structure, schematized in the following Table 6.

	Young CTRL	Old CTRL	Old N	Old EX	Old EX+N
Presynaptic side					
Axon diameter (µm)	↑↑↑↑	2.82 ± 0.53	↓	↑↑↑	↔
Nerve terminal perimeter (µm)	↔	314 ± 105.30	↓	↔	↔
Nerve terminal area (µm²)	↔	389.35 ± 183.94	↔	↔	↔
No. of branches	↓ (p = 0.05)	15.31 ± 8.96	↓↓↓↓	↓↓↓↓	↓↓↓
Average lenght of branches (µm)	↔	12.61 ± 6.34	↔	↑	↑
Complexity	↔	4.39 ± 0.48	↓↓↓	↓↓	↓↓
Postsynaptic side					
AChR perimeter (µm)	↔	293.95 ± 90.37	↓	↓	↔
AChR area (µm²)	↔	494.01 ± 165.86	↔	↔	↔
Endplate perimeter (µm)	↔	127.62 ± 27.20	↔	↔	↔
Endplate area (µm²)	↔	979.08 ± 374.16	↔	↔	↔
Compactness %	↔	51.72 ± 7.05	↑↑↑	↑↑↑↑	↔
Interaction and fragmentation					
Unoccupied AChR area (µm²)	↓↓	176.27 ± 72.66	↓ (p = 0.06)	↓	↓ (p = 0.05)
Overlap %	↑↑↑	63.56 ± 11.25	↔	↑	↔
No. of AChR clusters	↓↓↓	7.31 ± 6.06	↓↓↓	↓↓	↔
Average area of clusters (µm²)	↑↑	96.55 ± 57.46	↔	↔	↔
Fragmentation	↓↓	0.79 ± 0.11	↓	↓	↔

Table 6. Schematized values relative to the analysis of the Neuromuscular Junction (NMJ) morphology, divided in pre, post synaptic and the interaction among the two structures. *Values arise from the analysis of images processed by the Confocal Microscopy. Values of Old CTRL are represented as means ± SD and used as reference values for comparison with the other groups. Arrows represent*

the trend above or below the reference Old CTRL, based on statistical evaluations (student t-test between Young CTRL and Old CTRL and ordinary One-Way ANOVA for the comparison among all Old groups). ↔ indicates unchanged values compared to the Old CTRL.

The morphological parameters were analysed following the "NMJ-morph" macro commands for image analysis (through Fiji, ImageJ software), explained in detail by Jones and colleagues (Jones et al, 2016). Arrows mark all the significant changes in comparison with the reference Old CTRL group. At first sight, ageing mainly impacted on the superimposition and thus the interaction between the pre and postsynaptic structures, as well as the fragmentation (as evaluated in the timing evolution of mice from 2 to 28-mo, Cheng *et al*, 2013). Ageing thus reversed a young healthy condition in which the structures were fully overlapping, with a strong decreased fragmentation due to active crosstalk and activity-dependent maintenance of the structure, sustained by a hypertrophic axon terminal innervation.

The presynaptic remodelling seemed to be the most affected by all the interventions, separately and in combination, resembling the Young condition in most of the parameters. Postsynaptic values were ameliorated regarding the compactness of AChR spatial organization, in aged mice subjected to nitrate supplementation and exercise, separately. The neuromuscular plasticity thus reflected the adaptability in the remodelling of the components it is formed by, flattering in our case the evaluations regarding perimeters and areas of the NMJ separate sides. The junctions displayed a divergence among the Old mice and the Old treated ones, collocating the latter to an ameliorated structural organization which resemble the young condition (characterized most of the times by continuous AChR tubuli and linear structures, ref. to Image 38). Lastly, the overlap between the two sides of the junction was strongly ameliorated only in the exercised cohort, locating this trend closer to the young littermates, while a decrease in fragmentation and thus receptor clusters visibly occurred in N and EX groups, resembling even in this case a younger condition.

Overall, these data indicated a decline in the NMJ morphological organization in elderly mice, as well as the ability to respond to treatments with an appreciable remodelling of the junction at different degrees and levels. Endurance exercise in old mice was the most efficient treatment that drove the morphology to a beneficial spatial reorganization, closer to the young condition and thus to a widely functional crosstalk. Nitrate supplementation acted on some parameters (not all the same as the exercise ones) that at the end resulted again in a decreased fragmentation and smaller junctions (attributable to a higher remodelling occurring mainly in fast fibers; Mech *et al*, 2020). The combined treatment just showed an improvement in the complexity of the presynaptic side, with

any surprisingly cumulative beneficial effects from those seen in $NaNO_3$ supplementation and exercise training, singularly.

Different mechanisms could be explicative of a remodelling of the NMJ, and an intricate network of signalling molecules are causative of various effects that not only modulate the junction assembly, but also play important roles in skeletal muscle plasticity and promotion of health.

- *Dietary nitrate-related adaptations in elderly mice*

Nitrates supplementation decreased NCAM1 expression and the number of NCAM1 positive fibers suggesting an accomplished axonal attachment thus clearly indicating a beneficial effect on muscle denervation in old mice. In addition, a clear modulation of the intracellular synthetic pathway by nitrates intake was observed, based on the high levels of phosphorylated p70S6K and S6, factors directly involved in the initiation step of protein synthesis. As a consequence, a positive effect on fibers size was obtained. This is supported by *in vitro* evidence showing that L-Arginine supplementation enhances protein synthesis signalling pathway in an NO-dependent manner (Wang *et al*, 2018).

Recently, focus has been given to the connection between Akt/mTOR pathway and the maintenance of the NMJ, demonstrating that this complex axis goes beyond the canonical synthetic pathway, orchestrating factors involved in the stability and innervation of the junction (Baraldo *et al*, 2020, Castets *et al*, 2020). A reduced fragmentation and a simplistic and compacted structural organization can thus be guided by NO-dependent p70S6K and S6 activity.

Regarding muscle functionality, *ex vivo* resistance to fatigue and mitochondrial respiration were both enhanced by nitrates intake. This ameliorated outcome could be explained by the exogenous $NaNO_3$ supplementation we approached in this study, which il closely resembling physiological levels and can thus boost the respiration (Sakamuri *et al*, 2020). This beneficial effect challenges the dogma regarding the inhibitory and detrimental effects of NO, mainly based on the promotion of nitrosative damage directly on mitochondrial complexes, caused by high concentrations of NO, which is unlikely to occur by the action of endogenous NO (Poderoso *et al*, 2019). The mitochondrial aspect is of undoubted importance also in the light of evidence indicating that mitochondria may be either a primary trigger or at least an important player in NMJ instability in both junctional elements (Rygiel *et al*, 2016).

- *Endurance exercise-related adaptations in elderly mice*

Alongside the beneficial features of the remodelled morphology of both pre and postsynaptic sides, and the interaction between the two, observed in old mice following training, a reduction in NCAM1-stained positive fibers and expression was observed, indicating a beneficial effect on muscle denervation in old mice. In addition, a strong induction of neurotrophins (BDNF and NT4) was also found following exercise in elderly mice, directly correlated to the NMJ morphological ameliorations (Kreko-Pierce and Eaton, 2018). Therefore, the observed nerve terminal hypertrophy could be mediated by neurotrophins which guide the axon to reinnervation (Hoyng *et al*, 2014) and, once the active-dependent feedback signalling was established, neurofilaments increased in their assembly so as to promote a strong connection.

Exercise, moreover, promoted an increase in the expression of the regulatory factor SIRT1 which, through deacetylation and direct nuclear activity, can trigger a cascade of events beneficial for mitochondrial adaptations. It can thus be directly or indirectly (through PGC1α) responsible for TFAM induction, which is then recruited for mtDNA replication and transcription of mitochondrial genes (all relating to the ETC system). In agreement with this, a much more efficient and functional ETC was found in terms of decrease in proton leakage through the High-Resolution Respirometry technique. This was then accountable for an ameliorated oxidative phosphorylation coupling efficiency (Harper *et al*, 2021) observed in mice after 2 months' endurance exercise training. By the way, this mitochondrial functional improvement assessed in all treatments was not accountable to changes in mitochondrial mass and/or parameters regarding its dynamicisms, speculating an intrinsic beneficial outcome independent by molecular adaptations. As previously said, a feedback mechanism between NMJ and mitochondria is speculated in the literature, suggesting even in this case a connection among the ameliorated functionality of these organelles and the increased NMJ morphological outcomes.

Surprisingly, the nitrates and exercise combined intervention did not display any additive effects than the single ones. This aspect will need further investigation.

FUTURE PERSPECTIVES

Remodelling in response to nitrate supplementation and exercise occurs in skeletal muscle of elderly sarcopenic mice. The beneficial effects are achieved at NMJ, muscle size and mitochondrial respiration levels, proposing a model in which functionality is ameliorated and demonstrating that there is no excessive resistance to adaptations in elderly conditions. The results obtained encourage the study of nitrate supplementation in elderly humans to verify its efficacy in counteracting NMJ detrimental ageing.

Because sarcopenia, and all the debilitating outcomes it carries with, are highly affecting the quality of life of elderly fragile people, the evaluation of efficacy non-invasive strategies are nowadays covering a relevant role to ameliorate this condition. Moreover, some of the pathways and dysregulations occurring during ageing can be shared with neurodegenerative pathologies, and so the study of the NMJ and the pathways involved in its morphological improvement can be suggestive of approaches to mitigate the time course of events.

BIBLIOGRAPHY

Aare S, Spendiff S, Vuda M, Elkrief D, Perez A, Wu Q, Mayaki D, Hussain SNA, Hettwer S, Hepple RT. Failed reinnervation in aging skeletal muscle. *Skelet Muscle.* 2016; **6**(1):29

Adamovich Y, Shlomai A, Tsvetkov P, Umansky KB, Reuven N, Estall JL, Spiegelman BM, Shaul Y. The Protein Level of PGC-1α, a Key Metabolic Regulator, Is Controlled by NADH-NQO1. *Mol Cell Biol.* 2013; **33**(13):2603–2613

Adams L, Carlson BM, Henderson L, Goldman D. Adaptation of nicotinic acetylcholine receptor, myogenin, and MRF4 gene expression to long-term muscle denervation. *J Cell Biol.* 1995; **131**(5):1341-9

Adams ME, Anderson KNE, Froehner SC. The alpha-syntrophin PH and PDZ domains scaffold acetylcholine receptors, utrophin, and neuronal nitric oxide synthase at the neuromuscular junction. *J Neurosci.* 2010; **30**(33):11004-10

Anisimova AS, Alexandrov AI, Makarova NE, Gladyshev VN, Dmitriev SE. Protein synthesis and quality control in aging. *Aging (Albany NY).* 2018; **10**(12):4269–4288

Apel PJ, Alton T, Northam C, Ma J, Callahan M, Sonntag WE, Li Z. How age impairs the response of the neuromuscular junction to nerve transection and repair: An experimental study in rats. *J Orthop Res.* 2009; **27**(3):385-93

Arnold AS, Gill J, Christe M, Ruiz R, McGuirk S, St-Pierre J, Tabares L, Handschin C. Morphological and functional remodelling of the neuromuscular junction by skeletal muscle PGC-1α. *Nat Commun.* 2014; **5**:3569

Arnold JT, Oliver SJ, Lewis-Jones TM, Wylie LJ, Macdonald JH. Beetroot juice does not enhance altitude running performance in well-trained athletes. *Appl Physiol Nutr Metab.* 2015; **40**(6):590-5

Ascenzi F, Barberi L, Dobrowolny G, Villa Nova Bacurau A, Nicoletti C, Rizzuto E, Rosenthal N, Scicchitano BM, Musarò A. Effects of IGF-1 isoforms on muscle growth and sarcopenia. *Aging Cell.* 2019; **18**(3):e12954

Ashmore T, Roberts LD, Morash AJ, Kotwica AO, Finnerty J, West JA, Murfitt SA, Fernandez BO, Branco C, Cowburn AS, Clarke K, Johnson RS, Feelisch M, Griffin JL, Murray AJ. Nitrate enhances

skeletal muscle fatty acid oxidation via a nitric oxide-cGMP-PPAR-mediated mechanism. *BMC Biol.* 2015; **13**:110

Bailey SJ, Fulford J, Vanhatalo A, Winyard PG, Blackwell JR, DiMenna FJ, Wilkerson DP, Benjamin N, Jones AM. Dietary nitrate supplementation enhances muscle contractile efficiency during knee-extensor exercise in humans. *J Appl Physiol (1985).* 2010; **109**(1):135-48

Bailey SJ, Gandra PG, Jones AM, Hogan MC, Nogueira L. Incubation with sodium nitrite attenuates fatigue development in intact single mouse fibres at physiological PO_2. *J Physiol.* 2019; **597**(22):5429-5443

Bailey SJ, Winyard P, Vanhatalo A, Blackwell JR, Dimenna FJ, Wilkerson DP, Tarr J, Benjamin N, Jones AM. Dietary nitrate supplementation reduces the O_2 cost of low-intensity exercise and enhances tolerance to high-intensity exercise in humans. *J Appl Physiol (1985).* 2009; **107**(4):1144-55

Bao Z, Cui C, Chow SKH, Qin L, Wong RMY, Cheung WH. AChRs Degeneration at NMJ in Aging-Associated Sarcopenia–A Systematic Review. *Front Aging Neurosci.* 2020; **12**:597811

Baraldo M, Geremia A, Pirazzini M, Nogara L, Solagna F, Türk C, Nolte H, Romanello V, Megighian A, Boncompagni S, Kruger M, Sandri M, Blaauw B. Skeletal muscle mTORC1 regulates neuromuscular junction stability. *J Cachexia Sarcopenia Muscle.* 2020; **11**(1):208-225

Barns M, Gondro C, Tellam RL, Radley-Crabb HG, Grounds MD, Shavlakadze T. Molecular analyses provide insight into mechanisms underlying sarcopenia and myofiber denervation in old skeletal muscles of mice. *Int J Biochem Cell Biol.* 2014; **53**:174-85

Berry MJ, Miller GD, Kim-Shapiro DB, Fletcher MS, Jones CG, Gauthier ZD, Collins SL, Basu S, Heinrich TM. A randomized controlled trial of nitrate supplementation in well-trained middle and older-aged adults. *PLoS One.* 2020; **15**(6):e0235047

Bescós R, Ferrer-Roca V, Galilea PA, Roig A, Drobnic F, Sureda A, Martorell M, Cordova A, Tur JA, Pons A. Sodium nitrate supplementation does not enhance performance of endurance athletes. *Med Sci Sports Exerc.* 2012; **44**(12):2400-9

Bhardwaj G, Penniman CM, Jena J, Suarez Beltran PA, Foster C, Poro K, Junck TL, Hinton Jr AO, Souvenir R, Fuqua JD, Morales PE, Bravo-Sagua R, Sivitz WI, Lira VA, Abel ED, O'Neill BT. Insulin and

IGF-1 receptors regulate complex I-dependent mitochondrial bioenergetics and supercomplexes via FoxOs in muscle. *J Clin Invest.* 2021; **131**(18):e146415

Bianchi VE, Locatelli V, Rizzi L. Neurotrophic and Neuroregenerative Effects of GH/IGF1. *Int J Mol Sci.* 2017; **18**(11):2441

Bjørkøy G, Lamark T, Pankiv S, Øvervatn A, Brech A, Johansen T. Monitoring autophagic degradation of p62/SQSTM1. *Methods Enzymol.* 2009; **452**:181-97

Bodine SC, Baehr LM. Skeletal muscle atrophy and the E3 ubiquitin ligases MuRF1 and MAFbx/atrogin-1. *Am J Physiol Endocrinol Metab.* 2014; **307**(6):E469–E484

Bongers KS, Fox DK, Ebert SM, Kunkel SD, Dyle MC, Bullard SA, Dierdorff JM, Adams CM. Skeletal muscle denervation causes skeletal muscle atrophy through a pathway that involves both Gadd45a and HDAC4. *Am J Physiol Endocrinol Metab.* 2013; **305**(7):E907-15

Boorsma RK, Whitfield J, Spriet LL. Beetroot juice supplementation does not improve performance of elite 1500-m runners. *Med Sci Sports Exerc.* 2014; **46**(12):2326-34

Brack AS, Rando TA. Intrinsic changes and extrinsic influences of myogenic stem cell function during aging. *Stem Cell Rev.* 2007; **3**:226–237

Brocca L, McPhee JS, Longa E, Canepari M, Seynnes O, De Vito G, Pellegrino MA, Narici M, Bottinelli R. Structure and function of human muscle fibers and muscle proteome in physically active older men. *J Physiol.* 2017; **595**(14):4823-4844

Brown LA, Judge JL, Macpherson PC, Koch LG, Qi NR, Britton SL, Brooks SV. Denervation and senescence markers data from old rats with intrinsic differences in responsiveness to aerobic training. *Data Brief.* 2019; **27**:104570

Brunelli L, Yermilov V, Beckman JS. Modulation of catalase peroxidatic and catalatic activity by nitric oxide. *Free Radic Biol Med.* 2001; **30**(7):709-14

Bruneteau G, Simonet T, Bauché S, Mandjee N, Malfatti E, Girard E, Tanguy ML, Behin A, Khiami F, Sariali E, Hell-Remy C, Salachas F, Pradat PF, Fournier E, Lacomblez L, Koenig J, Romero NB, Fontaine B, Meininger V, Schaeffer L, Hantai D. Muscle histone deacetylase 4 upregulation in amyotrophic lateral sclerosis: potential role in reinnervation ability and disease progression. *Brain.* 2013; **136**(Pt 8):2359-68

Bujak AL, Crane JD, Lally JS, Ford RJ, Kang SJ, Rebalka IA, Green AE, Kemp BE, Hawke TJ, Schertzer JD, Steinberg GR. AMPK activation of muscle autophagy prevents fasting-induced hypoglycemia and myopathy during aging. *Cell Metab.* 2015; **21**(6):883-90

Caballano-Infantes E, Terron-Bautista J, Beltrán-Povea A, Cahuana GM, Soria B, Nabil H, Bedoya FJ, Tejedo JR. Regulation of mitochondrial function and endoplasmic reticulum stress by nitric oxide in pluripotent stem cells. *World J Stem Cells.* 2017; **9**(2):26-36

Cannavino J, Brocca L, Sandri M, Grassi B, Bottinelli R, Pellegrino MA. The role of alterations in mitochondrial dynamics and PGC-1α over-expression in fast muscle atrophy following hindlimb unloading. *J Physiol.* 2015; **593**(8):1981-95

Cantò C, Auwerx J. PGC-1alpha, SIRT1 and AMPK, an energy sensing network that controls energy expenditure. *Curr Opin Lipidol.* 2009; **20**(2):98-105

Carlson BM, Carlson JA, Dedkov EI, McLennan IS. Concentration of caveolin-3 at the neuromuscular junction in young and old rat skeletal muscle fibers. *J Histochem Cytochem.* 2003; **51**(9):1113-8

Carlström M. Nitric oxide signalling in kidney regulation and cardiometabolic health. *Nat Rev Nephrol.* 2021; **17**(9):575-590

Carnio S, LoVerso F, Baraibar MA, Longa E, Khan MM, Maffei M, Reischl M, Canepari M, Loefler S, Kern H, Blaauw B, Friguet B, Bottinelli R, Rudolf R, Sandri M. Autophagy impairment in muscle induces neuromuscular junction degeneration and precocious aging. *Cell Rep.* 2014; **8**(5):1509-21

Carreras MC, Franco MC, Finocchietto PV, Converso DP, Antico Arciuch VG, Holod S, Peralta JG, Poderoso JJ. The biological significance of mtNOS modulation. *Front Biosci.* 2007; **12**:1041-8

Castets P, Ham DJ, Ruegg MA. The TOR Pathway at the Neuromuscular Junction: More Than a Metabolic Player? *Front Mol Neurosci.* 2020; **13**:162

Cau SBA, Carneiro FS, Tostes RC. Differential modulation of nitric oxide synthases in aging: therapeutic opportunities. *Front Physiol.* 2012; **3**:218

Cermak NM, Gibala MJ, van Loon LJC. Nitrate supplementation's improvement of 10-km time-trial performance in trained cyclists. *Int J Sport Nutr Exerc Metab.* 2012; **22**(1):64-71

Cermak NM, Res P, Stinkens R, Lundberg JO, Gibala MJ, van Loon LJC. No improvement in endurance performance after a single dose of beetroot juice. *Int J Sport Nutr Exerc Metab.* 2012; **22**(6):470-8

Chai RJ, Vukovic J, Dunlop S, Grounds MD, Shavlakadze T. Striking Denervation of Neuromuscular Junctions without Lumbar Motoneuron Loss in Geriatric Mouse Muscle. *PLoS One.* 2011; **6**(12):e28090

Chang L, Daly C, Miller DM, Allen PD, Boyle JP, Hopkins PM, Shaw MA. Permeabilised skeletal muscle reveals mitochondrial deficiency in malignant hyperthermia-susceptible individuals. *Br J Anaesth.* 2019; **122**(5):613-621

Chen H, Vermulst M, Wang YE, Chomyn A, Prolla TA, McCaffery JM, Chan DC. Mitochondrial fusion is required for mtDNA stability in skeletal muscle and tolerance of mtDNA mutations. *Cell.* 2010; **141**(2):280-9

Chen ZP, McConell GK, Michell BJ, Snow RJ, Canny BJ, Kemp BE. AMPK signaling in contracting human skeletal muscle: acetyl-CoA carboxylase and NO synthase phosphorylation. *Am J Physiol Endocrinol Metab.* 2000; **279**(5):E1202–E1206

Cheng A, Morsch M, Murata Y, Ghazanfari N, Reddel SW, Phillips WD. Sequence of age-associated changes to the mouse neuromuscular junction and the protective effects of voluntary exercise. *PLoS One.* 2013; **8**(7):e67970

Chipman PH, Schachner M, Rafuse VF. Presynaptic NCAM Is Required for Motor Neurons to Functionally Expand Their Peripheral Field of Innervation in Partially Denervated Muscles. *J Neurosci.* 2014; **34**(32):10497-510

Christopher J Mann CJ, Perdiguero E, Kharraz Y, Aguilar S, Pessina P, Serrano AL, Muñoz-Cánoves P. Aberrant repair and fibrosis development in skeletal muscle. *Skelet Muscle.* 2011; **1**(1):21

Ciesielska S, Slezak-Prochazka I, Bil P, Rzeszowska-Wolny J. Micro RNAs in Regulation of Cellular Redox Homeostasis. *Int J Mol Sci.* 2021; **22**(11):6022

Clerc P, Rigoulet M, Leverve X, Fontaine E. Nitric oxide increases oxidative phosphorylation efficiency. *J Bioenerg Biomembr.* 2007; **39**(2):158-66

Coggan AR, Broadstreet SR, Mikhalkova D, Bole I, Leibowitz JL, Kadkhodayan A, Park S, Thomas DP, Thies D, Peterson LR. Dietary nitrate-induced increases in human muscle power: high versus low responders. *Physiol Rep.* 2018; **6**(2):e13575

Coggan AR, Hoffman RL, Gray DA, Moorthi RN, Thomas DP, Leibowitz JL, Thies D, Peterson LR. A Single Dose of Dietary Nitrate Increases Maximal Knee Extensor Angular Velocity and Power in Healthy Older Men and Women. *J Gerontol A Biol Sci Med Sci.* 2020; **75**(6):1154-1160

Cogliati S, Frezza C, Soriano ME, Varanita T, Quintana-Cabrera R, Corrado M, Cipolat S, Costa V, Casarin A, Gomes LC, Perales-Clemente E, Salviati L, Fernandez-Silva P, Enriquez JA, Scorrano L. Mitochondrial cristae shape determines respiratory chain supercomplexes assembly and respiratory efficiency. *Cell.* 2013; **155**(1):160-71

Cohen TJ, Choi MC, Kapur M, Lira VA, Yan Z, Yao TP. HDAC4 regulates muscle fiber type-specific gene expression programs. *Mol Cells.* 2015; **38**(4):343-8

Conley KE, Jubrias SA, Esselman PC. Oxidative capacity and ageing in human muscle. *J Physiol.* 2000; **526**(Pt 1):203-10

Contreras-Lopez R, Elizondo-Vega R, Luque-Campos N, Torres MJ, Pradenas C, Tejedor G, Paredes-Martínez MJ, Vega-Letter AM, Campos-Mora M, Rigual-Gonzalez Y, Oyarce K, Salgado M, Jorgensen C, Khoury M, de Los Ángeles Garcia-Robles M, Altamirano C, Djouad F, Luz-Crawford P. The ATP synthase inhibition induces an AMPK-dependent glycolytic switch of mesenchymal stem cells that enhances their immunotherapeutic potential. *Theranostics.* 2021; **11**(1):445-460

Cooke RM, Mistry R, Challiss RAJ, Straub VA. Nitric oxide synthesis and cGMP production is important for neurite growth and synapse remodeling after axotomy. *J Neurosci.* 2013; **33**(13):5626-37

Corleto KA, Singh J, Jayaprakasha GK, Patil BS. Storage Stability of Dietary Nitrate and Phenolic Compounds in Beetroot (*Beta vulgaris*) and Arugula (*Eruca sativa*) Juices. *J Food Sci.* 2018; **83**(5):1237-1248

Cruz-Jentoft AJ, Bahat G, Bauer J, Boirie Y, Bruyère O, Cederholm T, Cooper C, Landi F, Rolland Y, Sayer AA, Schneider SM, Sieber CC, Topinkova E, Vandewoude M, Visser M, Zamboni M. Sarcopenia: revised European consensus on definition and diagnosis. *Age Ageing.* 2019; **48**(1):16-31

Daum B, Walter A, Horst A, Osiewacz HD, Kühlbrandt W. Age-dependent dissociation of ATP synthase dimers and loss of inner-membrane cristae in mitochondria. *Proc Natl Acad Sci U S A.* 2013; **110**(38):15301-6

De Oliveira GV, Morgado M, Conte-Junior CA, Alvares TS. Acute effect of dietary nitrate on forearm muscle oxygenation, blood volume and strength in older adults: A randomized clinical trial. *PLoS One.* 2017; **12**(11):e0188893

Deepa S, Bhaskaran S, Espinoza S, Brooks SV, McArdle A, Jackson ML, Remmen HV, Richardson A. A new mouse model of frailty: the Cu/Zn superoxide dismutase knockout mouse. *Geroscience.* 2017; **39**(2):187-198

Del Campo A, Contreras-Hernández I, Castro-Sepúlveda M, Campos CA, Figueroa R, Tevy MF, Eisner V, Casas M, Jaimovich E. Muscle function decline and mitochondria changes in middle age precede sarcopenia in mice. *Aging (Albany NY).* 2018; **10**(1): 34–55

Deschenes MR, Roby MA, Eason MK, Harris MB. Remodeling of the Neuromuscular Junction Precedes Sarcopenia Related Alterations in Myofibers. *Exp Gerontol.* 2010; **45**(5):389–393

Di Massimo C, Scarpelli P, Di Lorenzo N, Caimi G, di Orio F, Tozzi Ciancarelli MG. Impaired plasma nitric oxide availability and extracellular superoxide dismutase activity in healthy humans with advancing age. *Life Sci.* 2006; **78**(11):1163-7

Dobrowolny G, Barbiera A, Sica G, Scicchitano BM. Age-Related Alterations at Neuromuscular Junction: Role of Oxidative Stress and Epigenetic Modifications. *Cells.* 2021; **10**(6):1307

Dulac M, Leduc-Gaudet JP, Cefis M, Ayoub MB, Reynaud O, Shams A, Moamer A, Nery Ferreira MF, Hussain SN, Gouspillou G. Regulation of muscle and mitochondrial health by the mitochondrial fission protein Drp1 in aged mice. *J Physiol.* 2021; **599**(17):4045-4063

Dupuis L, Gonalez de Aguilar JL, Echaniz-Laguna A, Eschbach J, Rene F, Oudart H, Halter B, Huze C, Schaeffer L, Bouillaud F, Loeffler JP. Muscle mitochondrial uncoupling dismantles neuromuscular junction and triggers distal degeneration of motor neurons. *PLoS One.* 2009; **4**(4):e5390

Ebert SM, Dyle MC, Kunkel SD, Bullard SA, Bongers KS, Fox DK, Dierdorff JM, Foster ED, Adams CM. Stress-induced skeletal muscle Gadd45a expression reprograms myonuclei and causes muscle atrophy. *J Biol Chem.* 2012; **287**(33):27290-301

Eigentler A, Draxl A, Gnaiger E. Laboratory Protocol. Citrate synthase: a mitochondrial marker enzyme. *Mitochondrial Physiology Network.* 2020; **04**:1-12

Engan HK, Jones AM, Ehrenberg F, Schagatay E. Acute dietary nitrate supplementation improves dry static apnea performance. *Respir Physiol Neurobiol.* 2012; **182**(2-3):53-9

Etherington SJ, Everett AW. Postsynaptic production of nitric oxide implicated in long-term depression at the mature amphibian (*Bufo marinus*) neuromuscular junction. *J Physiol.* 2004; **559**(Pt 2):507-17

Ezzat-Zadeh Z, Kim JS, Chase PB, Arjmandi BH. The cooccurrence of obesity, osteoporosis, and sarcopenia in the ovariectomized rat: a study for modeling osteosarcopenic obesity in rodents. *J Aging Res.* 2017; **2017**:1454103

Favaro G, Romanello V, Varanita T, Desbats A, Morbidoni V, Tezze C, Albiero M, Canato M, Gherardi G, De Stefani D, Mammucari C, Blaauw B, Boncompagni S, Protasi F, Reggiani C, Scorrano L, Salviati L, Sandri M. DRP1-mediated mitochondrial shape controls calcium homeostasis and muscle mass. *Nat Commun.* 2019; **10**(1):2576

Ferguson SK, Redinius KM, Harral JW, Pak DI, Swindle DC, Hirai DM, Blackwell JR, Jones AM, Stenmark KR, Buehler PW, Irwin DC. The effect of dietary nitrate supplementation on the speed-duration relationship in mice with sickle cell disease. *J Appl Physiol (1985).* 2020; **129**(3):474-482

Francaux M, Demeulder B, Naslain D, Fortin R, Lutz O, Caty G, Deldicque L. Aging Reduces the Activation of the mTORC1 Pathway after Resistance Exercise and Protein Intake in Human Skeletal Muscle: Potential Role of REDD1 and Impaired Anabolic Sensitivity. *Nutrients.* 2016; **8**(1):47

Franco MC and Estevez AG. Tyrosine nitration as mediator of cell death. *Cell Mol Life Sci.* 2014; **71**(20):3939-50

Frost RA, Nystrom GJ, Lang CH. Endotoxin and interferon-gamma inhibit translation in skeletal muscle cells by stimulating nitric oxide synthase activity. *Shock.* 2009; **32**(4):416-26

Garbern JC, Lee RT. Mitochondria and metabolic transitions in cardiomyocytes: lessons from development for stem cell-derived cardiomyocytes. *Stem Cell Res Ther.* 2021; **12**(1):177

Garcia ML, Fernandez A, Solas MT. Mitochondria, motor neurons and aging. *J Neurol Sci.* 2013; **330**(1-2):18-26

Garcia-Roves PM, Osler ME, Holmstrom MH, Zierath JR. Gain-of-function R225Q mutation in AMP-activated protein kinase gamma3 subunit increases mitochondrial biogenesis in glycolytic skeletal muscle. *J Biol Chem.* 2008; **283**(51):35724-34

Gath I, Ebert J, Godtel-Armbrust U, Ross R, Reske-Kunz AB; Forstermann U. NO synthase II in mouse skeletal muscle is associated with caveolin 3. *Biochem J.* 1999; **340**(Pt3):723-8

Gaugler M, Brown A, Merrell E, DiSanto-Rose M, Rathmacher JA, Reynolds TH. PKB signaling and atrogene expression in skeletal muscle of aged mice. *J Appl Physiol (1985).* 2011; **111**(1):192–199

Gill JF, Delezie J, Santos G, McGuirk S, Schnyder S, Frank S, Rausch M, St-Pierre J, Handschin C. Peroxisome proliferator-activated receptor γ coactivator 1α regulates mitochondrial calcium homeostasis, sarcoplasmic reticulum stress, and cell death to mitigate skeletal muscle aging. *Aging Cell.* 2019; **18**(5):e12993

Gilliard CN, Lam JK, Cassel KS, Park JW, Schechter AN, Piknova B. Effect of dietary nitrate levels on nitrate fluxes in rat skeletal muscle and liver. *Nitric Oxide.* 2018; **75**:1-7

Gillon A, Sheard P. Elderly mouse skeletal muscle fibers have a diminished capacity to upregulate NCAM production in response to denervation. *Biogerontology.* 2015; **16**(6):811-23

Giovarelli M, Zecchini S, Martini E, Garrè M, Barozzi S, Ripolone M, Napoli L, Coazzoli M, Vantaggiato C, Roux-Biejat P, Cervia D, Moscheni C, Perrotta C, Parazzoli D, Clementi E, De Palma C. Drp1 overexpression induces desmin disassembling and drives kinesin-1 activation promoting mitochondrial trafficking in skeletal muscle. *Cell Death Differ.* 2020; **27**(8):2383-2401

Glund S, Schoelch C, Thomas L, Niessen HG, Stiller D, Roth GJ, Neubauer H. Inhibition of acetyl-CoA carboxylase 2 enhances skeletal muscle fatty acid oxidation and improves whole-body glucose homeostasis in db/db mice. *Diabetologia.* 2012; **55**:2044–2053

Gnaiger E, Kuznetsov AV, Schneeberger S, Seiler R, Brandacher G, Steurer W, Margreiter R. Mitochondria in the Cold. *Life in the Cold. Springer*; Heiderlberg, Germany: 2000. pp. 431–442

Godfrey EW, Longacher M, Neiswender H, Schwarte RC, Browning DD. Guanylate cyclase and cyclic GMP-dependent protein kinase regulate agrin signaling at the developing neuromuscular junction. *Dev Biol.* 2007; **307**(2):195-201

Godfrey EW, Schwarte RC. The role of nitric oxide signaling in the formation of the neuromuscular junction. *J Neurocytol.* 2003; **32**(5-8):591-602

Goljanek-Whysall K, Soriano-Arroquia A, McCormick R, Chinda C, McDonagh B. miR-181a regulates p62/SQSTM1, parkin, and protein DJ-1 promoting mitochondrial dynamics in skeletal muscle aging. *Aging Cell.* 2020; **19**(4):e13140

Gomes LC, Di Benedetto G, Scorrano L. During autophagy mitochondria elongate, are spared from degradation and sustain cell viability. *Nat Cell Biol.* 2011; **13**(5):589-98

Gonzalez-Freire M, de Cabo R, Studenski SA, Ferrucci L. The Neuromuscular Junction: Aging at the Crossroad between Nerves and Muscle. *Front Aging Neurosci.* 2014; **6**:208

Gouspillou G, Bourdel-Marchasson I, Rouland R, Calmettes G, Franconi JM, Deschodt-Arsac V, Diolez P. Alteration of mitochondrial oxidative phosphorylation in aged skeletal muscle involves modification of adenine nucleotide translocator. *Biochim Biophys Acta.* 2010; **1797**(2):143-51

Gouspillou G, Picard M, Godin R, Burelle Y, Hepple RT. Role of peroxisome proliferator-activated receptor gamma coactivator 1-alpha (PGC-1α) in denervation-induced atrophy in aged muscle: facts and hypotheses. *Longev Healthspan.* 2013; **2**(1):13

Govoni M, Jansson EA, Weitzberg E, Lundberg JO. The increase in plasma nitrite after a dietary nitrate load is markedly attenuated by an antibacterial mouthwash. *Nitric Oxide.* 2008; **19**(4):333-7

Greising SM, Mantilla CB, Gorman BA, Ermilov LG, Sieck GC. Diaphragm muscle sarcopenia in aging mice. *Exp Gerontol.* 2013; **48**(9):881-7

Gumucio, JP, Mendias CL. Atrogin-1, MuRF-1, and sarcopenia. *Endocrine.* 2013; **43**(1):12-21

Gurd BJ, Yoshida Y, McFarlan JT, Holloway GP, Moyes CD, Heigenhauser GJF, Spriet L, Bonen A. Nuclear SIRT1 activity, but not protein content, regulates mitochondrial biogenesis in rat and human skeletal muscle. *Am J Physiol Regul Integr Comp Physiol.* 2011; **301**(1):R67-75

Hachisu M, Obayashi M, Kogo M, Ihara K. Psychosomatic Health in Elderly People for Preventing Frailty: The role of IGF-1 and BDNF in the Muscle and the Brain. *J Aging Sci.* 2020; **8**(1):1-3

Haider G, Folland JP. Nitrate supplementation enhances the contractile properties of human skeletal muscle. *Med Sci Sports Exerc.* 2014; **46**(12):2234-43

Hakim CH, Lessa TB, Jenkins GJ, Yang NN, Ambrosio CE, Duan D. An improved method for studying mouse diaphragm function. *Sci Rep.* 2019; **9**(1):19453

Hall DT, Griss T, Ma JF, Sanchez BJ, Sadek J, Tremblay AMK, Mubaid S, Omer A, Ford RJ, Bedard N, Pause A, Wing SS, Di Marco S, Steinberg GR, Jones RG, Gallouzi IE. The AMPK agonist 5-aminoimidazole-4-carboxamide ribonucleotide (AICAR), but not metformin, prevents inflammation-associated cachectic muscle wasting. *EMBO Mol Med.* 2018; **10**(7):e8307

Hall DT, Ma JF, Di Marco S, Gallouzi I. Inducible nitric oxide synthase (iNOS) in muscle wasting syndrome, sarcopenia, and cachexia. *Aging (Albany NY).* 2011; **3**(8):702-15

Handschin C, Kobayashi YM, Chin S, Seale P, Campbell KP, Spiegelman BM. PGC-1α regulates the neuromuscular junction program and ameliorates Duchenne muscular dystrophy. *Genes Dev.* 2007; **21**(7):770–783

Harper C, Gopalan V, Goh J. Exercise rescues mitochondrial coupling in aged skeletal muscle: a comparison of different modalities in preventing sarcopenia. *J Transl Med.* 2021; **19**:71

Hendrickse P, Galinska M, Hodson-Tole E, Degens H. An evaluation of common markers of muscle denervation in denervated young-adult and old rat gastrocnemius muscle. *Exp Gerontol.* 2018; **106**:159-164

Hepple RT, Rice CL. Innervation and neuromuscular control in ageing skeletal muscle. *J Physiol.* 2016; **594**(8):1965–1978

Hernandez A, Schiffer TA, Ivarsson N, Cheng AJ, Bruton JD, Lundberg JO, Weitzberg E, Westerblad H. Dietary nitrate increases tetanic $[Ca^{2+}]i$ and contractile force in mouse fast-twitch muscle. *J Physiol.* 2012; **590**(15):3575-83

Herzig S, Shaw RJ. AMPK: guardian of metabolism and mitochondrial homeostasis. *Nat Rev Mol Cell Biol.* 2018; **19**(2):121–135

Hettwer S, Dahinden P, Kucsera S, Farina C, Ahmed S, Fariello R, Drey M, Sieber CC, Vrijbloed W. Elevated levels of a C-terminal agrin fragment identifies a new subset of sarcopenia patients. *Exp Gerontol.* 2013; **48**(1):69-75

Hezel M, de Groat WC, Galbiati F. Caveolin-3 promotes nicotinic acetylcholine receptor clustering and regulates neuromuscular junction activity. *Mol Biol Cell.* 2010; **21**(2):302-10

Hirai DM, Musch TI, Poole DC. Exercise training in chronic heart failure: improving skeletal muscle O_2 transport and utilization. *Am J Physiol Heart Circ Physiol*. 2015; **309**(9):H1419-39

Hord NG, Tang Y, Bryan NS. Food sources of nitrates and nitrites: the physiologic context for potential health benefits. *Am J Clin Nutr.* 2009; **90**(1):1-10

Hoyng SA, De Winter F, Gnavi S, de Boer R, Boon LI, Korvers LM, Tannemaat MR, Malessy MJA, Verhaagen J. A comparative morphological, electrophysiological and functional analysis of axon regeneration through peripheral nerve autografts genetically modified to overexpress BDNF, CNTF, GDNF, NGF, NT3 or VEGF. *Exp Neurol.* 2014; **261**:578-93

https://www.istat.it/it/files/2021/07/Report-anziani-2019.pdf

Huang DD, Fan SD, Chen XY, Yan LX, Zhang XZ, Ma BW, Yu DY, Xiao WY, Zhuang CL, Yu Z. Nrf2 deficiency exacerbates frailty and sarcopenia by impairing skeletal muscle mitochondrial biogenesis and dynamics in an age-dependent manner. *Exp Gerontol.* 2019; **119**:61-73

Huang DD, Yan LX, Fan SD, Chen XY, Yan JY, Dong QT, Chen WZ, Lui NX, Chen XL, Yu Z. Nrf2 deficiency promotes the increasing trend of autophagy during aging in skeletal muscle: a potential mechanism for the development of sarcopenia. *Aging (Albany NY).* 2020; **12**(7):5977-5991

Huang QK, Qiao HY, Fu MH, Li G, Li WB, Chen Z, Wei J, Liang BS. MiR-206 Attenuates Denervation-Induced Skeletal Muscle Atrophy in Rats Through Regulation of Satellite Cell Differentiation via TGF-β1, Smad3, and HDAC4 Signaling. *Med Sci Monit.* 2016; **22**:1161–1170

Huffman DM, Quipildor GF, Mao K, Zhang X, Wan J, Apontes P, Cohen P, Barzilai N. Central insulin-like growth factor-1 (IGF-1) restores whole-body insulin action in a model of age-related insulin resistance and IGF-1 decline. *Aging Cell.* 2016; **15**(1):181-6

Hughes WE, Ueda K, Treichler DP, Casey DP. Effects of acute dietary nitrate supplementation on aortic blood pressure and aortic augmentation index in young and older adults. *Nitric Oxide.* 2016; **59**:21-7

Husmann F, Bruhn S, Mittlmeier T, Zschorlich V, Behrens M. Dietary Nitrate Supplementation Improves Exercise Tolerance by Reducing Muscle Fatigue and Perceptual Responses. *Front Physiol.* 2019; **10**:404

Ibebunjo C, Chick JM, Kendall T, Eash JK, Li C, Zhang Y, Vickers C, Wu Z, Clarke BA, Shi J, Cruz J, Fournier B, Brachat S, Gutzwiller S, Ma Q, Markovits J, Broome M, Steinkrauss M, Skuba E, Galarneau JR, Gygi SP, Glass DJ. Genomic and proteomic profiling reveals reduced mitochondrial function and disruption of the neuromuscular junction driving rat sarcopenia. *Mol Cell Biol.* 2013; **33**(2):194-212

Ivarsson N, Schiffer TA, Hernández A, Lanner JT, Weitzberg E, Lundberg JO, Westerblad H. Dietary nitrate markedly improves voluntary running in mice. *Physiol Behav.* 2017; **168**:55–61

Jang S, Javadov S. Elucidating the contribution of ETC complexes I and II to the respirasome formation in cardiac mitochondria. *Sci Rep.* 2018; **8**(1):17732

Jeffrey Man HS, Tsui AKY, Marsden PA. Nitric oxide and hypoxia signaling. *Vitam Horm.* 2014; **96**:161-92

Jespersen B, Tykocki NR, Watts SW, Cobbett PJ. Measurement of smooth muscle function in the isolated tissue bath-applications to pharmacology research. *J Vis Exp.* 2015; (95):52324

Jiang C, Moorthy BT, Patel DM, Kumar A, Morgan WM, Alfonso B, Huang J, Lampidis TJ, Isom DG, Barrientos A, Fontanesi F, Zhang F. Regulation of Mitochondrial Respiratory Chain Complex Levels, Organization, and Function by Arginyltransferase 1. *Front Cell Dev Biol.* 2020; **8**:603688

Johnson ML, Robinson MM, Nair KS. Skeletal muscle aging and the mitochondrion. *Trends Endocrinol Metab.* 2013; **24**(5):247-56

Jones AM, Grassi B, Christensen PM, Krustrup P, Bangsbo J, Poole DC. Slow Component of V˙O2 Kinetics: Mechanistic Bases and Practical Applications. *Med Sci Sports Exerc.* 2011; **43**(11):2046-62

Jones MA, Werle MJ. Agrin-induced AChR aggregate formation requires cGMP and aggregate maturation requires activation of cGMP-dependent protein kinase. *Mol Cell Neurosci.* 2004; **25**(2):195-204

Jones RA, Harrison C, Eaton SL, Hurtado ML, Graham LC, Alkhammash L, Oladiran OA, Gale A, Lamont DJ, Simpson H, Simmen MW, Soeller C, Wishart TM, Gillingwater TH. Cellular and Molecular Anatomy of the Human Neuromuscular Junction. *Cell Rep.* 2017; **21**(9):2348–2356

Jones RA, Reich CD, Dissanayake KN, Kristmundsdottir F, Findlater GS, Ribchester RR, Simmen MW, Gillingwater TH. NMJ-morph reveals principal components of synaptic morphology influencing structure–function relationships at the neuromuscular junction. *Open Biol.* 2016; **6**(12):160240

Joseph GA, Wang SX, Jacobs CE, Zhou W, Kimble GC, Tse HW, Eash JK, Shavlakadze T, Glass DJ. Partial Inhibition of mTORC1 in Aged Rats Counteracts the Decline in Muscle Mass and Reverses Molecular Signaling Associated with Sarcopenia. *Mol Cell Biol.* 2019; **39**(19):e00141-19

Ju Y, Lee H, Choi J, Choi M. The Role of Protein S-Nitrosylation in Protein Misfolding-Associated Diseases. *Life (Basel).* 2021; **11**(7):705

Justice JN, Gioscia-Ryan RA, Johnson LC, Battson ML, de Picciotto NE, Beck HJ, Jiang H, Sindler AL, Bryan NS, Enoka RM, Seals DR. Sodium nitrite supplementation improves motor function and skeletal muscle inflammatory profile in old male mice. *J Appl Physiol (1985)*. 2015; **118**(2):163-9

Kang H, Lichtman JW. Motor Axon Regeneration and Muscle Reinnervation in Young Adult and Aged Animals. *J Neurosci.* 2013; **33**(50):19480–19491

Kelly J, Fulford J, Vanhatalo A, Blackwell JR, French O, Bailey SJ, Gilchrist M, Winyard PG, Jones AM. Effects of short-term dietary nitrate supplementation on blood pressure, O_2 uptake kinetics, and muscle and cognitive function in older adults. *Am J Physiol Regul Integr Comp Physiol.* 2013; **304**(2):R73-83

Khan MM, Strack S, Wild F, Hanashima A, Gasch A, Brohm K, Reischl M, Carnio S, Labeit D, Sandri M, Labeit S, Rudolf R. Role of autophagy, SQSTM1, SH3GLB1, and TRIM63 in the turnover of nicotinic acetylcholine receptors. *Autophagy.* 2014; **10**(1):123-36

Kim C, Hwang JK. The 5,7-Dimethoxyflavone Suppresses Sarcopenia by Regulating Protein Turnover and Mitochondria Biogenesis-Related Pathways. *Nutrients.* 2020; **12**(4):1079

Kim KW, Cho HJ, Khaliq SA, Son KH, Yoon MS. Comparative Analyses of mTOR/Akt and Muscle Atrophy-Related Signaling in Aged Respiratory and Gastrocnemius Muscles. *Int J Mol Sci.* 2020; **21**(8):2862

Kimball SR, O'Malley JP, Anthony JC, Crozier SJ, Jefferson LS. Assessment of biomarkers of protein anabolism in skeletal muscle during the life span of the rat: sarcopenia despite elevated protein synthesis. *Am J Physiol Endocrinol Metab.* 2004; **287**(4):E772-80

Kobzik L, Reid MB, Bredt DS, Stamler JS. Nitric oxide in skeletal muscle. *Nature.* 1994; **372**(6506):546-8

Kobzik L, Stringer B, Balligand JL, Reid MB, Stamler JS. Endothelial type nitric oxide synthase in skeletal muscle fibers: mitochondrial relationships. *Biochem Biophys Res Commun.* 1995; **211**(2):375-81

Kodama S, Saito K, Tanaka S, Maki M, Yachi Y, Asumi M, Sugawara A, Totsuka K, Shimano H, Ohashi Y, Yamada N, Sone H. Cardiorespiratory fitness as a quantitative predictor of all-cause mortality and cardiovascular events in healthy men and women: a meta-analysis. *JAMA.* 2009; **301**(19):2024-35

Koltai E, Hart N, Taylor AW, Goto S, Ngo JK, Davies KJA, Radak Z. Age-associated declines in mitochondrial biogenesis and protein quality control factors are minimized by exercise training. *Am J Physiol Regul Integr Comp Physiol.* 2012; **303**(2):R127-34

Koneczny I, Cossins J, Vincent A. The role of muscle-specific tyrosine kinase (MuSK) and mystery of MuSK myasthenia gravis. *J Anat.* 2014; **224**(1):29-35

Kreko-Pierce T, Eaton BA. Rejuvenation of the aged neuromuscular junction by exercise. *Cell Stress.* 2018; **2**(2):25-33

Krishnan VS, White Z, Terrill JR, Hodgetts SI, Fitzgerald M, Shavlakadze T, Harvey AR, Grounds MD. Resistance wheel exercise from mid-life has minimal effect on sciatic nerves from old mice in which sarcopenia was prevented. *Biogerontology.* 2017; **18**:769–790

Kumar RA, Kelley RC, Hahn D, Ferreira LF. Dietary nitrate supplementation increases diaphragm peak power in old mice. *J Physiol.* 2020; **598**(19):4357-4369

Kung TA, Cederna PS, van der Meulen JH, Urbanchek MG, Kuzon Jr WM, Faulkner JA. Motor unit changes seen with skeletal muscle sarcopenia in oldest old rats. *J Gerontol A Biol Sci Med Sci.* 2014; **69**(6):657-65

Kurutas EB. The importance of antioxidants which play the role in cellular response against oxidative/nitrosative stress: current state. *Nutr J.* 2015; **15**:71

Kusner LL and Kaminski HJ. Nitric oxide synthase is concentrated at the skeletal muscle endplate. *Brain Res.* 1996; **730**(1-2):238-42

Laemmli UK. Cleavage of structural proteins during the assembly of the head of bacteriophage T4. *Nature.* 1970; **227**(5259):680-5

Lancaster Jr. Nitroxidative, nitrosative, and nitrative stress: kinetic predictions of reactive nitrogen species chemistry under biological conditions. *Chem Res Toxicol.* 2006; **19**(9):1160-74

Lansley KE, Winyard PG, Bailey SJ, Vanhatalo A, Wilkerson DP, Blackwell JR, Gilchrist M, Benjamin N, Jones AM. Acute dietary nitrate supplementation improves cycling time trial performance. *Med Sci Sports Exerc.* 2011; **43**(6):1125-31

Lansley KE, Winyard PG, Fulford J, Vanhatalo A, Bailey SJ, Blackwell JR, DiMenna FJ, Gilchrist M, Benjamin N, Jones AM. Dietary nitrate supplementation reduces the O2 cost of walking and running: a placebo-controlled study. *J Appl Physiol (1985).* 2011; **110**(3):591-600

Larsen FJ, Schiffer TA, Borniquel S, Sahlin K, Ekblom B, Lundberg JO, Weitzberg E. Dietary inorganic nitrate improves mitochondrial efficiency in humans. *Cell Metab.* 2011; **13**(2):149-59

Larsen FJ, Weitzberg E, Lundberg JO, Ekblom B. Effects of dietary nitrate on oxygen cost during exercise. *Acta Physiol (Oxf).* 2007; **191**(1):59-66

Larsen S, Nielsen J, Hansen CN, Nielsen LB, Wibrand F, Stride N, Schroder HD, Boushel R, Helge JW, Dela F & Hey-Mogensen M. Biomarkers of mitochondrial content in skeletal muscle of healthy young human subjects. *J Physiol.* 2012; **590**:3349–3360

Lavorato M, Gupta PK, Hopkins PM, Franzini-Armstrong C. Skeletal muscle microalterations in patients carrying malignant hyperthermia-related mutations of the e-c coupling machinery. *Eur J Transl Myol.* 2016; **26**:6105

Leduc-Gaudet JP, Picard M, Pelletier FSJ, Sgarioto N, Auger MJ, Vallee J, Robitaille R, St-Pierre DH, Gouspillou G. Mitochondrial morphology is altered in atrophied skeletal muscle of aged mice. *Oncotarget.* 2015; **6**(20):17923–17937

Lemieux P and Birot O. Altitude, Exercise, and Skeletal Muscle Angio-Adaptive Responses to Hypoxia: A Complex Story. *Front Physiol.* 2021; **12**:735557

Li L, Wang H, Hu L, Wu X, Zhao B, Fan Z, Zhang C, Wang J, Wang S. Age associated decrease of sialin in salivary glands. *Biotech Histochem.* 2018; **93**(7):505–511

Li Y, D'Aurelio M, Deng JH, Park JS, Manfredi G, Hu P, Lu J, Bai Y. An assembled complex IV maintains the stability and activity of complex I in mammalian mitochondria. *J Biol Chem.* 2007; **282**(24):17557-62

Li Y, Lee Y, Thompson WJ. Changes in Aging Mouse Neuromuscular Junctions Are Explained by Degeneration and Regeneration of Muscle Fiber Segments at the Synapse. *J Neurosci.* 2011; **31**(42):14910–14919

Lira VA, Brown DL, Lira AK, Kavazis AN, Soltow QA, Zeanah EH, Criswell DS. Nitric oxide and AMPK cooperatively regulate PGC-1α in skeletal muscle cells. *J Physiol.* 2010; **588**(Pt 18):3551-66

Lira VA, Slotow QA, Long JHD, Betters JL, Sellman JE, Criswell DS. Nitric oxide increases GLUT4 expression and regulates AMPK signaling in skeletal muscle. *Am J Physiol Endocrinol Metab.* 2007; **293**(4):E1062-8

Lowry OH, Rosebrough NJ, Farr AL, Randall RJ. Protein measurement with the Folin phenol reagent. *J Biol Chem.* 1951; **193**(1):265-75

Lundberg JO, Gladwin MT, Ahluwalia A, Benjamin N, Bryan NS, Butler A, Cabrales P, Fago A, Feelisch M, Ford PC, Freeman BA, Frenneaux M, Friedman J, Kelm M, Kevil CG, Kim-Shapiro DB, Kozlov AV, Lancaster Jr, Lefer DJ, McColl K, McCurry K, Patel RP, Petersson J, Rassaf T, Reutov VP, Richter-Addo GB, Schechter A, Shiva S, Tsuchiya K, van Faassen EE, Webb AJ, Zuckerbraun BS, Zweier JL, Weitzberg E. Nitrate and nitrite in biology, nutrition and therapeutics. *Nat Chem Biol.* 2009; **5**(12):865-9

Ma J, Shen J, Garrett JP, Lee CA, Li Z, Elsaidi GA, Ritting A, Hick J, Tan KH, Smith TL, Smith BP, Koman LA. Gene expression of myogenic regulatory factors, nicotinic acetylcholine receptor subunits, and GAP-43 in skeletal muscle following denervation in a rat model. *J Orthop Res.* 2007; **25**(11):1498-505

Ma W, Cai Y, Shen Y, Chen X, Zhang L, Ji Y, Chen Z, Zhu J, Yang X, Sun H. HDAC4 Knockdown Alleviates Denervation-Induced Muscle Atrophy by Inhibiting Myogenin-Dependent Atrogene Activation. *Front Cell Neurosci.* 2021; **15**:663384

MacDonald JA, Walsh MP. Regulation of smooth muscle myosin light chain phosphatase by multi-site phosphorylation of the myosin targeting subunit, MYPT1. *Cardiovasc Haematol Disorders-Drug Targets.* 2018; **18**(1):4-13

Makrecka-Kuka M, Krumschnabel G, Gnaiger E. High-Resolution Respirometry for Simultaneous Measurement of Oxygen and Hydrogen Peroxide Fluxes in Permeabilized Cells, Tissue Homogenate and Isolated Mitochondria. *Biomolecules.* 2015; **5**(3):1319–1338

Mann CJ, Perdiguero E, Kharraz Y, Aguilar S, Pessina P, Serrano AL, Muñoz-Cánoves P. Aberrant repair and fibrosis development in skeletal muscle. *Skelet Muscle.* 2011; **1**(1):21

Masiero E, Agatea L, Mammucari C, Blaauw B, Loro E, Komatsu M, Metzger D, Reggiani C, Schiaffino S, Sandri M. Autophagy is required to maintain muscle mass. *Cell Metab.* 2009; **10**(6):507-15

Matsumaru D, Motohashi H. The KEAP1-NRF2 System in Healthy Aging and Longevity. *Antioxidants (Basel).* 2021; **10**(12):1929

Mattagajasingh I, Kim C, Naqvi A, Yamamori T, Hoffman TA, Jung S, DeRicco J, Kasuno K, Irani K. SIRT1 promotes endothelium-dependent vascular relaxation by activating endothelial nitric oxide synthase. *Proc Natl Acad Sci U S A.* 2007; **104**(37):14855-60

McConell GK, Bradley SJ, Stephens TJ, Canny BJ, Kingwell BA, Lee-Young RS. Skeletal muscle nNOS mu protein content is increased by exercise training in humans. *Am J Physiol Regul Integr Comp Physiol.* 2007; **293**(2):R821-8

McGee SL, Howlett KF, Starkie RL, Cameron-Smith D, Kemp BE, Hargreaves M. Exercise increases nuclear AMPK alpha2 in human skeletal muscle. *Diabetes.* 2003; **52**(4):926-8

Mech AM, Brown AL, Schiavo G, Sleigh JN. Morphological variability is greater at developing than mature mouse neuromuscular junctions. *J Anat.* 2020; **237**(4):603-617

Mengel A, Chaki M, Shekariesfahlan A, Lindermayr C. Effect of nitric oxide on gene transcription – S-nitrosylation of nuclear proteins. *Front Plant Sci.* 2013; **4**:293

Mishra D, Patel V, Banerjee D. Nitric Oxide and S-Nitrosylation in Cancers: Emphasis on Breast Cancer. *Breast Cancer (Auckl).* 2020; **14**:1178223419882688

Miura P, Amirouche A, Clow C, Belanger G, Jasmin BJ. Brain-derived neurotrophic factor expression is repressed during myogenic differentiation by miR-206. *J Neurochem.* 2012; **120**(2):230-8

Mobley CB, Mumford PW, Kephart WC, Haun CT, Holland AM, Beck DT, Martin JS, Young KC, Anderson RG, Patel RK, Langston GL, Lowery RP, Wilson JM, Roberts MD. Aging in Rats Differentially Affects Markers of Transcriptional and Translational Capacity in Soleus and Plantaris Muscle. *Front Physiol.* 2017; **8**:518

Moon K, Hood BL, Kim B, Hardwick JP, Conrads TP, Veenstra TD, Song BJ. Inactivation of oxidized and S-nitrosylated mitochondrial proteins in alcoholic fatty liver of rats. *Hepatology.* 2006; **44**(5):1218-30

Mor Huertas A, Morton AB, Hinkey JM, Ichinoseki-Sekine N, Smuder AJ. Modification of Neuromuscular Junction Protein Expression by Exercise and Doxorubicin. *Med Sci Sports Exerc.* 2020; **52**(7):1477-1484

Moreillon M, Conde Alonso S, Broskey NT, Greggio C, Besson C, Rousson V, Amati F. Hybrid fiber alterations in exercising seniors suggest contribution to fast-to-slow muscle fiber shift. *J Cachexia Sarcopenia Muscle.* 2019; **10**(3):687-695

Moresi V, Williams AH, Meadows E, Flynn JM, Potthoff MJ, McAnally J, Shelton JM, Backs J, Klein WH, Richardson JA, Bassel-Duby R, Olson EN. Myogenin and class II HDACs control neurogenic muscle atrophy by inducing E3 ubiquitin ligases. *Cell.* 2010; **143**(1):35-45

Morris G, Walder K, Puri BK, Berk M; Maes M. The Deleterious Effects of Oxidative and Nitrosative Stress on Palmitoylation, Membrane Lipid Rafts and Lipid-Based Cellular Signalling: New Drug Targets in Neuroimmune Disorders. *Mol Neurobiol.* 2016; **53**:4638–4658

Mozos I, Tudor Luca C. Crosstalk between Oxidative and Nitrosative Stress and Arterial Stiffness. *Curr Vasc Pharmacol.* 2017; **15**(5):446-456

Muggeridge DJ, Howe CCF, Spendiff O, Pedlar C, James PE, Easton C. A single dose of beetroot juice enhances cycling performance in simulated altitude. *Med Sci Sports Exerc.* 2014; **46**(1):143-50

Murciano-Calles J, Coello A, Camara-Artigas A, Martinez JC. PDZ/PDZ interaction between PSD-95 and nNOS neuronal proteins. *J Mol Recognit.* 2020; **33**(4):e2826

Navratil M, Terman A, Arriaga EA. Giant mitochondria do not fuse and exchange their contents with normal mitochondria. *Exp Cell Res.* 2008; **314**(1):164-72

Nickels TJ, Reed GW, Drummond JT, Blevins DE, Lutz MC, Wilson DF. Does nitric oxide modulate transmitter release at the mammalian neuromuscular junction? *Clin Exp Pharmacol Physiol.* 2007; **34**(4):318-26

Nilwik R, Snijders T, Leenders M, Groen BB, van Kranenburg J, Verdijk LB, van Loon LJC. The decline in skeletal muscle mass with aging is mainly attributed to a reduction in type II muscle fiber size. *Exp Gerontol.* 2013; **48**(5):492-8

Nishimune H, Stanford JA, Mori Y. Role of exercise in maintaining the integrity of the neuromuscular junction. *Muscle Nerve.* 2014; **49**(3):315-24

Nisoli E, Clementi E, Paolucci C, Cozzi V, Tonello C, Sciorati C, Bracale R, Valerio A, Francolini M, Moncada S, Carruba MO. Mitochondrial biogenesis in mammals: the role of endogenous nitric oxide. *Science.* 2003; **299**(5608):896-9

Nisoli E, Tonello C, Cardile A, Cozzi V, Bracale R, Tedesco L, Falcone S, Valerio A, Cantoni O, Clementi E, Moncada S, Carruba MO. Calorie restriction promotes mitochondrial biogenesis by inducing the expression of eNOS. *Science.* 2005; **310**(5746):314-7

Niu Y, Wang T, Liu S, Yuan H, Li H, Fu L. Exercise-induced GLUT4 transcription via inactivation of HDAC4/5 in mouse skeletal muscle in an AMPKα2-dependent manner. *Biochim Biophys Acta Mol Basis Dis.* 2017; **1863**(9):2372-2381

Ntessalen M, Procter NEK, Schwarz K, Loudon BL, Minnion M, Fernandez BO, Vassiliou VS, Vauzour D, Madhani M, Constantin-Teodosiu D, Horowitz JD, Feelisch M, Dawson D, Crichton PG, Frenneaux MP. Inorganic nitrate and nitrite supplementation fails to improve skeletal muscle mitochondrial efficiency in mice and humans. *Am J Clin Nutr.* 2020; **111**(1):79-89

Nyakayiru J, Kouw IWK, Cermak NM, Senden JM, van Loon LJC, Verdijk LB. Sodium nitrate ingestion increases skeletal muscle nitrate content in humans. *J Appl Physiol (1985).* 2017; **123**(3):637-44

Nyakayiru JM, Jonvik KL, Pinckaers PJM, Sender J, van Loon LJC, Verdijk LB. No Effect of Acute and 6-Day Nitrate Supplementation on VO 2 and Time-Trial Performance in Highly Trained Cyclists. *Int J Sport Nutr Exerc Metab.* 2017; **27**(1):11-17

O'Leary MF, Vainshtein A, Iqbal S, Ostojic O, Hood DA. Adaptive plasticity of autophagic proteins to denervation in aging skeletal muscle. *Am J Physiol Cell Physiol.* 2013; **304**(5):C422-30

Oda K. Age changes of motor innervation and acetylcholine receptor distribution on human skeletal muscle fibres. *J Neurol Sci.* 1984; **66**(2-3):327-38

Park JW, Piknova B, Dey S, Noguchi CT, Schechter AN. Compensatory mechanisms in myoglobin deficient mice preserve NO homeostasis. *Nitric Oxide.* 2019; **90**:10-14

Park JW, Thomas SM, Schechter AN, Piknova B. Control of rat muscle nitrate levels after perturbation of steady state dietary nitrate intake. *Nitric Oxide.* 2021; **109-110**:42-49

Pascual-Fernández J, Fernández-Montero A, Córdova-Martínez A, Pastor D, Martínez-Rodríguez A, Roche E. Sarcopenia: Molecular Pathways and Potential Targets for Intervention. *Int J Mol Sci.* 2020; **21**(22):8844

Patel A, Zhao J, Yue Y, Zhang K, Duan D, Lai Y. Dystrophin R16/17-syntrophin PDZ fusion protein restores sarcolemmal nNOSμ. *Skelet Muscle.* 2018; **8**(1):36

Peleli M, Zollbrecht C, Montenegro MF, Hezel M, Zhong J, Persson EG, Holmdahl R, Weitzberg E, Lundberg JO, Carlström M. Enhanced XOR activity in eNOS-deficient mice: Effects on the nitrate-nitrite-NO pathway and ROS homeostasis. *Free Radic Biol Med.* 2016; **99**:472-484

Perez-Torres I, Manzano-Pech L, Rubio-Ruiz ME, Soto ME, Guarner-Lans V. Nitrosative Stress and Its Association with Cardiometabolic Disorders. *Molecules.* 2020; **25**(11):2555

Perry CG, Kane DA, Lin CT, Kozy R, Cathey BL, Lark DS, Kane CL, Brophy PM, Gavin TP, Anderson EJ, Neufer PD. Inhibiting myosin-ATPase reveals a dynamic range of mitochondrial respiratory control in skeletal muscle. *Biochem J.* 2011; **437**:215–222

Perry Jr RA, Brown LA, Lee DE, Brown JL, Baum JI, Greene NP, Washington TA. The Akt/mTOR pathway: Data comparing young and aged mice with leucine supplementation at the onset of skeletal muscle regeneration. *Data Brief.* 2016; **8**:1426-32

Pesta D, Gneiger E. High-resolution respirometry. OXPHOS protocols for human cell cultures and permeabilized fibers from small biopsies of human muscle. *Methods Mol Biol.* 2012; **810**;25–58

Pesta D, Hoppel F, Macek C, Messner H, Faulhaber M, Kobel C, Parson W, Burtscher M, Schocke M, Gnaiger E. Similar qualitative and quantitative changes of mitochondrial respiration following strength and endurance training in normoxia and hypoxia in sedentary humans. *Am J Physiol Regul Integr Comp Physiol.* 2011; **301**:R1078–87

Piantadosi CA, Suliman HB. Redox regulation of mitochondrial biogenesis. *Free Radic Biol Med.* 2012; **53**(11):2043-53

Picon-Pages P, Garcia-Buendia J, Munoz FJ. Functions and dysfunctions of nitric oxide in brain. *Biochim Biophys Acta Mol Basis Dis.* 2019; **1865**(8):1949-1967

Pigna E, Renzini A, Greco E, Simonazzi E, Fulle S, Mancinelli R, Moresi V, Adamo S. HDAC4 preserves skeletal muscle structure following long-term denervation by mediating distinct cellular responses. *Skelet Muscle.* 2018; **8**(1):6

Pinna M, Roberto S, Milia R, Marongiu E, Olla S, Loi A, Migliaccio GM, Padulo J, Orlandi C, Tocco F, Concu A, Crisafulli A. Effect of beetroot juice supplementation on aerobic response during swimming. *Nutrients.* 2014; **6**(2):605-15

Poderoso JJ, Helfenberger K, Poderoso C. The effect of nitric oxide on mitochondrial respiration. *Nitric Oxide.* 2019; **88**:61-72

Pollari E, Goldsteins G, Bart G, Koistinaho J, Giniatullin R. The role of oxidative stress in degeneration of the neuromuscular junction in amyotrophic lateral sclerosis. *Front Cell Neurosci.* 2014; **8**:131

Porcelli S, Ramaglia M, Bellistri G, Pavei G, Pugliese L, Montorsi M, Rasica L, Marzorati M. Aerobic Fitness Affects the Exercise Performance Responses to Nitrate Supplementation. *Med Sci Sports Exerc.* 2015; **47**(8):1643-51

Poudel SB, Dixit M, Neginskaya M, Nagaraj K, Pavlov E, Werner H, Yakar S. Effects of GH/IGF on the Aging Mitochondria. *Cells.* 2020; **9**(6):1384

Presnell CE, Bhatti G, Numan LS, Lerche M, Alkhateeb SK, Ghalib M, Shammaa M, Kavdia M. Computational insights into the role of glutathione in oxidative stress. *Curr Neurovasc Res.* 2013; **10**(2):185-94

Qin L, Liu X, Sun Q, Fan Z, Xia D, Ding G, Ling Ong H, Adams D, Gahl WA, Zheng C, Qi S, Jin L, Zhang C, Gu L, He J, Deng D, Ambudkar IS, Wang S. Sialin (SLC17A5) functions as a nitrate transporter in the plasma membrane. *Proc Natl Acad Sci U S A.* 2012; **109**(33):13434-9

Quiles JM, Gustafsson AB. Mitochondrial Quality Control and Cellular Proteostasis: Two Sides of the Same Coin. *Front Physiol.* 2020; **11**:515

Radak Z, Suzuki K, Posa A, Petrovszky Z, Koltai E, Boldogh I. The systemic role of SIRT1 in exercise mediated adaptation. *Redox Biol.* 2020; **35**:101467

Radi R. Nitric oxide, oxidants, and protein tyrosine nitration. *Proc Natl Acad Sci U S A.* 2004; **101**(12):4003-8

Rajan VR, Mitch WE. Muscle wasting in chronic kidney disease: the role of the ubiquitin proteasome system and its clinical impact. *Pediatr Nephrol.* 2008; **23**(4):527-35

Ramblod AS, Kostelecky B, Elia N, Lippincott-Schwarts J. Tubular network formation protects mitochondria from autophagosomal degradation during nutrient starvation. *Proc Natl Acad Sci U S A.* 2011; **108**(25):10190-5

Rameau GA, Tukey DS, Garcin-Hosfield ED, Titcombe RF, Misra C, Khatri L, Getzoff ED, Ziff EB. Biphasic coupling of neuronal nitric oxide synthase phosphorylation to the NMDA receptor regulates AMPA receptor trafficking and neuronal cell death. *J Neurosci.* 2007; **27**(13):3445-55

Rammos C, Hendgen-Cotta UB, Sobierajski J, Bernard A, Kelm M, Rassaf T. Dietary nitrate reverses vascular dysfunction in older adults with moderately increased cardiovascular risk. *J Am Coll Cardiol.* 2014; **63**(15):1584-5

Ratto D, Corana F, Mannucci B, Priori EC, Cobelli F, Roda E, Ferrari B, Occhinegro A, Di Iorio C, De Luca F, Cesaroni V, Girometta C, Bottone MG, Savino E, Kawagishi H, Rossi P. *Hericium erinaceus* Improves Recognition Memory and Induces Hippocampal and Cerebellar Neurogenesis in Frail Mice during Aging. *Nutrients.* 2019; **11**(4):715

Reiser PJ, Kline WO, Vaghy PL. Induction of neuronal type nitric oxide synthase in skeletal muscle by chronic electrical stimulation *in vivo*. *J Appl Physiol.* 1997; **82**(4):1250-5

Riuzzi F, Sorci G, Arcuri C, Giambanco I, Bellezza I, Minelli A, Donato R. Cellular and molecular mechanisms of sarcopenia: the S100B perspective. *J Cachexia Sarcopenia Muscle.* 2018; **9**(7):1255-1268

Robinson SW, Gutierrez Olmo M, Martin M, Smith TM, Morone N, Steinert JR. Endogenous Nitric Oxide Synthase activity regulates synaptic transmitter release. *Opera Med Physiol.* 2017; **3**(2):31-38

Roda E, Priori EC, Ratto D, De Luca F, Di Iorio C, Angelone P, Locatelli CA, Desiderio A, Goppa L, Savino E, Bottone MG, Rossi P. Neuroprotective Metabolites of *Hericium erinaceus* Promote Neuro-Healthy Aging. *Int J Mol Sci.* 2021; **22**(12):6379

Romanello V, Guadagnin E, Gomes L, Roder I, Sandri C, Petersen Y, Milan G, Masiero E, Del Piccolo P, Foretz M, Scorrano L, Rudolf R, Sandri M. Mitochondrial fission and remodelling contributes to muscle atrophy. *EMBO J.* 2010; **29**(10):1774-85

Romanello V, Sandri M. Mitochondrial Quality Control and Muscle Mass Maintenance. *Front Physiol.* 2016; **6**:422

Rudolf R, Khan MM, Labeit S, Deschenes MR. Degeneration of neuromuscular junction in age and dystrophy. *Front Aging Neurosci.* 2014; **6**:99

Rygiel KA, Grady JP, Turnbull DM. Respiratory chain deficiency in aged spinal motor neurons. *Neurobiol Aging.* 2014; **35**(10):2230-8

Rygiel KA, Picard M, Turnbull DM. The ageing neuromuscular system and sarcopenia: a mitochondrial perspective. *J Physiol.* 2016; **594**(16): 4499–4512

Saini J, Faroni A, Reid AJ, Mouly V, Butler-Browne G, Lightfoot AP, McPhee JS, Degens H, Al-Shanti N. Cross-talk between motor neurons and myotubes via endogenously secreted neural and muscular growth factors. *Physiol Rep.* 2021; **9**(8):e14791

Saito Y, Chikenji TS, Matsumura T, Nakano M, Fujimiya M. Exercise enhances skeletal muscle regeneration by promoting senescence in fibro-adipogenic progenitors. *Nat Commun.* 2020; **11**(1):889

Sakamuri SSVP, Sperling JA, Evans WR, Dholakia MH, Albuck AL, Sure VN, Satou R, Mostany R, Katakam PVG. Nitric oxide synthase inhibitors negatively regulate respiration in isolated rodent cardiac and brain mitochondria. *Am J Physiol Heart Circ Physiol.* 2020; **318**(2):H295-H300

Sakuma K, Kinoshita M, Ito Y, Aizawa M, Aoi W, Yamaguchi A. p62/SQSTM1 but not LC3 is accumulated in sarcopenic muscle of mice. *J Cachexia Sarcopenia Muscle.* 2016; **7**(2):204-12

Sakuma K, Yamaguchi A. The recent understanding of the neurotrophin's role in skeletal muscle adaptation. *J Biomed Biotechnol.* 2011; **2011**:201696

Samengo G, Avik A, Fedor B, Whittaker D, Myung KH, Wehling-Henricks M, Tidball JG. Age-related loss of nitric oxide synthase in skeletal muscle causes reductions in calpain S-nitrosylation that increase myofibril degradation and sarcopenia. *Aging Cell.* 2012; **11**(6):1036-45

Sandri M, Barberi L, Bijlsma AY, Blaauw B, Dyar KA, Milan G, Mammucari C, Meskers CGM, Pallafacchina G, Paoli A, Pion D, Roceri M, Romanello V, Serrano AL, Toniolo L, Larsson L, Maier AB, Muñoz-Cánoves P, Musarò A, Pende M, Reggiani C, Rizzuto R, Schiaffino S. Signalling pathways regulating muscle mass in ageing skeletal muscle. The role of the IGF1-Akt-mTOR-FoxO pathway. *Biogerontol.* 2013; **14**:pp303–323

Sandri M, Sandri C, Gilbert A, Skurk C, Calabria E, Picard A, Walsh K, Schiaffino S, Lecker SH, Goldberg AL. Foxo transcription factors induce the atrophy-related ubiquitin ligase atrogin-1 and cause skeletal muscle atrophy. *Cell.* 2004; **117**(3):399-412

Sandri M. Autophagy in skeletal muscle. *FEBS Lett.* 2010; **584**(7):1411-6

Sarti P, Forte E, Giuffrè A, Mastronicola D, Magnifico MC, Arese M. The Chemical Interplay between Nitric Oxide and Mitochondrial Cytochrome c Oxidase: Reactions, Effectors and Pathophysiology. *Int J Cell Biol.* 2012; **2012**:571067

Schicchitano BM, Pelosi L, Sica G, Musarò A. The physiopathologic role of oxidative stress in skeletal muscle. *Mech Ageing Dev.* 2018; **170**:37-44

Schroder EA, Wang L, Wen Y, Callahan LAP, Supinski GS. Skeletal muscle-specific calpastatin overexpression mitigates muscle weakness in aging and extends life span. *J Appl Physiol (1985).* 2021; **131**(2):630-642

Sebastián D, Sorianello E, Segalés J, Irazoki A, Ruiz-Bonilla V, Sala D, Planet E, Berenguer-Llergo A, Muñoz JP, Sánchez-Feutrie M, Plana N, Hernández-Álvarez MI, Serrano AL, Palacín M, Zorzano A. Mfn2 deficiency links age-related sarcopenia and impaired autophagy to activation of an adaptive mitophagy pathway. *EMBO J.* 2016; **35**(15):1677-93

Shang GK, Han L, Wang ZH, Liu YP, Yan SB, Sai WW, Wang D, Li YH, Zhang W, Zhong M. Sarcopenia is attenuated by TRB3 knockout in aging mice via the alleviation of atrophy and fibrosis of skeletal muscles. *J Cachexia Sarcopenia Muscle.* 2020; **11**(4):1104-1120

Shiao T, Fond A, Deng B, Wehling-Henricks M, Adams ME, Froehner SC, Tidball JG. Defects in neuromuscular junction structure in dystrophic muscle are corrected by expression of a NOS transgene in dystrophin-deficient muscles, but not in muscles lacking α- and β1-syntrophins. *Hum Mol Genet.* 2004; **13**(17):1873-84

Siervo M, Oggioni C, Jakovljevic DG, Trenell M, Mathers JC, Houghton D, Celis-Morales C, Ashor AW, Ruddock A, Ranchordas M, Klonizakis M, Williams EA. Dietary nitrate does not affect physical activity or outcomes in healthy older adults in a randomized, cross-over trial. *Nutr Res.* 2016; **36**(12):1361-1369

Silvagno F, Xia H, Bredt DS. Neuronal nitric-oxide synthase-mu, an alternatively spliced isoform expressed in differentiated skeletal muscle. *J Biol Chem.* 1996; **271**(19):11204-8

Soendenbroe C, Bechshøft CJL, Heisterberg MF, Jensen SM, Bomme E, Schjerling P, Karlsen A, Kjaer M, Andersen JL, Mackey AL. Key Components of Human Myofibre Denervation and Neuromuscular Junction Stability are Modulated by Age and Exercise. *Cells.* 2020; **9**(4):893

Soendenbroe C, Heisterberg MF, Schjerling P, Karlsen A, Kjaer M, Andersen JL, Mackey AL. Molecular indicators of denervation in aging human skeletal muscle. *Muscle Nerve.* 2019; **60**(4):453-463

Srihirun S, Park JW, Teng R, Sawaengdee W, Piknova B, Schechter AN. Nitrate uptake and metabolism in human skeletal muscle cell cultures. *Nitric Oxide.* 2020; **94**:1-8

Srikuea R, Hirunsai M, Charoenphandhu N. Regulation of vitamin D system in skeletal muscle and resident myogenic stem cell during development, maturation, and ageing. *Scientific Reports.* 2020; **10**:8239

Stamler JS, Meissner G. Physiology of nitric oxide in skeletal muscle. *Physiol Rev.* 2001; **81**(1):209-237

Tadaishi M, Miura S, Kai Y, Kawasaki E, Koshinaka K, Kawanaka K, Nagata J, Oishi Y, Ezaki O. Effect of exercise intensity and AICAR on isoform-specific expressions of murine skeletal muscle PGC-1α mRNA: a role of β_2-adrenergic receptor activation. *Am J Physiol Endocrinol Metab.* 2011; **300**(2):E341-9

Tamir S and Tannenbaum SR. The role of nitric oxide (NO●) in the carcinogenic process. *Biochim Biophys Acta*. 1996; **1288**(2):F31-6

Tanaka H, Ueno S, Aoyagi R, Hatamoto Y, Jackowska M, Shiose K, Higaki Y. Easily performed interval exercise induces to increase in skeletal muscle PGC-1α gene expression. *Integr Mol Med.* 2017; **4**(4):1-4

Tanner RE, Brunker LB, Agergaard J, Barrows KM, Briggs RA, Kwon OS, Young LM, Hopkins PN, Volpi E, Marcus RL, LaStayo PC, Drummond MJ. Age-related differences in lean mass, protein synthesis and skeletal muscle markers of proteolysis after bed rest and exercise rehabilitation. *J Physiol.* 2015; **593**(Pt 18):4259–4273

Taylor CT. Mitochondria and cellular oxygen sensing in the HIF pathway. *Biochem J*. 2008; **409**(1):19-26

Tengan CH, Rodrigues GS, Godinho RO. Nitric Oxide in Skeletal Muscle: Role on Mitochondrial Biogenesis and Function. *Int J Mol Sci.* 2012; **13**(12):17160–17184

Tews DS, Goebel HH, Schneider I, Gunkel A, Stennert E, Neiss WF. Expression of different isoforms of nitric oxide synthase in experimentally denervated and reinnervated skeletal muscle. *J Neuropathol Exp Neurol.* 1997; **56**(12):1283-9

Thomas DD. Breathing new life into nitric oxide signaling: A brief overview of the interplay between oxygen and nitric oxide. *Redox Biol.* 2015; **5**:225-233

Tidball JG, Lavergne E, Lau KS, Spencer MJ, Stull JT, Wehling M. Mechanical loading regulates NOS expression and activity in developing and adult skeletal muscle. *Am J Physiol.* 1998; **275**(1):C260-6

Tilokani L, Nagashima S, Paupe V, Prudent J. Mitochondrial dynamics: overview of molecular mechanisms. *Essays Biochem.* 2018; **62**(3):341–360

Timpani CA, Hayes A, Rybalka E. Therapeutic strategies to address neuronal nitric oxide synthase deficiency and the loss of nitric oxide bioavailability in Duchenne Muscular Dystrophy. *Orphanet J Rare Dis.* 2017; **12**(1):100

Timpani CA, Mamchaoui K, Butler-Browne G, Rybalka E. Nitric Oxide (NO) and Duchenne Muscular Dystrophy: NO Way to Go? *Antioxidants (Basel).* **2020**; 9(12):1268 Tintignac LA, Brenner HR, Rüegg MA. Mechanisms Regulating Neuromuscular Junction Development and Function and Causes of Muscle Wasting. *Physiol Rev.* 2015; **95**(3):809-52

Tirone M, Tran NL, Ceriotti C, Gorzanelli A, Canepari M, Bottinelli R, Raucci A, Di Maggio S, Santiago C, Mellado M, SaclierM, François S, Careccia G, He M, De Marchis F, Conti V, Ben Larbi S, Cuvellier S, Casalgrandi M, Preti A, Chazaud B, Al-Abed Y, Messina G, Sitia G, Brunelli S, Bianchi ME, Vénéreau E. High mobility group box 1 orchestrates tissue regeneration via CXCR4. *J Exp Med.* 2018; **215**(1):303–318

Tripathi P, Moinuddin, Dixit K, Mir AR, Habib S, Alam K, Ali A. Peroxynitrite modified DNA presents better epitopes for anti-DNA autoantibodies in diabetes type 1 patients. *Cell Immunol.* 2014; **290**(1):30-8

Volpi E, Sheffield-Moore M, Rasmussen BB, Wolfe RR. Basal muscle amino acid kinetics and protein synthesis in healthy young and older men. *JAMA.* 2001; **286**(10):1206-12

Wahren J, Saltin B, Jorfeldt L, Pernow B. Influence of age on the local circulatory adaptation to leg exercise. *Scand J Clin Lab Invest.* 1974; **33**(1):79-86

Wang R, Jiao H, Zhao J, Wang X, Lin H. L-Arginine Enhances Protein Synthesis by Phosphorylating mTOR (Thr 2446) in a Nitric Oxide-Dependent Manner in C2C12 Cells. *Oxid Med Cell Longev.* 2018; **2018**:7569127

Wang X, Blagden C, Fan J, Nowak S, Taniuchi I, Littman DR, Burden SJ. Runx1 prevents wasting, myofibrillar disorganization, and autophagy of skeletal muscle. *Genes Dev.* 2005; **19**(14):1715-22

Webb AJ, Patel N, Loukogeorgakis S, Okorie M, Aboud Z, Misra S, Rashid R, Miall P, Deanfield J, Benjamin N, MacAllister R, Hobbs AJ, Ahluwalia A. Acute blood pressure lowering, vasoprotective, and antiplatelet properties of dietary nitrate via bioconversion to nitrite. *Hypertension.* 2008; **51**(3):784-90

Wenz T, Tossi SG, Rotundo RL, Spiegelman BM, Moraes CT. Increased muscle PGC-1α expression protects from sarcopenia and metabolic disease during aging. *Proc Natl Acad Sci U S A.* 2009; **106**(48):20405–20410

Wilkerson DP, Hayward GM, Bailey SJ, Vanhatalo A, Blackwell JR, Jones AM. Influence of acute dietary nitrate supplementation on 50-mile time trial performance in well-trained cyclists. *Eur J Appl Physiol.* 2012; **112**(12):4127-34

Willadt S, Nash M, Slater C. Age-related changes in the structure and function of mammalian neuromuscular junctions. *Ann N Y Acad Sci.* 2018; **1412**(1):41-53

Woessner M, Smoglia JM, Tarzia B, Stabler T, van Bruggen M, Allen JD. A stepwise reduction in plasma and salivary nitrite with increasing strengths of mouthwash following a dietary nitrate load. *Nitric Oxide.* 2016; **54**:1-7

Wu G, Morris Jr SM. Arginine metabolism: nitric oxide and beyond. *Biochem J.* 1998; **336**(Pt.1)1-17

Wylie LJ, Park JW, Vanhatalo A, Kadach S, Black MI, Stoyanov Z, Schechter AN, Jones AM, Piknova B. Human skeletal muscle nitrate store: influence of dietary nitrate supplementation and exercise. *J Physiol.* 2019; **597**(23):5565-5576

Xie WQ, He M, Yu DJ, Wu YX, Wang XH, Lv S, Xiao WF, Li YS. Mouse models of sarcopenia: classification and evaluation. *J Cachexia Sarcopenia Muscle.* 2021; **12**(3):538-554

Yamakura F and Kawasaki H. Post-translational modifications of superoxide dismutase. *Biochim Biophys Acta.* 2010; **1804**(2):318-25

Yang B, Larson DF, Watson RR. Modulation of iNOS activity in age-related cardiac dysfunction. *Life Sci.* 2004; **75**,655–667

Yoon MS. mTOR as a Key Regulator in Maintaining Skeletal Muscle Mass. *Front Physiol.* 2017; **8**:788

Yoshihara T, Tsuzuki T, Chang SW, Kakigi R, Sugiura T, Naito H. Exercise preconditioning attenuates hind limb unloading-induced gastrocnemius muscle atrophy possibly via the HDAC4/Gadd45 axis in old rats. *Exp Gerontol.* 2019; **122**:34-41

Yu R, Lendahl U, Nister M, Zhao J. Regulation of Mammalian Mitochondrial Dynamics: Opportunities and Challenges. *Front Endocrinol (Lausanne).* 2020; **11**:374

Zamora R, Vodovotz Y, Billiar TR. Inducible Nitric Oxide Synthase and Inflammatory Diseases. *Mol Med.* 2000; **6**:347-373

Zeng Z, Liang J, Wu L, Zhang H, Lv J, Chen N. Exercise-Induced Autophagy Suppresses Sarcopenia Through Akt/mTOR and Akt/FoxO3a Signal Pathways and AMPK-Mediated Mitochondrial Quality Control. *Front Physiol.* 2020; **11**:583478

Zhang G, Han H, Zhuge Z, Dong F, Jiang S, Wang W, Guimarães DD, Schiffer TA, Lai EY, Ribeiro Antonino Carvalho LR, Barbosa Lucena R, Braga VA, Weitzberg E, Lundberg JO, Carlstrom M. Renovascular effects of inorganic nitrate following ischemia-reperfusion of the kidney. *Redox Biol.* 2021; **39**:101836

Zhang J, Wang X, Vikash V, Ye Q, Wu D, Liu Y, Dong W. ROS and ROS-Mediated Cellular Signaling. *Oxid Med Cell Longev.* 2016; **2016**:4350965

Zuccarelli L, Baldassarre G, Magnesa B, Degano C, Comelli M, Gasparini M, Manferdelli G, Marzorati M, Mavelli I, Pilotto A, Porcelli S, Rasica L, Šimunič B, Pišot R, Narici M, Grassi B. Peripheral impairments of oxidative metabolism after a 10-day bed rest are upstream of mitochondrial respiration. *J Physiol.* 2021; **599**(21):4813-4829

Zucchi E, Lu CH, Cho Y, Chang R, Adiutori R, Zubiri I, Ceroni M, Cereda C, Pansarasa O, Greensmith L, Malaspina A, Petzold A. A motor neuron strategy to save time and energy in neurodegeneration: adaptive protein stoichiometry. *J Neurochem.* 2018; **146**(5):631-641

Zweier JL, Wang P, Samouilov A, Kuppusamy P. Enzyme-independent formation of nitric oxide in biological tissues. *Nat Med.* 1995; **1**(8):804-9